Radiation Induced Synthesis of Conducting Polymers and their Metal Nanocomposites

Zhenpeng Cui

NNT : 2017SACLS165

THESE DE DOCTORAT
DE
L'UNIVERSITE PARIS-SACLAY
PREPAREE A
L'UNIVERSITE PARIS-SUD

ECOLE DOCTORALE N °571
Sciences chimiques : molécules, matériaux, instrumentation et biosystèmes (2MIB)

Spécialité de doctorat: Chimie

Par

Zhenpeng Cui

Radiation induced synthesis of conducting polymers and their metal nanocomposites

Thèse présentée et soutenue à Orsay, le 14 Septembre 2017 :

Composition du Jury :

Mme Laure Catala	Professeure	Université Paris-Saclay	Présidente
M. Jean-Marc Jung	Professeur	Université de Strasbourg	Rapporteur
M. Hyacinthe Randriamahazaka	Professeur	Université Paris-Diderot	Rapporteur
Mme Sophie Le Caër	Chargée de Recherche	Université Paris-Saclay, CEA	Examinatrice
M. Fabrice Goubard	Professeur	Université de Cergy-Pontoise	Examinateur
M. Cyrille Sollogoub	Maître de Conférences	CNAM et ENSAM	Examinateur
M. Samy Remita	Professeur	Université Paris-Saclay et CNAM	Directeur de thèse

Acknowledgements

For the moment, it is almost at the end of my thesis and my doctoral research in Laboratoire de Chimie Physique (LCP) is going to finish. My thesis can't be completed without earnest instructions and inspiring helps from my supervisor, referees, cooperators, colleagues, friends and family. Here, I would like to express my sincere thanks to them for their contributions and participation for my research and my thesis.

I would like to thank my advisor Prof. Samy Remita for his guidance of my research and supervision of my thesis. His abundant knowledge, scientific training and helpful suggestions let me find the directions of my research and master various useful skills for doctoral research. I would like to express my sincere appreciate for his patience and hard work on my thesis. His preciseness and his kindness enables me to overcome difficulties in my research.

I am grateful to Prof. Jean-Marc Jung and Prof. Randriamahazaka Hyacinthe for their acceptance of being the reviewers of my thesis. I would like to thank Prof. Laure Catala, Prof. Sophie Le Caer, Prof. Cyrille Sollogoub and Prof. Fabrice Goubard for their acceptance of being the referees of my defense. It is my glory to invite all the members of doctoral thesis defence committee to attend my defense and I would like to express my sincere thanks to all of you.

I would like to thank Prof. Philippe Maître as the director of LCP for his kind help. I would like to thank Prof. Mehran Mostafavi for his inspiring suggestions. I would like to thank Prof. Hynd Remita as the leader of TEMiC group for her friendly and helpful assistances.

I would like to thank all the cooperators Alexandre Dazzi, Ariane Deniset-Besseau, Rolando Rebois, Patrice Lefrançois, Matthieu Gervais, Stéphane Néron, Sarah Baiz, Pieere-Henri Aubert, Jean-louis Marignier, Jean-Michel Guigner for their beneficial collaborations and kind help.

I would like to thank my colleagues Cecilia Coletta, Teseer Bahry, Xiaojiao Yuan and all the members of TEMiC group for their kind help and happy accompaniment. They give me many help in my research and bring me a lot of fun in daily life.

I would like to thank China Scholar Council (CSC) for offering me scholarship for my research.

I would like to thank Mireille Benoit and Alexandre Demarque for kind assistances during the experiments. I would like to thank Séverine Bourguignon, Anne Morel for their helps with administrative work.

I would like to say thanks to my friends for their kind help and the happy time we spent together. Last but not least, I would like to thank my family for their supports and encouragements.

Acronyms list

AFM-IR	atomic force microscopy-based infrared nano spectroscopy
Ani	aniline
ATR-FTIR	attenuated total reflection fourier transform infrared spectroscopy
CMC	critical micelle concentration
CPs	conducting polymers
Cryo-TEM	cryogenic-transmission electron microscopy
D	dose
EDOT	3,4-ethylenedioxythiophene
EDX	energy dispersive X-Ray spectroscopy
G	radiolytic yield
Gy	gray
PANI	polyaniline
PEDOT	poly(3,4-ethylenedioxythiophene)
PPy	polypyrrole
Py	pyrrole
SEM	scanning electron microscopy
SHE	standard hydrogen electrode
TGA	thermogravimetric analysis
UV-vis	ultraviolet-visible
ε	molar extinction coefficient

Contents

Résumé

Depuis la découverte de la conductivité électrique du polyacétylène, $(CH)_x$, et des nombreuses caractéristiques particulièrement intéressantes liées à ce type de matériaux, les travaux de recherche sur les polymères conducteurs (PCs) se sont multipliés. Les PCs constituent désormais des matériaux de choix, qui sont utilisés dans de très nombreuses applications. Différentes méthodologies ont été utilisées pour la préparation de polymères conducteurs et de leurs nanocomposites. Le plus souvent, les PCs sont synthétisés par des méthodes chimiques ou électrochimiques traditionnelles, grâce à l'oxydation initiale des monomères. Néanmoins, différentes méthodes alternatives ont été proposées, comme les méthodes enzymatique, photochimique ou par sonication.

Très récemment, une méthodologie radiolytique originale a été développée au sein de notre laboratoire pour la préparation de PCs en solution aqueuse. Cette méthodologie alternative permet, en effet, l'oxydation des monomères dissous dans l'eau. Cette oxydation est assurée par les radicaux oxydants produits *in situ* par la radiolyse de l'eau, suite à la pénétration dans le milieu d'un rayonnement ionisant de forte énergie, que ce soit des rayons ou des électrons accélérés. Des études de radiolyse pulsée menées par notre équipe ont par ailleurs démontré que le processus de croissance des PCs résultait d'un mécanisme par stades et non d'un mécanisme en chaîne.

L'objectif du présent travail est de démontrer la versatilité de notre méthodologie radiolytique et de l'étendre à la synthèse de différents PCs dans l'eau, sous différentes conditions expérimentales. Le poly(3,4-ethylènedioxythiophène), PEDOT, et le polypyrrole, PPy, ont ainsi été préparés avec succès et caractérisés en solution aqueuse, ou après dépôt sur substrat, par des techniques spectroscopiques et microscopiques complémentaires. La stabilité thermique et la conductivité électrique de ces matériaux radiosynthétisés ont été étudiées et comparées aux propriétés des PCs produits par les méthodologies traditionnelles.

Dans ce manuscrit, nous avons étudié l'influence et l'impact de la nature des espèces radiolytiques oxydantes, de la force ionique du milieu, du pH de la solution et de la présence de surfactants, qu'ils soient libres ou auto-assemblés, sur le mécanisme de croissance des PCs, sur le rendement de polymérisation, sur la morphologie des matériaux radiosynthétisés ainsi que sur les propriétés optiques et électriques de ces derniers. Comme démontré, la présence d'auto-assemblages organiques ne permet pas la préparation quantitative de PCs à cause de réactions compétitives d'oxydation des surfactants par les espèces radiolytiques. Au contraire,

la nature très acide du milieu favorise la préparation efficace de PCs, qui sont alors, de surcroît, caractérisés par des propriétés spectroscopiques originales.

Nous avons par ailleurs, montré dans ce travail que les PCs pouvaient être produits, non seulement par oxydation radioinduite des monomères, mais également par réduction radiolytique de ceux-ci. Ainsi, grâce à l'utilisation d'espèces radiolytiques réductrices, telles que les électrons solvatés, une toute nouvelle voie de synthèse par réduction des monomères a été développée pour la synthèse de PCs en solution aqueuse. Les matériaux ainsi préparés ont été comparés à ceux produits par oxydation des monomères. Non seulement la morphologie est similaire, mais les propriétés physico-chimiques sont également comparables.

Nous avons finalement utilisé la radiolyse pour la synthèse de nanocomposites hybrides à base de PCs et de métaux de transition. Plusieurs voies de synthèse ont été développées : synthèse en une ou deux étapes, par oxydation ou réduction des monomères. Bien entendu, l'architecture des nanocomposites obtenus ainsi que leurs propriétés sont très dépendantes de la voie de synthèse utilisée. Ces résultats ont été interprétés en termes de mécanismes de croissance des PCs d'une part, et des nanoparticules métalliques d'autre part, en termes de constantes de vitesse (qui ont été déterminées par radiolyse impulsionnelles) et en tenant compte des interactions intermoléculaires de faible énergie mises en jeu.

La nouvelle stratégie de synthèse par radiolyse, qui est décrite dans ce manuscrit, ouvre la voie à la préparation de très nombreuses familles de PCs et de leurs composites, que ce soit en solution aqueuse ou dans des environnements alternatifs (en milieu organique, sur support, en milieu hétérogène), ce qui laisse augurer de nombreuses applications fort prometteuses.

Chapter 1: A brief introduction of research background

In 2000, the noble prize in chemistry was jointly awarded to Alan J. Heeger, Alan G. MacDiarmid and Hideki Shirakawa "for the discovery and development of conductive polymers" (Figure 1.1).[1]

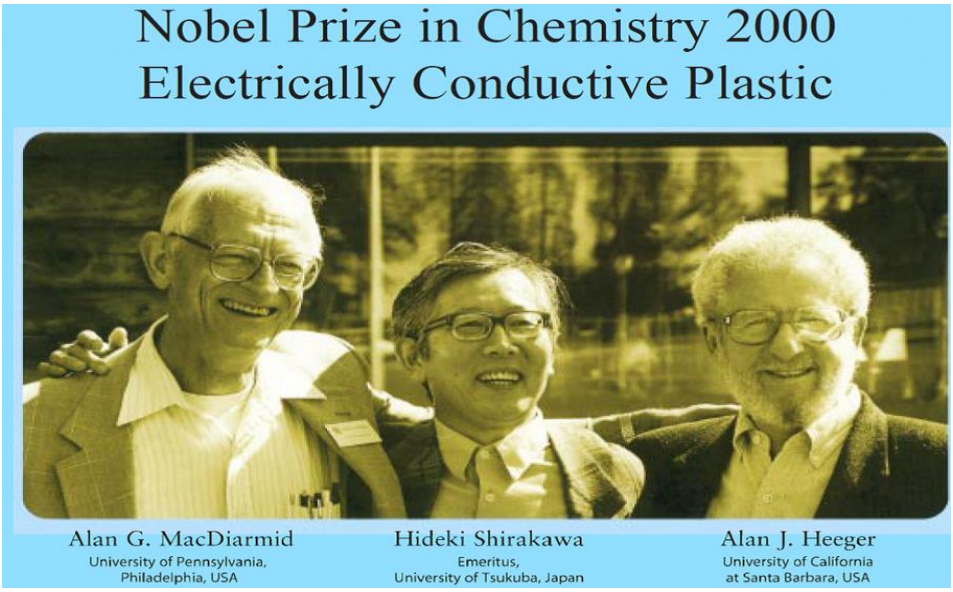

Figure 1.1 Nobel Laureates in chemistry 2000.[1]

1.1 Conducting polymers (CPs)

Conducting polymers (CPs) have opened a new research field and attracted great interests for their advantageous properties and excellent performances as a new generation of polymer materials.[1-3] Since the first discovery in 1970s, a wide variety of electrically conductive polymers as well as their derivatives have been developed and widely applied in various fields.[1,3] The super characters and promising applications of conducting polymer materials have promoted their quick development and will definitely bring about great profits in a wide range of areas.[4-7]

What are CPs? They are particular kinds of polymers exhibiting electrical conductivity arising from the π-conjugated systems in the polymer structures.[2] In general, conventional organic polymers are known to be good electrical insulators without free π-electrons along

their backbone. On the contrary, there are delocalized π-electrons in the conjugated systems of CPs which endow conducting polymers an intrinsic electrical conductivity.[3] Therefore, CPs are also known as π-conjugated polymers.[3,8]

1.1.1 Representative CPs

Since the discovery of polyacetylene $(CH)_x$, as the first conducting polymers, deep understanding of basic principles of CPs was accelerated. In addition, more and more CPs were rapidly discovered and synthetic methods of CPs underwent a quick development. Now, CPs are a big family containing a large variety of electrically conducting polymers.[3,9] Here are some examples of widely investigated CPs (Figure 1.2).[3]

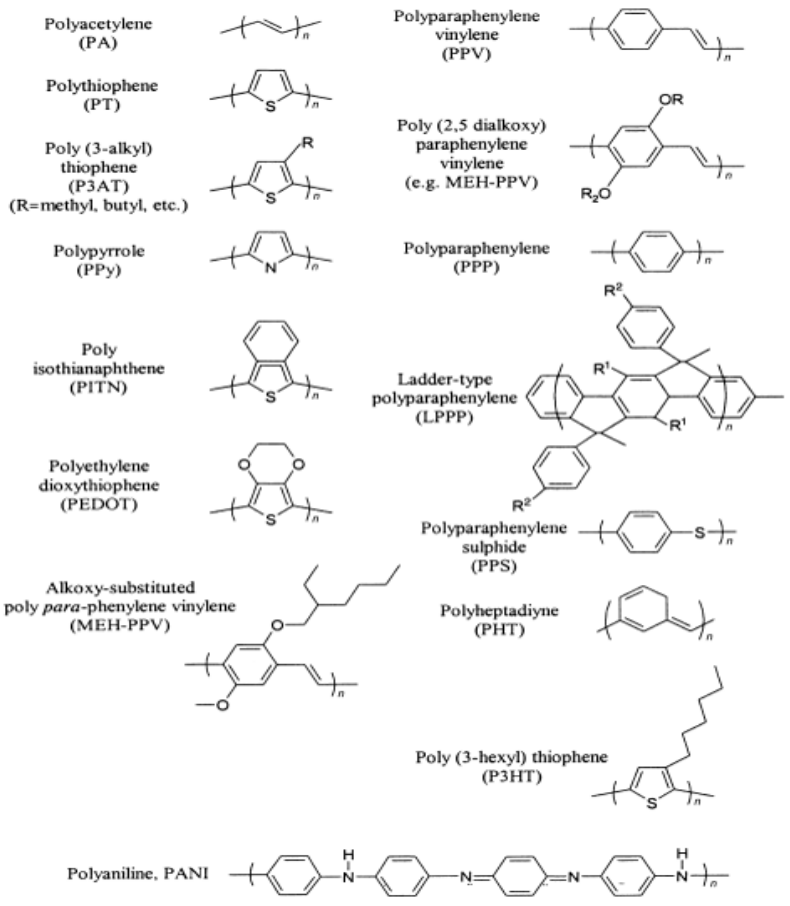

Figure 1.2 Examples of conjugated conducting polymers.[3]

It is clear that all the CPs possess π-conjugated system in their backbones whatever the side groups or functional groups. The incorporation of different side chains and functional groups on the basic unit of CPs can not only improve the physical and chemical properties but also

endow the pristine polymers new expected functionalities. To obtain CPs with specific and multiple functionalities, the design and synthesis of multiple CPs are still on the way and rapid progress is being maintained based on great research interest all over the world. The discovery of CPs opens a new field of the application of polymers and makes CPs the fourth generation of polymer materials.[3,10,11]

Among the various CPs, poly(3,4-ethylenedioxythiophene) (PEDOT), polypyrrole (PPy) and polyaniline (PANI) have been mostly investigated due to easy synthesis, good processability and excellent properties.[12-16] Due to the advantageous characters of these CPs, synthesis and processing of these three kinds of representative conducting polymers and their derivatives are of great interests as they are promising candidates for organic polymer conductors. Therefore, investigations on the mechanism and principles of the electrical conductivity of CPs are of great importance.

1.1.2 Electrical conductivity

As the first conducting polymers reported, polyacetylene $(CH)_x$ was found to become electrically conductive when treated with halogen (Figure 1.3).[9] Although Natta *et al.* synthesized polyacetylene powders no later than 1958, the $(CH)_x$ films were successfully prepared by Hedeki Shirakawa using Ziegler-Natta catalyst and changed from insulator to conductor after halogenation.[1,3,9,17] Compared with the *cis*-isomer (1.7×10^{-9} S/cm), *trans*-isomer (4.4×10^{-5} S/cm) is thermodynamically stable and has a higher electrical conductivity at room temperature (Figure 1.3). However, remarkable increase of electrical conductivity of the $(CH)_x$ films was found when treated with halogen vapor, indicating the formation of conducting polymers of $(CH)_x$.[9]

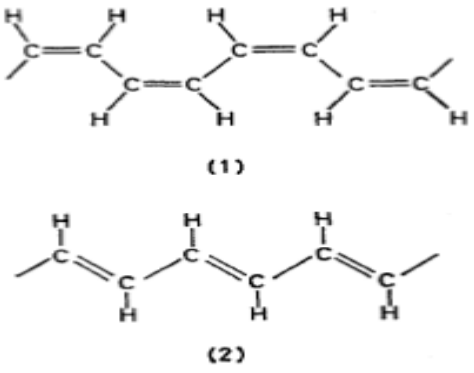

Figure 1.3 *Cis*-isomer (1) and *trans*-isomer (2) of polyacetylene.[9]

According to the electrical conductivity, materials can be divided into four categories: insulator, semiconductor, conductor and superconductor.[18] In general a material with a conductivity less than 10^{-7} S/cm is regarded as an insulator and a material with a conductivity in the range of 10^{-7}~10 S/cm is considered as a semiconductor. A metal can show an electrical conductivity higher than 10^{3} S/cm.[18] From the point of view of electrical conductivity, the $(CH)_x$ polymers should be regarded as semiconductors (*trans*-isomer) or insulators (*cis*-isomer) due to the relatively low electrical conductivity (Figure 1.4).[2] However, a doping process (i.e. halogenation) brings about an increase of electrical conductivity by many orders of magnitude and results in the transformation of $(CH)_x$ films into electrical conductors (Figure 1.4). This result changes the common perception that the traditional polymers are non-electrical conductor and proves that the electrical conductivity of π-conjugated polymers could vary in a wide range from insulators to conductors. Therefore, CPs are also called as "Synthetic Metals".[2]

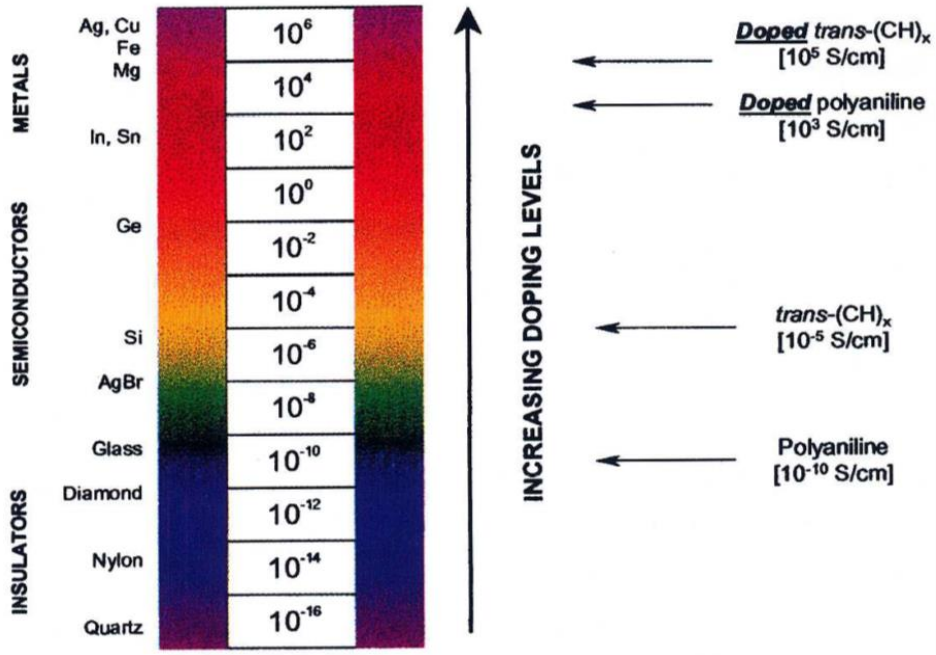

Figure 1.4. Electrical conductivity range divisions and the electrical conductivity of CPs.[2]

The principle of electrical conductivity of different materials can be explained by the traditional band gap theory.[19] In the solid materials, the energy level distributions of electrons are divided into valence band, forbidden band and conduction band (Figure 1.5). Electrons occupy the valence band with lower energy and jump to the conduction band when they are

excited. Between the top of the valence band (the highest occupied molecular orbital, HOMO) and the bottom of the conduction band (the lowest unoccupied molecular orbital, LUMO) is the forbidden band where no electrons exist. The difference between HOMO and LUMO is called the bandgap (E_g) (Figure 1.5). After excitation, when the electrons are distributed in the conduction band, they can move freely and form the current when an electrical field is added. In the metallic materials, overlaps of the valence band and conduction band make metal have no bandgap and result in the free movement of electrons in valence band. As a result, metal has a good electrical conductivity at room temperature. On the contrary, the E_g value of dielectric materials is large and the transition of electrons from valence band to conduction band is not possible. Hence, insulator has a poor electrical conductivity. The E_g value of semiconductive materials is relatively smaller than that of insulators and electrons can jump from the valence band to the conduction band when heated or optically excited (Figure 1.5). As a result, semiconductor is able to conduct the electrical current only under certain conditions. Therefore, the different E_g values determine the abilities of different materials to conduct electrical current.[20]

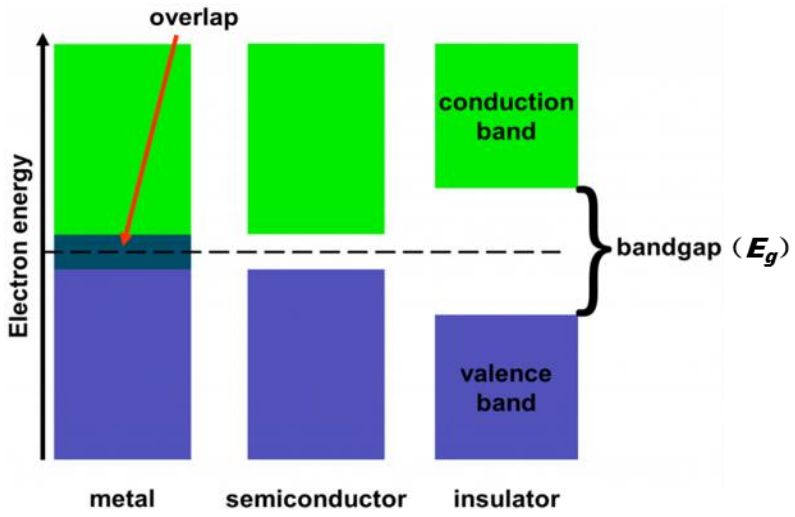

Figure 1.5 Energy band structures of conductors, semiconductors and insulators.

In order to determine the E_g values of different materials, the absorption edge wavelength (λ_{edge}) is necessary to be known and the E_g values can be calculated according to the following equation:

$$E_g = \frac{1240}{\lambda_{edge}\ (nm)}\ (eV) \tag{1.1}$$

By measuring the UV-visible absorption spectra of different materials which display the onset of absorption bands, the λ_{edge} of different materials can be deduced using absorption spectroscopy (Figure 1.6).[21] The E_g value of insulators is normally larger than 6 eV and the E_g value of semiconductors is around 1 eV.[20] In general, the E_g values of most conjugated polymers fall in the range of 1.0~3.0 eV suggesting that most intrinsic conducting polymers are semiconductors.[18,22]

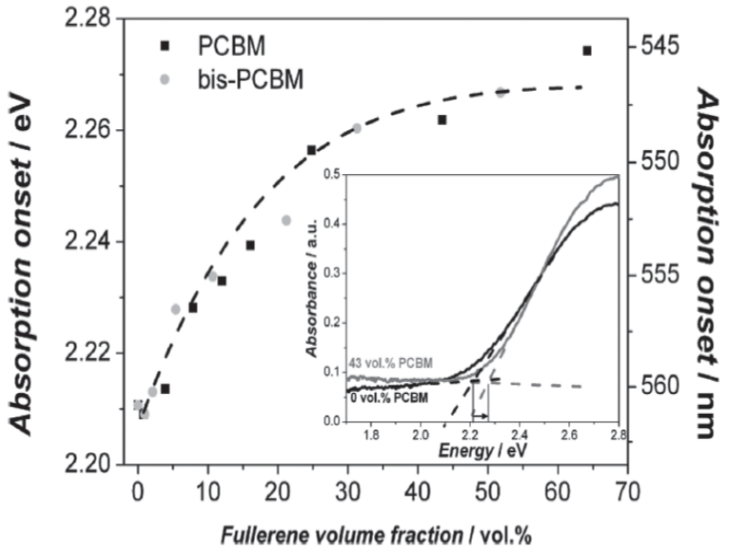

Figure 1.6 Absorption edge position of phenyl-C_{61}-butyric acid methyl ester (PCBM) and bis-PCBM. The absorption spectra of poly(3-hexylthiophene) (P3HT) and P3HT:PCBM (43 vol%) showing the shift of the absorption edge and the way for determining its value is shown in the inset.[21]

In the semiconductive materials, when an electron is excited from the valence band, an empty position is left. A hole is formed at the position of an excited electron in the valence band.[23] Neighboring electrons move to the vacant position and repeat similar movement generating the electrical current. The formation of electrical current is equivalent to the movement of a particle with positive charge. Positively charged holes are also able to conduct the electrical conductivity with comparable effectiveness as electrons. Therefore, both electrons in conduction band and holes in valence band can be carriers of the electrical current. If the electrical current in a semiconductor is mainly conducted by electrons with negative charges, it is called n-type semiconductor. On the contrary, p-type semiconductor applies more positively charged holes as the main carriers. Since most CPs are semiconductors, the transformation of CPs from semiconductors to conductors normally needs additional treatment called doping process.

1.1.3 Doping concept

As mentioned above, polyacetylene $(CH)_x$ as the first example of conducting polymers, can be changed from insulator to conductor by a doping process. Based on the final conducting mode of the CPs, the doping treatment can be divided into two kinds: *p*-doping and *n*-doping. Taking the chemical doping of $(CH)_x$ for example, *p*-doping and *n*-doping can be expressed as follows:

Oxidation with halogen (*p*-doping): $(CH)_x + 3n/2I_2 \rightarrow (CH)_x^{n+} + nI_3^-$ (1.2)

Reduction with alkali metal (*n*-doping): $(CH)_x + nNa \rightarrow (CH)_x^{n-} + nNa^+$ (1.3)

Concerning the *p*-doping, oxidation of the CPs occurs forming cations by extracting electrons from polymer backbones. The oxidant becomes anions by reduction and works as the counter ions. After sufficient *p*-doping, CPs become p-type conductors. Inversely, reduction of the CPs happens during the *n*-doping injecting electrons to the polymer backbones, forming negatively charged CPs while reductant is oxidized into cations. As a result, *n*-doping makes CPs n-type conductors. To achieve doping of CPs, many different methods can be applied: chemical doping, electrochemical doping, protonation by acid-base chemistry, photo-doping, charge injection have been successfully performed.[3] Here are some important CPs and their electrical conductivities after doping (Figure 1.7).[24]

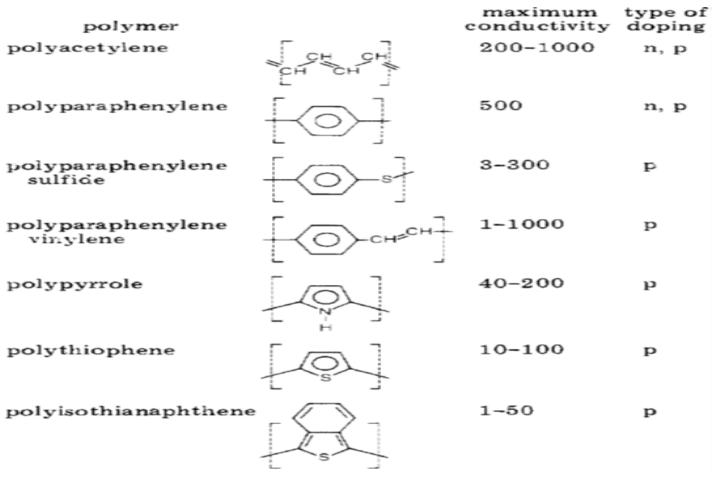

Figure 1.7 Structure, maximum conductivities (in Ω^{-1} cm^{-1}), and type of doping (n or p) for some of the more important conducting polymers.[24]

The doping concept of CPs is different from that applied in inorganic semiconductors as redox reaction occurs and counter ions are incorporated.[25] It is clear that the polymer chains of CPs are charged upon doping process and that there are counter ions which maintain the electrical nature rather than atom replacement. The concept of doping is the unique, central, underlying, and unifying theme which distinguishes conducting polymers from all other types of polymers.[2] During the doping process, dramatic changes of electrical conductivity is realized by transferring the CPs from semiconductor to metallic conductor. Therefore, a doping process is the key trigger of electrical conductivity of electrically conducting polymers.

In the electronic structure of conjugated polymers, charge carriers (electrons or holes), appearing on polymer chains, are energetically favorable to be localized and coupled to the distortions in the backbone. This process causes the presence of localized electronic stated in the band gap due to the shift of the valence band and conduction band.[24] At lower doping level, excitation across the valence band and conduction band creates the self-localized, nonlinear excitations of conducting polymers: solitons (in degenerate ground state systems), polarons, and bipolarons (in nondegenerate ground state systems).[3,26]

A soliton is a charge associated with a boundary or domain wall between the two possible degenerate ground-state configurations.[3,24] The presence of a soliton results in the appearance of a localized electronic level at the mid-gap. In the new electronic level, a neutral soliton is half-occupied and a positively or negatively charged soliton is empty (Figure 1.8).[24]

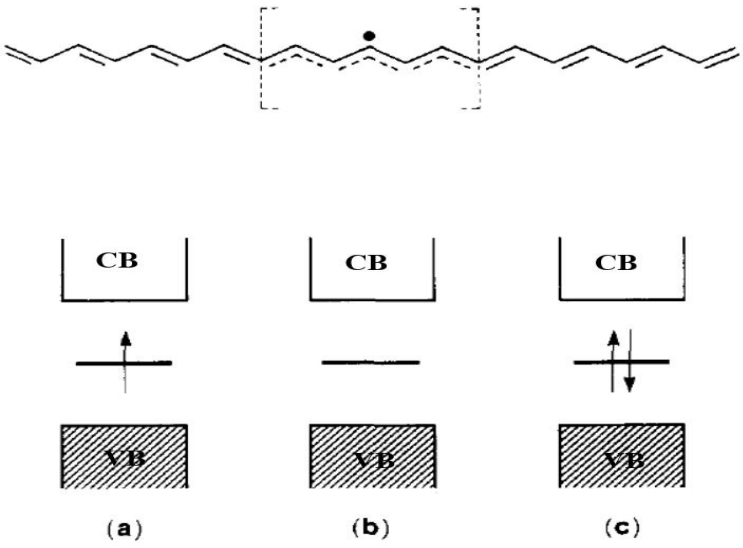

Figure 1.8 Top: schematic illustration of the geometric structure of a neutral soliton of a *trans*-polyacetylene chain. Bottom: band structure for a *trans*-polyacetylene chain containing (a) a neutral soliton, (b) a positively charged soliton, and (c) a negatively charged soliton.[24]

A polaron is a radical ion associated with a lattice distortion and the presence of localized electronic states in the gap referred as polaron states.[24] A polaron can be thought as a bound state of a charged soliton and a neutral soliton whose mid-gap energy states hybridize to form bonding and antibonding levels.[3] In the nondegenerate ground state of the pristine conducting polymers, a doping process creates charge carriers with ionized polymer chains. At lower charge concentrations, a polaron appears with a charge at one end and a free electron at the other showing a measurable spin (Figure 1.9).[27]

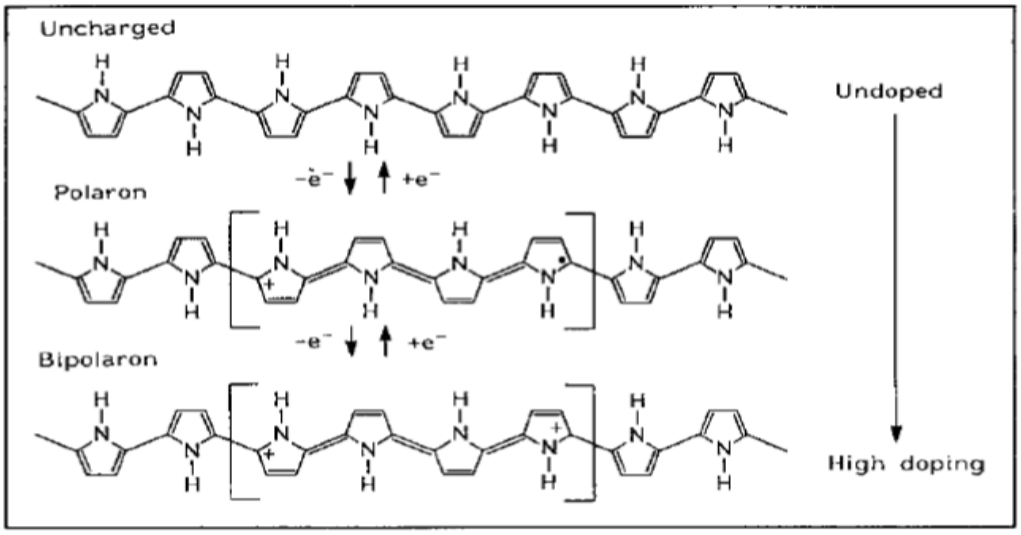

Figure 1.9 Formation of polaron and biopolaron along a polypyrrole chain.[27]

Similarly, a bipolaron is defined as a pair of like charges associated with a strong local lattice distortion.[3,24,27] A bipolaron is a bound state of two charged solitons of like charge (or two polarons whose neutral solitons annihilate each other) with two corresponding mid-gap levels.[3] The formation of a bipolaron indicates that the energy gained by the interaction with the lattice is larger than that of the Coulomb repulsion between the two like charges confined in the same location.[24] At high doping level, the charge density along the polymer chains increases, a section containing two like charges emerges representing the bipolaron (Figure 1.9).[27]

As the doping level increases, polaron and bipolaron are formed until the formation of bipolaron bands resulting from the overlap of bipolaron states (Figure 1.10).[24,28] The high electrical conductivity of conducting polymers at high doping levels is thus reasonable. Therefore, the electrical conductivity of conjugated polymer can be well controlled by the doping process.[26]

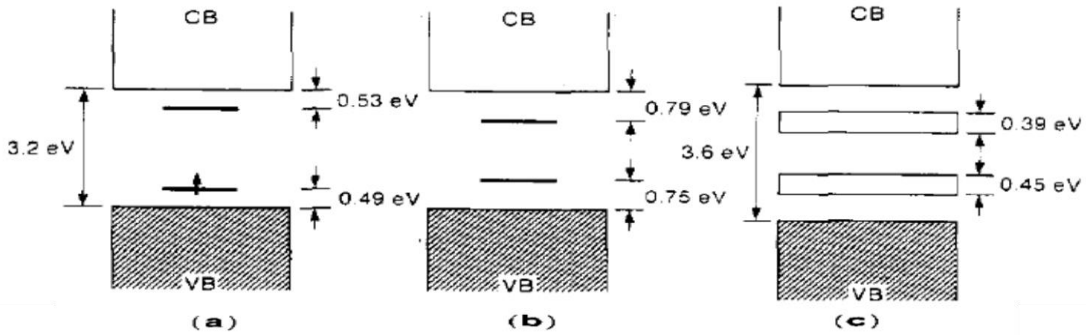

Figure 1.10 Evolution of the polypyrrole band structure upon doping: (a) low doping level, polaron formation; (b) moderate doping level, bipolaron formation; (c) high (33 mol %) doping level, formation of bipolaron bands.[24]

1.1.4 Potential applications

Since the discovery of CPs, the potential applications have attracted great research interest and conducting polymer materials have been widely applied in a variety of areas.[3,4] Based on the chemical and physical properties, various applications of CPs as coating materials have been extensively investigated (Figure 1.11).[29] The potential application of CPs mainly include: conducting coatings, catalysts, sensors, electrochromic devices, field effect transistors, solar cells, photovoltaic devices, etc.[4,30-34]

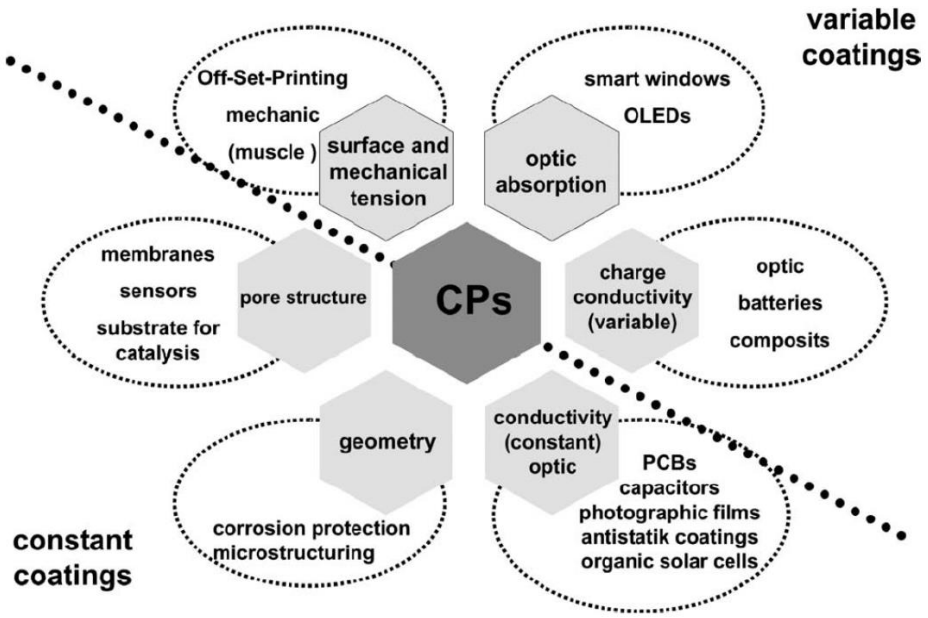

Figure 1.11 Overview for functional properties of CPs and resulting application possibilities.[29]

Shirakawa *et al.* discovered that polyacetylene $(CH)_x$ shows good electrical conductivity as that of metal when treated with halogen.[9] Cho *et al.* synthesized single-crystal nanowires of PEDOT polymers which have ultrahigh electrical conductivity up to 8797 S/cm. Zhou *et al.* reported the application of PPy polymers based catalysts for the redox reaction of I_3^- ions.[6] Ghosh *et al.* found that poly(diphenylbutadiyne) (PDPB) exhibites excellent photocatalytic ability for the degradation of phenol or methyl orange.[35] Huang *et al.* easily produced nanofibers of PANI polymers for chemical sensor applications.[36] Balint *et al.* summarized that PEDOT, PPy and PANI were important materials for biosensors, neural implants, drug delivery devices and tissue engineering scaffolds.[5]

Among the various extraordinary properties of CPs, the most attracting properties are their tunable electrical conductivity and excellent optical properties which enable CPs to possess unique electrical conductivity and good transparency. Conducting polymer blends of poly(3,4-ethylenedioxythiophene) (PEDOT) and poly(styrene sulfonate) (PEDOT/PSS), namely Baytron P, have been commercialized and applied as efficient antistatic coatings, flexible electrode materials and highly conducting coatings (Figure 1.12).[12,37]

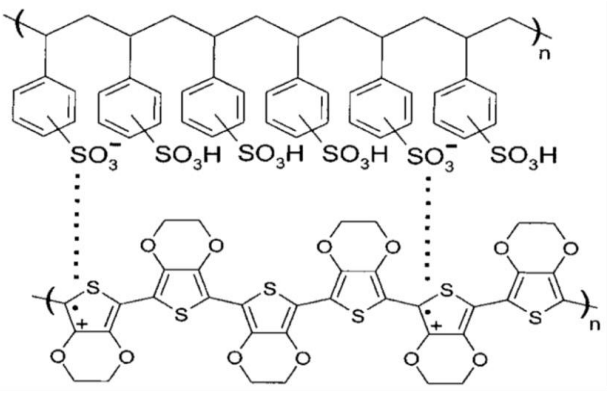

Figure 1.12 Scheme of PEDOT/PSS blend (Baytron P, Bayer AG, Leverkusen, Germany), which is a dispersion of the oxidized polymer PEDOT and the polyanion PSS in water.[12]

Heuer *et al.* reported that PEDOT/PSS hybrids have potential application as electrochromic devices for their apparent and efficient color change originating from the charge transfer of the polymers (Figure 1.13).[30] Laforgue *et al.* fabricated self-standing PEDOT nanofibers mat that was electrically conductive. When the PEDOT nanofibers mat was coated with thermochromic inks, controlled colour-changing could be realized by applying current to the mat. Schwendeman *et al.* produced perfluoroalkanoate-substituted PEDOT for electrochromic device applications.[38]

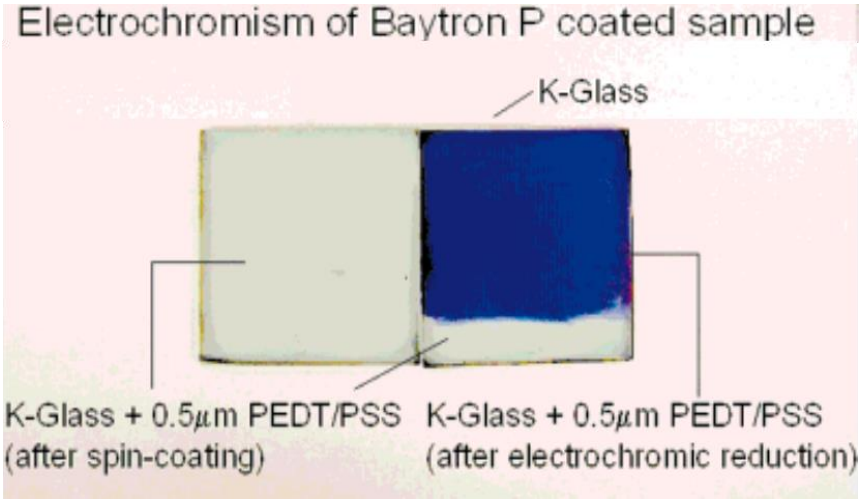

Figure 1.13 Electrochromism of PEDOT/PSS (PEDOT/PSS in the Figure).[30]

In addition, PEDOT/PSS are considered to be promising materials for optoelectronic organic devices because they enable cost-effective roll-to-roll mass production and can be applied on flexible substrates.[12,39] Yan *et al.* used PEDOT/PSS to form the full polymer filed-effect transistors with good electrical properties and mechanical flexibility.[40] Kim *et al.* applied highly conductive PEDOT/PSS films as stand-alone electrodes for organic solar cells.[41] Kim *et al.* prepared organic photovoltaic using PEDOT/PSS and graphene oxide with high power conversion efficiency.[42] Saranya *et al.* reviewed that PEDOT, PPy and PANI polymers and their hybrid with different materials all had good photovoltaic performance.[33]

Therefore, the applications of CPs have brought great progress in coating materials and have potential applications in energy harvest. Thus, further studies on the applications of conducting polymer materials will continue and definitely bring more profits in the future.

1.1.5 Synthesis of CPs

In order to synthesize CPs with different functionalities, various candidate monomers have been selected and many synthetic methods have been developed. The monomers of 3,4-ethylenedioxythiophene (EDOT), pyrrole (Py) and aniline (Ani) and their derivatives are mostly used as their corresponding polymers are of great research interest. In addition, many monomers with different functional groups are being developed for different applications. The synthesis of CPs can be realized with traditional polymerization methods. Moreover, new alternative synthetic methodologies are developed for the synthesis of CPs.

1.1.5.1 Polymerization methodologies

In general, the preparation of CPs can be realized with similar methods to the synthesis of common polymers. Traditional chemical and electrochemical methods are applied to obtain CPs from the polymerization of the monomers.[4,43-46] To the chemical method, oxidative chemicals that can work as initiators and induce the polymerization of the monomers into the polymers are used (Figure 1.14). The chemical oxidants have higher redox potential than that of monomers and oxidize the monomers into cations which undergo further polymerization into polymers. The chemical method induced polymerization has been proposed to proceed according to a step-by step growth procedure and not according to chain reaction (Figure 1.14).[47]

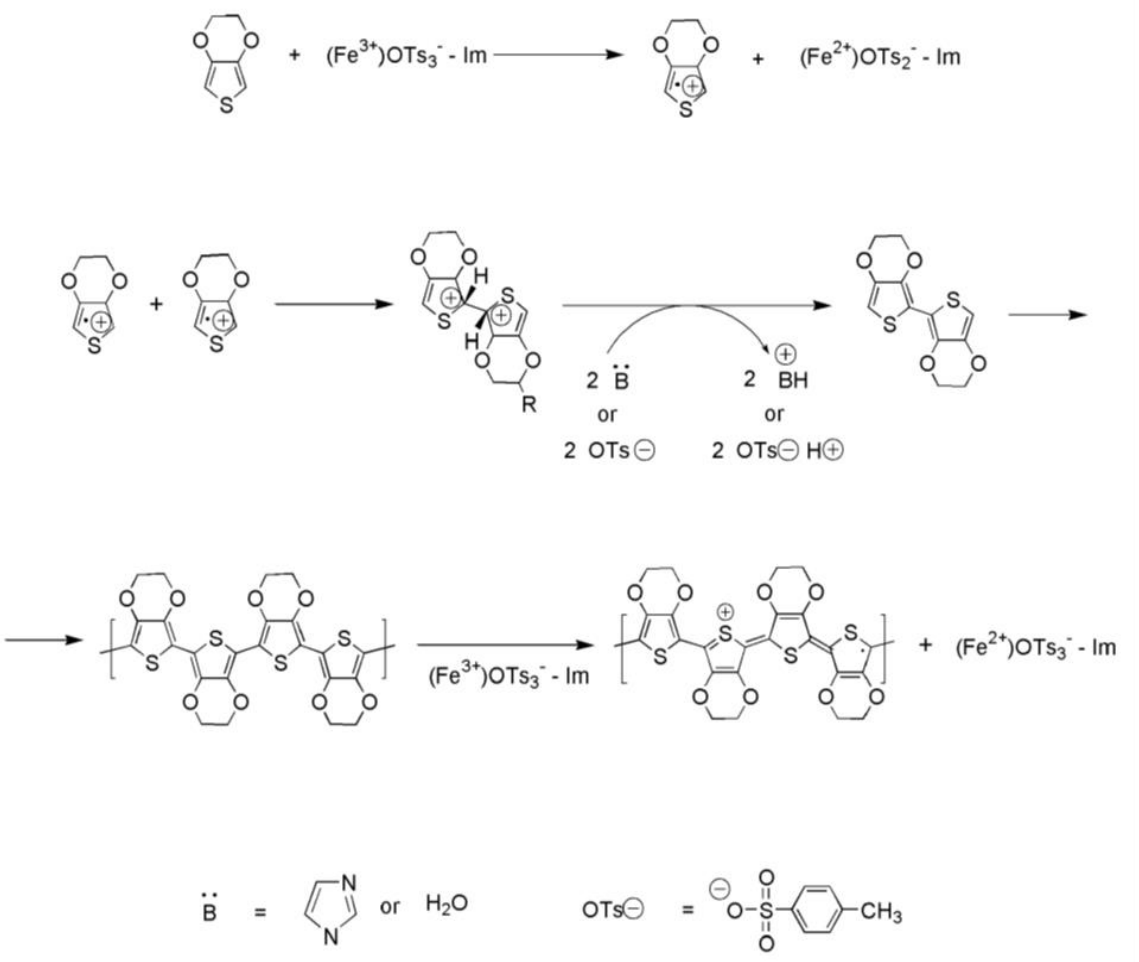

Figure 1.14 Schematic description of the oxidative step-growth chemical polymerization of EDOT into PEDOT. Note that imidazole acts to reduce the reactivity of $Fe(OTs)_3$ thereby leading to slower polymerization kinetics and lower doping levels.[47]

Depending on the redox potential of different monomers, different oxidants with various redox potentials can be applied. For example, $FeCl_3$ is often used as the initiator for monomers with low redox potential while $K_2S_2O_8$ is applied as stronger oxidant.[44,45] Meanwhile, chemical reductants such as hydrazine (N_2H_4) and lithium aluminum hydride ($LiAlH_4$) are also used as the initiator.[48,49] According to the species which initiate the polymerization of monomers, the polymerization processes can be divided into oxidation polymerization and reduction polymerization.[48-50] For the chemical method, synthesis of polymers using reduction polymerization has been reported while oxidative polymerization is more commonly used.[51]

Concerning the electrochemical method, initiation of monomers polymerization is achieved by applying an oxidation potential on the working electrode. The monomers are oxidized into radical cations which dimerize by eliminating two H atoms. Then, dimers are oxidized and react with dimer cations producing the oligomers. Elongation of oligomers through the same procedure finally results in the polymers on the surface of working electrode (Figure 1.15).[4] By adjusting the oxidation potential, the oxidation of different monomers can be successfully realized. Therefore, both traditional chemical and electrochemical methods more generally involve the oxidation of monomers to initiate the polymerization and a step-by-step mechanism is often proposed. Nevertheless, chain reaction mechanism is alternatively proposed as it is suggested that radical cations can directly react with monomers forming a dimer cation.[52]

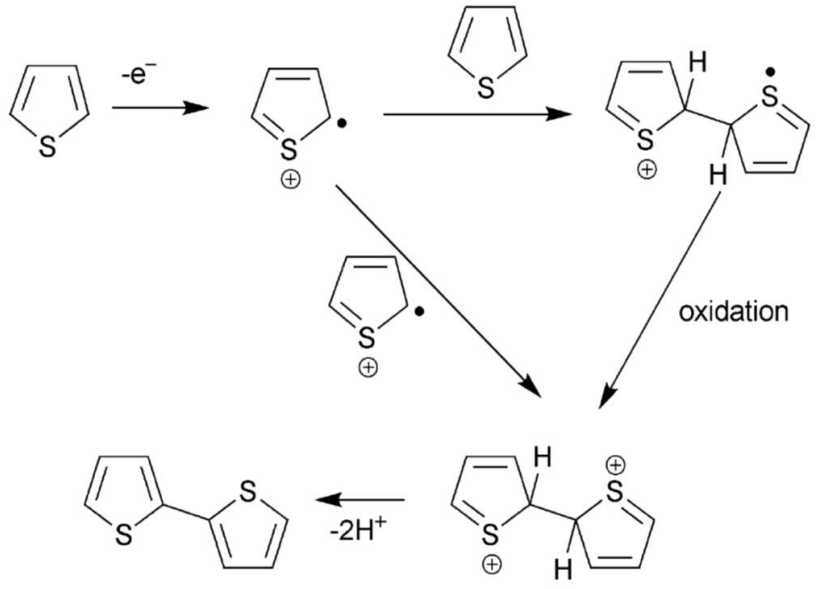

Figure 1.15 Schematic description of electrochemical polymerization process of thiophene.[4]

There is no doubt that traditional chemical and electrochemical methods are very useful methods for the synthesis of CPs. However, the application of chemical oxidants causes pollutions to the environment making the chemical method less preferred.[53] During the electrochemical polymerization, reactions are confined to the surfaces of the conductive working electrodes making the production of a large amount of CPs in a short time impossible.[4] In order to overcome the disadvantages of the traditional methods, some alternative methods have been reported such as catalytic method, enzymatic method and radiation method, etc.

Nagarajan, et al. used biocatalytic method to synthesize PEDOT polymers at milder pH with soybean peroxidase (SBP) as the catalyst.[53] Kumru, *et al.* prepared PANI using copper catalyzed air oxidation process. [54] Bouldin *et al.* synthesize PPy with fewer structural defects using enzyme catalysis.[55] Gizdavic-Nikolaidis *et al.* developed a rapid and easy route for the synthesis of PANI with microwave radiation.[56] Furthermore, radiation method coupled with chemical method was used for the synthesis of CPs. Karim *et al.* synthesized PPy using gamma (γ)-radiation induced oxidative polymerization with ammonium peroxy-disulfate (APS) as chemical oxidant.[57] Similarly, Pillalamarri *et al.* used γ-radiolysis to synthesize PANI nanofibers in the presence of APS as chemical initiator.[58] In addition, Li *et al.* applied ultrasonic irradiation in preparing PEDOT polymers.[59] Ghosh *et al.* adopted photochemical method to synthesize PDPB polymer nanostructures for photocatalysis under visible light.[35]

Radiation method based extensively on radiation chemistry with γ-irradiation or pulse radiolysis for the synthesis of CPs has recently been reported. Samy Remita's team synthesized PEDOT polymers for the first time using γ radiolysis of water.[60] Lattach *et al.* produced PEDOT polymers with different morphologies using γ irradiation by adjusting the reactive species.[61] Coletta *et al.* studied the growth mechanism of PEDOT polymers initiated by accelerated electrons.[62] Using radiation method not only avoids the application of chemical oxidant but also produces bulk quantity of CPs. Therefore, radiation method based on γ-irradiation may offer a useful method for the synthesis of CPs. This methodology is that we used in the present work in particular for the synthesis of PEDOT and PPy. It will be described in detail in the manuscript.

1.1.5.2 Effect of synthetic conditions

In order to improve the physical and chemical properties of CPs, the synthetic conditions are also needed to be controlled and improved. It is well known that the application of

templates and that the appropriate choice of pH values can affect the morphology and properties of the obtained CPs.[36]

To realize controllable synthesis of CPs with uniform morphology, templates are often used during the polymerization process.[63,64] According to the nature of the templates, they can be divided into two main categories: hard templates and soft templates. Wang *et al.* prepared uniform polyaniline nano-fibrils using hard template composed of anodic aluminum oxide (AAO).[65] Cai *et al.* synthesized PPy and poly(3-methylthiophene) (PMT) with nuclepore membranes containing linear, cylindrical pores.[66] The advantages of using hard templates are the control of morphology while the post-treatment remains complex since the hard templates are needed to be removed.[67] On the contrary, soft templates can achieve fine morphological control by selecting appropriate surfactants and are relatively easy to be removed. Han *et al.* used the surfactant sodium dodecyl sulfate (SDS) to prepare PEDOT nanofibers.[64] Ghosh *et al.* fabricated hexagonal mesophases with cetyltrimethylammonium bromide (CTAB) as the soft template for the synthesis of PEDOT and PDPB.[35,68] Therefore, synthesis of CPs with soft templates (SDS, CTAB) is more commonly applied and of great use.

Furthermore, the pH applied during the synthesis affects the properties of CPs as the pH values can affect the oxidation degree of CPs.[69] Charging of the polymer beyond a certain limit leads to the overoxidation of the polymers.[70] Debiemme-Chouvy *et al.* studied the overoxidation of PPy by hydroxyl radicals resulting in the formation of an insulating material.[71] The overoxidation potential strongly depends on the pH values.[72] At higher pH, the redox potential for the overoxidation of the CPs decreases resulting in the cleavage of the conjugation pathways.[69] Therefore, the synthesis of CPs in acidic medium maintains the electrical activity of CPs.

In addition, in order to improve the electrical conductivity of CPs, post treatment can be applied by further physical or chemical procedures. Kim *et al.* enhanced the electrical conductivity of PEDOT/PSS by chemical treatment with ethylene glycol (EG) and thermal treatment.[41] Ouyang reported that electrical conductivity of PEDOT/PSS hybrid reaches as high as indium tin oxide (ITO) through a treatment with mild and weak organic acids.[73] Yun *et al.* enhanced the electrode performance of composite films of multiwalled carbon tubes and PEDOT/PSS using HCl and methanol treatment.[74] Chou *et al.* treated PEDOT/PSS films with dimethyl sulfoxide (DMSO) for ITO-free liquid crystal display.[75]

In this work, we checked the effect of pH and influence of the presence of surfactants self-assembled into micelles on the radiation induced synthesis of CPs, especially of PEDOT.

1.2 CPs nanocomposites

Nanocomposites which are composed of organic and inorganic building blocks, can combine the properties from the parent constituents and generate new properties to meet current and future demands in functional materials.[76] The combination of conducting polymers (CPs) with inorganic nanoparticles produces composites of CPs which can not only maintain the properties of CPs and inorganic nanoparticles but also endow the CPs composites new properties.[76-78] Moreover, the incorporation of inorganic nanoparticles can compensate the defects of CPs by modifying their physical properties.[78] CPs nanocomposites have attracted great research as they may offer new materials with improved multiple functions for various applications in many fields.

1.2.1 Compositions and applications

There are a lot of reports on the nanocomposites of CPs and extensive research works have been carried out on these new materials.[76,77] In the CPs nanocomposites, CPs normally serve as the polymer matrix and inorganic nanoparticles are imbedded into the parent polymers to form the hybrid with CPs as the carriers of nanoparticles.[78] Besides, inorganic nanoparticles can be surrounded by the CPs to form core-shell structures.[79] The diversity of structures and morphologies of CPs and inorganic nanoparticles make the CPs nanocomposites more unique and useful.

As there are a large variety of both CPs and inorganic nanoparticles, appropriate combination of CPs with inorganic nanoparticles can form a large number of CPs nanocomposites and designing special CPs nanocomposites by selecting specific CPs and nanoparticles can realize specialized targets. The preparation of CPs nanocomposites can extend the application range of CPs and offer new useful materials. Some representative nanocomposites of interest and their applications are listed (Figure 1.16).[77]

Compared with CPs, CPs nanocomposites possess comparable or even improved properties enabling CPs nanocomposites to have similar potential applications including: electrical conductors, sensors, catalysts, electrochromic devices, photovoltaic devices, etc.[32,78,80,81] Semaltianos *et al.* incorporated ZnO nanoparticles into PEDOT/PSS based materials and increased the electrical conductivity of the polymer by almost two times.[82] Park *et al.* constructed silver nanoparticles decorated nanotubes of PEDOT polymers as chemical sensors of NH_3.[83] Bogdanović *et al.* synthesized nanocomposites of PANI/Au for electrocatalytic

oxygen reduction reaction (ORR).[84] Mumtaz et *al.* synthesized PEDOT/PSS materials with Ag or Au nanoparticles with improved electrochromic coloration efficiency.[85] Lu et *al.* fabricated PEDOT nanoflowers with germanium (Ge) with enhanced optoelectronic properties for promising photovoltaic applications.[86] Therefore, the synthesis of CPs nanocomposites is another practical way to improve the properties of CPs and may offer new materials with improved and interesting properties.

nanocomposite of interest		
polymer (shell)	inorganic particle (core)	significant characterization/applications
PPy and PAn	SiO_2 (1 μm, ~35 nm, 20 nm), SnO_2−Sb (10 nm), stringy SiO_2 (40−300 nm long)	nanocomposites in stable colloidal form, showing "raspberry" morphology and inorganic particle rich surface
PPy and PAn	CeO_2 (0.52 μm), CuO (1.6 μm), α-Fe_2O_3 (spherical, polyhedral and spindle shaped), NiO (3.8 μm), SiO_2 (0.46 μm)	colloidally stable nanocomposite having extremely low dc conductivity was formed without using any polymerization initiator
PPy and PAn	$BaSO_4$ (20 nm), colloidal gold with particles 7−9 nm and Al_2O_3 membrane	in situ formation of colloidal nanocomposite within the microemulsion or inside the Al_2O_3 membrane
PPy, PAn, NVC, and PPV	ZrO_2 (20−30 nm), Fe_2O_3 (25−50 nm), SiO_2, n-TiO_2 (~10 nm), Al_2O_3 (35−50 nm), MgO (2−4 μm), CB	nanocomposites in macroscopic precipitate form or with limited colloidal stability but improved thermal and electrical properties and novel transport properties
PPy and PAOABSA	MS (5−30 nm), Fe_xO_y (14 nm), Fe_2O_3 (15−50 nm), γ-Fe_2O_3 (~85 nm)	nanocomposites with significant magnetic susceptibility
PPy and PAn	BT (~1 μm), $LiMnO_2$, $LiMn_2O_4$, V_2O_5, β-MnO_2, PMo_{12}, $H_3PMo_{12}O_{40}$, CB, Fe_2O_3 (4 nm, 40 nm).	nanocomposites with important charge storage and dielectric properties; materials suitable for cathode applications
PPy, PAn, PTh, and PEDOT	Pt (~ 4 nm), PtO_2, Pt, Cu, Pd, SiO_2 (20 nm) and bimetallic couples	nanocomposites containing catalytically important metals; important for catalytic applications
PPy and PAn	SiO_2 (20 nm)	surface functionalized nanocomposites; important for immunodiagnostic assays
PPy	SiO_2, PB, MnO_2, Ta_2O_5, TiO_2	electrochemically synthesized composite films having improved charge storage properties
PPy and PAn	WO_3	nanocomposite films with important ECD application and optical activity

Figure 1.16 Nanocomposites of conducting polymers and specific applications.[77]

1.2.2 CPs/noble metal nanocomposites

Among various CPs nanocomposites, the composites composed by CPs and noble metal nanoparticles have been of great research interest.[87,88] It is well known that silver (Ag) as well as gold (Au) are noble metals and their nanoparticles are of great importance. The combination of Ag or Au nanoparticles with CPs have been widely used for analysis, water purification, diagnostics, catalysis, etc.[89-91] As Ag is superior in electrical and thermal conductivities and has the ability to enhance electrical and optical properties of the polymer composites, the synthesis and potential applications of CPs/Ag nanocomposites have been widely studied.

As an important and characteristic kind of CPs nanocomposites, CPs/Ag nanocomposites have similar applications as other CPs nanocomposites including conductors, sensors, catalysts, solar cell, etc.[83,92-94] Škodová *et al.* prepared PPy/Ag nanocomposites possessing good electrical conductivity.[93] Radhakrishnan *et al.* fabricated nanocomposite films of PPy/PEDOT/Ag for label-free electrochemical DNA sensing. Balamurugan *et al.* synthesized PEDOT/Ag nanocomposites for catalytic reduction of 4-nitrophenol.[92] Ghazy *et al.* incorporated Ag nanoparticles into PEDOT/PSS for the application in organic solar cells.[95] Therefore, the synthesis and applications of CPs/Ag nanocomposites are meaningful and of great importance.

1.2.3 Synthesis of CPs nanocomposites

Similar to the synthesis of CPs, the preparation of CPs nanocomposites can generally be achieved by traditional chemical and electrochemical methods.[77,96] Moreover, synthesis of CPs nanocomposites with radiation method has been reported.[97]

As CPs nanocomposites are composed by both electrical conducting polymers and inorganic nanoparticles, the synthesis of CPs nanocomposites includes both the synthesis of CPs by polymerization and production of inorganic nanoparticles by reduction of metal ions. The formation of CPs nanocomposites is illustrated (Figure 1.17).[77] To prepare CPs nanocomposites, different synthetic procedures can be used to synthesize CPs and inorganic nanoparticles. According to the synthetic procedures, the synthesis of CPs nanocomposites can be realized in two steps or one step.[92,93]

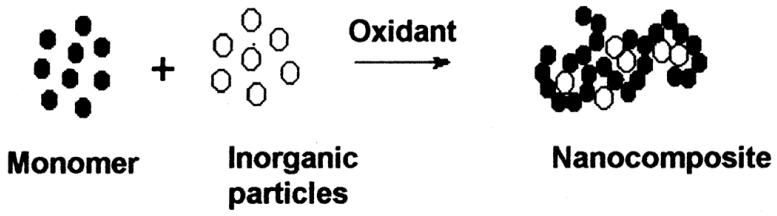

Figure 1.17 Formation of nanocomposite from the constituents.[77]

When the CPs nanocomposites are prepared in two steps (two-step method), the polymerization of monomers and synthesis of inorganic nanoparticles are carried out in different times. The synthesis of CPs can be done first and then the reduction of metal ions

onto the surfaces of polymers resulting in CPs blended with nanoparticles. In this process, the preformed CPs work as the template. Behniafar *et al.* prepared PEDOT/Ag nanocomposites using chemical oxidation of EDOT monomers and chemical reduction synthesis of Ag nanoparticles.[98]

On the contrary, when nanoparticles are formed first, then the polymerization of monomers will occur around the nanoparticles forming the core/shell nanostructures which has a polymeric shell.[99] Kim *et al.* constructed nanocomposites of PEDOT/PSS/Au with core−shell structure where Au nanoparticles were located in the center and coated by PEDOT/PSS. Therefore, the synthetic procedures can affect the final morphology of CPs nanocomposites.

To simplify the synthetic procedures, the polymerization of monomers and reduction of metal ions can be realized in one step (one-pot method).[100] Using the one-pot method, the preparation of CPs and nanoparticles can be realized at the same time where the inorganic salt may work as the oxidant initiating the polymerization of monomers.[101] Fujii *et al.* prepared nanocomposite microspheres of Fe/PPy/Pd in one step.[100] Singh *et al.* used one-pot method to synthesize free standing and flexible PPy/Ag nanocomposites.[102]

Radiation-induced chemical oxidative polymerization method has been applied for the synthesis of CPs nanocomposites.[95,97,103] Karim *et al.* prepared core-shell structured silver–polyaniline nanocomposites by γ radiolysis method with APS as chemical oxidant.[97] Pillalamarri *et al.* fabricated polyaniline nanofibers with APS as chemical oxidant and decorated them with noble-metal (Ag or Au) nanoparticles using γ radiolysis.[104] Ali *et al.* synthesized copper/poly(vinyl alcohol) nanocomposites by radiation-induced synthesis.[103] As is mentioned before, synthesis of CPs using radiation method has been developed and applied. Therefore, synthesis of CPs and CPs nanocomposites with radiation method is worth studying and may offer a new synthetic approach. In this work, we consider more specifically the synthesis of PEDOT/Ag nanocomposites by two-step or one-pot methods by using exclusively radiation chemistry.

1.3 Research object

The aim of my research is mainly focused on synthesizing CPs as well as CPs nanocomposites by using γ-irradiation and studying their potential applications. To make the study easy and for comparison purpose, we selected two kinds of CPs, PEDOT and PPy as the research targets. In addition, the inorganic nanoparticles applied here are Ag nanoparticles. My research work will be carried out as follows:

In chapter 2, all the chemical agents, synthetic methods and characterization techniques applied for the synthesis of CPs and CPs nanocomposites are briefly introduced and explained;

In chapter 3, an original radiolytic methodology developed by Samy Remita's team (that I was in as a member) for the synthesis of CPs is reviewed. The state of art of synthesis of CPs with this new alternative method is summarized;

In chapter 4, pyrrole is used as alternative monomer instead of EDOT and the versatility of radiolytical methodology is checked by synthesizing another CPs, namely PPy;

In chapter 5, synthesis of PEDOT induced by gamma irradiation is selected as the research target and effects of synthetic conditions on the polymerization of EDOT are investigated. The influence of soft template, pH and ionic strength on the polymerization of EDOT and on the properties of PEDOT are studied;

In chapter 6, synthesis of PEDOT by a simple γ-rays-based reduction–polymerization route instead of oxidation route under nitrogen (N_2) atmosphere at room temperature is described for the first time;

In chapter 7, preparation of PEDOT/Ag nanocomposites starting from EDOT monomers and Ag^+ silver ions dissolved in water with simple γ-rays-based radiolytic methodologies is described in details.

Finally, the main achievements realized in my work are summarized to draw general conclusions and synthesis of CPs with radiolytic methodologies as well as the potential applications of radiosynthesized CPs are outlooked in perspectives.

References

[1] Shirakawa, H., The Discovery of Polyacetylene Film: The Dawning of an Era of Conducting Polymers (Nobel Lecture). *Angew. Chem. Int. Ed.* **2001,** *40* (14), 2574-2580.

[2] MacDiarmid, A. G., "Synthetic Metals": A Novel Role for Organic Polymers (Nobel Lecture). *Angew. Chem. Int. Ed.* **2001,** *40* (14), 2581-2590.

[3] Heeger, A. J., Semiconducting and metallic polymers: The fouth gererнation of polymeric materials (nobel Lecture). *Angew. Chem. Int. Ed.* **2001,** *40*, 2591-2611.

[4] Li, C.; Bai, H.; Shi, G., Conducting polymer nanomaterials: electrosynthesis and applications. *Chemical Society reviews* **2009,** *38* (8), 2397-409.

[5] Balint, R.; Cassidy, N. J.; Cartmell, S. H., Conductive polymers: towards a smart biomaterial for tissue engineering. *Acta biomaterialia* **2014,** *10* (6), 2341-2353.

[6] Zhou, Q.; Shi, G., Conducting Polymer-Based Catalysts. *J. Am. Chem. Soc.* **2016,** *138* (9), 2868-2876.

[7] Guo, X.; Baumgarten, M.; Müllen, K., Designing π-conjugated polymers for organic electronics. *Prog. Polym. Sci.* **2013,** *38* (12), 1832-1908.

[8] Harun, M. H.; Saion, E.; Kassim, A.; Yahya, N.; Mahmud, E., Conjugated Conducting Polymers: A Brief Overview. *JASA* **2007,** *2*, 63-68.

[9] Shirakawa, H.; Louis, E. J.; MacDiarmid, A. G.; Chiang, C. K.; Heeger, A. J., Synthesis of electrically conducting organic polymers : halogen derivatives of polyacetylene,(CH)x. *J. Chem. Soc., Chem. Commun.* **1977**, 578-580.

[10] Heeger, A. J., Semiconducting polymers: the Third Generation. *Chemical Society reviews* **2010,** *39* (7), 2354-2371.

[11] Gedde, U. W., A Brief Introduction to Polymer Science. *Polymer Physics* **1999**, 15.

[12] Groenendaal, L. B.; Jonas, F.; Freitag, D.; Pielartzik, H.; Reynolds, J. R., Poly(3,4-ethylenedioxythiophene) and Its Derivatives: Past, Present, and Future. *Adv. Mater.* **2000,** *12* (7), 481-494.

[13] Roncali, J.; Blanchard, P.; Frere, P., 3,4-Ethylenedioxythiophene (EDOT) as a versatile building block for advanced functional [small pi]-conjugated systems. *Journal of Materials Chemistry* **2005,** *15* (16), 1589-1610.

[14] Kirchmeyer, S.; Reuter, K., Scientific importance, properties and growing applications of poly(3,4-ethylenedioxythiophene). *Journal of Materials Chemistry* **2005,** *15* (21), 2077.

[15] De Jesus, M. C.; Fu, Y.; Weiss, R. A., Conductive polymer blends prepared by in situ polymerization of pyrrole: A review. *Polym Eng Sci* **1997,** *37* (12), 1936-1943.

[16] Syed, S. A.; Dinesan, M. K., Review: Polyaniline—A novel polymeric material. *Talanta* **1991,** *38* (8), 815-837.

[17] Natta, G.; Mazzanti, G.; Corradini, P., Stereospecific polymerization of acetylene. *Atti Accad. Naz. Lincei, Rend. Cl. Sci. Fis., Mat. Nat. 1958, 25, 3-12.* **1958,** *25*, 3-12.

[18] Wan, M. X., Conducting Polymers with Micro or Nanometer Structure. *Tsinghua University Press, Beijing and Springer-Verlag GmbH Berlin Heidelberg* **2008**, 1.

[19] Salzner, U.; Lagowski, J. B.; Pickup, P. G.; Poirier, R. A., Design of low band gap polymers employing density functional theory—hybrid functionals ameliorate band gap problem. *Journal of Computational Chemistry* **1997,** *18* (15), 1943-1953.

[20] Millman, J.; Halkias, C. C., Integrated Electronics:along and digital circuits and systems. *Tata McGraw-Hill Education* **2001**, 16.

[21] Guilbert, A. A. Y.; Schmidt, M.; Bruno, A.; Yao, J.; King, S.; Tuladhar, S. M.; Kirchartz, T.; Alonso, M. I.; Goñi, A. R.; Stingelin, N.; Haque, S. A.; Campoy-Quiles, M.; Nelson, J., Spectroscopic Evaluation of Mixing and Crystallinity of Fullerenes in Bulk Heterojunctions. *Advanced Functional Materials* **2014,** *24* (44), 6972-6980.

[22] Furukawa, Y., Electronic Absorption and Vibrational Spectroscopies of Conjugated Conducting Polymers. *The Journal of Physical Chemistry* **1996,** *100* (39), 15644-15653.

[23] Millman, J.; Halkias, C. C., Integrated Electronics:along and digital circuits and systems. *Tata McGraw-Hill Education* **2001**, 17.

[24] Bredas, J. L.; Street, G. B., Polarons, bipolarons, and solitons in conducting polymers. *Accounts of Chemical Research* **1985,** *18* (10), 309-315.

[25] Wan, M. X., Conducting Polymers with Micro or Nanometer Structure. *Tsinghua University Press, Beijing and Springer-Verlag GmbH Berlin Heidelberg* **2008**, 5.

[26] Heeger, A. J.; Kivelson, S.; Schrieffer, J. R.; Su, W. P., Solitons in conducting polymers. *Reviews of Modern Physics* **1988,** *60* (3), 781-850.

[27] Walton, D. J., Electrically Conducting Polymers. *MATERIALS & DESIGN* **1990,** *11* (30), 142-151.

[28] Kiess, H., Conjugated Conducting Polymers. *Springer-Verlag, solid-state sciences* **1992,** *102*, 147.

[29] Schultze, J. W.; Karabulut, H., Application potential of conducting polymers. *Electrochimica Acta* **2005,** *50* (7–8), 1739-1745.

[30] Heuer, H. W.; Wehrmann, R.; Kirchmeyer, S., Electrochromic window based on conducting poly(3,4-ethylenedioxythiophene)-poly(styrene sulfonate). *Adv. Funct. Mater.* **2002,** *12* (2), 89-94.

[31] Laforgue, A., Electrically controlled colour-changing textiles using the resistive heating properties of PEDOT nanofibers. *J. Mater. Chem.* **2010,** *20* (38), 8233-8235.

[32] Ramanavičius, A.; Ramanavičienė, A.; Malinauskas, A., Electrochemical sensors based on conducting polymer—polypyrrole. *Electrochimica Acta* **2006,** *51* (27), 6025-6037.

[33] Saranya, K.; Rameez, M.; Subramania, A., Developments in conducting polymer based counter electrodes for dye-sensitized solar cells – An overview. *European Polymer Journal* **2015,** *66*, 207-227.

[34] Ameen, S.; Akhtar, M. S.; Seo, H.; Shin, H. S., Distinctive polypyrrole nanobelts as prospective electrode for the direct detection of aliphatic alcohols: Electrocatalytic properties. *Applied Catalysis B: Environmental* **2014,** *144*, 665-673.

[35] Ghosh, S.; Kouamé, N. A.; Ramos, L.; Remita, S.; Dazzi, A.; Deniset-Besseau, A.; Beaunier, P.; Goubard, F.; Aubert, P. H.; Remita, H., Conducting polymer nanostructures for photocatalysis under visible light. *Nat Mater* **2015,** *14* (5), 505-511.

[36] Huang, J. X.; Virji, S.; Weiller, B. H.; Kaner, R. B., Polyaniline Nanofibers: Facile Synthesis and Chemical Sensors. *J. AM. CHEM. SOC.* **2003,** *125*, 314-315.

[37] Crispin, X.; Jakobsson, F. L. E.; Crispin, A.; Grim, P. C. M.; Andersson, P.; Volodin, A.; van Haesendonck, C.; Van der Auweraer, M.; Salaneck, W. R.; Berggren, M., The Origin of the High Conductivity of Poly(3,4-ethylenedioxythiophene)−Poly(styrenesulfonate) (PEDOT−PSS) Plastic Electrodes. *Chem. Mater.* **2006,** *18* (18), 4354-4360.

[38] Schwendeman, I.; Gaupp, C. L.; Hancock, J. M.; Groenendaal, L.; Reynolds, J. R., Perfluoroalkanoate-Substituted PEDOT for Electrochromic Device Applications. *Advanced Functional Materials* **2003,** *13* (7), 541-547.

[39] Xia, Y. J.; Sun, K.; Ouyang, J. Y., Solution-Processed Metallic Conducting Polymer Films as Transparent Electrode of Optoelectronic Devices. *Advanced Materials* **2012,** *24* (18), 2436-2440.

[40] Yan, Y.; Huang, L. **B.**; Zhou, Y.; Han, S. T.; Zhou, L.; Zhuang, J. Q.; Xu, Z. X.; Roy, V. A. L., Self-aligned, full solution process polymer field-effect transistor on flexible substrates. *Scientific Reports* **2015,** *5*, 15770.

[41] Kim, Y. H.; Sachse, C.; Machala, M. L.; May, C.; Müller-Meskamp, L.; Leo, K., Highly Conductive PEDOT:PSS Electrode with Optimized Solvent and Thermal Post-Treatment for ITO-Free Organic Solar Cells. *Advanced Functional Materials* **2011,** *21* (6), 1076-1081.

[42] Kim, H. P.; Lee, S. J.; Mohd Yusoff, A. R.; Jang, J., A high performance organic photovoltaic utilizing PEDOT:PSS and graphene oxide. *RSC Advances* **2016,** *6* (34), 28599-28606.

[43] Baik, W.; Luan, W. Q.; Zhao, R. H.; Koo, S.; Kim, K. S., Synthesis of highly conductive poly(3,4-ethylenedioxythiophene) fiber by simple chemical polymerization. *Synt. Met.* **2009,** *159* (13), 1244-1246.

[44] Paradee, N.; Sirivat, A., Synthesis of poly(3,4-ethylenedioxythiophene) nanoparticles via chemical oxidation polymerization. *Polym. Int.* **2014,** *63* (1), 106-113.

[45] Zhang, X. Y.; Manohar, S. K., Bulk synthesis of polypyrrole nanofibers by a seeding approach. *J. AM. CHEM. SOC.* **2004,** *126*, 12714-12715.

[46] Gospodinova, N.; Terlemezyan, L., Conducting polymers prepared by oxidative polymerization: polyaniline. *Progress in Polymer Science* **1998,** *23* (8), 1443-1484.

[47] Ha, Y. H.; Nikolov, N.; Pollack, S. K.; Mastrangelo, J.; Martin, B. D.; Shashidhar, R., Towards a Transparent, Highly Conductive Poly(3,4-ethylenedioxythiophene). *Advanced Functional Materials* **2004,** *14* (6), 615-622.

[48] Kitada, K.; Ozaki, S., Reductive Polymerization of Halothiophene. *Polym Journal* **1995,** *27* (12), 1161-1166.

[49] Snyder, H. R.; Putnam, R. E., Reductive Polymerization of α,β-Unsaturated Amides. I. N,N-Diethylcrotonamide. *J. Am. Chem. Soc* **1954,** *76* (1), 33-35.

[50] Abu-Thabit, N. Y., Chemical Oxidative Polymerization of Polyaniline: A Practical Approach for Preparation of Smart Conductive Textiles. *Journal of Chemical Education* **2016,** *93* (9), 1606-1611.

[51] Inzelt, G., Conducting Polymers A New Era in Electrochemistry. *Springer Berlin Heidelberg* **2012**, 14.

[52] Sadki, S.; Schottland, P.; Brodie, N.; Sabouraud, G., The mechanisms of pyrrole electropolymerization. *Chemical Society reviews* **2000,** *29* (5), 283-293.

[53] Nagarajan, R.; Kumar, J.; Bruno, F. F.; Samuelson, L. A.; Nagarajan, R., Biocatalytically synthesized poly(3,4-ethylenedioxythiophene). *Macromolecules* **2008,** *41*, 3049-3052.

[54] Kumru, B.; Bicak, N., Polymerization of Aniline in Microemulsion by Catalytic Air Oxidation. *Macromolecular Symposia* **2015,** *352* (1), 42-45.

[55] Bouldin, R.; Ravichandran, S.; Kokil, A.; Garhwal, R.; Nagarajan, S.; Kumar, J.; Bruno, F. F.; Samuelson, L. A.; Nagarajan, R., Synthesis of polypyrrole with fewer structural defects using enzyme catalysis. *Synthetic Metals* **2011,** *161* (15–16), 1611-1617.

[56] Gizdavic-Nikolaidis, M. R.; Stanisavljev, D. R.; Easteal, A. J.; Zujovic, Z. D., A rapid and facile synthesis of nanofibrillar polyaniline using microwave radiation. *Macromolecular rapid communications* **2010,** *31* (7), 657-661.

[57] Karim, M. R.; Lee, C. J.; Lee, M. S., Synthesis of conducting polypyrrole by radiolysis polymerization method. *Polymers for Advanced Technologies* **2007,** *18* (11), 916-920.

[58] Pillalamarri, S. K.; Blum, F. D.; Tokuhiro, A. T.; Story, J. G.; Bertino, M. F., Radiolytic Synthesis of Polyaniline Nanofibers: A New Templateless Pathway. *Chemistry of Materials* **2005,** *17* (2), 227-229.

[59] Li, W. K.; Chen, J.; Zhao, J. J.; Zhang, J. R.; Zhu, J. J., Application of ultrasonic irradiation in preparing conducting polymer as active materials for supercapacitor. *Materials Letters* **2005,** *59* (7), 800-803.

[60] Lattach, Y.; Deniset-Besseau, A.; Guigner, J. M.; Remita, S., Radiation chemistry as an alternative way for the synthesis of PEDOT conducting Polymers under "soft" Conditions. *Radiat. Phys. Chem.* **2013,** *82*, 44-53.

[61] Lattach, Y.; Coletta, C.; Ghosh, S.; Remita, S., Radiation-Induced Synthesis of Nanostructured Conjugated Polymers in Aqueous Solution: Fundamental Effect of Oxidizing Species. *Chemphyschem* **2014,** *15* (1), 208-218.

[62] Coletta, C.; Cui, Z.; Archirel, P.; Pernot, P.; Marignier, J. L.; Remita, S., Electron-induced growth mechanism of conducting polymers: a coupled experimental and computational investigation. *J. Phys. Chem. B* **2015,** *119* (16), 5282-5298.

[63] Yang, Y.; Jiang, Y.; Xu, J.; Yu, J., Conducting polymeric nanoparticles synthesized in reverse micelles and their gas sensitivity based on quartz crystal microbalance. *Polymer* **2007,** *48* (15), 4459-4465.

[64] Han, M. G.; Foulger, S. H., Facile synthesis of poly(3,4-ethylenedioxythiophene) nanofibers from an aqueous surfactant solution. *Small* **2006,** *2* (10), 1164-1169.

[65] Wang, Z.; Chen, M.; Li, H. L., Preparation and characterization of uniform polyaniline nano-fibrils using the anodic aluminum oxide template. *Materials Science and Engineering: A* **2002,** *328* (1–2), 33-38.

[66] Cai, Z. H.; Martin, C. R., Electronically conductive polymer fibers with mesoscopic diameters show enhanced electronic conductivities. *J. Am. Chem. Soc.* **1989,** *111* (11), 4138-4139.

[67] Xiao, R.; Cho, S.; Liu, R.; Lee, S. B., Controlled Electrochemical Synthesis of Conductive Polymer Nanotube Structures. *J. AM. CHEM. SOC.* **2007,** *129*, 4483-4489.

[68] Ghosh, S.; Remita, H.; Ramos, L.; Dazzi, A.; Deniset-Besseau, A.; Beaunier, P.; Goubard, F.; Aubert, P. H.; Brisset, F.; Remita, S., PEDOT nanostructures synthesized in hexagonal mesophases. *New Journal of Chemistry* **2014,** *38* (3), 1106-1115.

[69] Tehrani, P.; Kanciurzewska, A.; Crispin, X.; Robinson, N.; Fahlman, M.; Berggren, M., The effect of pH on the electrochemical over-oxidation in PEDOT:PSS films. *Solid State Ion.* **2007,** *177* (39-40), 3521-3527.

[70] Krische, B.; Zagorska, M., Overoxidation in conducting polymers. *Synthetic Metals* **1989,** *28* (1), 257-262.

[71] Debiemme-Chouvy, C.; Tran, T. T. t. M., An insight into the overoxidation of polypyrrole materials. *Electrochemistry Communications* **2008,** *10* (6), 947-950.

[72] Lewis, T. W.; Wallace, G. G.; Kim, C. Y.; Kim, D. Y., Studies of the overoxidation of polypyrrole. *Synthetic Metals* **1997,** *84* (1), 403-404.

[73] Ouyang, J. Y., Solution-processed PEDOT:PSS films with conductivities as indium tin oxide through a treatment with mild and weak organic acids. *ACS applied materials & interfaces* **2013,** *5* (24), 13082-13088.

[74] Yun, D. J.; Jeong, Y. J.; Ra, H.; Kim, J. M.; Park, J. H.; Park, S.; An, T. K.; Seol, M.; Park, C. E.; Jang, J.; Chung, D. S., Effective Way To Enhance the Electrode Performance of Multiwall Carbon Nanotube and Poly(3,4-ethylenedioxythiophene): Poly(styrene sulfonate) Composite Using HCl–Methanol Treatment. *J. Phys. Chem. C* **2016,** *120* (20), 10919-10926.

[75] Chou, T. R.; Chen, S. H.; Chiang, Y. T.; Lin, Y. T.; Chao, C. Y., Highly conductive PEDOT:PSS films by post-treatment with dimethyl sulfoxide for ITO-free liquid crystal display. *Journal of Materials Chemistry C* **2015,** *3* (15), 3760-3766.

[76] Kao, J.; Thorkelsson, K.; Bai, P.; Rancatore, B. J.; Xu, T., Toward functional nanocomposites: taking the best of nanoparticles, polymers, and small molecules. *Chemical Society reviews* **2013,** *42* (7), 2654-2678.

[77] Gangopadhyay, R.; De, A., Conducting Polymer Nanocomposites: A Brief Overview. *Chemistry of Materials* **2000,** *12* (3), 608-622.

[78] Zhan, C.; Yu, G.; Lu, Y.; Wang, L.; Wujcik, E.; Wei, S., Conductive polymer nanocomposites: a critical review of modern advanced devices. *Journal of Materials Chemistry C* **2017,** *5* (7), 1569-1585.

[79] Deng, J.; Ding, X.; Zhang, W.; Peng, Y.; Wang, J.; Long, X.; Li, P.; Chan, A., Magnetic and conducting Fe3O4–cross-linked polyaniline nanoparticles with core–shell structure. *Polymer* **2002,** *43* (8), 2179-2184.

[80] Lu, X.; Zhang, W.; Wang, C.; Wen, T.; Wei, Y., One-dimensional conducting polymer nanocomposites: Synthesis, properties and applications. *Progress in Polymer Science* **2011,** *36* (5), 671-712.

[81] Nguyen, T. P., Polymer-based nanocomposites for organic optoelectronic devices. A review. *Surface and Coatings Technology* **2011,** *206* (4), 742-752.

[82] Semaltianos, N. G.; Logothetidis, S.; Hastas, N.; Perrie, W.; Romani, S.; Potter, R. J.; Dearden, G.; Watkins, K. G.; French, P.; Sharp, M., Modification of the electrical properties of PEDOT:PSS by the incorporation of ZnO nanoparticles synthesized by laser ablation. *Chemical Physics Letters* **2010,** *484* (4–6), 283-289.

[83] Park, E.; Kwon, O. S.; Park, S. J.; Lee, J. S.; You, S.; Jang, J., One-pot synthesis of silver nanoparticles decorated poly(3,4-ethylenedioxythiophene) nanotubes for chemical sensor application. *J. Mater. Chem.* **2012,** *22*, 1521–1526.

[84] Bogdanović, U.; Pašti, I.; Ćirić-Marjanović, G.; Mitrić, M.; Ahrenkiel, S. P.; Vodnik, V., Interfacial Synthesis of Gold–Polyaniline Nanocomposite and Its Electrocatalytic Application. *ACS applied materials & interfaces* **2015,** *7* (51), 28393-28403.

[85] Mumtaz, M.; Ouvrard, B.; Maillaud, L.; Labrugere, C.; Cloutet, E.; Cramail, H.; Delville, M. H., Hybrid PEDOT–Metal Nanoparticles – New Substitutes for PEDOT:PSS in Electrochromic Layers – Towards Improved Performance. *European Journal of Inorganic Chemistry* **2012,** *2012* (32), 5360-5370.

[86] Lu, P.; Yang, P. H., Poly(3,4-ethylenedioxythiophene)/germanium organic-inorganic hybrid thin films: substrate-induced synthesis, enhanced photoelectrochemical and photocatalytic properties. *RSC Advances* **2016,** *6* (1), 601-606.

[87] Folarin, O. M.; Sadiku, E. R.; Maity, A., Polymer-noble metal nanocomposites: Review. *International Journal of the Physical Sciences* **2011,** *6* (21), 4869-4882.

[88] Xu, P.; Han, X.; Zhang, B.; Du, Y.; Wang, H., Multifunctional polymer-metal nanocomposites via direct chemical reduction by conjugated polymers. *Chemical Society reviews* **2014,** *43* (5), 1349-1360.

[89] Pradeep, T.; Anshup, Noble metal nanoparticles for water purification: A critical review. *Thin Solid Films* **2009,** *517* (24), 6441-6478.

[90] Larguinho, M.; Baptista, P. V., Gold and silver nanoparticles for clinical diagnostics — From genomics to proteomics. *Journal of Proteomics* **2012,** *75* (10), 2811-2823.

[91] Sau, T. K.; Rogach, A. L.; F., J.; Klar, T. A.; Feldmann, J., Properties and Applications of Colloidal Nonspherical Noble Metal Nanoparticles. *Advanced Materials* **2010,** *22* (16), 1805-1825.

[92] Balamurugan, A.; Ho, K.-C.; Chen, S.-M., One-pot synthesis of highly stable silver nanoparticles-conducting polymer nanocomposite and its catalytic application. *Synthetic Metals* **2009,** *159* (23-24), 2544-2549.

[93] Škodová, J.; Kopecký, D.; Vrňata, M.; Varga, M.; Prokeš, J.; Cieslar, M.; Bober, P.; Stejskal, J., Polypyrrole–silver composites prepared by the reduction of silver ions with polypyrrole nanotubes. *Polym. Chem.* **2013,** *4*, 3610-3616.

[94] Zhang, X. Y.; Lee, J. S.; Lee, G. S.; Cha, D. K.; Kim, M. J.; Yang, D. J.; Manohar, S. K., Chemical Synthesis of PEDOT Nanotubes. *Macromolecules* **2006,** *39*, 470-472.

[95] Ghazy, O. A.; Ibrahim, M. M.; I., A. E. F.; Hosni, H. M.; Shehata, E. M.; Deghiedy, N. M.; Balboul, M. R., PEDOT:PSS incorporated silver nanoparticles prepared by gamma radiation for the application in organic solar cells. *Journal of Radiation Research and Applied Sciences* **2015,** *8* (2), 166-172.

[96] Parvin, M.; Pirnia, M.; Arjomandi, J., Electrochemical synthesis, in situ spectroelectrochemistry of conducting indole-titanium dioxide and zinc oxide polymer nanocomposites for rechargeable batteries. *Electrochimica Acta* **2015,** *185*, 276-287.

[97] Karim, M. R.; Lim, K. T.; Lee, C. J.; Bhuiyan, M. T.; Kim, H. J.; Park, L.; Lee, M. S., Synthesis of core-shell silver–polyaniline nanocomposites by gamma radiolysis method. *Journal of Polymer Science Part A: Polymer Chemistry* **2007,** *45* (24), 5741-5747.

[98] Behniafar, H.; Yousefzadeh, D., Chemical synthesis of PEDOT/Ag nanocomposites via emulsion technique in silver colloid. *Designed Monomers and Polymers* **2015,** *18* (1), 6-11.

[99] Mo, Z. L.; Zuo, D. D.; Chen, H.; Sun, Y. X.; Zhang, P., Synthesis of graphite nanosheets/AgCl/polypyrrole composites via two-step inverse microemulsion method. *Eur. Polym. J.* **2007,** *43* (2), 300-306.

[100] Fujii, S.; Hamasaki, H.; Abe, H.; Yamanaka, S.; Ohtaka, A.; Nakamura, E.; Nakamura, Y., One-step synthesis of magnetic iron-conducting polymer-palladium ternary nanocomposite microspheres with applications as a recyclable catalyst. *Journal of Materials Chemistry A* **2013,** *1* (14), 4427-4430.

[101] Fujii, S.; Aichi, A.; Akamatsu, K.; Nawafune, H.; Nakamura, Y., One-step synthesis of polypyrrole-coated silver nanocomposite particles and their application as a coloured particulate emulsifier. *J.Mater.Chem.* **2007,** *17* (36), 3777-3779.

[102] Singh, A.; Salmi, Z.; Jha, P.; Joshi, N.; Kumar, A.; Decorse, P.; Lecoq, H.; Lau-Truong, S.; Aswal, D. K.; Gupta, S. K.; Chehimi, M. M., One step synthesis of highly ordered free standing flexible polypyrrole-silver nanocomposite films at air-water interface by photopolymerization. *RSC Advances* **2013,** *3* (32), 13329-13336.

[103] Ali, Z. I.; Ghazy, O. A.; Meligi, G.; Saleh, H. H.; Bekhit, M., Radiation-Induced Synthesis of Copper/Poly(vinyl alcohol) Nanocomposites and Their Catalytic Activity. *Advances in Polymer Technology* **2016**, 21675.

[104] Pillalamarri, S. K.; Blum, F. D.; Tokuhiro, A. T.; Bertino, M. F., One-Pot Synthesis of Polyaniline-Metal Nanocomposites. *Chem. Mater.* **2005,** *17*, 5941-5944.

Chapter 2: Materials, synthetic methods and characterizations

In this chapter, all the chemical agents, synthetic methods and characterizations applied in this work for the synthesis of conducting polymers (CPs) and CPs nanocomposites are briefly introduced and explained. First, all the chemicals applied including monomers, oxidants and target CPs and CPs nanocomposites are listed. Then, the radiation method used for the preparation of CPs and CPs nanocomposites is described and explained in detail. Finally, all analytical methods and specific characterizations performed to CPs and CPs nanocomposites are summarized.

2.1 Chemicals

All the chemicals applied in the experiments and their basic information are listed (Table 2.1). All the monomers are commercially available and used directly without further treatment.

Table 2.1 List of all the applied chemicals.

Chemicals	**Molecular formula**	**Molecular weight**	**Application**	**Purity**	**Producer**
3,4-ethylenedioxythiophene	$C_6H_6O_2S$	142.18	monomer	≥ 98%	Sigma-Aldrich
pyrrole	C_4H_5N	67.09	monomer	≥ 98%	Sigma-Aldrich
potassium persulfate	$K_2S_2O_8$	270.32	oxidant	reagent grade	Touzart & Magnon
nitrogen	N_2	28.00	atmosphere	99.99%	Air Liquid Co.
nitrous oxide	N_2O	44.01	atmosphere scavenger	99.99%	Air Liquid Co.

oxygen	O_2	32.00	atmosphere scavenger	99.99%	Air Liquid Co.
sodium azide	NaN_3	65.01	scavenger	≥ 99.5%,	Sigma-Aldrich
isopropanol	C_3H_8O	60.09	scavenger	≥ 95%	Sigma-Aldrich
tert-butanol	$C_4H_{10}O$	74.12	scavenger	≥ 95%	Sigma-Aldrich
hydrochloric acid	HCl	36.46	acid scavenger	ACS grade	VWR International S.A.S.
perchloric acid	$HClO_4$	100,46	acid scavenger	ACS grade	Sigma-Aldrich
sodium perchlorate	$NaClO_4$	122.44	inorganic salt	98%,	Sigma-Aldrich
silver perchlorate	$AgClO_4$	207.32	inorganic salt	99%	Sigma-Aldrich
sodium dodecyl sulfate	$C_{12}H_{25}NaO_4S$	288,37	surfactant	≥ 98.5%,	Sigma-Aldrich
poly(4-styrenesulfonic acid)	$(C_8H_8O_3S)_n$	~75000	plasticizer	18%	Sigma-Aldrich
nitrosyl tetrafluoroborate	$NOBF_4$	116.81	dopant	≥ 95%	Sigma-Aldrich
dimethyl sulfoxide	C_2H_6OS	78.13	solvent	ACS grade	Sigma-Aldrich
acetonitrile	C_2H_3N	41.05	solvent	≥ 99.8%	Sigma-Aldrich
deionized water	H_2O	18.01	solvent	18.2 MΩ cm	Millipore system

2.2 Solutions preparation

2.2.1 Dissolution of monomers

Pyrrole (Py) monomers are dissolved in deionized water (Millipore system, 18.2 MΩ cm, LCP, University Paris-Sud) in volumetric flasks within the concentration range of 1~20 mM. The concentrations of aqueous solutions of Py are lower than that of the solubility of Py at room temperature which is reported to be 0.67 M.[1] Py monomers are a weak base and the redox potential of pyrrole monomers is 0.80 V_{SHE}.[2,3] The chemical structure of pyrrole monomers is shown (Figure 2.1). The polymerization occurs by connecting pyrrole monomers at α and α' positions forming polypyrrole (PPy, Figure 2.1). In addition, the α and β' coupling is also possible at the α and β' positions.[4] After deposition, PPy polymers usually appear to be yellow green.[5]

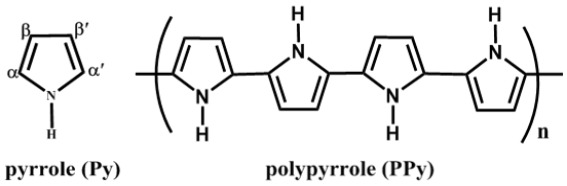

Figure 2.1 Chemical structures of pyrrole monomers (Py) and polypyrrole polymers (PPy). The free α, α′ positions at which polymerization occurs are shown in the pyrrole structure.

3,4-ethylenedioxythiophene (EDOT) monomers are solubilized in deionized water with the concentration ranges from 1 to 10 mM. This concentration range is lower than the solubility of EDOT which is reported to be 11 mM at room temperature.[6] EDOT monomers are one kind of derivatives of thiophen which is the most simple and basic component of the electrically conducting polymer materials.[7] The chemical structure of EDOT monomers is presented (Figure 2.2). Compared with the structure of thiophen, it is easy to see that there is an ethylenedioxy group locating at the 3 and 4 positions (β and β') of the thiophen ring and the functional group takes up the β and β' inhibiting the polymerization of EDOT monomers at these positions. Therefore, the polymerization of EDOT monomers can occur only at the 2 and 5 positions (α and α') of each thiophen ring. The redox potential of EDOT monomers is about 1.4 $V_{Ag/AgCl}$.[8] When the C-H bonds at α and α' positions of each thiophen ring are broken, EDOT monomers are

connected together by coupling reactions forming poly(3,4-ethylenedioxythiophene) (PEDOT, Figure 2.2) polymers. Generally, PEDOT polymers appear to be dark blue in the reduced state with a band gap of 1.6 eV and become light blue after oxidation.[9,10]

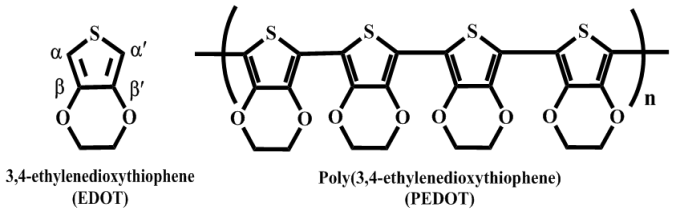

Figure 2.2 Chemical structures of 3,4-ethylenedioxythiophene (EDOT) monomer and poly (3,4-ethylenedioxythiophene) (PEDOT) polymer. EDOT structure shows free α,α' positions where coupling reactions may occur.

2.2.2 Variation of experimental conditions

In order to use the soft template during radiolysis, the anionic surfactant sodium dodecyl sulfate (SDS) is applied (Figure 2.3).[11]

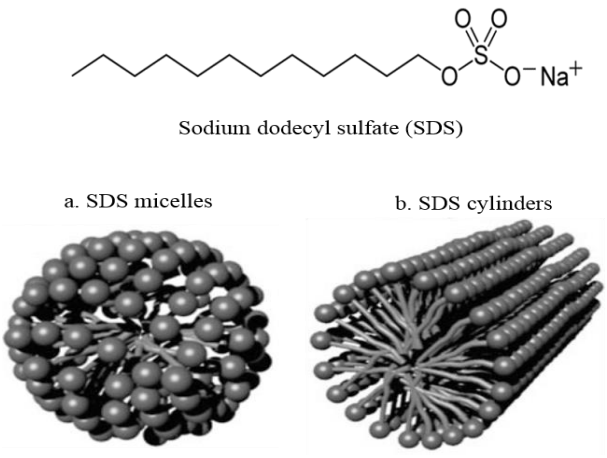

Figure 2.3 Structural formula of SDS and spherical (a) and cylindrical (b) structures formed by SDS..[11]

It is well known that the critical micelle concentrations (CMC) of SDS are 8.3 mM (CMC I, 25 ^{0}C) and 70 mM (CMC II, 25 ^{0}C).[11,12] SDS can be used to form the soft template with different shapes such as spherical (between CMC I and CMC II) or cylindrical (above CMC II)

nanostructures which can work as the soft template and affect the final morphology of CPs (Figure 2.3).[11] When the soft template formed by SDS is applied, the solubility of EDOT monomers is also increased from 11 mM to 73 mM which overcomes the solubility problem of EDOT in water.[6]

In order to check the influence of the pH on the polymerization, perchloric acid ($HClO_4$) or hydrochloric acid (HCl) (1~1000 mM) is used to adjust the pH of the prepared solutions. The pH values of all the solutions are measured using a pH-meter (CyberScan pH 500).

To study the effect of ionic strength on the polymerization, sodium perchlorate ($NaClO_4$) or sodium chloride (NaCl) (1000 mM) salt is added to the prepared aqueous solutions of EDOT monomers (10 mM).

In order to prepare nanocomposites of PEDOT/Ag by radiolytic method, silver perchlorate salt ($AgClO_4$) (1~10 mM) is added to the aqueous solutions of EDOT monomers (10 mM) as Ag^+ source for silver nanoparticles synthesis.

2.2.3 Chemical oxidation by $S_2O_8^{2-}$

In order to compare radiolytic method with chemical method, potassium persulfate ($K_2S_2O_8$) is used as chemical oxidant for the synthesis of PPy in water by traditional chemical method. It is known that persulfate anion ($S_2O_8^{2-}$) is a very strong oxidant and can initiate the polymerization of pyrrole monomers by oxidation polymerization.[13] To realize complete polymerization of Py monomers, the concentration of $K_2S_2O_8$ (40 mM) is two times that of Py monomers (20 mM).

Persulfate ion ($S_2O_8^{2-}$) is often used in literature as an initiator of conducting materials polymerization. Indeed, it is a powerful oxidant, with a strong redox potential of 2.1 V_{SHE} which enables it to oxidize organic monomers.[14] It is generally assumed that persulfate oxidation mechanism is through free radicals. With the presence of some catalysts, like heat, persulfate can homolytically dissociate according to the following reaction:[15]

$$S_2O_8^{2-} \rightarrow 2\ SO_4^{\bullet -} \qquad (2.1)$$

This reaction leads to sulfate radical which is one of the strongest oxidizing species with a redox potential which is estimated to be 2.6 V_{SHE}, similar to that of hydroxyl radical (2.7 V_{SHE} in acidic

solutions and 1.8 V_{SHE} in neutral solutions).[16,17] Although the persulfate anion by itself is a strong oxidizer, its reaction kinetics is often relatively slow. However, generation of sulfate radicals by heat activation can significantly enhance the oxidation kinetics by persulfate.[18]

2.2.4 Degassing and addition of alcohols for radiolytic oxidation or reduction

In order to remove the dissolved oxygen (O_2) in the aqueous solutions and when atmosphere components need to be inert, nitrogen (N_2) is used to degas all the aqueous solutions. Nitrous oxide (N_2O) is also alternatively used to degas the aqueous solutions and works as the scavenger of solvated electrons (e_{aq}^-) as it will be seen later.

In order to scavenge hydroxyl radicals (HO•) formed during γ-radiolysis, isopropanol or *tert*-butanol (0.2 M) are added in excess into the aqueous monomer solutions for reduction polymerization.

2.3 Samples irradiation

2.3.1 Radiolysis of water

Radiation method is based on the radiolysis of solvent which produces various oxidizing and reducing species.[19] The initiators produced using radiation method can induce the oxidation of organic monomers making it a new method for the synthesis of CPs and reduction of metal ions into metal nanoparticles. Compared with traditional chemical method, radiation method avoids the addition of chemical oxidants or reducing species while just needs the common solvent making the polymerization process clean and environment friendly. Furthermore, radiation method can realize the production of large quantity of CPs or CPs nanocomposites which overcomes the limitation of electrochemical method.[20]

The history of radiation chemistry is long and investigations on radiation chemistry of different solvents have already been carried out.[21-23] However, both complex physical and chemical reactions happen during the radiation process. For the moment, the mechanism of radiolysis of water is relatively well understood.[22]

As the most commonly used and abundant solvent, water (H_2O) is of great importance and the radiolysis of water is meaningful. Ionizing radiation can be initiated by gamma (γ)-rays, X-rays and accelerated particles (electrons, α-particles) which possess high energy. When water is exposed to ionizing radiation, both physical and chemical stages undergo as a function of the time (Figure 2.4).[24]

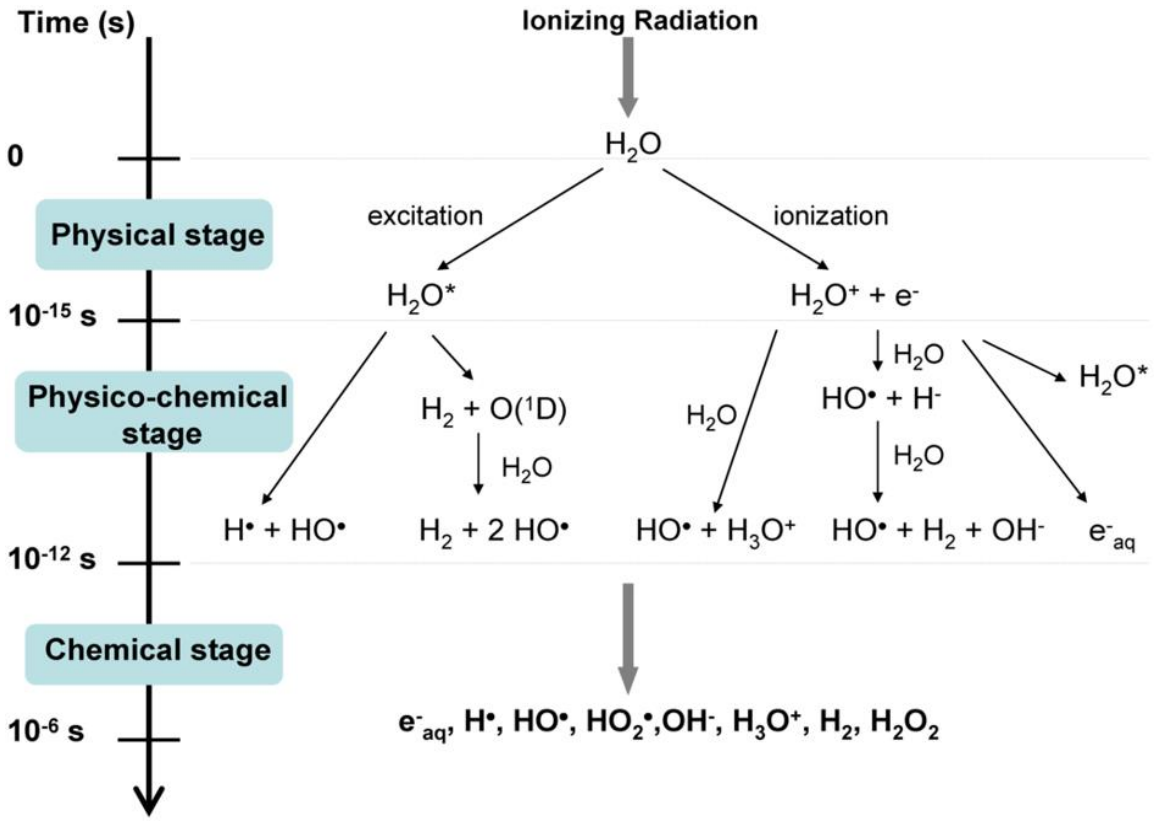

Figure 2.4 Main reactions during the three stages of water radiolysis at neutral pH under nitrogen atmosphere.[24]

After the physico-chemical stage, complex reactions occur and stable species are produced at the ns time scale. At the chemical stage, the kinds and amounts of species produced are possible to be known. Therefore, the radiolysis of water under N_2 atmosphere at neutral pH can be summarized as follows:[23]

$$H_2O \rightarrow HO\bullet, H\bullet, e_{aq}^-, H_3O^+, H_2O_2, H_2 \qquad (2.2)$$

In order to quantify the amounts of the different species produced by radiolysis of water, the concept of radiolytic yield (G value) is used to express the production or consumption of different species. G value is defined as the amount of species (mol) formed or disappeared in the medium when one joule (J) is absorbed and the commonly used unit of radiolytic yield is mol J^{-1}.[25] In the early literature, G value is termed as the number of molecules produced when the energy of 100 eV is absorbed.[23] They could be transferred into each other by:

$$1 \text{ molecule } (100 \text{ eV})^{-1} = 1.036 \times 10^{-7} \text{ mol } J^{-1} \quad (2.3)$$

The G values of different radiolytic species which evidently depend on the experimental condition are summarized and listed for different radiation types and pH values under N_2 atmosphere (Table 2.2).[24]

Table 2.2 Radiolytic yields (μmol J^{-1}) as a function of the type of radiation and the pH under N_2 atmosphere .[24]

Radiation	e_{aq}^-	HO•	H•	H_2	H_2O_2	$HO_2^•$
γ Electrons (0.1–10 MeV) pH = 3–11	0.28	0.28	0.06	0.047	0.073	0.0027
γ Electrons (0.1–10 MeV) pH = 0.5	0	0.301	0.378	0.041	0.081	0.0008
5.3 MeV α particles (^{210}Po) pH = 0.5	0	0.052	0.062	0.163	0.150	0.011

According to Table 2.2, γ radiolysis of water under N_2 atmosphere in neutral medium produces different species and the G values of which are:[23]

$$G_{HO\cdot} = 2.8 \times 10^{-7} \text{ mol } J^{-1} \quad (2.4)$$

$$G_{e_{aq}^-} = 2.8 \times 10^{-7} \text{ mol } J^{-1} \quad (2.5)$$

$$G_{H\bullet} = 0.6 \times 10^{-7} \text{ mol } J^{-1} \quad (2.6)$$

$$G_{H_2} = 0.46 \times 10^{-7} \text{ mol } J^{-1} \quad (2.7)$$

$$G_{H_2O_2} = 0.73 \times 10^{-7} \text{ mol } J^{-1} \quad (2.8)$$

$$G_{HO_2\bullet} = 0.027 \times 10^{-7} \text{ mol } J^{-1} \quad (2.9)$$

It is clear that among the various species produced by the γ radiolysis of water under N_2 atmosphere in neutral medium, HO• and e_{aq}^- are the major species.

The effect of pH on G values of different species produced during the radiolysis of water by γ rays and accelerated electrons are shown (Figure 2.5).[26] Therefore, the production of different species can be adjusted by controlling the pH values. In addition, the G values of different species can be controlled by adding scavengers during the radiolysis. Under different conditions, by adding specific scavengers or changing the pH values, the amount of different species can be varied and both reducing species and oxidizing species can be obtained. Therefore, the species produced can be adjusted by changing the radiolytic conditions.[27-29]

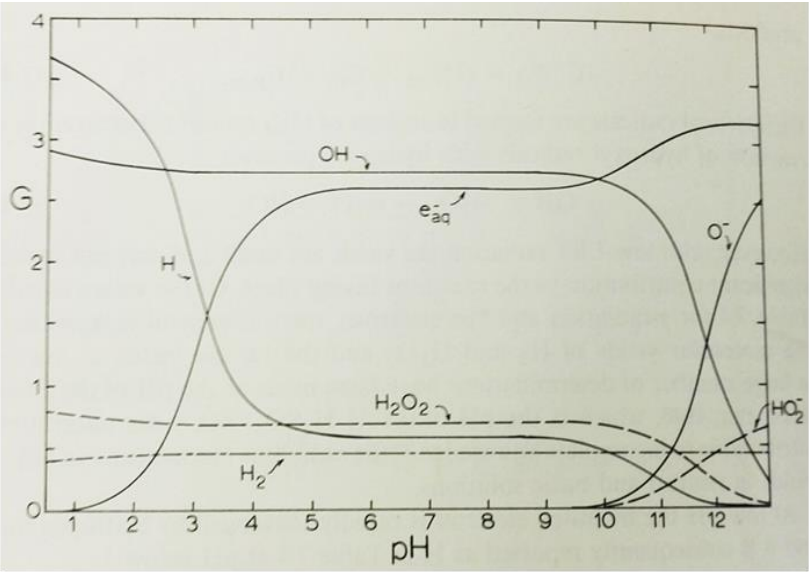

Figure 2.5 Effect of pH on the primary products of water irradiation. Yields are for γ-rays and fast electrons under N_2 atmosphere with energies of the of the order of 1 to 20 MeV.[26]

2.3.2 γ-source, absorbed dose and dose rate

As an important ionizing radiation source, γ-rays released by radioactive cobalt (^{60}Co) have been widely applied in both industry and research. The decay of ^{60}Co produces γ-rays with high energy and the half-life period of ^{60}Co is 5.27 years (Figure 2.6).[30] It is well known that γ-rays are highly energetic waves and the penetration ability of gamma photons is strong which needs to be protected by the lead wall.

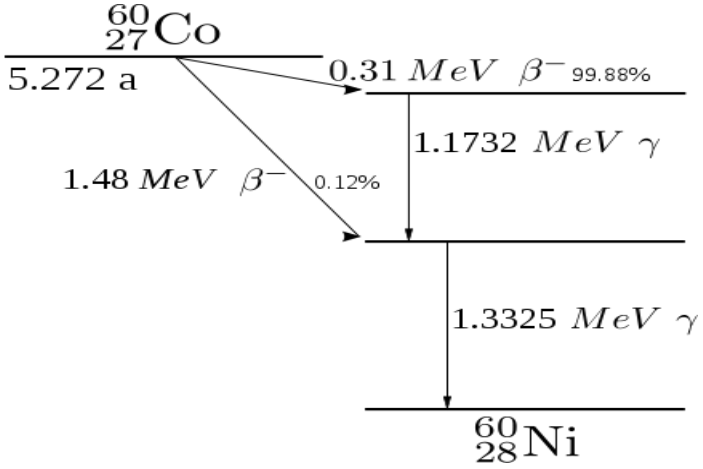

Figure 2.6 Schematic illustration of the decay of ^{60}Co.[30]

In order to describe the energy absorbed during the γ-irradiation, the concept of dose (D) is introduced to quantify the amount of energy deposited in the irradiated aqueous samples. Normally, D is counted with the unit of gray (Gy) which is defined as the energy of 1 J absorbed by 1 kg or 1 L (water density being 1 g/ml). Therefore, the dose of 1 Gy corresponds to 1 J/kg or 1 J/L.[31] In addition, within a per unit time (min or h), the amount of energy deposited is termed as the dose rate (Gy/min or kGy/h). Thus, the energy absorbed during the γ radiation of water can be calculated as follows:

$$\text{D (Gy)} = \text{Dose rate (Gy/min or Gy/h)} \times \text{Time (min or h)}. \quad (2.10)$$

In the gamma source (LCP, University Paris-Sud), the ^{60}Co is stored in a lead jar and mechanically lifted up for irradiation which is controlled by the operator (Figure 2.7 left). To

irradiate the samples by γ rays, all the glass vials containing aqueous solutions are put on the plat at fixed positions (Figure 2.7 right). The dose rates at different positions depend on the distance to the source and are determined with Fricke's dosimetry.[32]

Figure 2.7 Photograph of ^{60}Co gamma source (LCP, Paris-Sud University). Control panel (left) and irradiation plate (right).

As a result, when the dose rate is determined, the total energy deposited by γ irradiation can be calculated according to equation (2.10). Knowing the G values of the different radiolytic species, their concentrations can be determined according to the following equation:

$$C\ (mol \cdot L^{-1}) = D\ (Gy) \times G\ (mol \cdot J^{-1}) \qquad (2.11)$$

In the same way, the dose which is necessary to quantitatively oxidize or reduce a solute in the solution can be deduced from this equation knowing the yield of its disappearance.

2.3.3 Irradiation in oxidizing conditions

As mentioned before, the radiolysis of water with γ rays produces a wide variety of species and the G values of the different species depend on the radiolytic conditions. During the radiolysis of water, both oxidizing and reducing species are formed. As a result, the produced oxidizing

species may work as initiators to induce the polymerization and have the potential application for the synthesis of CPs. Nevertheless, with this aim, reducing species (such as e_{aq}^-) should be scavenged and converted into secondary radicals to optimize and to increase the yield of oxidation. In order to quantify the polymerization of monomers with the oxidizing species produced by γ radiolysis of water, it is necessary to know the kinds and amounts of all oxidizing species produced under the given experimental conditions.

Irradiation under O_2

When the radiolysis of water undergoes under oxygen (O_2) atmosphere, H• atoms and e_{aq}^- are scavenged by O_2 to produce respectively perhydroxyl radicals ($HO_2^{\bullet}$) and superoxide radicals ($O_2^{\bullet-}$) which are the two acido-basic forms of the couple $HO_2^{\bullet}/O_2^{\bullet-}$ (pKa ($HO_2^{\bullet}/O_2^{\bullet-}$) = 4.8 at 298 K).[22] As a consequence, when irradiating aerated aqueous solutions at neutral pH, only two short-lived transient species are formed: HO• and $O_2^{\bullet-}$ with the following radiolytic yields:[17]

$$G_{HO\bullet} = 2.8 \times 10^{-7} \text{ mol J}^{-1} \quad (2.12)$$

$$G(O_2^{\bullet-}) = G_{H\bullet} + G_{e_{aq}^-} = 3.4 \times 10^{-7} \text{ mol J}^{-1} \quad (2.13)$$

It is well known that HO• is a strong oxidizing species since its apparent standard redox potential at pH = 7 amounts to $E°(HO\bullet/H_2O) = 2.2\ V_{SHE}$.[17] Nevertheless, $O_2^{\bullet-}$ is almost a poor oxidizing species with a redox potential $E°(O_2^{\bullet-}/H_2O_2) = 0.9\ V_{SHE}$.[22]

Irradiation under N_2O

When irradiating nitrous oxide (N_2O, 25 mM) saturated aqueous solutions at neutral pH, e_{aq}^- is quantitatively converted into HO• according to the following reaction:[33]

$$e_{aq}^- + N_2O + H_2O \rightarrow HO\bullet + HO^- + N_2 \quad (2.14)$$

Therefore, the main oxidizing species produced under N_2O atmosphere is HO• radicals with the radiolytic yield of:

$$G(HO\bullet) = G_{HO\bullet} + G_{e_{aq}^-} = 5.6 \times 10^{-7} \text{ mol J}^{-1} \quad (2.15)$$

Note that H• atoms are still present in such conditions. Nevertheless, due to its relatively small amount and unknown reactivity, the presence of H• atoms are often neglected.

Irradiation under N_2O in presence of NaN_3

When the radiolysis of water occurs under N_2O atmosphere and in the presence of sodium azide (NaN_3) (100 mM), HO• radicals are very quickly scavenged by N_3^- ions leading to the quantitative formation of azide radicals ($N_3^\bullet$) according to:[34,35]

$$HO\bullet + N_3^- \rightarrow HO^- + N_3^\bullet \quad (2.16)$$

It is well known that $N_3^\bullet$ radicals are an alternative oxidizing system more selective than HO•. It is a soft one-electron oxidant $E°(N_3^\bullet/N_3^-) = 1.33\ V_{SHE}$ at pH=7.[34-36] Thus, when irradiating N_2O-saturated aqueous solutions at neutral pH in the presence of NaN_3, the main oxidizing species produced is $N_3^\bullet$ radicals with a radiolytic yield of formation of which amounts to:

$$G(N_3^\bullet) = G_{HO\bullet} + G_{e_{aq}^-} = 5.6 \times 10^{-7} \text{ mol J}^{-1} \quad (2.17)$$

Irradiation under N_2O in acidic medium

When the radiolysis of water happens under N_2O atmosphere in acidic medium, e_{aq}^- is quickly transformed into H• atoms by reacting with hydronium ions (H^+):[28]

$$e_{aq}^- + H^+ \rightarrow H\bullet \quad (2.18)$$

But, its competitive transformation into HO• radicals also happens according to equation (2.14).

The radiolytic yields of $H^{\cdot}$ atoms and HO• radicals in acidic medium under N_2O atmosphere can be estimated as it will be done in chapter 5.

When perchloric acid ($HClO_4$) is used in the aqueous solution, perchlorate ion (ClO_4^-) is unreactive to the species produced by radiolysis resulting in the formation of HO• radicals and H• atoms as the main species.[37] Therefore, the main oxidizing species produced by radiolysis of acidic aqueous solution containing $HClO_4$ is HO•.

When the neutral aqueous solution is added with hydrochloride acid (HCl) instead of $HClO_4$, HO• is finally converted to $Cl_2^{\cdot -}$ according to the following reactions:[29]

$$HO\bullet + Cl^- \rightarrow ClOH^{\cdot -} \quad (2.19)$$

$$ClOH^{\cdot -} + H^+ \rightarrow Cl^{\cdot} + H_2O \quad (2.20)$$

$$Cl^{\cdot} + Cl^- \rightarrow Cl_2^{\cdot -} \quad (2.21)$$

Therefore, in addition to H• atoms, the main oxidizing species produced by radiolysis of acidic aqueous solution containing HCl is $Cl_2^{\cdot -}$.[28] The redox potential of $E^o(Cl_2^{\cdot -}/Cl^-)$ amounts to 2.09 V_{SHE} indicating that $Cl_2^{\cdot -}$ is a strong oxidant.[27]

Radiation induced polymerization

It is reported that radiation induced polymerization of organic monomer could only proceed through a recurrent oxidation process.[19] Taking the radiation induced polymerization of EDOT for example, HO• radicals first react with EDOT monomers, then with dimers, then with oligomers. The quantitative synthesis of PEDOT polymers throughout such a step-by-step mechanism necessarily implies the use of two HO• radicals for the oxidation of one EDOT molecule (in α and α' positions).[19] Thus, in order to initiate the oxidation of organic monomers and realize complete polymerization of CPs, the amount of oxidizing species should be twice that of the amount of organic monomers as already demonstrated.[19,38,39] Therefore, the total dose needed for the production of needed amount of oxidizing radicals and quantitative oxidation of organic monomers can be determined as follows:[19]

$$D_{max}\ (Gy) = \frac{2[monomer]_0\ (mol\ L^{-1})}{G(oxidant)\ (mol\ J^{-1})} \quad (2.22)$$

Knowing the dose rate during γ irradiation, for a given solution with a fixed concentration of organic monomers, in order to conduct oxidation polymerization, the total time needed for irradiation can be determined by dividing the total dose by the dose rate.

2.3.4 Irradiation in reducing condition

The radiolysis of water also produces reducing species which may have potentials to induce the synthesis of CPs by reduction polymerization and produce metal nanoparticles by reduction of metal ions. Among primary radiolytic radicals formed under N_2 atmosphere in neutral medium, it is well known that e_{aq}^- is very reducing species with a redox potential of −2.8 V_{SHE}.[33]

Irradiation under N_2 atmosphere in the presence of alcohol

When radiolysis of water takes place under N_2 atmosphere with isopropanol (0.2 M), HO• radicals and H• atoms quantitatively react with isopropanol and isopropanol radical ($(CH_3)_2C•OH$) is generated according to:[40,41]

$$(CH_3)_2CHOH + HO• \rightarrow (CH_3)_2C•OH + H_2O \quad (2.23)$$

$$(CH_3)_2CHOH + H• \rightarrow (CH_3)_2C•OH + H_2 \quad (2.24)$$

The redox potential of this alcohol radical $(CH_3)_2C•OH$ which is also a reducing species amounts to −1.8 V_{SHE} at pH=7.[40] Although H• atoms are also powerful reducing species with a redox potential of -2.3 V_{SHE}, both the HO• radicals and H• atoms are tranformed into $(CH_3)_2C•OH$.[42] Therefore, radiolysis of water under N_2 atmosphere with isopropanol produces two main reducing species e_{aq}^- and $(CH_3)_2C•OH$ with the radiolytic yields:

$$G_{e_{aq}^-} = 2.8 \times 10^{-7}\ mol\ J^{-1} \quad (2.25)$$

$$G((CH_3)_2C\bullet OH) = G_{HO\bullet} + G_{H\bullet} = 3.4 \times 10^{-7} \text{ mol J}^{-1} \quad (2.26)$$

When the radiolysis of water takes place under N_2 atmosphere with *tert*-butanol (0.2 M) instead of isopropanol, HO• radicals and H• atoms once again quantitatively react with *tert*-butanol, and *tert*-butanol radical is generated:[40,41]

$$(CH_3)_3COH + HO\bullet \rightarrow \bullet CH_2(CH_3)_2COH + H_2O \quad (2.27)$$

$$(CH_3)_3COH + H\bullet \rightarrow \bullet CH_2(CH_3)_2COH + H_2 \quad (2.28)$$

However, contrarily to isopropanol radical, *tert*-butanol radical is a stable and unreactive species. Thus, the radiolysis of water under N_2 atmosphere in the presence of *tert*-butanol, produces a single reducing species namely e_{aq}^- with the radiolytic yields:[41]

$$G_{e_{aq}^-} = 2.8 \times 10^{-7} \text{ mol J}^{-1} \quad (2.29)$$

Radiation induced synthesis of metal nanoparticles and polymerization

Synthesis of metal nanoparticles using radiolytic method has been already intensively investigated and widely applied.[40,43] Nanoparticles can be prepared by the reduction of metal ions using reducing species produced by radiolysis of water. The well-known and applied reducing species are e_{aq}^- and $(CH_3)_2C\bullet OH$ which can reduce metal ions into metal atoms which aggregate leading to inorganic nanoparticles.[44,45] Among various metal nanoparticles, the synthesis of Ag nanoparticles using radiation chemistry has been reported and intensively investigated.[43-45]

Taking the formation of Ag nanoparticles for example, the reduction of silver ions and formation of silver nanoparticles is as follows:[46]

$$Ag^+ + e_{aq}^- \rightarrow Ag^0 \quad (2.30)$$

$$Ag^+ + (CH_3)_2C\bullet OH \rightarrow Ag^0 + (CH_3)_2CO + H^+ \quad (2.31)$$

$$Ag^0 + Ag^0 \rightarrow Ag_2{}^0 \quad (2.32)$$

$$Ag^0 + Ag^+ \rightarrow Ag_2{}^+ \quad (2.33)$$

$$\vdots$$

$$Ag_m{}^{x+} + Ag_n{}^{y+} \rightarrow Ag_{m+n}{}^{(x+y)+} \quad (2.34)$$

Since both oxidative and reductive species can be produced by radiolysis, both radiation induced polymerization by oxidation or reduction of organic monomers and synthesis of inorganic nanocomposites by reduction of metal ions are feasible. Therefore, it is also possible to apply radiation method for the synthesis of CPs nanocomposites as it will be described in this manuscript in chapter 7.

2.4 Kinetic study by pulse radiolysis

Electron accelerator is of great importance in the basic research of ultra-fast chemical reactions. The electron accelerator analyzing system coupled with time-resolved spectroscopy enables the analysis of fast chemical reactions and makes the pulse radiolysis study a powerful tool. In order to understand the mechanism of polymerization and determine the rate constants of fast reactions induced by hydrated electrons or hydroxyl radicals, pulse radiolysis experiments is implemented on the picosecond laser-triggered electron accelerator (ELYSE, Paris-Sud University) coupled with a time-resolved absorption spectroscopic detection system (Figure 2.8).[47]

In pulsed radiolysis, a solution irradiated by a short pulse of high-energy electrons produces a significant concentration of radical species. As is mentioned above, if the system is an aqueous solution at neutral pH, under N_2 atmosphere, water radiolysis leads to the production of the following reactive species: HO•, H•, e_{aq}^-, H_3O^+, H_2O_2, H_2 (reaction 2.2). Among the formed species, e^-_{aq} and HO• radicals are the most abundant species and have higher reactivity.

In order to study the specific action of hydrated electrons, e^-_{aq}, with organic monomers and in order to determine its rate constant, an aqueous solution containing 1 mM in EDOT and 0.2 M in *tert*-butanol is prepared, degassed with N_2 and then studied by pulse radiolysis. It is known that *tert*-butanol is an efficient scavenger of HO• radicals according to reaction (2.27) which leading

to a racial which is known to be unreactive. Thus, in these conditions, e_{aq}^- is the only reducing species which can be involved in reduction polymerization and synthesis of CPs nanocomposites.

Figure 2.8 ELYSE electron accelerator source (Laboratoire de Chimie Physique, LCP, Paris-Sud University).

During the pulse study, the 15 ps pulses, which are characterized by a charge of 4~6 nC and an electron energy of 7.6 MeV, are delivered at a repetition frequency of 5 Hz. The dose per pulse is derived from the absorbance of the hydrated electron at 660 nm with $\varepsilon_{660nm,\ (e\text{-}aq)} = 1.8\times10^4$ L.mol^{-1} cm^{-1}, and $G_{3ns,\ (e\text{-}aq)} = 3.45\times10^{-7}$ mol.J^{-1}. For each pulse, the dose deposited in water is 40.5 Gy in the irradiated volume (i.e., $[e^-_{aq}] \approx 1.4\times10^{-5}$ M).[48]

A N_2-purged stock aqueous solution of 200 mL is used which circulated in the 10×10 mm fused silica irradiation cell at a flow rate of 100 mL/min by means of a peristaltic pump. The solution is then renewed between each pulse and, for each kinetic measurement, it is possible to apply up to 400 pulses.

Absorption measurements are performed using the white light beam of a homemade Xenon flash lamp.[49] The light is focused through the sample collinearly with the electron beam and then directed onto the slit of a flat field spectrograph (Chromex 250IS), equipped with three 150 grooves/mm grating blazed at 300, 500 and 800 nm which dispersed the light on the entrance optics of a streak-camera (model C-7700 from Hamamatsu).[38] The time-resolved absorbance of the sample is calculated using average images obtained on the streak-camera (with and without the electron pulses). The full spectra from 245 to 650 nm are obtained by two series of absorption

measurements using two different optical filters (UG5 and GG325) to optimize the light intensity on a specific spectral domain (250-400 and 360-700 nm, respectively). Also, the spectral overlap between 360 and 400 nm enables checking the good stability and the reproducibility of all irradiation measurements.

2.5 Materials treatment

After irradiation, aqueous solutions or suspensions are obtained and materials dispersed in liquid state are characterized without treatment. In order to carry out analyses and characterizations in solid state, material powders are obtained by treating aqueous solutions or suspensions with drying process or lyophilization and material films or membranes are formed by spin coating treatment or drying process (Figure 2.9).

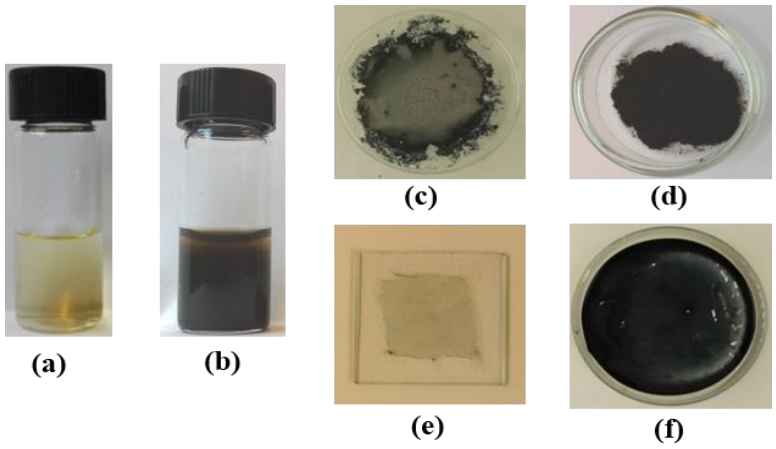

Figure 2.9 Photographs of obtained materials after irradiation in different states. Aqueous solution of SDS after irradiation for 70 kGy (a); aqueous suspension of pyrrole after irradiation for 70 kGy (b); PEDOT powders obtained by drying process(c); PPy powders obtained by lyophilization (d); PEDOT film formed by spin coating (e); PEDOT/PSS membrane prepared by drying process (f).

Drying and lyophilization

After irradiation, aqueous solutions containing polymers or composites are centrifugated and washed with water. The obtained materials are then dried in the Frollabo AP 60 oven at 50 ^{o}C for 24 h (Figure 2.10).

Figure 2.10 Frollabo AP 60 oven (Laboratoire de Chimie Physique, LCP, Paris-Sud University).

The solutions after gamma irradiation are dried by lyophilization with a Heto PowerDry® LL1500 (Thermo Electron Co., France) to obtain dehydrated powders (Figure 2.11). The drying procedures are done as follows: first, all the solutions are transfered to culture dishes and frozen into ices; then, the frozen samples are moved to the drying chamber and lyophilized at -110 ^{o}C for 48 h.

Figure 2.11 Heto PowerDry® LL1500 lyophilizer (Équipe Industries Agroalimentaires, Département Chimie Vivant Santé, Conservatoire National des Arts et Métiers).

Film preparation by spin coating

After irradiation, a few drops of the irradiated aqueous solutions are deposited onto the glass substrates by spin coating with a SCC-200 spin coater with a speed of 100 rpm for 60 s leading to the formation of a film (Figure 2.12 left). During the spin coating, the glass substrates are held by the vacuum formed by the pump (Figure 2.12 right). The spin coating is carried out by spinning at a speed of 100 rpm for 60 s (Laboratoire de Chimie Physique, LCP, Paris-Sud University) or 1000 rpm for 30 s (Laboratoire de Physicochimie des polymères et Interfaces, LPPI, Cergy-Pontoise University).

Figure 2.12 SCC-200 spin coater (left) and coupled pump for vacuum (right) (Laboratoire de Chimie Physique, LCP, Paris-Sud University).

Nitrosyl tetrafluoroborate ($NOBF_4$) is dissolved in acetonitrile at a concentration of 20 mM and used as the dopant. Acetonitrile solution of $NOBF_4$ is dropped on to the films prepared by spin coating. The doping process of electrically conducting polymers is realized by the oxidative nitrosonium cation (NO^+) with a redox potential of 0.87 V_{SHE}.[50] As is mentioned before, the doping type of PEDOT and PPy is p-doping.[51]

PEDOT/PSS membrane preparation

To prepare PEDOT/PSS membranes, PEDOT polymers are mixed with poly(4-styrenesulfonic acid) (PSSH) and dimethyl sulfoxide (DMSO) to form a membrane and realize a homogeneous distribution. The mixture is dried in the oven at 50 ^{o}C for 24 h.

2.6 Materials Characterizations

After irradiation, aqueous solutions or suspensions containing synthesized materials are characterized. In the same way, the powders obtained after drying or lyophilization as well as films and membranes prepared by spin coating and drying process are studied.

2.6.1 UV-vis absorption spectroscopy

Ultraviolet-visible (UV-vis) spectra of aqueous solutions of monomers, polymers and nanocomposites prepared using chemical oxidation or gamma irradiation are recorded on a UV-vis scanning spectrophotometer (HP 8453) in quartz cells with an optical path length of 0.1 or 0.2 cm (Figure 2.13). To measure the UV-vis spectra of the samples, appropriate dilution is carried out to the samples. The reference is always ultrapure water.

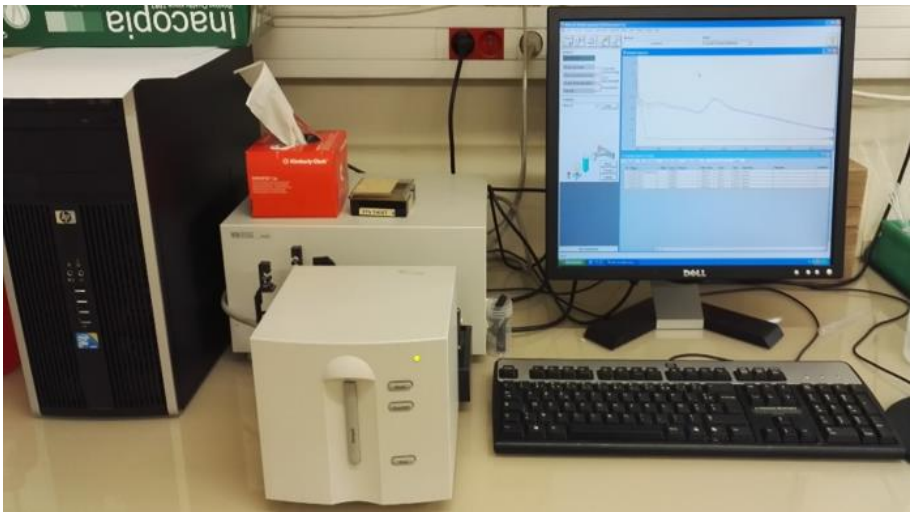

Figure 2.13 UV-vis scanning spectrophotometer (Laboratoire de Chimie Physique, LCP, Paris-Sud University).

2.6.2 Cryo-transmission electron microscopy and EDX analysis

To observe the original morphology of the as-prepared samples in aqueous solutions, *in situ* observation of the morphology is carried out on a transmission electron microscope in a

cryogenic environment (Cryo-TEM), known to be adapted to low density contrasts (Institut de Minéralogie et de Physique des Milieux Condensés, IMPMC, Pierre and Marie Curie University). A drop of each solution is deposited on ‘‘quantifoil’’® (Quantifoil Micro Tools Gmbh, Germany) 200 mesh holey-carbon-coated grids. After being blotted with filter paper, the grids are quench-frozen by being rapidly plunged into liquid ethane in order to form a thin ice film avoiding water crystallization. The grids are then transferred into the microscope using a side entry Gatan 626 cryoholder cooled at -180 ^{o}C with liquid nitrogen. Images are taken with an Ultrascan 2k CCD camera (Gatan, USA) by using a LaB6 JEOL JEM 2100 (JEOL, Japan) (Figure 2.14). Advantages of Cryo-TEM are not only ensuring the observation of soft nanostructures but also avoiding the phase transition and aggregation which should result from the drying procedures.

Figure 2.14 JEOL 2100 Cryo-TEM (Institut de Minéralogie et de Physique des Milieux Condensés, IMPMC, Pierre and Marie Curie University).

Energy dispersive X-Ray (EDX) analysis is carried out to identify the chemical composition of the materials during the characterizations by Cryo-TEM (Institut de Minéralogie et de Physique des Milieux Condensés, IMPMC, Pierre and Marie Curie University). During Cryo-TEM observations, *in situ* EDX spectroscopy is used to check the chemical composition and to perform

the elemental analysis within a selected area of the samples. An EDX JEOL Si(Li) detector mounted on the cryo-microscope is used with a resolution of 140 eV.

2.6.3 ATR-FTIR spectroscopy

To identify the obtained products and their chemical composition, Fourier transform infrared (FTIR) spectra of lyophilized polymers are recorded using a FTIR spectrometer (Bruker Vertex 70) with diamond attenuated total reflection (ATR) attachment (PIKEMIRACLE crystal plate diamond/ZnSe) and MCT detector with a liquid nitrogen cooling system (Figure 2.15). The dried powders are deposited onto the ZnSe diamond and scanning is conducted from 4000 to 600 cm^{-1} with a 4 cm^{-1} spectral resolution for 100 times and averaged for each spectrum.

Figure 2.15 ATR-FTIR spectrometer (Laboratoire de Chimie Physique, LCP, Paris-Sud University).

2.6.4 AFM-IR nanospectroscopy

In order to check the morphology and the chemical nature of radiosynthesized products, a small drop of the aqueous solution is deposited onto the upper surface of ZnSe prism (transparent in the mid-IR) and dried naturally. The dried deposit is observed by nanoIR^{TM} (@Anasys Instruments) an AFM-IR system that combines the AFM with a pulsed infrared OPO laser to perform spectromicroscopy (Figure 2.16).

Figure 2.16 AFM-IR microscope (Laboratoire de Chimie Physique, LCP, Paris-Sud University).

AFM which has a visible laser focusing on the cantilever and a four quadrants detector measuring its deflection is used for the superficial morphology characterization in contact mode.[52-54] To obtain relevant infrared spectra, the pulsed infrared laser setup covers the wavenumbers from 3600 cm^{-1} to 1000 cm^{-1} (Figure 2.17).

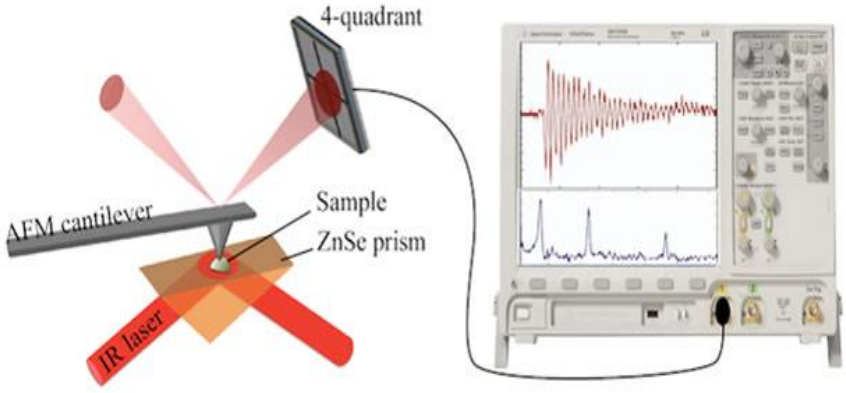

Figure 2.17 Schematic representation of AFM-IR technique.

During the measurements, the tip of the AFM remains in contact with the object. When the sample absorbs IR laser pulse, the absorbing region warms via the photothermal effect and a

rapid thermal expansion occurs which then impacts the tip of the AFM cantilever and causes its oscillation. As the amplitude of oscillations is proportional to the absorption, scanning the surface with a given wavenumber enables the drawing of chemical map of the sample, while changing the wavelength on a fixed position of the tip gives a local infrared spectrum (Figure 2.17).

2.6.5 SEM microscopy and EDX analysis

In order to check the morphology of the samples after deposition, powders obtained after lyophilization are sprinkled onto carbon tape adhered to aluminum mounts and the images are obtained with EVO MA10 scanning electron microscope (SEM) (Figure 2.18, left). In order to obtain better observation of the morphology, the product is coated with gold in some cases (Figure 2.18, right). The Magnification, accelerating voltage and scale bar are adjusted to obtain the SEM images of the samples (Laboratoire Procédés et Ingénierie en Mécanique et Matériaux, PIMM, Conservatoire National des Arts et Métiers, CNAM, Paris).

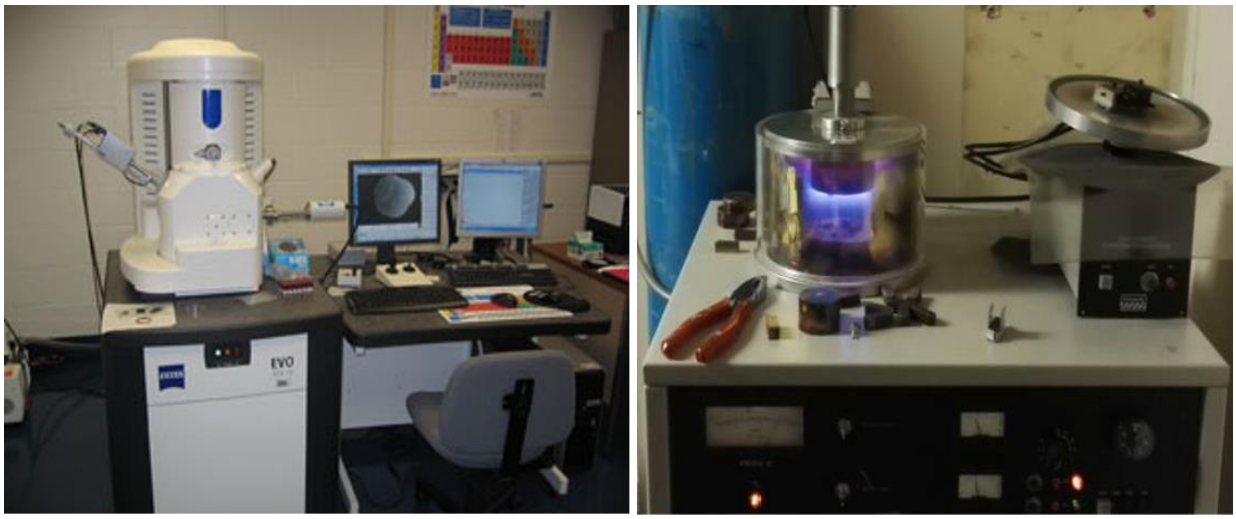

Figure 2.18 EVO MA10 SEM (left) and SC-6 Pelco Sputter Coater (Laboratoire Procédés et Ingénierie en Mécanique et Matériaux, PIMM, Conservatoire National des Arts et Métierss, CNAM, Paris).

During the observations by SEM, EDX analysis is also carried out to identify the chemical composition of the materials (Laboratoire Procédés et Ingénierie en Mécanique et Matériaux, PIMM, Conservatoire National des Arts et Métiers, CNAM, Paris). EDX spectroscopy is used to

check the chemical composition and to perform the elemental analysis within a selected area of the samples. All the EDX spectra are recorded with a beam energy of 15.0 keV.

2.6.6 TGA analysis

The thermal stability and composition analysis of the obtained polymers and nanocomposites after radiolysis are performed on a thermogravimetric analysis instrument TGA Q500 (TA instruments, USA) (Figure 2.19). The thermal degradation of the samples is carried out under a nitrogen flow of 50 mL/min within the temperature range of 40 to 800 ^{0}C at a heating rate of 20 ^{0} C/min (Laboratoire Procédés et Ingénierie en Mécanique et Matériaux, PIMM, Conservatoire National des Arts et Métiers, CNAM, Paris).

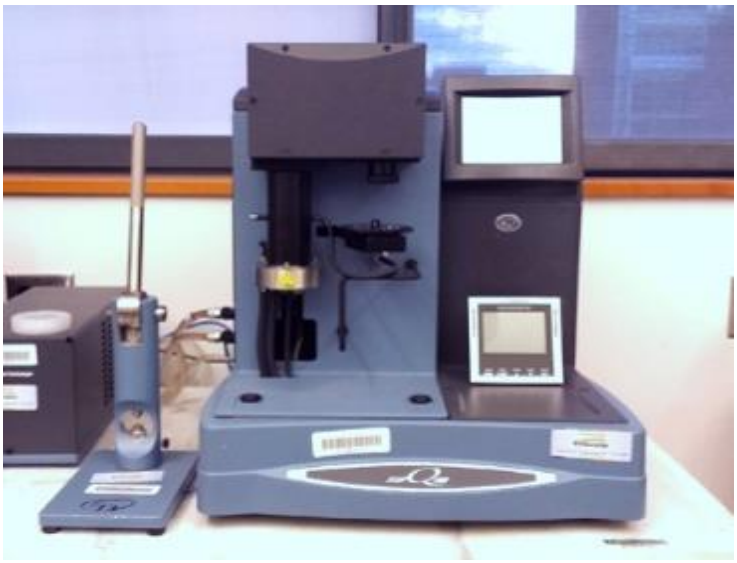

Figure 2.19 Thermogravimetric analysis (TGA) instrument (Laboratoire Procédés et Ingénierie en Mécanique et Matériaux, PIMM, ENSAM, Conservatoire National des Arts et Métiers, CNAM, Paris).

2.6.7 Electrical conductivitys

The electrical conductivity of spin coated films prepared after radiolysis is measured by the traditional four-point probe method.[55] The resistances of the samples are measured using a Keithley 2420 system (Figure 2.20) (Laboratoire de Physicochimie des Polymères et Interfaces,

LPPI, Cergy-Pontoise University). Each sample is checked at three different positions and the resistance values are averaged.

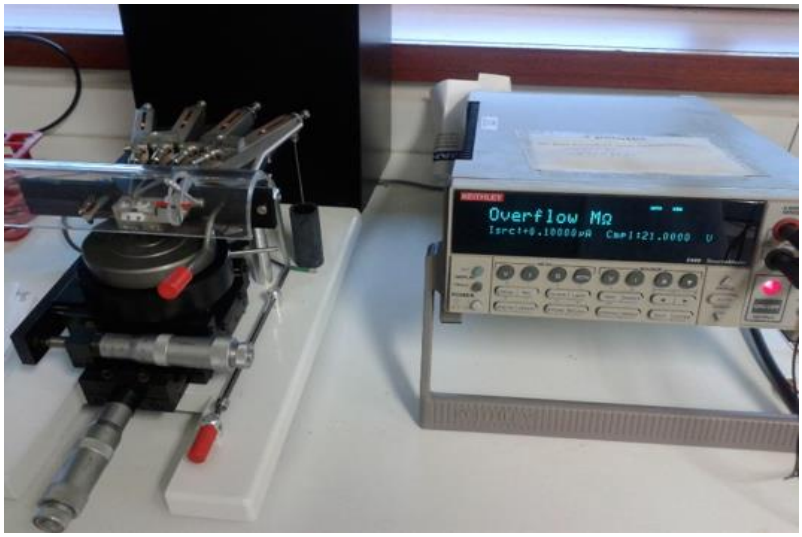

Figure 2.20 Kelvin four-point probe technique coupled with a Keithley 2420 system (Laboratoire de Physicochimie des Polymères et Interfaces, LPPI, Cergy-Pontoise University).

The thickness of the spin coated samples is measured on a 3 Veeco Dektak 150 surface profiler (Figure 2.21). The thickness of each sample is also measured three times and averaged.

Figure 2.21 Surface profiler (Laboratoire de Physicochimie des Polymères et Interfaces, LPPI, Cergy-Pontoise University).

The conductivity, ρ ($S \cdot cm^{-1}$) is then determined thanks to the following equation:[56]

$$\rho = \left(\frac{\pi}{\ln 2} \times \frac{V}{I} \times t \right)^{-1} \quad (2.35)$$

where V is the voltage difference (V), t the film thickness (cm) and I the applied current (A).

References

[1] Riddick, J. A.; Bunger, W. B.; Sakano, T. K., Techniques of Chemistry 4th ed. John Wiley and Sons. 1985, 2, 631.

[2] Zhou, M.; Heinze, J., Electropolymerization of Pyrrole and Electrochemical Study of Polypyrrole. 3. Nature of "Water Effect" in Acetonitrile. The Journal of Physical Chemistry B 1999, 103 (40), 8451-8457.

[3] Tan, Y.; Ghandi, K., Kinetics and mechanism of pyrrole chemical polymerization. Synthetic Metals 2013, 175, 183-191.

[4] Roncali, J., Conjugated poly(thiophenes): synthesis, functionalization, and applications. Chemical Reviews 1992, 92 (4), 711-738.

[5] Camurlu, P., Polypyrrole derivatives for electrochromic applications. RSC Advances 2014, 4 (99), 55832-55845.

[6] Sakmeche, N.; Aeiyach, S.; Aaron, J. J.; Jouini, M.; Lacroix, J. C.; Lacaze, P. C., Improvement of the Electrosynthesis and Physicochemical Properties of Poly(3,4-ethylenedioxythiophene) Using a Sodium Dodecyl Sulfate Micellar Aqueous Medium. Langmuir 1999, 15 (7), 2566-2574.

[7] Mehmood, U.; Al-Ahmed, A.; Hussein, I. A., Review on recent advances in polythiophene based photovoltaic devices. Renewable and Sustainable Energy Reviews 2016, 57, 550-561.

[8] Roncali, J.; Blanchard, P.; Frere, P., 3,4-Ethylenedioxythiophene (EDOT) as a versatile building block for advanced functional [small pi]-conjugated systems. Journal of Materials Chemistry 2005, 15 (16), 1589-1610.

[9] Lee, S.; Gleason, K. K., Enhanced Optical Property with Tunable Band Gap of Cross-linked PEDOT Copolymers via Oxidative Chemical Vapor Deposition. Adv. Funct. Mater. 2015, 25 (1), 85-93.

[10] Heuer, H. W.; Wehrmann, R.; Kirchmeyer, S., Electrochromic window based on conducting poly(3,4-ethylenedioxythiophene)-poly(styrene sulfonate). Adv. Funct. Mater. 2002, 12 (2), 89-94.

[11] Han, M. G.; Foulger, S. H., Facile Synthesis of Poly(3,4-ethylenedioxythiophene) Nanofibers from an Aqueous Surfactant Solution. Small 2006, 2 (10), 1164-1169.

[12] Zhao, J.; Fung, B. M., NMR study of the transformation of sodium dodecyl sulfate micelles. Langmuir 1993, 9 (5), 1228-1231.

[13] Liang, C.; Bruell, C. J.; Marley, M. C.; Sperry, K. L., Persulfate oxidation for in situ remediation of TCE. I. Activated by ferrous ion with and without a persulfate–thiosulfate redox couple. Chemosphere 2004, 55 (9), 1213-1223.

[14] Yang, S. W.; Cheng, J. H.; Sun, J.; Hu, Y. Y.; Liang, X. Y., Defluorination of Aqueous Perfluorooctanesulfonate by Activated Persulfate Oxidation. PLOS ONE 2013, 8 (10), e74877.

[15] Liang, C. J.; Su, H. W., Identification of Sulfate and Hydroxyl Radicals in Thermally Activated Persulfate. Industrial & Engineering Chemistry Research 2009, 48 (11), 5558-5562.

[16] Deng, Y.; Ezyske, C. M., Sulfate radical-advanced oxidation process (SR-AOP) for simultaneous removal of refractory organic contaminants and ammonia in landfill leachate. Water Research 2011, 45 (18), 6189-6194.

[17] Buxton, G. V.; Greenstock, C. L.; Helman, W. P.; Ross, A. B., Critical Review of rate constants for reactions of hydrated electrons, hydrogen atoms and hydroxyl radicals (·OH/·O− in Aqueous Solution. Journal of Physical and Chemical Reference Data 1988, 17 (2), 513-886.

[18] Coletta, C.; Cui, Z. P.; Dazzi, A.; Guigner, J. M.; Néron, S.; Marignier, J. L.; Remita, S., A pulsed electron beam synthesis of PEDOT conducting polymers by using sulfate radicals as oxidizing species. Radiation Physics and Chemistry 2016, 126, 21-31.

[19] Lattach, Y.; Deniset-Besseau, A.; Guigner, J. M.; Remita, S., Radiation chemistry as an alternative way for the synthesis of PEDOT conducting Polymers under "soft" Conditions. Radiat. Phys. Chem. 2013, 82, 44-53.

[20] Karim, M. R.; Lee, C. J.; Lee, M. S., Synthesis of conducting polypyrrole by radiolysis polymerization method. Polymers for Advanced Technologies 2007, 18 (11), 916-920.

[21] Spinks, J. W. T.; Woods, R. J., An introduction to radiation chemistry. John Wiley & Sons, Inc. 1990, 3, 251-256.

[22] Ferradini, C.; Jay-Gerin, J. P., Radiolysis of water and aqueous solutions-history and present state of the science. Can. J. Chem. 1999, 77, 1542-1575.

[23] Ferradini, C.; Jay-Gerin, J. P., The effect of pH on water radiolysis: A still open question - A minireview. Res. Chem. Intermed. 2000, 26 (6), 549-565.

[24] Le Caër, S., Water Radiolysis: Influence of Oxide Surfaces on H2 Production under Ionizing Radiation. Water 2011, 3 (4), 235-253.

[25] Ma, J., Ultrafast electron transfer in solutions studied by picosecond pulse radiolysis. Doctoral thesis 2015.

[26] Spinks, J. W. T.; Woods, R. J., An introduction to radiation chemistry. John Wiley & Sons, Inc. 1990, 3, 260.

[27] Schwarz, H. A.; Dodson, R. W., Equilibrium between Hydroxyl Radicals and Thallium(I I) and the Oxidation Potential of OH (aq). The Journal of Physical Chemistry 1984, 88 (16), 3643-3647.

[28] Elliot, A. J.; Geertsen, S.; Buxton, G. V., Oxidation of Thiocyanate and Iodide Ions by Hydrogen Atoms in Acid Solutions. J. Chern. Soc., Faraday Trans. I 1988, 84 (4), 1101-1112.

[29] Jayson, G. G.; Parsons, B. J.; Swallow, A. J., Some simple, highly reactive, inorganic chlorine derivatives in aqueous solution. Their formation using pulses of radiation and their role in the mechanism of the Fricke dosimeter. J. Chem. Soc., Faraday Trans. 1 1973, 69, 1597-1607.

[30] Cherry, P.; Duxburyh, A., Practical Radiotherapy: Physics and Equipment. Oxford University Press 1998, 119.

[31] Grupen, C., Introduction to radiation protection: practical knowledge for handling radioactive source. Springer 2010, 7.

[32] Jayson, G. G.; Parsons, B. J.; Swallow, A. J., The mechanism of the fricke dosimeter. International Journal for Radiation Physics and Chemistry 1975, 7 (2), 363-370.

[33] Hart, E. J., Research potentials of the hydrated electron. Acc. Chem. Res. 1969, 2, 161-167.

[34] Jonsson, M.; Lind, J.; Eriksen, T. E.; Merenyi, G., Redox and Acidity Properties of 4-Substituted Aniline Radical Cations in Water. Journal of the American Chemical Society 1994, 116 (4), 1423-1427.

[35] Lind, J.; Shen, X.; Eriksen, T. E.; Merenyi, G., The one-electron reduction potential of 4-substituted phenoxyl radicals in water. Journal of the American Chemical Society 1990, 112 (2), 479-482.

[36] Alfassi, Z. B.; Harriman, A.; Huie, R. E.; Mosseri, S.; Neta, P., The redox potential of the azide/azidyl couple. The Journal of Physical Chemistry 1987, 91 (8), 2120-2122.

[37] Domae, M.; Katsumura, Y.; Jiang, P. Y.; Nagaishi, R.; Ishigure, K.; Kozawa, T.; Yoshida, Y., Pulse and [gamma]-radiolysis of concentrated perchloric acid solutions. Journal of the Chemical Society, Faraday Transactions 1996, 92 (12), 2245-2250.

[38] Coletta, C.; Cui, Z. P.; Archirel, P.; Pernot, P.; Marignier, J. L.; Remita, S., Electron-Induced Growth Mechanism of Conducting Polymers: A Coupled Experimental and Computational Investigation. The Journal of Physical Chemistry B 2015, 119 (16), 5282-5298.

[39] Lattach, Y.; Coletta, C.; Ghosh, S.; Remita, S., Radiation-induced synthesis of nanostructured conjugated polymers in aqueous solution: fundamental effect of oxidizing species. Chemphyschem : a European journal of chemical physics and physical chemistry 2014, 15 (1), 208-218.

[40] Belloni, J.; Mostafavi, M.; Remita, H.; Marignier, J. L.; Delcourt, M. O., Radiation-induced synthesis of mono- and multi-metallic clusters and nanocolloids. New J. Chem., 1998, 1239-1255.

[41] Piechowski, M. V.; Thelen, M.; Hoigné, J.; Bühler, R. E., tert-Butanol as an OH-Scavenger in the Pulse Radiolysis of Oxygenated Aqueous Systems. Ber. Bunsenges. Phys. Chem. 1992, 96 (10), 1448-1454.

[42] Spinks, J. W. T.; Woods, R. J., An introduction to radiation chemistry. John Wiley & Sons, Inc. 1990, 3, 276.

[43] He, L.; Dumee, L. F.; Liu, D.; Velleman, L.; She, F.; Banos, C.; Davies, J. B.; Kong, L., Silver nanoparticles prepared by gamma irradiation across metal-organic framework templates. RSC Advances 2015, 5 (14), 10707-10715.

[44] Janata, E.; Henglein, A.; Ershov, B. G., First Clusters of Ag+ Ion Reduction in Aqueous Solution. The Journal of Physical Chemistry 1994, 98 (42), 10888-10890.

[45] Belloni, J., Nucleation, growth and properties of nanoclusters studied by radiation chemistry: Application to catalysis. Catalysis Today 2006, 113 (3–4), 141-156.

[46] Remita, S., Effect of ligands on thermadynamics, kinetics and spectral properties of metalic aggregates synthesized by radiloysis. Doctoral thesis 1995, 98.

[47] Belloni, J.; Monard, H.; Gobert, F.; Larbre, J. P.; Demarque, A.; De Waele, V.; Lampre, I.; Marignier, J. L.; Mostafavi, M.; Bourdon, J. C.; Bernard, M.; Borie, H.; Garvey, T.; Jacquemard, B.; Leblond, B.; Lepercq, P.; Omeich, M.; Roch, M.; Rodier, J.; Roux, R., ELYSE—A picosecond electron accelerator for pulse radiolysis research. Nuclear Instruments and Methods in Physics Research Section A: Accelerators, Spectrometers, Detectors and Associated Equipment 2005, 539 (3), 527-539.

[48] Coletta, C., Study of growth mechanism of conducting polymers by pulse radiolysis. Ph.D thesis 2016, 37.

[49] Marignier, J. L.; de Waele, V.; Monard, H.; Gobert, F.; Larbre, J. P.; Demarque, A.; Mostafavi, M.; Belloni, J., Time-resolved spectroscopy at the picosecond laser-triggered electron accelerator ELYSE. Radiation Physics and Chemistry 2006, 75 (9), 1024-1033.

[50] Connelly, N. G.; Geiger, W. E., Chemical Redox Agents for Organometallic Chemistry. Chem. Rev. 1996, 96 (2), 877-910.

[51] Bredas, J. L.; Street, G. B., Polarons, bipolarons, and solitons in conducting polymers. Accounts of Chemical Research 1985, 18 (10), 309-315.

[52] Dazzi, A. P., R.; Glotin, F.; Ortega, J. M., Local infrared microspectroscopy with subwavelength spatial resolution with an atomic force microscope tip used as a photothermal sensor. Optics Letters, 2005, 30 (18), 2388-2390.

[53] Policar, C.; Waern, J. B.; Plamont, M.-A.; Cle`de, S.; Mayet, C.; Prazeres, R.; Ortega, J.-M.; Vessie`res, A.; Dazzi, A., Subcellular IR Imaging of a Metal–Carbonyl Moiety Using Photothermally Induced Resonance. Angew. Chem., Int. Ed. 2011, 50 (4), 860–864.

[54] Dazzi, A.; Prater, C. B.; Hu, Q. C.; Bruce Chase, D.; Rabolt, J.; F.; Marcott, C., AFM–IR: Combining atomic force microscopy and infrared spectroscopy for nanoscale chemical characterization. Appl. Spectrosc. 2012, 66, 1365−1384.

[55] Smits, F. M., Measurement of Sheet Resistivities with the Four-Point Probe. Bell System Technical Journal 1958, 37, 711-718.

[56] Ghosh, S.; Remita, H.; Ramos, L.; Dazzi, A.; Deniset-Besseau, A.; Beaunier, P.; Goubard, F.; Aubert, P. H.; Brisset, F.; Remita, S., PEDOT nanostructures synthesized in hexagonal mesophases. New Journal of Chemistry 2014, 38 (3), 1106-1115.

Chapter 3: Radiation chemistry as a new method for the synthesis of PEDOT: a state of the art

As is mentioned before, the synthesis of conducting polymers (CPs) with radiation method has been developed by Samy Remita's team. Synthesis of conducting poly(3,4-ethylenedioxythiophene) (PEDOT) was achieved through an original soft alternative way: gamma (γ) radiolysis of aerated aqueous solutions of 3,4-ethylenedioxythiophene (EDOT) in the absence of any external chemical initiators. Then, the original radiolytic methodology was extended to the synthesis of PEDOT polymers in N_2O-saturated aqueous solutions of EDOT. In addition, pulse radiolysis was used to study the mechanism of HO•-induced polymerization of PEDOT where a step-by-step mechanism has been found. Even if this preliminary work began before my joining Samy Remita's group and it was not exclusively carried out for my thesis. In fact, I took part in this research work and made some of the experiments related below.

3.1 Synthesis of CPs by an alternative radiolytic methodology

Contrarily to chemical and electrochemical methods, radiolytic methodology, which is based on the interaction of high energy ionizing radiations with matter, is not really used in the field of conducting polymers. It is well known that gamma (γ-) rays and X-rays radiolysis are very often used at ambient temperature and pressure in order to initiate, in the absence of external chemical initiators, oxidation or reduction reactions through the control of the initiator radicals which depend on the nature of the medium (atmosphere, solvent, potential solute).[1-4] Besides, radiolysis is known as an interesting method for the synthesis of non-conducting polymers and is also described as an alternative way leading to the formation of layers of controlled thickness at the interfaces.[5-7] Using radiolysis should also lead to chemical processes which can be switched on and off upon exposure or removal of ionizing radiation instead of using initiator or stopper molecules.

Despite all these advantages, only few works concerning both radiation chemistry and conducting polymers have been reported. Moreover, the preparation of CPs using gamma irradiation was always accompanied by the addition of chemical oxidants. Karim *et al.* synthesized PPy using γ radiation induced oxidative polymerization with ammonium peroxy-

disulfate (APS) as chemical oxidant.[8] Similarly, Pillalamarri *et al.* used γ radiolysis to synthesize PANI nanofibers in the presence of APS.[9] However, the radiolysis method has never been used alone for the synthesis of CPs.

Starting from monomers dissolved in water, a simple γ-rays-based radiolytic way which enables the synthesis of conducting polymers under air at room temperature, and contrarily to the chemical routes, in the absence of any external chemical initiators, was described for the first time. In addition, when compared with the usual electrochemical methods, this new γ-rays-based radiolytic way presented some advantages concerning the easy preparation of the samples, where no supporting electrolyte was needed, and the ability to work under atmospheric conditions without purging solutions with an inert gas. Besides, contrarily to the electrochemical way which leads to the direct deposition of CPs onto conducting substrates, the described radiolysis method leads to the formation of CPs dispersed in water enabling their further deposition over conducting or even non-conducting surfaces.

3.2 Gamma radiation induced PEDOT polymerization under air

3,4-ethylenedioxythiophene (EDOT) molecules are soluble in water and present some specific chemical properties which make them interesting building blocks for the synthesis of functional π-conjugated systems such as PEDOT (Figure 2.2, chapter 2).

In fact, due to their strong electron donor effect, the ether groups at the β and β' positions of thiophene rings, which confer a high reactivity to the free α and α' positions, prevent the formation of parasite α-β' linkages during polymerization. PEDOT acquires a prominent position among various CPs due to moderate band gap and low oxidation potential conferring on PEDOT an exceptional stability to the oxidized charged state which furthermore exhibits high conductivity and good optical properties in the visible spectral region.[10]

3.2.1 Solutions preparation and gamma irradiation under air

Aqueous solutions of different concentrations of EDOT ranging between 1 and 10 mM were first prepared at room temperature in the presence (for comparison with electrochemically synthesized PEDOT polymers) or in the absence of $LiClO_4$ (100 mM) and then irradiated under

air with increasing doses up to 70 kGy in order to radiosynthesize PEDOT polymers. The γ-ray dose rate was 1.4 kGy·h^{-1} in all cases. Irradiations were carried out with a ^{60}Co γ-rays source. EDOT concentrations higher than 10 mM have not been studied because of the limited solubility of EDOT in water and because of the possible direct ionization of EDOT molecules which could occur during radiolysis.[11]

In the presence of air, H• atoms and solvated electrons (e_{aq}^-) are scavenged by molecular oxygen O_2 to produce respectively perhydroxyl radicals ($HO_2^•$) and superoxyde radicals ($O_2^{•-}$) which are the two acido-basic forms of the couple $HO_2^•/O_2^{•-}$ (pKa ($HO_2^•/O_2^{•-}$) = 4.8 at 298 K).[12] As a consequence, when irradiating aerated aqueous solutions at neutral pH, as in the case of EDOT solutions (initial pH = 7.2), only two short-lived transient species are formed: hydroxyl radicals (HO•) and $O_2^{•-}$ with radiolytic yields of 2.8×10^{-7} mol J^{-1} (equation 2.12, chapter 2) and 3.4×10^{-7} mol J^{-1} (equation 2.13, chapter 2).

Note that when sodium formate (HCOONa) at a concentration of 100 mM is added to aerated aqueous solutions, hydroxyl radicals are quantitatively scavenged by formate anions leading to $COO^{•-}$ radicals which are subsequently oxidized into $O_2^{•-}$. Then in the presence of formate ions, the radiolytic yield of formation of $O_2^{•-}$ reaches the value of 6.2×10^{-7} mol J^{-1}.

Since protons are formed during γ-radiolysis, steady-state irradiation leads to a continuous pH decrease. As a consequence, when the pH of the solution becomes lower than 4.8 ((pKa ($HO_2^•/O_2^{•-}$) value), $HO_2^•$ radicals become predominant. Then below pH = 4.8, the two species which must be considered are HO• and $O_2^{•-}$. It is noted that even at very low pHs, EDOT molecules remain stable. In particular, no acid hydrolysis could affect the etheroxyde groups in EDOT.

3.2.2 Mechanistic study of EDOT oxidation

It is clear that EDOT in water displays two absorption maxima at 235 and 255 nm as shown for a concentration of 1 mM in EDOT (Figure 3.1).[13] From varying EDOT concentration, two molar extinction coefficients at these wavelengths are estimated:

$$\varepsilon_{235} = 5650 \pm 10 \text{ L mol}^{-1} \text{ cm}^{-1} \quad \varepsilon_{255} = 7048 \pm 200 \text{ L mol}^{-1} \text{ cm}^{-1} \tag{3.1}$$

These absorption maxima and the corresponding values of the extinction coefficients are consistent with literature data concerning heteroaromatic compounds, in particular with those of thiophene (which absorbs at 231 nm in hexane with ε_{231} = 7100 L mol^{-1} cm^{-1}) and its derivatives.[14] In addition, auxochromic substitution (by the ethylenedioxy group) in EDOT which should lead to a bathochromic effect can explain the shift of the absorption maximum from 231 to 255 nm.

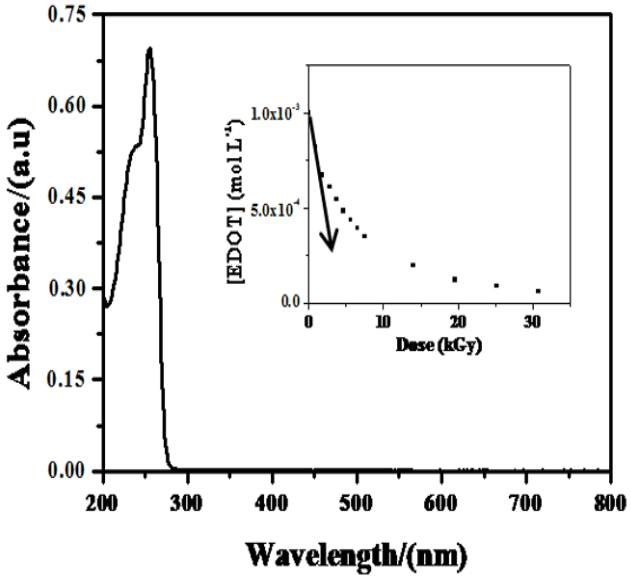

Figure 3.1 UV-vis absorption spectrum of an aqueous solution containing 1 mM in EDOT. The optical path length was 0.1 cm. The reference was water. Insert: variation of EDOT concentration as a function of the dose. The initial radiolytic yield of EDOT consumption corresponds to the initial slope of the curve.[13]

Aqueous solutions containing 1 mM in EDOT were irradiated at increasing doses up to 30 kGy. The evolution of the UV-visible absorption spectrum of this solution as a function of the irradiation dose displays a continuous decrease in the absorption at 235 and 255 nm indicating the progressive consumption of EDOT. From the two previously calculated values of the extinction coefficients at 235 and 255 nm, the variation in EDOT concentration with the dose is deduced (Insert of Figure 3.1). At the first steps of irradiation, this consideration is correct since EDOT remains predominant. Nevertheless, these as-calculated concentrations are necessary overestimated at high doses since, in addition to EDOT, other species may also absorb in the UV part of the spectrum.

Starting from 1 mM in EDOT, insert of Figure 3.2 displays the variation of EDOT concentration as a function of the irradiation dose. The initial radiolytic yield of EDOT consumption, $G_{-EDOT\ 0}$, is given by the value of the initial slope of the curve which can be deduced thanks to an exponential fit of the experimental curve:

$$G_{-EDOT\ 0}\,(\text{mol J}^{-1}) = -\left(\frac{\text{d[EDOT] (mol L}^{-1})}{\text{dDose (Gy)}}\right)_0 = 2.7 \times 10^{-7}\ \text{mol J}^{-1} \tag{3.2}$$

Note that the same value of the yield is obtained when considering only the first points of the experimental curve (up to 7 kGy). Thanks to our experimental results, it is found that:

$$G_{-EDOT\ 0} = G_{HO\bullet} \tag{3.3}$$

Also, when irradiations were performed in the presence of 100 mM in formate ions, which are scavengers of HO• radicals, no consumption of EDOT was observed. These results first indicate that a concentration of 1 mM in EDOT is sufficient to scavenge all the hydroxyl radicals and second demonstrate that only hydroxyl radicals react with EDOT. Indeed, since the apparent standard redox potential at pH = 7 amounts to $E°(HO\bullet/H_2O) = 2.2\ V_{SHE}$, HO• is a strong oxidizing species enables oxidation of EDOT.[12] On the contrary, $O_2^{\bullet-}$ is almost a poor oxidizing species with a redox potential $E°(O_2^{\bullet-}/H_2O_2) = 0.9\ V_{NHE}$.[12] As a consequence, the relatively low apparent redox potential of $O_2^{\bullet-}$ does not allow the reaction with EDOT the oxidation potential of which amounts to $1.4\ V_{Ag/AgCl}$.[15]

Note that with increasing dose, due to the increase in H_3O^+ amount, the medium becomes more acidic. As a consequence, when the pH of the solution becomes lower than 4.8 (pKa ($HO_2^{\bullet}/O_2^{\bullet-}$) value) which is the case after an irradiation of a few kGy, $HO_2^{\bullet}$ radical (perhydroxyl radical), which is known to be a strong oxidant, becomes predominant and its implication in EDOT oxidation processes couldn't be neglected.[12]

The reactivity of hydroxyl radicals towards thiophene (Th) molecules has already been studied by pulsed radiolysis.[16] It has been found that HO• radical adds preferentially to the α position in Th leading to a short-lived α-hydroxythienyl (Th-OH)• radical. This latter subsequently undergoes a second order radical-radical reaction with itself to produce α, α'-bithiophene which

absorbs at both 246 and 301 nm. On another hand, for α-thiophene oligomers in chloroform solution, the wavelengths values of the absorption maxima have been shown to increase with the number (n) of thiophene units: from 305 nm for n = 2 to 350~450 nm for n comprised between 3 and 8.[17]

In this work, whatever EDOT concentration ranging from 1 to 10 mM, EDOT disappearance parallels the formation of species which absorb at both 290 and 350 nm as shown in the case of 10 mM in EDOT (Figure 3.2).[13]

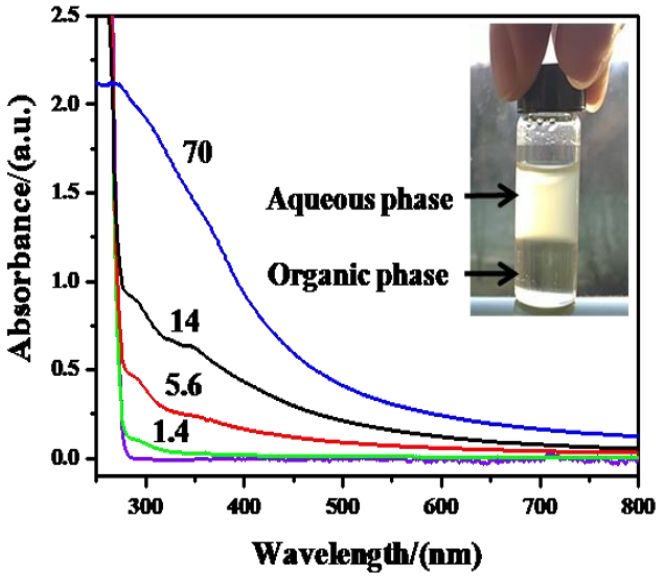

Figure 3.2 Absorption spectra of an aqueous solution containing 10 mM in EDOT irradiated with increasing doses: 0, 1.4 kGy, 5.6 kGy, 14 kGy and 70 kGy. The optical path length was 0.1 cm. The reference was water. Insert: image of the aqueous EDOT solution irradiated at 70 kGy after the addition of dichloromethane as a denser organic phase (v/v): PEDOT suspension remains in the upper aqueous phase.[13]

These absorption maxima should be attributed to dimers and oligomers of EDOT which could be formed according to the following mechanism:[13,18]

$$EDOT + HO^{\bullet} \rightarrow (EDOT\text{-}HO)^{\bullet} \text{ or } EDOT^{\bullet+} + HO^{-} \quad (3.4)$$

$$2\,(EDOT\text{-}HO)^{\bullet} \text{ or } 2EDOT^{\bullet+} \rightarrow \text{dimers then oligomers} \quad (3.5)$$

First, HO• adds to the α position in EDOT leading to the oxidized (EDOT-HO)• or abstracts electron from EDOT leading to $EDOT^{\bullet+}$ radical cation which are not observable by steady-state radiolysis. Then, the adduct or radical cation reacts with itself leading to dimers (and afterwards to oligomers) which absorb at both 290 and 350 nm. Once again, auxochromic substitution (by the ethylenedioxy group) in EDOT dimers can explain the shift in their absorption maxima as compared with those of bithiophene molecules (246 and 301 nm).[16]

As observed in insert of Figure 3.1, the yield of EDOT oxidation, $G_{\text{-EDOT }0}$ decreases with the dose and becomes much lower than G_{HO}. at high doses. This is because of the competitive reactions of hydroxyl radicals with EDOT dimers and oligomers which take place in the medium and which become more and more preponderant as the amount of EDOT decreases. Indeed, the oxidation potential of the dimers and the oligomers is lower than that of the monomers enabling their oxidation by hydroxyl radicals. So the process of oxidative coupling of the units continues as the polymer grows.[19]

Different aqueous solutions with EDOT concentrations higher than 1 mM were irradiated at increasing doses. For each initial EDOT concentration, the initial yield of EDOT oxidation is calculated and it is almost constant with the following mean value:

$$G_{\text{-EDOT }0} = 2.7 \pm 0.2\ 10^{-7}\ \text{mol J}^{-1} \tag{3.6}$$

The fact that the yield of EDOT consumption does not depend on the initial EDOT concentration demonstrates that the process which will be attributed to PEDOT radioinduced synthesis does not proceed through a chain reaction.[12] In particular, (EDOT-OH)• adduct or $EDOT^{\bullet+}$ radical cation does not react with EDOT. This is consistent with the pulsed radiolysis results obtained in literature in the case of thiophene monomers and with the results we obtained and which will be presented later in this chapter.[16] Indeed, it has been demonstrated that the reaction between (Th-OH)• adduct and Th does not take place since it is too slow.

As a consequence, PEDOT radioinduced synthesis could only proceed through a recurrent HO• oxidation process: HO• reacts with EDOT monomers, then with dimers, then with oligomers. The quantitative synthesis of PEDOT polymers throughout such a step-by-step mechanism necessarily implies the use of two HO• radicals for the oxidation of one EDOT molecule (in α and α' positions). Thus, the theoretical irradiation dose (D_{max}) which should lead to the total

oxidation of EDOT into PEDOT can be calculated (equation 2.22, chapter 2). For instance, 7.4 kGy and 74 kGy are necessary for the total oxidation of 1 and 10 mM in EDOT respectively.

3.2.3 Highlighting PEDOT radioinduced synthesis

While relatively low concentrations in EDOT monomers up to 4 mM were needed for succeeding in the follow-up of their oxidation mechanism by UV-vis absorption spectroscopy, higher concentrations were necessary for the characterization of PEDOT polymers either in aqueous solution or after their deposition onto substrate as it will be presented in the case of 10 mM in EDOT.

Aqueous solutions containing 10 mM in EDOT were irradiated at increasing doses up to 70 kGy. The evolution of the UV-visible absorption spectrum of this solution as a function of the irradiation dose was shown (Figure 3.2).[13] In the present case (10 mM in EDOT) with the used optical path length (0.1 cm), EDOT disappearance couldn't be quantified nor observed due to the relatively high values of the molar extinction coefficients at 235 and 255 nm. Nevertheless, at 70 kGy (which is close to the supposed D_{max}) the presence of a shoulder in the spectrum around 250 nm should indicate that EDOT has almost completely disappeared.

From the beginning of the irradiation and as already described in the case of 1 mM in EDOT, two absorption bands attributable to EDOT dimers and oligomers appear and grow up at 290 and 350 nm giving to the solution a yellow coloration. Nevertheless, with the increase in the irradiation dose no clear shift to longer wavelengths is observed for the absorption maxima. Only, a continuous scattering whose intensity increases with irradiation dose is observed. This is explained as follows: a yellow suspension appears in the medium and is clearly noticeable for doses higher than 14 kGy. This suspension becomes denser and the solution more turbid as the irradiation dose increases. As it will be demonstrated thanks to ATR-FTIR spectroscopic measurements, this suspension corresponds to PEDOT polymers formed at high doses thanks to the recurrent step-by-step HO• oxidation process.

The turbid solution obtained after a 70 kGy irradiation was centrifuged in order to recuperate a polymer-containing solid phase. The isolated yellow powder was washed, lyophilized and then characterized by ATR-FTIR spectroscopy in order to investigate the structure of the obtained polymer and to confirm the presence of PEDOT.

The ATR-FTIR spectrum of the radiosynthesized polymer is presented (Figure 3.3, spectrum a) in the wavenumber region 1550-600 cm^{-1} together with those of electrosynthesized PEDOT (Figure 3.3, spectrum b) and of pure non irradiated EDOT liquid sample (bottom of Figure 3.3).[13] Note that the difference between the intensity of polymers spectra (a and b) and the intensity of EDOT spectrum results from the types of deposition on the ATR-FTIR crystal. The deposition of EDOT liquid phase is translated by a better resolution when compared with the solid phase deposition of polymer films.

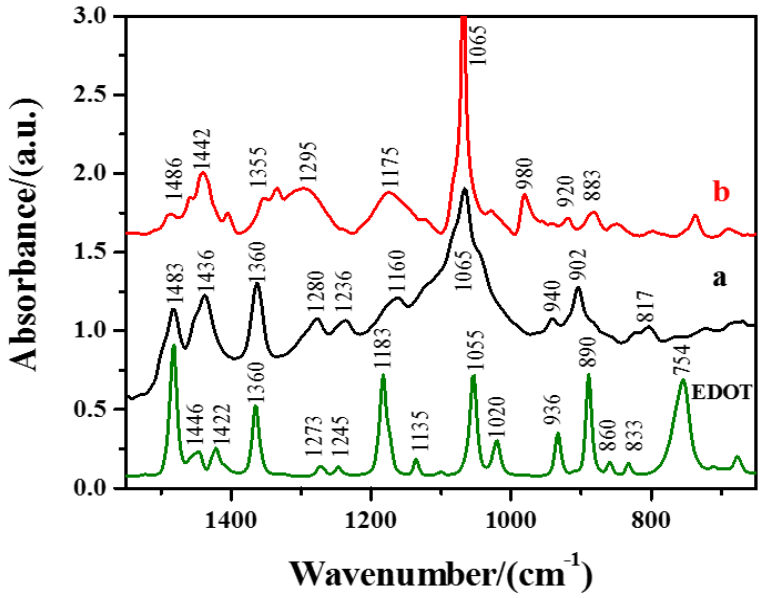

Figure 3.3 ATR-FTIR spectra of pure EDOT (lower spectrum), 70 kGy-radiosynthesized PEDOT isolated after centrifugation, washing and lyophilisation steps (spectrum a) and electrosynthesized PEDOT formed by chronoamperometry during 30 sec (spectrum b).[13]

The three obtained spectra are in good agreement with those previously reported for EDOT and PEDOT in literature.[20-23] In addition, no considerable differences exist between spectrum a and spectrum b. Only small shifts in the vibration modes can be observed. Starting from what is known in literature about EDOT and electrosynthesized PEDOT, vibrations at 1483, 1436 and 1360 cm^{-1}, observed in spectrum a, can be attributed to the stretching modes of C=C and C-C in the thiophene ring. The vibrations at 1280, 1236, 1160 and 1065 cm^{-1} can be assigned to the stretching modes of the ethylenedioxy group (C-C and C-O-R-O-C) while the vibration modes of the C-S bond which is present in the thiophene ring can be observed at 940, 902 and 817 cm^{-1}.

All these bands are present in the spectra of Figure 3.3 even if they appear relatively slightly displaced.

Whereas the (C-H) stretching band at 754 cm^{-1} is clearly observed in EDOT spectrum, one can observe the absence of such a band in the spectrum of radiosynthesized PEDOT polymers (Figure 3.3, spectrum a).[13] Thus, spectroscopic results demonstrate without any ambiguity that EDOT radioinduced polymerization takes place thanks to α-α' coupling reactions, as in the case of electrochemically induced method, and that the resulting yellow powder obtained after centrifugation is effectively composed of PEDOT polymers. Nevertheless, since the powder was washed before its characterization, the absence of the stretching band at 754 cm^{-1} can't definitely prove the total consumption of EDOT after a 70 kGy-irradiation.

The PEDOT nature of the radiosynthesized polymer which composes the solid phase was also proved thanks to the determination of its melting point. Indeed, a temperature of 145 °C was observed which is very close to the PEDOT melting point value (146 °C) reported.[24] This result should also prove the absence of impurities in our product.

After irradiation at high doses (from 14 to 70 kGy) (Figure 3.2), a very slow precipitation of the polymer suspension is observed. This precipitation corresponds to a sedimentation process of the radiosynthesized PEDOT polymers of high molecular weight. This precipitation can't be assigned to the hydrophobia of radiosynthesized polymers. Indeed, after adding either cyclohexane (density = 0.8) or dichloromethane (density = 1.3) to the aqueous PEDOT suspensions (v/v), the polymer particles stay in the aqueous phase while both organic phases remain colourless as illustrated in the case of dichloromethane (Insert of Figure 3.2) confirming the hydrophilic properties of radiosynthesized PEDOT. Besides, hydrophilic properties of PEDOT polymers have already been established since it has been demonstrated that they can interact by hydrogen bonds with water molecules thanks to the ethylenedioxy functions present onto their EDOT residues.[15,25] On another hand, if HO• hydroxyl radicals would react, according to a previously proposed recurrent oxidation process, radiosynthesized PEDOT polymers should contain along their polymeric chains, in agreement with ATR-FTIR observations, numerous –OH hydroxyl groups which should enhance their hydrophilic properties.

Aqueous solutions containing 10 mM in EDOT and irradiated at 70 kGy were observed by Cryo-transmission electron microscopy just after irradiation and before any sedimentation. Representative images showed the presence of low density globular structures forming

polydisperse spherical nanoparticles with a mean diameter of 200 nm (Figure 3.4).[13] Since no other low density objects were observed during our Cryo-TEM experiments, it can be deduced that these spherical nanoparticles are made up of radiosynthesized PEDOT polymers.

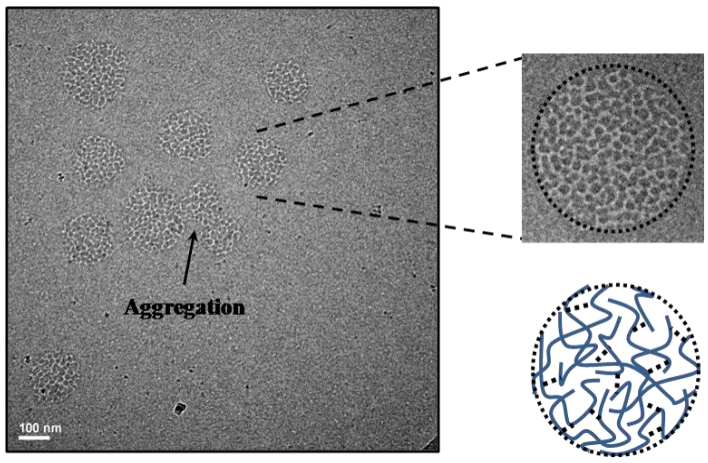

Figure 3.4 Cryo-TEM image of an aqueous sample containing 10 mM in EDOT irradiated at 70 kGy. It exhibits spherical low density objects with a mean diameter of 200 nm attributed to self-assembled hydrophilic PEDOT polymers. An aggregation process of these spherical objects is also observable. Zoom: a single spherical polymer nanoparticule with its schematic representation exhibiting hydrogen bonds interactions between the chains.[13]

Each observed nanoparticle has a complex structure and seems to be composed of interdigitated nano-objects (zoom of Figure 3.4). Since no parasite α-β' linkages could occur during polymerization, radiosynthesized PEDOT must be composed of chain polymers which are no branched nor networked. Thus, each globular structure observed on Figure 3.5 should correspond to a self-assembly of independent amorphous PEDOT polymer chains as schematically represented on Figure 3.5. This is in agreement with the usual morphology of the polymers in the amorphous state which follows the "random coil" model.[26] Once again, the probable simultaneous presence of both ethylenedioxy functions (H-bond acceptors) and hydroxyl groups (H-bond donors) along the polymer chains should explain not only the hydrosolubility and the solvation of PEDOT polymers but also the packing and the nano-structuration of the observed spherical supramolecular PEDOT self-assemblies.

Intermolecular hydrogen bonds should also explain the aggregation process of the globular radiosynthesized PEDOT self-assemblies observed on Figure 3.4. This spontaneous aggregation process explains the polydispersity of the system as well as the formation of polymer self-

assemblies of high molecular weight which afterwards slowly precipitate. In order to characterize the morphology of the polymers after a deposition procedure, a drop of the solution containing the PEDOT yellow suspension obtained after a 70 kGy-irradiation (polymer self-assemblies of Figure 3.5) was deposited onto gold substrate and dried. The surface was then imaged by dynamic mode Atomic Force Microscopy (Figure 3.5).[13]

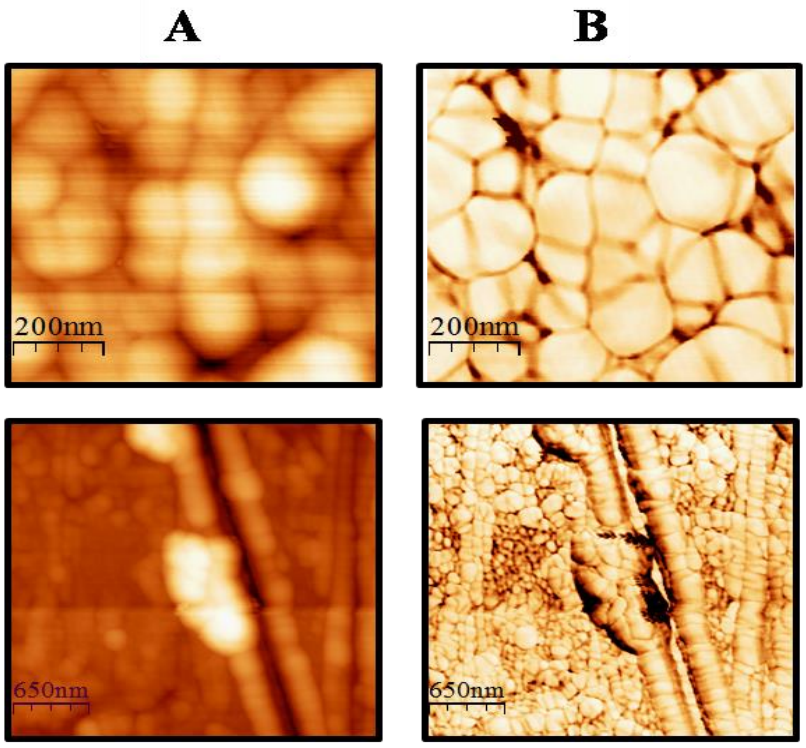

Figure 3.5 AFM topography (**A)** and phase contrast (**B)** images in dynamic mode of PEDOT nanostructures obtained after irradiation at 70 kGy and deposition onto gold substrates. Both kinds of images are displayed at two different scales.[13]

Topography and phase contrast images in dynamic mode of radiosynthesized PEDOT polymers indicate the presence of very close-packed spheroid polymeric nanoparticles (Figure 3.5). Nevertheless, as observed from bottom images of Figure 3.5, a preferential linear packing is observable which leads to some self-assemblies with fibrillar morphologies. Note that in the present work phase images are only used to reinforce the contrast of topography ones.

The nanoparticles observed by AFM after deposition should come from the globular structures already observed in aqueous solution by Cryo-TEM (Figure 3.4). Then, as previously mentioned,

each nanoparticle should be made up of self-assembled PEDOT chain polymers. The packing of the particles and their flattening onto the substrate when deposited then dried should explain the more or less spherical shape of the nanoparticles and could also explain the polydispersity in size observed on Figure 3.5.

As deduced from upper images of Figure 3.5, the diameter of the particles ranges from 100 to 200 nm which is not far from the mean diameter of the globular structures observed in solution by Cryo-TEM. Two explanations could be proposed. First possibility: the nano-objects observed in solution and onto gold substrates (respectively by Cryo-TEM and AFM) are strictly the same. This would imply the existence of very strong hydrogen-bonds interactions into each nanoparticle since no significant change in the morphology occurs during the isolation and the drying process. Second possibility: the mass lost of each globular nanostructure during its drying process is counterbalanced by an increase in size due to the aggregation which generally parallels such a phase transition.

3.2.4 Conclusions

For the first time, a new γ-radiolysis-based alternative way for synthesizing conducting polymers in solution was successfully developed. When compared with the usual electrochemical methods, this methodology allows the further deposition of the polymers onto either conducting or non-conducting surfaces. Starting from EDOT monomers, the radiolytic methodology enabled the preparation of PEDOT polymers under soft conditions: in water, at ambient temperature, in the presence of air and in the absence of any external oxidizing species. The synthesized PEDOT materials were evidenced by ATR-FTIR spectroscopy.

It was proved that radioinduced polymerization proceeds through a step-by-step mechanism which involves a recurrent oxidation process by hydroxyl radicals produced by water radiolysis. The probable presence along the polymeric chains of –OH functionalities, which should come from the addition of hydroxyl radicals, could explain the hydrophilic properties of radiosynthesized PEDOT polymers. It could also justify the existence in aqueous solution of the globular self-assembled structures made up of PEDOT polymeric chains which have been observed for the first time, in this work, thanks to Cryo-TEM experiments.

After deposition onto substrate, radiosynthesized PEDOT films are composed of more or less spherical PEDOT nanoparticles as revealed by AFM observations. While radiosynthesized PEDOT-containing layers present optical properties which are close to those of electrosynthesized PEDOT materials, their conducting efficiency remains relatively lower (results not shown).[13] This could result from the –OH functionalization of radiosynthesized PEDOT chains which should induce conformational constraints due to hydrogen bonds interactions.

3.3 Effect of oxidizing species on radiation-induced synthesis of PEDOT

As is mentioned before, γ-radiolysis is used as an original simple alternative way for synthesizing conjugated PEDOT polymers in solution for the first time.[13] It is demonstrated that radiation induced PEDOT polymerization proceeds through a recurrent step-by-step mechanism which involves a recurrent oxidation process by hydroxyl radicals formed during water radiolysis. This new γ-rays-based radiolytic way presents some advantages concerning the easy preparation of the samples, where no supporting electrolyte is needed, and the ability to work under atmospheric conditions without purging solutions with an inert gas. Besides, contrarily to the electrochemical way which leads to the direct deposition of CPs onto conducting substrates, radiolysis method leads to the formation of CPs dispersed in water enabling their further deposition over conducting or even non-conducting surfaces.

In this part, the original radiolytic methodology is extended to the synthesis of PEDOT polymers in N_2O-saturated aqueous solutions of EDOT.[27] In these conditions, and depending on the presence of sodium azide salt, two different oxidizing species are formed, namely hydroxyl radicals) (HO•) and azide radicals ($N_3^{\bullet}$). Since the redox potentials of these two oxidative radicals (which are higher than that of EDOT monomers) and since their well-known oxidation mechanisms are quite different, one can expect the formation of two kinds of PEDOT polymers with tuned characteristics. Thus the aim of this work is the study of the influence of the oxidation mechanism onto the structure and the properties of PEDOT polymers. Since the role of polymerization mechanism is poorly investigated in literature in the field of conducting materials, the present study is certainly important in order to optimize the general preparation of nanostructured conducting polymers and in order to enhance their physico-chemical properties.

3.3.1 Solutions preparation and gamma irradiation under N_2O

Aqueous solutions containing 1mM or 10 mM in EDOT were prepared in the presence or in the absence of NaN_3 (10 mM for 1mM in EDOT or 100 mM for 10 mM in EDOT), under stirring, at room temperature and in the dark to prevent any photochemical reaction. The chosen EDOT concentration, which is lower than its solubility in water, was always checked by UV-vis absorption spectroscopy since the spectrum of EDOT had earlier been determined (ε_{235} = 5650 L mol^{-1} cm^{-1}, ε_{255} = 7048 ± 200 L mol^{-1} cm^{-1}).[11,13] The pHs of the solutions measured before irradiation, in the presence or in the absence of NaN_3, were found to be close to 7. Note that no drastic change in the pH was observed after irradiation. All the solutions were deaerated by bubbling with nitrous oxide (N_2O) and then irradiated with increasing doses up to 70 kGy in order to radiosynthesize PEDOT polymers.

In aqueous solutions saturated by nitrous oxide (25 mM in N_2O), e_{aq}^- are quantitatively and immediately converted into HO• (reaction 2.14, chapter 2). As a consequence, when irradiating N_2O-saturated aqueous solutions at neutral pH, as in the case of our EDOT solutions, only two short-lived transient species are formed: HO• and H• (hydrogen atoms). The radiolytic yield of formation of HO• becomes 5.6×10^{-7} mol J^{-1} (equation 2.15, chapter 2).

In aqueous solutions containing sodium azide (NaN_3 at 10 mM or 100 mM, dissociated into Na^+ and N_3^- ions) and saturated by nitrous oxide, HO• radicals are very quickly scavenged by N_3^- ions leading to the quantitative formation of $N_3^\bullet$ (reaction 2.16, chapter 2). In the presence of NaN_3, the concentration of EDOT monomers being always ten times lower than that of N_3^- ions, the direct oxidation of EDOT by HO• can be neglected. Thus, when irradiating N_2O-saturated aqueous solutions at neutral pH in the presence of NaN_3, as in the case of EDOT solutions, the radiolytic yield of formation of $N_3^\bullet$ amounts to 5.6×10^{-7} mol J^{-1} (equation 2.17, chapter 2). In these conditions, $N_3^\bullet$, which are known to be soft and selective oxidizing species, constitute 90% of the total amount of reactive radicals in the medium.[28] Note that H• can also react with N_3^- ions leading to $NH_2^\bullet$ radicals.[29] Nevertheless, the reactivity of these minority species, such as that of H•, has not been well established. This will allow us to neglect their presence.

In summary, depending on the presence of NaN_3 salt in the irradiated N_2O-saturated aqueous solutions of EDOT, two different oxidizing species can be generated: HO• or $N_3^\bullet$ radicals. Both are used in order to oxidize EDOT monomers into PEDOT polymers.

3.3.2 HO• and N_3• radicals induced EDOT oxidation

In the previous work, it is demonstrated that γ-irradiation (which produces both HO• and $O_2^{\bullet-}$) of aerated aqueous solutions containing EDOT molecules leads to the oxidation of these latter by hydroxyl radicals and to the synthesis of PEDOT polymers.

The yield of EDOT monomers consumption, which is strictly equal to the yield of HO• formation during the irradiation of aerated aqueous solutions of EDOT, does not depend on the initial monomers concentration.[13] This demonstrates that PEDOT radioinduced synthesis does not proceed through a chain reaction.[12] In fact, polymerization proceeds through a recurrent step-by-step mechanism which involves a repeated oxidation process by hydroxyl radicals formed during water radiolysis: HO• species react with EDOT monomers, then with dimers, then with oligomers. As a consequence, the quantitative synthesis of PEDOT polymers throughout such a step-by-step mechanism implies the use of two HO• radicals per EDOT molecule. Thus, the theoretical irradiation dose (D_{max}) which should lead to the quantitative formation of PEDOT in aerated aqueous solutions is twice the dose necessary for the total oxidation of EDOT monomers and can be calculated (equation 2.22, chapter 2).

As already explained and justified, under N_2O in the absence of NaN_3, HO• radicals can be considered as the only oxidizing species and their radiolytic yield of formation (G(HO•) = 5.6×10^{-7} mol J^{-1}) is increased in comparison with that obtained in aerated conditions ($G_{HO^\bullet}$ = 2.8×10^{-7} mol J^{-1}). In the absence of NaN_3, the total irradiation dose (D_{max}) which should enable the quantitative synthesis of PEDOT in N_2O-saturated aqueous solutions is thus twice the dose necessary for the total oxidation of EDOT monomers and, as a consequence, can be calculated as previously explained, but by using G(HO•) instead of $G_{HO^\bullet}$ (equation 2.15, chapter 2). In a N_2O-saturated aqueous solution containing 1 mM and 10 mM in EDOT, the dose which is necessary for the total oxidation of EDOT, amounts to 1.8 and 18 kGy respectively and the dose D_{max} which is necessary for the complete synthesis of PEDOT, amounts to 3.6 and 36 kGy, respectively.

In the absence of sodium azide salt, UV-visible absorption spectrum of N_2O-saturated aqueous solution containing 1 mM in EDOT irradiated at increasing doses up to 4 kGy was recorded (Figure 3.6).[27] The evolution of the UV-visible absorption spectrum of this solution as a function of the irradiation dose, up to 2 kGy, displays a continuous decrease in the absorption of EDOT at 235 and 255 nm which parallels a grow up in the absorbance at both 290 and 350 nm. The

presence of an isosbestic point indicates that a single process occurs up to 2 kGy, which implies EDOT oxidation by HO• radicals and the formation of a product which absorbs at both 290 and 350 nm. Since thiophene dimers are known to absorb at both 246 and 301 nm, the observed two absorption bands can be attributed to EDOT dimers.[16] Indeed, auxochromic substitution by the ethylenedioxy group in EDOT is responsible of the shift in its absorption maxima as compared with those of thiophene.[13] In the same way, auxochromic substitution could explain the difference in the absorption behavior between EDOT dimers and bithiophene molecules.

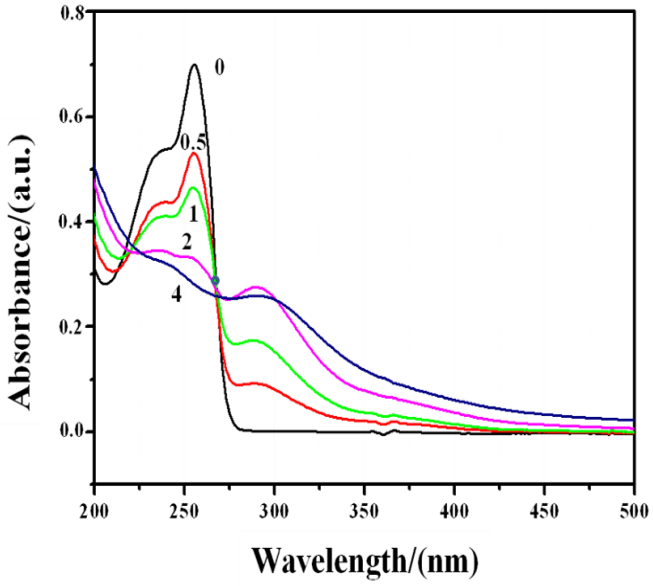

Figure 3.6 UV-visible absorption spectra of N_2O-saturated aqueous solution containing 1 mM in EDOT irradiated in the absence of NaN_3 with increasing doses: 0, 0.5, 1, 2 and 4 kGy. The optical path length was 0.1 cm. The reference was water. An isosbestic point is observed at lower doses.[27]

At 2 kGy, the residual absorption at 235 and 255 nm (Figure 3.6) indicates the quasi-total disappearance of EDOT, whose initial concentration was 1 mM. Now, 2 kGy is close to the dose (1.8 kGy) which enables the formation of 1 mM in hydroxyl radical thanks to water radiolysis. Therefore, as long as EDOT monomers are present in aqueous solution, hydroxyl radicals react exclusively with them. Yet, the oxidation potential of the dimers is always lower than that of the monomers enabling their further oxidation in particular by hydroxyl radicals.[19] Thus, the fact that hydroxyl radicals don't react with dimers at doses lower than 2 kGy could be explained by kinetic considerations: dimers oxidation should be very much slower than EDOT oxidation.

At doses higher than 2 kGy, the spectral evolution appears different (Figure 3.6): the isosbestic point is no longer observed and a progressive shift in the absorption bands occurs. Since at these doses, no EDOT is still present, such a spectral evolution indicates that hydroxyl radicals oxidize EDOT dimers, progressively leading to PEDOT oligomers. Such an interpretation is plausible since it has been shown in literature that the wavelengths values of the absorption maxima of α-thiophene oligomers increase with the number of thiophene units.[17]

While a concentration of 1mM in EDOT monomers was needed for succeeding in the follow-up of their oxidation mechanism, 10 mM in EDOT were necessary for the characterization of PEDOT polymers either in aqueous solution or after their deposition onto substrate. In the absence of sodium azide salt, N_2O-saturated aqueous solutions containing 10 mM in EDOT were irradiated at increasing doses up to 70 kGy. This latter dose is enough to ensure the total polymerization of EDOT (at 10 mM). The evolution of the UV-visible absorption spectrum of this solution as a function of the dose is displayed (Figure 3.7).[27]

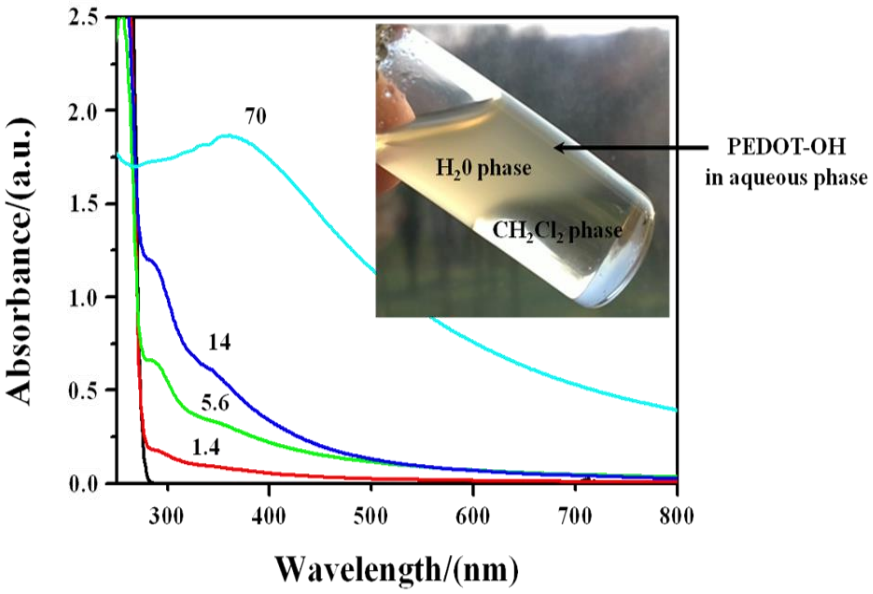

Figure 3.7 UV-vis absorption spectra of N_2O-saturated aqueous solution containing 10 mM in EDOT irradiated in the absence of NaN_3 with increasing doses: 0, 1.4, 5.6, 14 and 70 kGy. The optical path length was 0.1 cm. The reference was water. Insert: image of the aqueous solution irradiated at 70 kGy after the addition of dichloromethane as a denser organic phase (v/v): PEDOT-OH suspension remains in the upper aqueous phase.[27]

In the present case (10 mM in EDOT) and contrarily to the previous case (1 mM in EDOT), EDOT disappearance as well as the isosbestic point (observed on Figure 3.6) could not be observed due to the relatively high values of the molar extinction coefficients at 235 and 255 nm.[13] Nevertheless, as previously observed for 1 mM in EDOT, at low irradiation doses, up to about 20 kGy (the dose which produces 10 mM in hydroxyl radicals), two absorption bands grow up at 290 and 350 nm demonstrating the formation of dimers (Figure 3.7). In the present case (10 mM in EDOT) and contrarily to the previous case (1 mM in EDOT), EDOT disappearance as well as the isosbestic point (observed on Figure 3.6) could not be observed due to the relatively high values of the molar extinction coefficients at 235 and 255 nm.[13] Nevertheless, as previously observed for 1 mM in EDOT, at low irradiation doses, up to about 20 kGy (the dose which produces 10 mM in hydroxyl radicals), two absorption bands grow up at 290 and 350 nm demonstrating the formation of dimers (Figure 3.7).

Above 20 kGy, no absorption band is observed around 250 nm. This clearly indicates that EDOT has completely disappeared. When the dose becomes higher than the total irradiation dose, as observed in the case of the 70 kGy-irradiation (Figure 3.7), the absorption bands of dimers disappear and an intense absorption band grows up around 370 nm together with a continuous scattering whose intensity increases with irradiation dose. This should result from the lengthening of EDOT oligomers. In fact, at doses higher than 36 kGy, the appearance of a continuous scattering component, in the extinction spectrum of the irradiated solutions, is due to the formation in the bulk of a brown-yellow suspension. This suspension becomes denser and the solution appears more turbid as the irradiation dose increases. After the deposition of this suspension onto ITO substrate, the resulting film displays an intense absorption band at 550 nm. As it will be further demonstrated, this indicates that the suspension is made of polymers, noted PEDOT-OH, formed at high doses thanks to the recurrent step-by-step $HO^{\cdot}$ oxidation process.

After irradiation at high doses (from 36 to 70 kGy), a very slow precipitation of the suspension is observed. This precipitation corresponds to a sedimentation process of the PEDOT-OH polymers of relatively high molecular weights. This precipitation can't be assigned to the hydrophobia of radiosynthesized polymers. Indeed, after adding either cyclohexane or dichloromethane solvents to the aqueous suspensions (v/v) and after stirring and decantation, the polymer particles always remain in the aqueous phase while organic phases appear colourless as

illustrated in the case of dichloromethane (insert of Figure 3.7). This result proves the hydrophilic properties of PEDOT-OH polymers.

As previously explained, under N_2O and in the presence of NaN_3, HO• radicals are scavenged by N_3^- leading to $N_3^\bullet$ radicals which can then be considered as the only oxidizing species able to react with EDOT. $N_3^\bullet$ radicals are known as an alternative oxidizing system more selective than HO•. It is a soft one-electron oxidant $E°(N_3^\bullet/N_3^-) = 1.33\ V_{SHE}$ at pH=7 and it is used in this work for oxidizing EDOT.[30-32]

In the presence of sodium azide salt, N_2O-saturated aqueous solution containing 1 mM in EDOT was irradiated at increasing doses up to 4 kGy. The evolution at low doses of the UV-visible absorption spectrum of this solution as a function of the irradiation dose (results not shown) is similar to that obtained in the absence of azide salt even if the intensities of the spectra are somewhat different. Indeed, a continuous decrease in the absorption of EDOT parallels a grow-up in the absorbance at both 290 and 350 nm. Once again, the presence of an isosbestic point indicates that EDOT monomers are oxidized into dimers. This also proves that, such as hydroxyl radicals, $N_3^\bullet$ species are able to oxidize EDOT into dimers. In addition, as long as EDOT monomers remain present in aqueous solution, $N_3^\bullet$ reacts exclusively with them. The further formation of EDOT oligomers and polymers could be achieved only at higher doses. By analogy with the case of hydroxyl radicals, in the presence of NaN_3, the total irradiation dose (D_{max}) which should enable the quantitative synthesis of PEDOT in N_2O-saturated aqueous solutions is twice the dose necessary for the total oxidation of EDOT monomers and can be calculated as previously explained, but by using $G(N_3^\bullet)$ instead of $G_{HO\bullet}$ (equation 2.17, chapter 2). In a N_2O-saturated aqueous solution containing 10 mM in EDOT in the presence of azide salt, the dose which enables the total oxidation of EDOT amounts to 18 kGy and the dose D_{max} which is necessary for the complete production of PEDOT is then about 36 kGy.

In the presence of sodium azide salt, N_2O-saturated aqueous solutions containing a higher concentration in EDOT (10 mM) were irradiated at increasing doses up to 70 kGy. The evolution of the UV-visible absorption spectrum of this solution as a function of the dose is displayed (Figure 3.8).[27]

At low irradiation doses, up to about 20 kGy (the dose which produces 10 mM in azide radicals), two shoulders appear and grow up at 290 and 350 nm demonstrating the formation of dimers. When the dose becomes higher than the total irradiation dose, as observed in the case of

the 70 kGy-irradiation on Figure 3.8, the absorption bands of dimers disappear and a more intense absorption band grows up around 370 nm. Again, this should result from the lengthening of EDOT oligomers. Moreover, a brown-colored suspension is observable within the bulk which quickly deposits at the bottom of the solution. Note that the fast precipitation process, observed here, explains the absence of any scattering component in the extinction spectra of Figure 3.8. After the deposition of this suspension onto ITO substrate, the resulting film displays a broad absorption between 500 and 600 nm. As it will be further demonstrated, this indicates that the suspension is made of polymers, noted PEDOT-N_3, formed at high doses thanks to the $N_3^{\bullet}$-induced oxidation process.

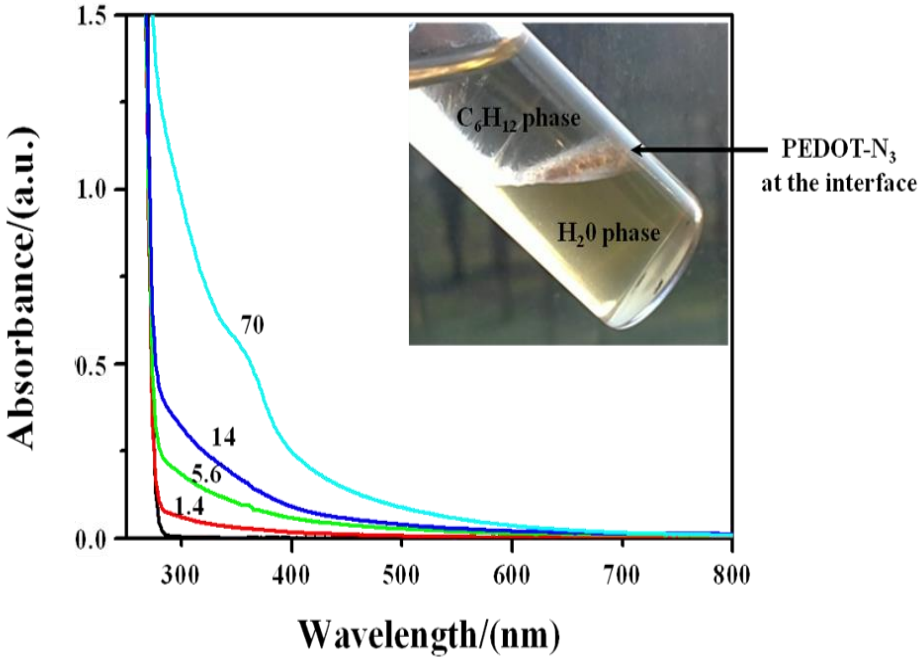

Figure 3.8 UV-vis spectra of N_2O-saturated aqueous solution containing 10 mM in EDOT irradiated in the presence of NaN_3 with increasing doses: 0, 1.4, 5.6, 14 and 70 kGy. The optical path length was 0.1 cm. The reference was water. Insert: image of the aqueous solution irradiated at 70 kGy after the addition of cyclohexane as a less dense organic phase (v/v): PEDOT-N_3 polymers remains at the interface between the two liquid phases.[27]

After irradiations at high doses (from 36 to 70 kGy), a precipitate is systematically observed. This precipitation is not only due to a sedimentation process of the PEDOT-N_3 polymers of relatively high molecular weight. It also results from the poor hydrophilic properties of these

systems. Indeed, after adding either cyclohexane or dichloromethane solvents to the aqueous suspensions (v/v) and after stirring and decantation, the polymer particles always remain at the organic solvent-water interface as illustrated in the case of cyclohexane (Insert of Figure 3.8). This result proves the amphiphilic properties of PEDOT-N_3 polymers. Note that at the interface, these polymers appear as clustered fibers.

One can note that, for the same initial concentration in EDOT (10 mM), the spectral evolution in the presence of NaN_3 (Figure 3.8) is similar to that observed in the absence of this salt (Figure 3.7). However, when comparing both evolutions, one can note that for a given irradiation dose, the maximal absorption is always lower in the presence of NaN_3. Even if hydroxyl radicals and azide radicals oxidize EDOT and induce polymerization through the formation of EDOT dimers, it seems that the two implied mechanisms are somewhat different. Maybe the kinetic growth of dimers, oligomers and polymers is slower in the case of $N_3^{\bullet}$. This would induce a lower polymerization yield and lower values of the maximal absorbance. However, such an interpretation is not in agreement with the observed dose effect. On another hand, the products of EDOT oxidation could be chemically and structurally different depending on $N_3^{\bullet}$ or HO• nature of the oxidizing radicals. This could explain the different spectral properties of the products obtained either in the presence or in the absence of azide salt. In addition, the poor hydrophilic properties of the products formed in the presence of NaN_3 lead to their deposition at the bottom of the solution and their adsorption onto the walls of the samples.

3.3.3 Characterization of PEDOT-OH and PEDOT-N_3

The ATR-FTIR spectra of PEDOT-OH and PEDOT-N_3 polymers, radiosynthesized at 70 kGy, which are similar to those obtained at 36 kGy, are presented in the wave number region 4000-700 cm^{-1} together with the spectrum of pure non irradiated EDOT (Figure 3.9).[27]

Between 1600 and 700 cm^{-1}, the three obtained spectra are in good agreement with those previously reported for PEDOT and EDOT in literature.[13,20-23] The vibrations at 1483, 1446 and 1360 cm^{-1} are attributed to the stretching modes of C=C and C-C in the thiophene ring, while those observed at 1280, 1236, 1160 and 1065 cm^{-1} are assigned to the stretching modes of the ethylenedioxy group (C-C and C-O-R-O-C). The vibration modes of the C-S bond which are

present in the thiophene ring can be observed at 940, 902 and 817 cm^{-1}. All these bands are present in all spectra of Figure 3.9 even if they appear relatively slightly displaced.

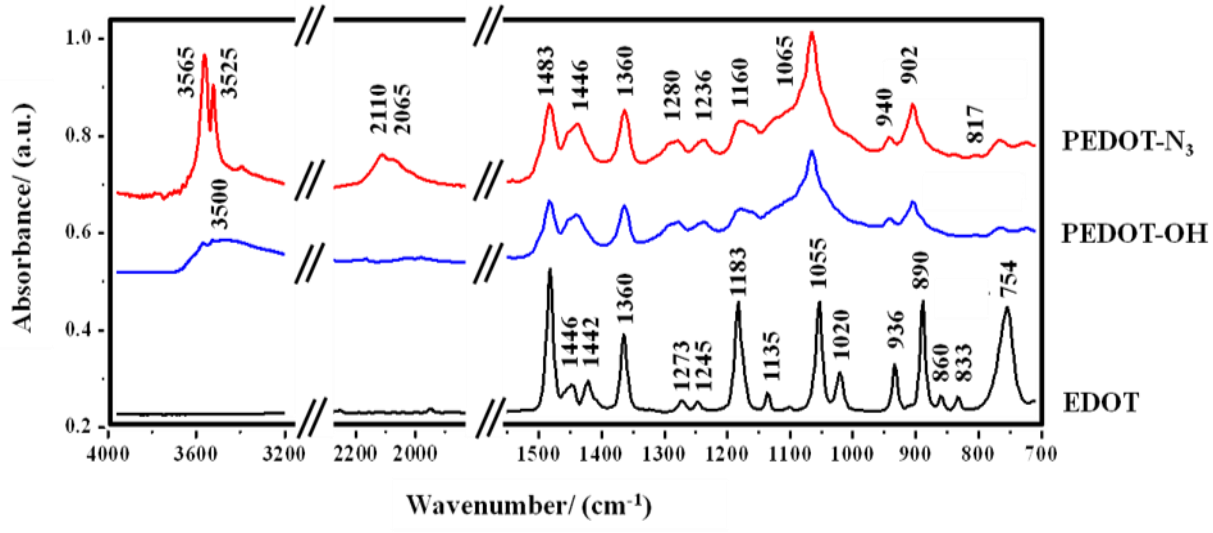

Figure 3.9 ATR-FTIR spectra of pure EDOT (lower spectrum) and of PEDOT polymers radiosynthesized at 70 kGy under N_2O atmosphere, both in presence (PEDOT-N_3) or in absence (PEDOT-OH) of NaN_3 salt, isolated after centrifugation and lyophilisation steps.[27]

The C-H stretching band at 754 cm^{-1} which is observed in EDOT spectrum, is clearly absent in the ATR-FTIR spectra of both radiosynthesized PEDOT polymers (Figure 3.9).[14] This demonstrates, without any ambiguity, that $N_3^{\bullet}$ and HO•-induced EDOT polymerizations have both taken place thanks to α-α' coupling reactions and that the resulting solid powders obtained after centrifugation are effectively composed of PEDOT polymers. Nevertheless, since the powders were centrifuged before their characterization, the absence of the C-H stretching band at 754 cm^{-1} can't prove here the total consumption of EDOT after a 70 kGy-irradiation.

The PEDOT nature of the radiosynthesized polymers, which compose the obtained solid phases was also proved thanks to the determination of their melting point after centrifugation and washing procedure. Indeed, it is found for both PEDOT-OH and PEDOT-N_3 a temperature of 145 ℃ which is very close to the PEDOT melting point value (146 ℃) already reported.[24] This result demonstrates the high purity of our products and thus the efficiency of our procedure.

Contrarily to the wave number region 4000-700 cm^{-1} where the spectra of PEDOT-OH and PEDOT-N_3 are very much alike, significant differences can be observed above 2000 cm^{-1}. Indeed,

the spectrum of PEDOT-OH exhibits a very large band between 3200 cm^{-1} and 3600 cm^{-1} while the spectrum of PEDOT-N_3 is characterized by an absorption in two different infrared regions: between 2110-2065 cm^{-1} and between 3565-3525 cm^{-1}.

In order to understand these spectral differences and to propose a reasonable interpretation, it is need to check the differences which exist between the chemical reactivity of hydroxyl radicals and azide radicals towards aromatic compounds, such as our EDOT monomers. In general, hydroxyl radicals add onto double bonds between two carbon atoms in aromatic molecules, while azide radicals lead to the formation of radical cations through electron abstraction as it has been demonstrated in the case of oxidized purines or in the case of tryptamine.[33,34] Note that depending on the pH, the OH-adducts may undergo a dehydration reaction giving the one-electron oxidized radicals.[33] Also, the reactivity of hydroxyl radicals towards thiophene molecules and of azide radicals towards pyrrole compounds was studied by pulsed radiolysis.[16] In agreement with all the previous results, it has been found that HO• radicals add preferentially to the α position in Th leading to (Th-HO)• adduct.[16] Differently, $N_3^{\bullet}$ abstract electrons of pyrrole derivatives leading to radical cations.[30] In our case and according to literature, EDOT monomers should then be oxidized by HO• and $N_3^{\bullet}$ radicals according to two different ways:

$$EDOT + HO\bullet \rightarrow (EDOT\text{-}HO)\bullet \qquad (3.6)$$

$$EDOT + N_3^{\bullet} \rightarrow EDOT^{\bullet+} + N_3^{-} \qquad (3.7)$$

Nevertheless, the reaction of HO• with EDOT which leads to $EDOT^{\bullet+}$ can't be excluded according to:

$$EDOT + HO\bullet \rightarrow EDOT^{\bullet+} + HO^{-} \qquad (3.8)$$

The (EDOT-HO)• hydroxyl adduct as well as the $EDOT^{\bullet+}$ radical cation subsequently undergo a second order radical-radical reaction with themselves to produce EDOT dimers as observed experimentally in this work and as demonstrated in literature in the case of both thiophene systems and pyrrole derivatives.[16,30]

In the field of conducting polymers, experiments concerning the photodegradation of polythiophene-based polymers demonstrated in the same way that HO• radicals lead to hydroxyl adduct, while $N_3^{\bullet}$ species give cation radicals of the polymers.[35] Since radiation induced polymerization proceeds through a recurrent step by step oxidation mechanism, both HO• and $N_3^{\bullet}$ radicals should react successively on EDOT dimers then oligomers producing continuously hydroxyl adducts in the case of HO• and radical cations in the case of $N_3^{\bullet}$. Then, one can expect the presence of hydroxyl groups exclusively into the HO•-induced radiosynthesized PEDOT polymers. Contrarily to PEDOT-N_3, PEDOT-OH should then contain alcohol functionalities.

As observed on Figure 3.9, the spectrum of PEDOT-OH polymers exhibits a very large band between 3600 cm^{-1} and 3200 cm^{-1}. Such a broad absorption in this spectral region is characteristic of O-H bonds and is traditionally observed in samples containing water molecules which are known to absorb between 3560 and 3520 cm^{-1}.[14] However, since our samples were conscientiously freeze-dried, the possible presence of water molecules must be ruled out. Besides, the absence of such a band in the spectrum of PEDOT-N_3 validates our assumption. On another hand, it is well known that free hydroxyl groups (-OH) in alcohols and phenols intensively absorb between 3650 cm^{-1} and 3584 cm^{-1}.[14] Nevertheless, in the presence of intermolecular H-bonds between the solutes, it is established that a very large band appears between 3550 and 3200 cm^{-1} at the expense of the band of free hydroxyl groups.[14] Then, the presence of a band in this exact region of the FTIR-spectrum in the case of PEDOT-OH (Figure 3.9) first proves the presence of hydroxyl groups all along the polymers as predicted from the growth mechanism, and second demonstrates the existence of strong intermolecular interactions between the functionalized polymers through hydrogen bonds. The presence of hydroxyl groups also confers to PEDOT-OH polymers hydrophilic properties which explain their poor solubility into organic solvents as previously discussed.

Contrarily to PEDOT-OH, PEDOT-N_3 polymers, which result from $N_3^{\bullet}$-induced EDOT oxidation, shouldn't contain alcohol functionalities. This is proved by the absence of large band of O-H in the ATR-FTIR spectrum of PEDOT-N_3 (Figure 3.9). The absence of such a polar group into the PEDOT-N_3 polymer impacts on its solubility in water and explains its poor hydrophilic properties.

After irradiation, for ATR-FTIR measurements, the samples were centrifuged, then freeze dried. As a consequence, in the case of PEDOT-N_3 which has been synthesized in the presence of

dissolved sodium azide, Na^+ and N_3^- ions were kept in the samples, and elimination of water molecules induced the precipitation of NaN_3 as an ionic solid together with the solid polymers. In the spectrum of PEDOT-N_3, two bands are observed at 3565 cm^{-1} and 3525 cm^{-1} and two others are present at 2110 cm^{-1} and 2065 cm^{-1} (Figure 3.9). These bands are attributable to the presence of azide anions. Indeed, azido group is generally characterized by the asymmetric stretching frequency in the region 2160-2090 cm^{-1} which often appears as a doublet.[14] In the solid state, due to the presence of cations which perturb the internal vibrations of the N_3^- anions, azide salts are known to generally absorb in two different infrared regions: 3400-3150 cm^{-1} and 2150-2025 cm^{-1}.[36] In particular, the spectrum of sodium azide salt has been shown to display an absorption band centered at 2106 cm^{-1} in addition to two other bands around 3500 cm^{-1} in agreement with our results.[36] This definitely confirms the presence of NaN_3 in our solid sample as expected from samples preparation. Note that functionalization of PEDOT-N_3 polymers by azido groups should be ruled out since azide radicals are known to only abstract electrons without any possible addition.

Amine molecules also absorb between 3500 and 3300 cm^{-1} in solutions. In particular, N-H bonds of primary amines are characterized in this spectral region by two bands (a doublet) which are always more narrow than O-H stretching bands.[14] These bands may sometimes be displaced to higher wavenumbers.[14] In addition, in the case of primary amines, these two peaks are associated to a shoulder which appears at lower wavenumbers and which corresponds to the angular deformation of N-H bond. Thus, the two bands observed in Figure 3.9 at 3565 cm^{-1} and 3525 cm^{-1} as well as the shoulder present around 3450 cm^{-1} in the case of PEDOT-N_3 could also be due to the presence in our sample of hydrazoic acid, HN_3, which is the acidic form of azide ion ($pKa(HN_3/N_3^-) = 4.6$ in aqueous solution) and which contains N-H bond.[37]

Aqueous solutions containing 10 mM in EDOT and irradiated at 36 and 70 kGy in the absence of NaN_3 were observed by Cryo-transmission electron microscopy just after irradiation and before any sedimentation or centrifugation. Representative images show the presence of low density globular structures forming polydisperse spherical nanoparticles with a diameter comprised between 100 and 300 nm as observed (Figure 3.10, mean diameter of 200 nm).[27]

These observations are consistent with our previous results which concerned hydroxyl-induced radiosynthesis of PEDOT under air atmosphere.[13] Since no other low density objects were observed during Cryo-TEM experiments, it can be deduced that these spherical nanoparticles are

made up of PEDOT-OH polymers. Note that the size and the shape of our polymer nanostructures are the same at both 36 and 70 kGy doses. This means that the irradiation dose has no noticeable influence on the structure of PEDOT-OH above the total irradiation dose (D_{max}).

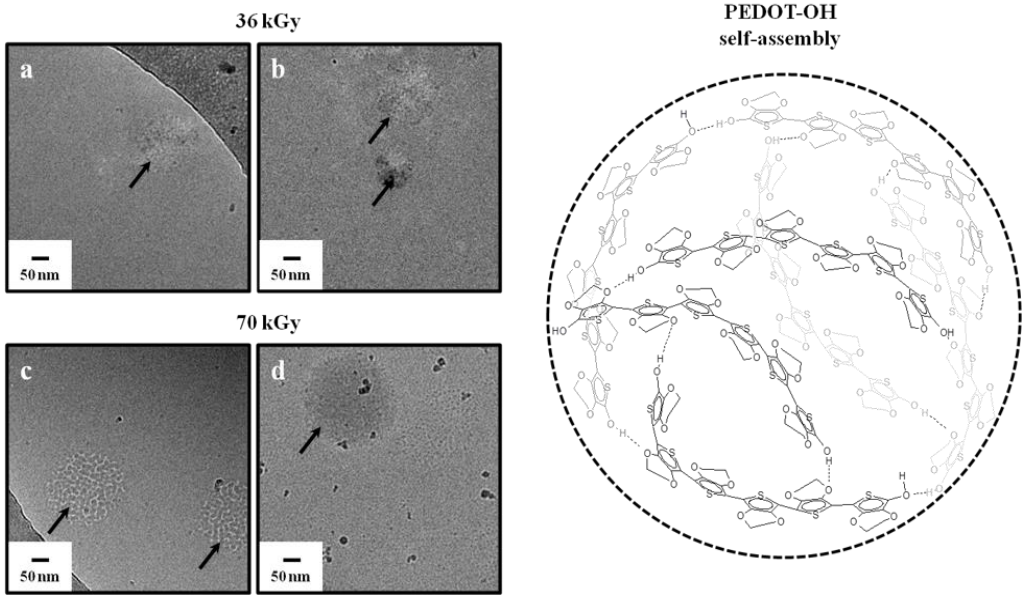

Figure 3.10 Cryo-TEM images of aqueous samples containing 10 mM in EDOT irradiated at 36 (a and b) and 70 kGy (c and d) under N_2O atmosphere in the absence of NaN_3. They exhibit spherical nanoobjects with a mean diameter of 200 nm attributed to self-assembled hydrophilic PEDOT-OH polymers. A schematic representation of a single spherical polymer nanoparticle highlights hydrogen bonds interactions between the chains.[27]

Each observed nanoparticle has a complex structure and seems to be composed of interdigitated polymer chains (see in particular Figure 3.10c). Since no parasite α–β' linkages could occur during polymerization, radiosynthesized PEDOT-OH nanostructures must be composed of linear chain polymers which are neither branched nor networked. Thus, each globular structure observed on Figure 3.10 should correspond to a self-assembly of independent amorphous PEDOT-OH chain polymers as schematically represented (Figure 3.10, right part). The presence of hydroxyl groups, which has previously been demonstrated, should explain not only the hydrosolubility of PEDOT-OH polymers but also the as-observed packing and nano-structuration of the spherical supramolecular PEDOT-OH self-assemblies (Figure 3.10). Note that ethylenedioxy groups (H-bond acceptors) present all along the polymer chains could also be involved in hydrogen-bonds with the hydroxyl groups.

Aqueous solutions containing 10 mM in EDOT and irradiated at 36 and 70 kGy, but this time in the presence of NaN_3, were also observed by Cryo-TEM just after irradiation and before any sedimentation or centrifugation. Instead of a compact spheroid surface morphology which was found in the case of PEDOT-OH, the obtained images clearly display nanoobjects forming fibrillar or lamellar (plate-like) nanostructures, more or less folded, with a maximal fiber thickness of 10 nm and a length which can reach several microns (Figure 3.11).[27]

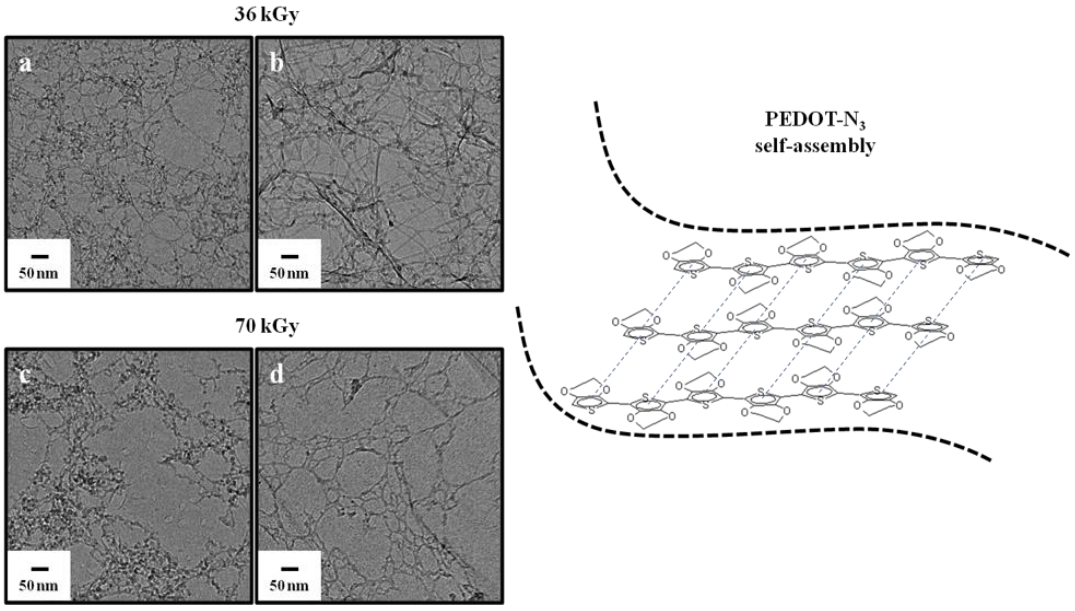

Figure 3.11 Cryo-TEM images of aqueous samples containing 10 mM in EDOT irradiated at 36 (a and b) and 70 kGy (c and d) under N_2O atmosphere in the presence of NaN_3. They exhibit fibrillar or lamellar (plate-like) nanostructures attributed to self-assembled amphiphilic PEDOT-N_3 polymers. A schematic representation of a single nanostructure highlights π-stacking interactions between the chains.[27]

Since no other low density objects were observed during our Cryo-TEM experiments, it can be deduced that these nanostructures are made up of PEDOT-N_3 polymers. Note that above the total irradiation dose (D_{max}), no effect of the dose is noticeable on the size and the shape of the polymer nanostructures.

Since no parasite α-β' linkages could occur during polymerization, the nanofibers are not branched nor bonded to each other. Then nodes observed on Figure 3.11 correspond to the crossing between independent nanofibers. Due to the thickness of the fibers, each of them should correspond to a self-assembly of linear PEDOT-N_3 polymer chains as schematically represented

(Figure 3.11, right part). Since hydroxyl groups are not present in PEDOT-N_3 polymers, the packing of these polymers can't result from H-bonds. This self-assembling should come from π-stacking interactions between conjugated polymers (and aromatic monomers) which maintain the polymer chains parallel to each other and which can maybe confer to the polymers a lamellar structure. On another hand, this self-assembling could explain the macroscopic observation of PEDOT-N_3 polymers as clustered fibers at the interface between water and organic solvent. Also, the fact that PEDOT-N_3 polymers can either interact by van der Waals interactions (π-stacking interactions) or by hydrogen bonds, thanks to the presence of ethylenedioxy groups, could explain the amphiphilic properties of these polymers.

In order to characterize the morphology of the polymers after a deposition procedure, drops of the aqueous solution containing the PEDOT-OH suspension obtained after a 70 kGy-irradiation (polymer self-assemblies of Figure 3.10) were deposited onto gold substrate and dried. The surface was then imaged by Scanning Electron Microscopy. The images indicate the presence of very close-packed spheroid polymeric particles (Figure 3.12, image a).[27]

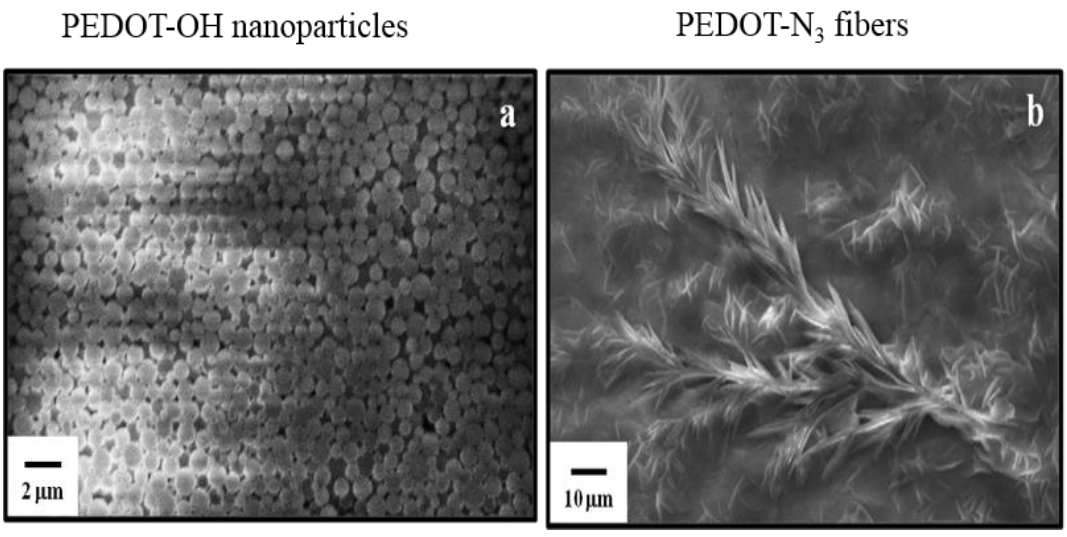

Figure 3.12 SEM images of PEDOT polymers after deposition onto gold substrates. Polymers were obtained after a 70 kGy-irradiation: (a) in the absence of NaN_3 (PEDOT-OH), (b) in the presence of NaN_3 (PEDOT-N_3).[27]

These structures should come from the globular nanostructures already observed in aqueous solution by Cryo-TEM (Figure 3.10). The particles observed by SEM after deposition are

polydisperse in size with a diameter comprised between 200 nm and 1 μm. Their size is then slightly bigger than that of the globular nanostructures observed by Cryo-TEM in solution. The flattening of the particles when deposited onto the substrate and their aggregation when dried due to phase transition should explain the increase and the polydispersity in size observed (Figure 3.12, image a).

In order to characterize the morphology of PEDOT-N_3 in the solid state, drops of the aqueous solution containing the suspension obtained after a 70 kGy-irradiation (polymer self-assemblies of Figure 3.11) were deposited onto gold substrate then dried. The SEM images demonstrate the presence of close-packed lamellar (plate-like) structures characterized by a maximal thickness of about 1 μm (Figure 3.12, image b). These structures should come from the aggregation of the fibrillar nanostructures which had previously been observed in aqueous solution by Cryo-TEM (Figure 3.11).

It is found that substantial differences exist between the structural properties of PEDOT-OH and PEDOT-N_3 polymers after deposition. It is generally admitted that the morphology of polymers in the solid state results from the contributions of three macro-conformations (Figure 3.13):[26]

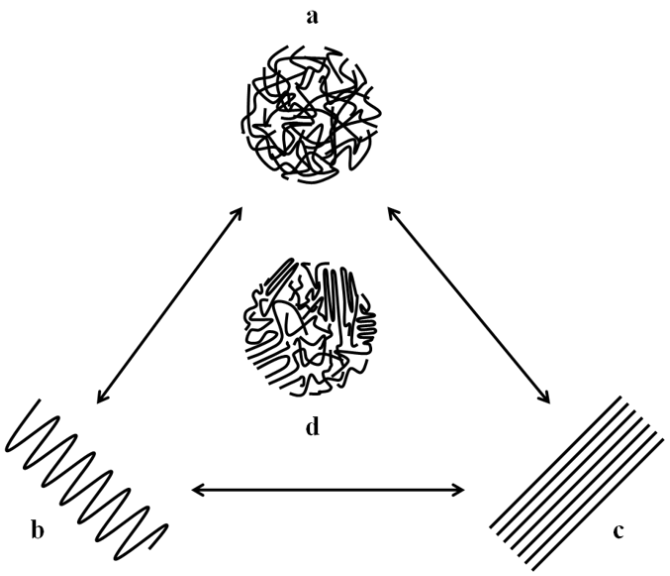

Figure 3.13 Schematic drawing of the different macro-conformations in solid linear polymers. (a) random, glassy, (b) folder chain, lamellar, (c) extended chain, (d) fringed micelle, mixture of a, b and c.[26]

(a) the random coil or irregularly folded molecules as found in the glassy state, (b) the folded chains, as found in lamellar structures and (c) the extended chains. The fringed micelles (d) can be seen, in summary, as a mixture of the three previous conformations. While the morphology of solid PEDOT-N_3 polymers agrees with the folded chain model found in lamellar structures, the morphology found for solid PEDOT-OH polymers is in good agreement with the random coil model found in the amorphous state. In solid state, as it has been proposed in aqueous solution, PEDOT-N_3 lamellar structures should correspond to self-assemblies of organized PEDOT-N_3 chain polymers which remain almost parallel thanks to π-stacking interactions. Due to the presence of hydroxyl pendant groups which induce hydrogen bonds interactions, PEDOT-OH chain polymers cannot pack together regularly enough to form lamellar structures at the solid state. Differently, the chains coil, entangle and randomly self-assemble in amorphous globular structures.

3.3.4 Conclusions

In the present work, the original radiolytic methodology is successfully extended to the synthesis of PEDOT conjugated polymers in N_2O-saturated aqueous solutions at ambient temperature and in the absence of any external oxidizing species. Starting from EDOT monomers and depending on the presence of sodium azide salt, two different oxidizing species are formed thanks to water radiolysis: hydroxyl radical (HO•) and azide radical ($N_3^{\bullet}$). Both species are shown to oxidize EDOT monomers into PEDOT polymers (called PEDOT-OH and PEDOT-N_3 respectively).

Thanks to ATR-FTIR experiments, it is demonstrated that contrarily to PEDOT-N_3 and PEDOT-OH polymers contain O-H functionalities. This noticeable difference between the two kinds of polymers was explained by the difference which exists between the well-known oxidizing behaviors of HO• and $N_3^{\bullet}$: while HO• radical adds onto aromatic molecules leading to radical adducts in addition radical cation, $N_3^{\bullet}$ radical exclusively forms radical cations through electron abstraction. Since radioinduced PEDOT polymerization proceeds through a step-by-step mechanism which involves a recurrent oxidation process as already demonstrated, HO• radicals contrarily to $N_3^{\bullet}$ species lead to PEDOT-OH adducts.

While unfunctionalized PEDOT-N_3 polymers are insoluble in water, PEDOT-OH are highly soluble in aqueous solutions thanks to the presence of hydroxyl groups. Many works were conducted in literature in order to modify the chemical structure of EDOT building blocks and thus to improve the solubility of the resulting functionalized PEDOT polymers.[10] In this work, without any pre-functionalization of EDOT monomers, synthesis of hydrophilic PEDOT polymers succeeded thanks to the use of hydroxyl radicals as oxidizing species.

Due to the presence of -OH functionalities which enable hydrogen-bond interactions, PEDOT-OH polymers self-assemble in aqueous solutions into globular nanostructures as observed by Cryo-TEM. Differently, unfunctionalized PEDOT-N_3 polymers self assemble in water, by π-stacking interactions, into fibrillar or lamellar nanostructures. Interestingly, the shapes of all these structures remain unchanged after deposition and drying procedure. Thus, the simple choice of the oxidizing species which further determines the whole oxidation mechanism, has not only a clear influence on the chemical structure and the hydrophilic properties of synthesized polymers, but also plays a crucial role on the final morphology of polymers nanostructures.

Current research aims to develop new synthesis strategies and new conducting polymers with tuned morphologies and properties. However, the study of the influence of polymerization mechanism remains poorly investigated in literature in the field of conducting materials. Thus, pulsed radiolysis studies coupled with structural and spectroscopic characterizations have been undertaken in order to identify the first steps of the polymerization mechanism and in order to better understand the growth process of PEDOT polymers in aqueous solution. This work has been down during the thesis of Cecilia Coletta.[38] In particular, I participated in the characterization of the synthesized materials.

3.4 Pulse radiolysis study of PEDOT polymerization

In the previous work, it has been proved that radiolytic methodology enables the synthesis of conjugated polymers under soft-conditions. Hydrophilic PEDOT polymers without any pre-functionalization of EDOT monomers are obtained in N_2O saturated aqueous solution. Moreover, it is demonstrated that a step-by-step mechanism is involved during PEDOT polymerization.[13] Indeed, the yield of EDOT monomers consumption, which is strictly equal to the yield of formation of HO• oxidizing radicals, does not depend on the initial concentration of the

monomers. On the other hand, the amount of oxidizing species which is needed for quantitative polymerization of PEDOT is twice that of EDOT monomers.[25] These previous results indicate that no chain reaction should happen. Thus, polymerization should proceed through recurrent oxidation reactions: HO• radicals should oxidize EDOT monomers, then dimers, then oligomers, and so on.

In the present part, time resolved absorption spectroscopy coupled with pulsed radiolysis is used in order, first, to study EDOT oxidation mechanism and, second, to definitely identify the nature of PEDOT growth process. This "fast" technique offers several advantages: it enables, thanks to the pulsed electrons accelerator, (i) the generation of oxidizing species in the aqueous irradiated medium in a very short time, (ii) the quantitative knowledge of oxidizing species concentration, (iii) the real-time following by absorption spectroscopy of the appearance and disappearance of transient species produced during EDOT oxidation and the estimation of the rate constants of the involved consecutive reactions. In particular, the reaction of EDOT monomers with hydroxyl radicals produced by water radiolysis was investigated with the aim to identify the different transient species involved in the first steps of HO•-induced PEDOT polymerization. Spectrokinetic analysis of experimental data and molecular simulations of absorption spectra were used as complementary methodologies to confirm the rate constants values and the transient and stable species identification (results not shown here but developed in the thesis of Cecilia Coletta).[38]

With the aim to demonstrate the step-by-step PEDOT polymerization mechanism and in order to synthesize conducting polymers thanks to a new alternative method based on electron beam irradiation, the electron accelerator was also used as a "simple" electron irradiator: EDOT solution was irradiated using consecutive accumulated pulses in order to produce a high concentration in oxidative species for ensuring a quantitative polymerization of PEDOT. The resulting polymers were finally characterized by different physicochemical techniques in aqueous solution or after deposition onto substrates.

3.4.1 Solutions preparation and pulse radiolysis study

Aqueous solutions containing 1 mM or 10 mM in EDOT monomers were prepared. The natural pH of EDOT aqueous solutions is neutral, about 8. The pH was changed by adding $HClO_4$

to obtain acidic solutions at pH = 4, 5 and 6 or by adding NaOH to obtain alkaline solution at pH = 13. The pH was measured before and after irradiation and only a slight decrease in the pH value was observed in the acidic and neutral solution, due to the production of H^+ ions during water radiolysis. All solutions were deaerated by bubbling with nitrous oxide, N_2O, prior to irradiation, then irradiated with an electron beam.

The experiments were carried out on the picosecond laser-triggered electron accelerator (ELYSE, University Paris-Sud) coupled with a time resolved absorption spectroscopic detection system.[39,40] Experimental conditions were described before (section 2.4, chapter2) and this study was also explained in detail in the thesis of Cecilia Colletta.[38] An N_2O-purged stock solution of 200 mL was used which circulated in the 10 x 10 mm fused silica irradiation cell at a flow rate of 100 mL/min by means of a peristaltic pump. Since the electron pulses were applied at a frequency of 5 Hz, the solution was renewed between each pulse and it was possible to apply up to 400 pulses for each kinetic measurement.

In this work, a pulsed radiolysis study coupled with molecular simulations, with thermodynamic calculations and with spectrokinetic analysis was used to study the mechanism of HO•-induced oxidation of EDOT in aqueous solution. The mechanistic scheme of EDOT oxidation by hydroxyl radical was established, the rate constants were determined and the transient species involved in the oxidation process were identified thanks to the comparison of their experimental and simulated UV-Vis absorption spectra. A mixed simulation method was used, using the monte-carlo (MC) sampling of the molecular geometries, the density functional theory (DFT) calculation of the electron structures and the polarized continuum (PCM) modeling of the solvent.

In acidic and neutral aqueous solutions, HO•-induced oxidation of EDOT implies the oxidation of EDOT into a transient species, $EDOT^{\bullet+}$ cation radical or (EDOT-HO)• addut, which dimerizes and deprotonates leading to a stable product, namely $EDOT_2$ dimer. In alkaline medium, this mechanism is mostly different since HO• deprotonates into its alkaline form, oxide radical, which adds onto EDOT monomer. This addition leads to an open cycle and prevents any dimerization of EDOT and consequently any polymerization of PEDOT.

In acidic and neutral aqueous solutions, after one pulse irradiation (40 Gy), no other products than $EDOT_2$ dimers were observed, demonstrating that no polymerization takes place. This proves that PEDOT polymerization is not a chain reaction. On the contrary, it has been

demonstrated to proceed through a step-by-step mechanism made up of the following recurrent steps: (i) oxidation/activation, (ii) growth/chain length increase, (iii) deprotonation.[18] The amount of hydroxyl radicals generated by one pulse during the pulsed radiolysis study is then not enough to ensure polymerization. It only enables the incomplete transformation of EDOT monomers into dimers. The quantitative polymerization of EDOT into PEDOT requires a very much higher concentration in hydroxyl radicals which should reach at least twice that of EDOT.

3.4.2 Electron beam irradiation induced EDOT polymerization

In pulse radiolysis experiment, the dose per pulse can't be significantly increased. Then, in order to check whether EDOT polymerization effectively proceeds through a step-by-step oxidation process and with the aim to synthesize conducting PEDOT polymers by using an electron beam, aqueous solutions containing 10 mM in EDOT in a closed cell under N_2O atmosphere were irradiated with a series of consecutive electron pulses of 40 Gy (delivered at a frequency of 10 Hz). Under these conditions, a high concentration of oxidative species is produced. Note that in these experimental conditions, the electron accelerator was used as a high-energy electrons irradiator. This work has also been done in Cecilia Coletta's thesis.[38] Nevertheless, I took part in the characterizations of the as-prepared products.

Taking into account the step by step polymerization process described in the previous sections, 10 mM in hydroxyl radicals are needed for the quantitative dimerization of 10 mM in EDOT into 5 mM in $EDOT_2$, then an additional amount of 5 mM in HO• is needed for the quantitative transformation of $EDOT_2$ into 2.5 mM in $EDOT_4$ and so on. This means that at least 20 mM in hydroxyl radicals are necessary to ensure the quantitative polymerization of EDOT monomers into PEDOT polymers. The use of two HO• radicals for one EDOT molecule is understandable since each EDOT monomer is bound to two EDOT neighbors inside the same polymer chain, which means that it has been twice oxidized. The theoretical irradiation dose (D_{max}) which should lead to the total oxidation of EDOT into PEDOT by $HO^{\cdot}$ radicals can be determined (equation 2.22, chapter 2). Thus, 37 kGy are necessary for the total polymerization of 10 mM in EDOT. Knowing that each pulse corresponds to a dose of 40 Gy, complete polymerization requires more than about 1000 successive pulses.

In order to quantitatively polymerize EDOT, the colorless and limpid aqueous solution of 10 mM in EDOT was irradiated at a dose of 180 kGy which corresponds to the accumulation of 4500 pulses of 40 Gy/pulse. After such an irradiation, the solution became turbid and its UV-Vis absorption spectrum is displayed (Figure 3.14).[18]

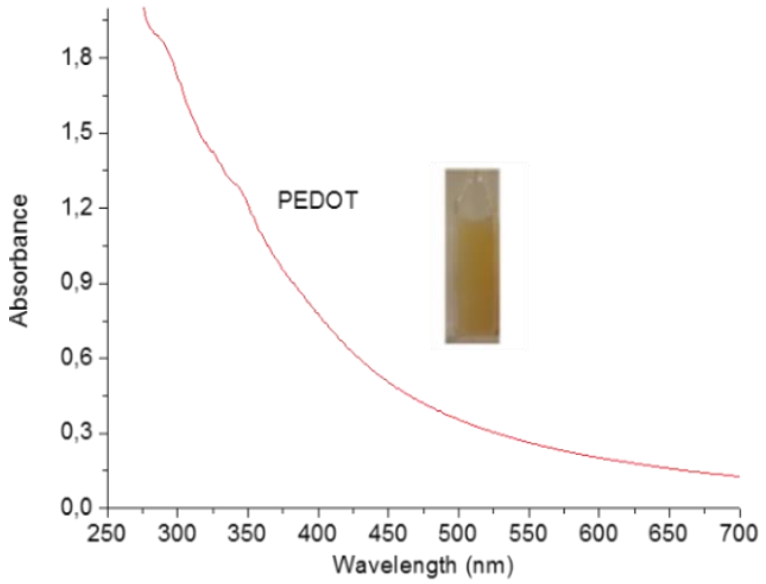

Figure 3.14 UV-vis absorption spectrum of a N_2O-satured aqueous solution of EDOT (10 mM) irradiated by an electron beam at a dose of 180 kGy (4500 pulses, 40 Gy/pulse). The reference is water and pathlength is 0.1 cm; (inset) image of a cell containing PEDOT aqueous suspension radiosynthesized by electron beam.[18]

No noticeable absorption band is present in the spectrum. Nevertheless, a continuous scattering appears due to the presence of a brown-yellow suspension in the bulk of the irradiated solution (inset of Figure 3.14). This spectrum and the turbidity of the solution are in good agreement with the results previously obtained by steady state γ radiolysis suggesting that polymerization effectively took place.[13]

In order to demonstrate that the radiosynthesized products are PEDOT polymers, the turbid solution obtained after 180 kGy electron beam irradiation was centrifuged in order to recuperate a solid phase. The isolated brown powder was lyophilized to eliminate any residual water molecules which could be trapped in the polymer containing solid phase (inset of Figure 3.15). The solid sample was then characterized by ATR-FTIR spectroscopy in order to investigate the chemical nature of the obtained polymers (Figure 3.15).[18]

The ATR-FTIR spectrum of the polymer powder is presented in the upper part of Figure 3.15 in the wave number region 1600-600 cm^{-1} together with the spectrum of pure non irradiated EDOT (bottom of Figure 3.15). The two spectra are in good agreement with those our group previously reported for PEDOT and EDOT when polymerization was induced by γ-rays. The IR spectrum of the polymer powder displays vibrations at 1485, 1441 and 1365 cm^{-1} which are attributed to C=C and C-C stretching modes in the thiophene ring. The vibrations observed at 1288, 1240, 1171 and 1059 cm^{-1} are assigned to the stretching modes of the ethyledioxy groups (C-C and C-O-R-O-C). The vibration modes of C-S bond which are present in the thiophene ring can be observed at 941 and 901 cm^{-1}. Note that the intense C-H stretching band at 754 cm^{-1}, observed in the spectrum of EDOT, is clearly absent in the ATR-FTIR spectrum of polymers. This definitely demonstrates, without any ambiguity, that EDOT polymerization quantitatively took place thanks to α,α'-coupling reactions and that the resulting solid powder obtained after lyophilisation is effectively composed of PEDOT polymers.

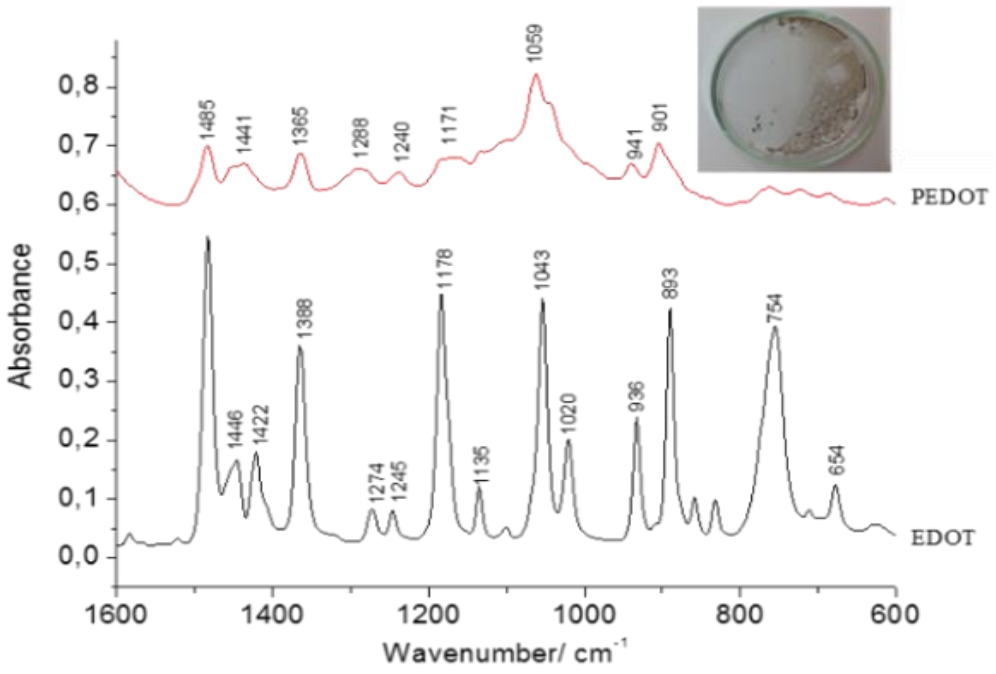

Figure 3.15 ATR-FTIR spectra of pure EDOT (bottom spectrum) and PEDOT polymers radiosynthesized at 180 kGy by electron beam (top spectrum); (inset) photograph of a cup containing the lyophilized radiosynthesized PEDOT powder.[18]

This demonstrates that such as γ-irradiation, electron beam irradiation enables the radiosynthesis of PEDOT polymers.[25] While one electron pulse leads to the formation of $EDOT_2$ dimers as stable products, the use of a series of successive pulses is necessary to generate enough hydroxyl radicals to form PEDOT polymers. It is evidenced that not only electron irradiation can be used as an alternative way for the synthesis of PEDOT polymers, but also that PEDOT growth effectively proceeds through a step by step oxidation process as expected.

Aqueous solutions containing 10 mM in EDOT and irradiated by electron beam at 180 kGy were observed by Cryo-transmission electron microscopy just after irradiation in order to investigate the structure and morphology of PEDOT polymers in aqueous solution. Representative images show the presence of low density globular structures forming spherical nanoparticles with a diameter ranging between 200 and 250 nm (Figure 3.16).[18]

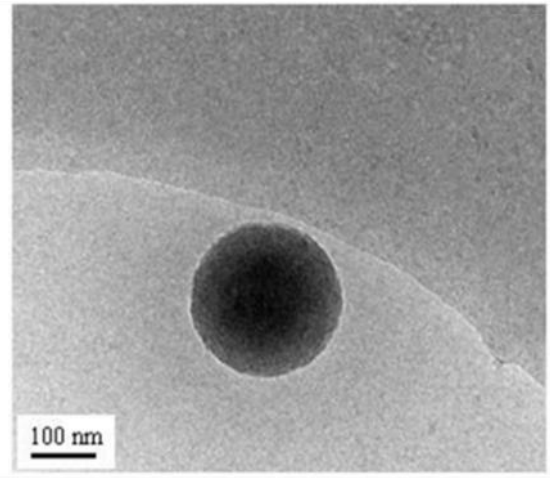

Figure 3.16 Cryo-TEM image of PEDOT radiosynthesized by electron beam at 180 kGy in aqueous solution. A PEDOT nanoparticle of around 250 nm is observed.[18]

This result is in agreement with polymer size and shape found after γ-rays induced PEDOT synthesis. Since no other low density objects were observed during our Cryo-TEM experiments, these spherical nanoparticles are supposed to be made up of PEDOT polymers. Each observed nanoparticle should be composed of interdigitated polymer chains. Since no α-β' linkages could occur during polymerization, radiosynthesized PEDOT nanostructures should be composed of linear chain polymers which are no branched nor networked. Thus the globular structure observed on Figure 3.16.c should correspond to a self-assembly of independent amorphous

PEDOT chain polymers. The presence of ethylenedioxy groups (H-bond acceptors) should explain not only the hydrosolubility of PEDOT polymers but also the as-observed packing and nano-structuration of the spherical supramolecular PEDOT self-assemblies.

In order to characterize the morphology of the polymers after a deposition procedure, the 180 kGy-irradiated sample was lyophilized and the black powder obtained was deposited then characterized by SEM microscopy. The images indicate the presence of very close packed polymeric particles (Figure 3.17).[18] Once again PEDOT polymers appear as spherical nanoparticles. These structures should come from the globular nanostructures already observed in aqueous solution by Cryo-TEM. The particles observed by SEM are almost monodisperse in size with a mean diameter of 220 nm which is close to that observed by Cryo-TEM in aqueous solution. This proves that neither phase transition nor deposition procedure affect the size and shape of PEDOT nanoparticles. This would imply the existence of very strong hydrogen-bond interactions into each polymer nanoparticle.

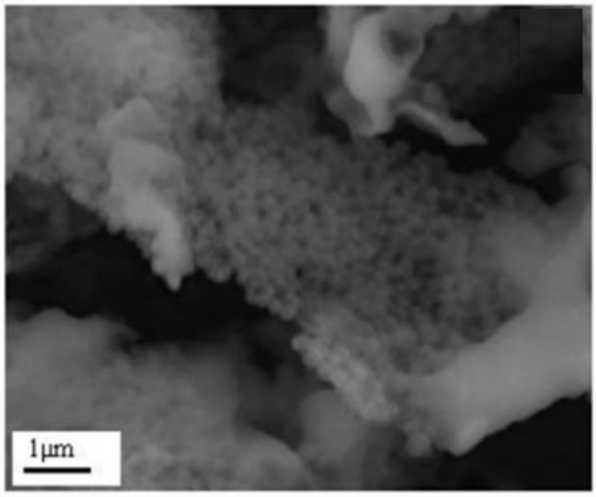

Figure 3.17 SEM image of lyophilized PEDOT radiosynthesized by electron beam at 180 kGy. Aggregates of spherical PEDOT nanoparticles are observed.[18]

Therefore, the synthesis of PEDOT polymers is successful thanks to the electrons beam irradiation of EDOT aqueous solution. The radiosynthesized PEDOT polymers form monodisperse nanoparticles the morphology of which is kept after deposition onto substrate.

3.4.3 Conductivity measurements

Since chemically and electrochemically synthesized PEDOT polymers are very often used for their conducting properties, the PEDOT radiosynthesized by electron beam at 180 kGy are also characterized by four point probe technique to check such interesting electrical properties.

After irradiation and lyophilization, the obtained PEDOT powder was dissolved and treated by a chemical oxidant $NOBF_4$ (10^{-2} M) in acetonitrile. The solution was spin-coated onto a glass substrate and a PEDOT layer was obtained. The average thickness of the doped PEDOT film was measured on a surface profiler and was found to be 105 nm. According to (equation 2.35, chapter 2), the mean value of the electrical conductivity was determined to be 9×10^{-4} S cm^{-1}. This conductivity is comparable to the highest conductivities reported in literature for PEDOT.[41,42]

3.4.4 Conclusions

In this work, a pulsed radiolysis study coupled with molecular simulations, with thermodynamic calculations and with spectrokinetic analysis was used to study the mechanism of $HO^{\cdot}$-induced oxidation of EDOT in aqueous solution. In acidic and neutral aqueous solutions, $HO^{\cdot}$-induced oxidation of EDOT implies the oxidation of EDOT into a transient species, namely $EDOT^{\cdot+}$ cation radical and also probably into (EDOT-HO)• adduct, which dimerizes and deprotonates leading to a stable product, namely $EDOT_2$ dimer. In alkaline medium, the mechanism is mostly different since $HO^{\cdot}$ deprotonates into its alkaline form, oxide radical, which adds onto EDOT monomer. This addition leads to an open cycle and prevents any dimerization of EDOT and consequently any polymerization of PEDOT.

In acidic and neutral aqueous solutions, after one pulse irradiation (40 Gy), no other products than $EDOT_2$ dimers were observed, demonstrating that no polymerization takes place. This proves that PEDOT polymerization is not a chain reaction. On the contrary, it proceeds through a step by step mechanism made up of the following recurrent steps: (i) oxidation/activation, (ii) growth/chain length increase, (iii) deprotonation. The amount of hydroxyl radicals generated by one pulse during the pulsed radiolysis study is then not enough to ensure polymerization. It only enables the incomplete transformation of EDOT monomers into dimers. The quantitative

polymerization of EDOT into PEDOT requires a very much higher concentration in hydroxyl radicals which should reach at least twice that of EDOT.

In order to prove that PEDOT polymerization effectively proceeds through a step by step oxidation process and with the aim to synthesize conducting PEDOT polymers, the electron beam, usually employed in fast kinetic studies, was used as a high energy electrons irradiator. Successfully, the irradiation with a series of 4500 consecutive electron pulses (180 kGy total dose) of EDOT aqueous solution enabled the production of a very high concentration in hydroxyl radicals and thus the quantitative synthesis of PEDOT polymers, demonstrating that PEDOT growth proceeds through a step by step oxidation process as expected.

The chemical nature of radiosynthesized PEDOT polymers was confirmed by ATR-FTIR spectroscopy while their morphology was checked in solution by Cryo-TEM microscopy and after lyophilisation and deposition by SEM microscopy. Radiosynthesized PEDOT polymers were found to form monodisperse nanoparticles whose morphology was kept after deposition onto solid substrate. Finally, the electrical conductivity of radiosynthesized PEDOT was evaluated at 9×10^{-4} S cm^{-1}. This conductivity is comparable to conductivities already reported in literature concerning PEDOT polymers synthesized by conventional methods.

The present study bears witness to the tremendous potential of such a new electrons-based methodology and gives us a glimpse of future promising industrial applications in the field of conducting polymers synthesis. Indeed, thanks to the accelerated electrons-based nano-beams which are nowadays available, it should appear possible to synthesize conducting polymers onto conducting or even non conducting substrates with a high spatial resolution in order to produce conductive patterns at a nanometric scale. The fact that conducting polymer growth proceeds through a step by step mechanism, and not according to a chain reaction, should enable the control of the chain length thanks to the adjustment of the irradiation dose.

3.5 Summary

According to the work of Samy Remita's team, synthesis of conducting polymers (CPs) with radiation method has been developed by the synthesis of conducting poly(3,4-ethylenedioxythiophene) (PEDOT). Using γ-radiolysis of aerated aqueous solutions of 3,4-ethylenedioxythiophene (EDOT) in the absence of any external chemical initiators, PEDOT

polymers were successfully synthesized with spherical appearance. The polymerization mechanism was proposed to be a step-by-step procedure. By adjusting the oxidizing species, PEDOT nanoparticles and nanofibers were prepared using γ-irradiation of aqueous solutions of EDOT degased with N_2O. It is proved that PEDOT-OH polymers self-assemble in aqueous solutions into globular nanostructures thanks to hydrogen-bond interactions. While, PEDOT-N_3 polymers self-assembling should come from π-stacking interactions between conjugated polymers forming fibrillar nanostructures. Pulse radiolysis study proved the formation of $EDOT^{\bullet+}$ radical cation and probably that of (EDOT-HO)• adduct which lead to the $EDOT_2$ dimers. Furthermore, it is suggested that EDOT monomers undergo degradation under high pH and the synthesis of CPs with electron beam is feasible.

However, the versatility of this radiolytic method needs to be checked. The synthesis of other CPs such as polypyrrole (PPy) by using γ-irradiation is worth studying. The effect of synthetic conditions (pH and soft template) on the polymerization of EDOT needs to be further studied. Both the effect of pH and application of soft template on the polymerization of EDOT and on the morphology of PEDOT is of great interest since they may affect the final properties of PEDOT polymers.

References

[1] Remita, S., Radioinduced lipid peroxidation: factors determining the oxidizability of liquids. *Can. J. Physiol. Pharmacol.* **2001,** *79*, 144-153.

[2] Varmenot, N.; Remita, S.; Abedinzadeh, Z.; Wisniowski, P.; Strzelczak, G.; Bobrowski, K., Oxidation Processes of N,S-Diacetyl-l-cysteine Ethyl Ester: Influence of S-Acetylation. *The Journal of Physical Chemistry A* **2001,** *105* (28), 6867-6875.

[3] Remita, S.; Fontaine, P.; Lacaze, E.; Borensztein, Y.; Sellame, H.; Farha, R.; Rochas, C.; Goldmann, M., X-ray radiolysis induced formation of silver nano-particles: A SAXS and UV–visible absorption spectroscopy study. *Nuclear Instruments and Methods in Physics Research Section B: Beam Interactions with Materials and Atoms* **2007,** *263* (2), 436-440.

[4] Attia, J.; Rémita, S.; Jonic, S.; Lacaze, E.; Fauré, M. C.; Larquet, E.; Goldmann, M., Radiation-Induced Synthesis and Cryo-TEM Characterization of Silver Nanoshells on Linoleate Spherical Micelles. *Langmuir* **2007,** *23* (19), 9523-9526.

[5] Chapiro, A., Radiation induced polymerization. *Radiation Physics and Chemistry (1977)* **1979,** *14* (1), 101-116.

[6] Muller, F.; Fontaine, P.; Remita, S.; Fauré, M. C.; Lacaze, E.; Goldmann, M., Synthesis of Nanostructured Metal−Organic Films: Surface X-ray Radiolysis of Silver Ions Using a Langmuir Monolayer as a Template. *Langmuir* **2004,** *20* (12), 4791-4794.

[7] Fontaine, P.; Fauré, M.-C.; Remita, S.; Muller, F.; Goldmann, M., X-ray surface radiolysis: Kinetics of the metal-organic interface formation. *The European Physical Journal Special Topics* **2009,** *167* (1), 157-162.

[8] Karim, M. R.; Lee, C. J.; Lee, M. S., Synthesis of conducting polypyrrole by radiolysis polymerization method. *Polymers for Advanced Technologies* **2007,** *18* (11), 916-920.

[9] Pillalamarri, S. K.; Blum, F. D.; Tokuhiro, A. T.; Story, J. G.; Bertino, M. F., Radiolytic Synthesis of Polyaniline Nanofibers: A New Templateless Pathway. *Chemistry of Materials* **2005,** *17* (2), 227-229.

[10] Roncali, J.; Blanchard, P.; Frere, P., 3,4-Ethylenedioxythiophene (EDOT) as a versatile building block for advanced functional [small pi]-conjugated systems. *Journal of Materials Chemistry* **2005,** *15* (16), 1589-1610.

[11] Pigani, L.; Heras, A.; Colina, Á.; Seeber, R.; López-Palacios, J., Electropolymerisation of 3,4-ethylenedioxythiophene in aqueous solutions. *Electrochemistry Communications* **2004,** *6* (11), 1192-1198.

[12] Ferradini, C.; Jay-Gerin, J. P., Radiolysis of water and aqueous solutions-history and present state of the science. *Can. J. Chem.* **1999,** *77*, 1542-1575.

[13] Lattach, Y.; Deniset-Besseau, A.; Guigner, J. M.; Remita, S., Radiation chemistry as an alternative way for the synthesis of PEDOT conducting Polymers under "soft" Conditions. *Radiat. Phys. Chem.* **2013,** *82*, 44-53.

[14] Silverstein, R. M.; Bassler, G. C.; Morrill, T. C., Spectrometric identification of organic compounds (Fifth Edition). *Organic Mass Spectrometry* **1991,** *26* (9), 813-813.

[15] Lattach, Y.; Archirel, P.; Remita, S., Influence of the Chemical Functionalities of a Molecularly Imprinted Conducting Polymer on Its Sensing Properties: Electrochemical Measurements and Semiempirical DFT Calculations. *The Journal of Physical Chemistry B* **2012,** *116* (5), 1467-1481.

[16] Saunders, B. B.; Kaufman, P. C.; Matheson, M. S., Reactions of thiophene with radiolytically produced radicals. 1. The hydroxyl radical. *The Journal of Physical Chemistry* **1978,** *82* (2), 142-150.

[17] Tour, J. M.; Wu, R. L., Synthesis and UV-visible properties of soluble α-thiophene oligomers. Monomer to octamer. *Macromolecules* **1992,** *25* (7), 1901-1907.

[18] Coletta, C.; Cui, Z. P.; Archirel, P.; Pernot, P.; Marignier, J. L.; Remita, S., Electron-Induced Growth Mechanism of Conducting Polymers: A Coupled Experimental and Computational Investigation. *The Journal of Physical Chemistry B* **2015,** *119* (16), 5282-5298.

[19] Bhattacharya, A.; De, A.; Mandal, P. C., Carbonate radical induced polymerisation of pyrrole: A steady state and flash photolysis study. *Journal of Radioanalytical and Nuclear Chemistry* **1998,** *230* (1), 91-95.

[20] Randriamahazaka, H.; Noël, V.; Chevrot, C., Nucleation and growth of poly(3,4-ethylenedioxythiophene) in acetonitrile on platinum under potentiostatic conditions. *Journal of Electroanalytical Chemistry* **1999,** *472* (2), 103-111.

[21] Kvarnström, C.; Neugebauer, H.; Blomquist, S.; Ahonenc, H. J.; Kankarec, J.; Ivaska, A., In situ spectroelectrochemical characterization of poly(3,4-ethylenedioxythiophene). *Electrochim. Acta* **1999,** *44*, 273-2750.

[22] Bazzaoui, E. A.; Aeiyach, S.; Lacaze, P. C., Electropolymerization of bithiophene on Pt and Fe electrodes in an aqueous sodium dodecylsulfate (SDS) micellar medium. *Synthetic Metals* **1996,** *83* (2), 159-165.

[23] Neugebauer, H.; Nauer, G.; Neckel, A.; Tourillon, G.; Garnier, F.; Lang, P., In situ investigations of the 3-methylthiophene polymer with attenuated total reflection Fourier transform infrared spectroscopy. *The Journal of Physical Chemistry* **1984,** *88* (4), 652-654.

[24] Irwin, M. D.; Roberson, D. A.; Olivas, R. I.; Wicker, R. B.; MacDonald, E., Conductive polymer-coated threads as electrical interconnects in e-textiles. *Fibers and Polymers* **2011,** *12* (7), 904.

[25] Lattach, Y.; Garnier, F.; Remita , S., Influence of Chemical and Structural Properties of Functionalized Polythiophene-Based Layers on Electrochemical Sensing of Atrazine. *Chemphyschem : a European journal of chemical physics and physical chemistry* **2012,** *13* (1), 281-290.

[26] Van Krevelen, D. W.; Nijenhuis, K. T., Properties of Polymers. *Elsevier* **2009**.

[27] Lattach, Y.; Coletta, C.; Ghosh, S.; Remita, S., Radiation-induced synthesis of nanostructured conjugated polymers in aqueous solution: fundamental effect of oxidizing species. *Chemphyschem : a European journal of chemical physics and physical chemistry* **2014,** *15* (1), 208-218.

[28] Lind, J.; Shen, X.; Eriksen, T. E.; Merenyi, G., The one-electron reduction potential of 4-substituted phenoxyl radicals in water. *Journal of the American Chemical Society* **1990,** *112* (2), 479-482.

[29] Neta, P.; Huie, R. E.; Ross, A. B., Rate Constants for Reactions of Inorganic Radicals in Aqueous Solution. *Journal of Physical and Chemical Reference Data* **1988,** *17* (3), 1027-1284.

[30] Beaver, B.; Teng, Y.; Guiriec, P.; Hapiot, P.; Neta, P., Mechanisms of Oxidation of 1,2,5-Trimethylpyrrole: Kinetic, Spectroscopic, and Electrochemical Studies. *The Journal of Physical Chemistry A* **1998,** *102* (30), 6121-6128.

[31] Alfassi, Z. B.; Harriman, A.; Huie, R. E.; Mosseri, S.; Neta, P., The redox potential of the azide/azidyl couple. *The Journal of Physical Chemistry* **1987,** *91* (8), 2120-2122.

[32] Ram, M. S.; Stanbury, D. M., Electron-transfer reactions involving the azidyl radical. *The Journal of Physical Chemistry* **1986,** *90* (16), 3691-3696.

[33] Singh, T. A.; Madhava Rao, B. S.; O’ Neill, P., Radical Chemistry of 8-Oxo-7,8-dihydro-2′ -deoxyadenosine and 8-Oxo-7,8-dihydro-2′ -deoxyguanosine: A Pulse Radiolysis Study. *The Journal of Physical Chemistry B* **2010,** *114* (49), 16611-16617.

[34] Gaikwad, P.; Priyadarsini, K. I.; Naumov, S.; Rao, B. S. M., Oxidation of Tryptamine and 5-Hydroxytryptamine: A Pulse Radiolysis and Quantum Chemical Study. *The Journal of Physical Chemistry A* **2009,** *113* (29), 8249-8257.

[35] Koch, M.; Nicolaescu, R.; Kamat, P. V., Photodegradation of Polythiophene-Based Polymers: Excited State Properties and Radical Intermediates. *The Journal of Physical Chemistry C* **2009,** *113* (27), 11507-11513.

[36] Nyquist, R. A.; Kagel, R. O.; Putzig, C. L.; Leugers, M. A., Handbook of Infrared and Raman spectra of inorganic compounds and organic salts. *Boston Academic Press* **1997,** *3*.

[37] Patnaik, P., Handbook of Inorganic Chemicals. *Ed. McGraw-Hill* **2002**.

[38] Coletta, C., Study of growth mechanism of conducting polymers by pulse radiolysis. *Ph.D thesis* **2016,** *1*, 37.

[39] Belloni, J.; Monard, H.; Gobert, F.; Larbre, J. P.; Demarque, A.; De Waele, V.; Lampre, I.; Marignier, J. L.; Mostafavi, M.; Bourdon, J. C.; Bernard, M.; Borie, H.; Garvey, T.; Jacquemard, B.; Leblond, B.; Lepercq, P.; Omeich, M.; Roch, M.; Rodier, J.; Roux, R., ELYSE—A picosecond electron accelerator for pulse radiolysis research. *Nuclear Instruments and Methods in Physics Research Section A: Accelerators, Spectrometers, Detectors and Associated Equipment* **2005,** *539* (3), 527-539.

[40] Marignier, J. L.; de Waele, V.; Monard, H.; Gobert, F.; Larbre, J. P.; Demarque, A.; Mostafavi, M.; Belloni, J., Time-resolved spectroscopy at the picosecond laser-triggered electron accelerator ELYSE. *Radiation Physics and Chemistry* **2006,** *75* (9), 1024-1033.

[41] Jones, B. H.; Cheng, K. Y.; Holmes, R. J.; Lodge, T. P., Nanoporous Poly(3,4-ethylenedioxythiophene) Derived from Polymeric Bicontinuous Microemulsion Templates. *Macromolecules* **2012,** *45* (1), 599-601.

[42] Ghosh, S.; Remita, H.; Ramos, L.; Dazzi, A.; Deniset-Besseau, A.; Beaunier, P.; Goubard, F.; Aubert, P. H.; Brisset, F.; Remita, S., PEDOT nanostructures synthesized in hexagonal mesophases. *New Journal of Chemistry* **2014,** *38* (3), 1106-1115.

Chapter 4: Radiation induced synthesis of PPy: demonstration of the versatility of radiolytic method

Since the discovery of conducting polymers (CPs) in 1970s, a variety of π-conjugated CPs have been developed and these typical CPs include poly(3,4-ethylenedioxythiophene) (PEDOT), polypyrrole (PPy), polyaniline (PANI) and their derivatives.[1-3] All these CPs are characterized by both environmental stability and high conductivity which are currently attracting great interests.[4] Among these typical CPs, PPy has been mostly investigated due to its relatively easier synthesis and greater stability.

Similar to the synthesis of PEDOT polymers, PPy polymers can be synthesized by the polymerization of pyrrole (Py) monomers (Figure 2.1, chapter 2) using both traditional chemical (e.g., $K_2S_2O_8$, $FeCl_3$, H_2O_2) and electrochemical methods while some alternative ways, such as enzymatic method, remain rarely proposed in literature.[5-9]

To the polymerization technologies of chemical and electrochemical methods, the first step of polymerization corresponds to the preliminary oxidation of Py monomers into their ionic states (Figure 4.1).[10] It is worth noting that the cationization of Py monomers is favorable at the α and α′ positions. Then, dimerization of two Py cations leads to the formation of Py dimers by eliminating two H atoms. Later, the formed Py dimers then repeat the previous oxidation reaction forming the Py dimer cation and undergo coupling reaction with another Py cation. Finally, the PPy polymers are formed according to this step-by-step mechanism.[10] This mechanism which has been highlighted in Samy Remita's team by pulse radiolysis during the thesis of Cecilia Coletta is comparable to that of PEDOT polymerization.[11,12]

Although the synthesis of PPy polymers has been widely studied for a long time, many efforts are still being spent on simplifying their preparation and optimizing their properties.[13,14] Compared with the common chemical and electrochemical methods, radiolytic method is based on the interaction of high energy ionizing radiations with matter. Instead of using external oxidative chemicals to initiate polymerization as in the case of chemical method, γ-radiolysis of aqueous solution leads to the quantitative and selective *in situ* production of radicals which come from the more abundant species present in the medium: the solvent molecules. These radicals, such as hydroxyl radicals (HO•) which are known to be very oxidative species should then act as

initiators of PPy synthesis.[15] In this way, the synthetic procedure is easier and environmentally friendly. In other words, water is used as the solvent without addition of chemical oxidants.

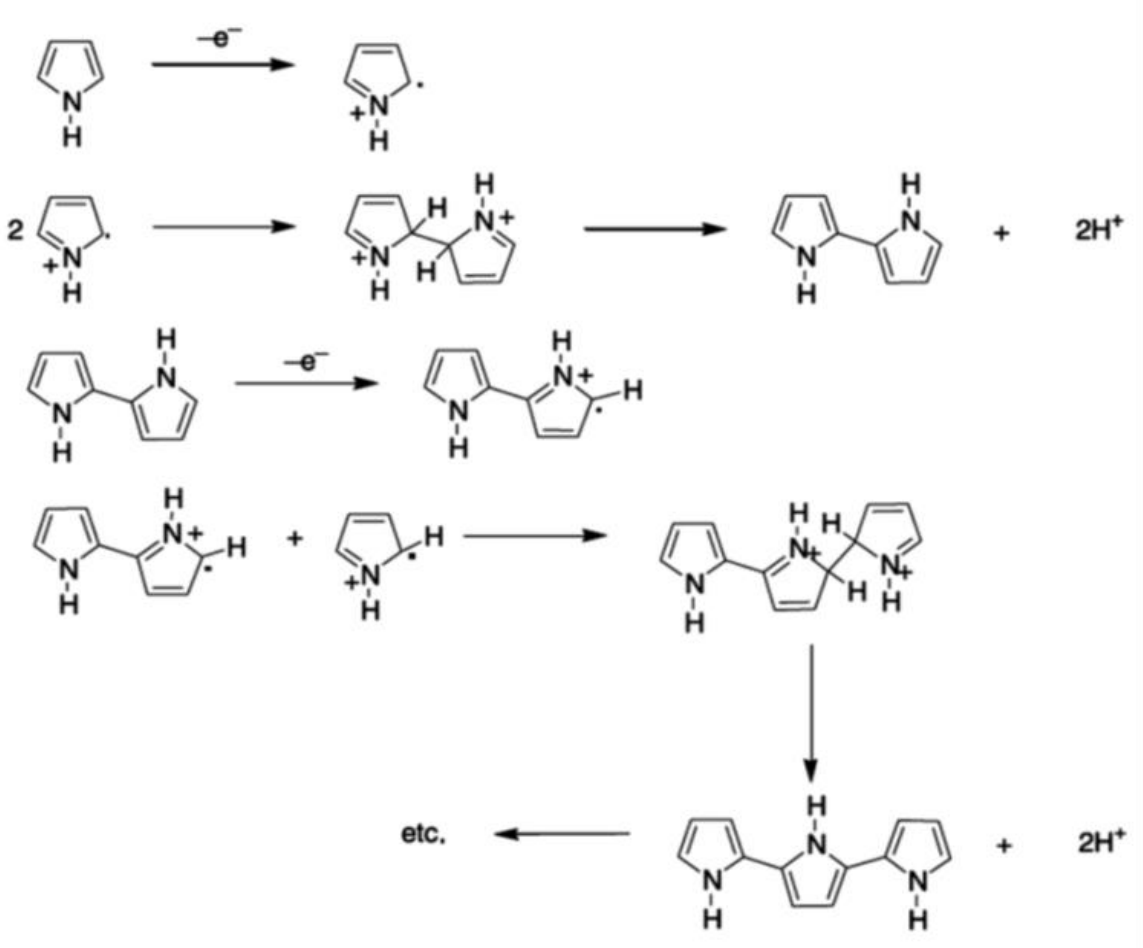

Figure 4.1 Proposed mechanism for electropolymerization of pyrrole.[10]

In the previous part (chapter 3), PEDOT polymers are successfully synthesized thanks to the use of different oxidizing species produced by water radiolysis.[12,16,17] It is demonstrated that the polymerization growth of PEDOT proceeds through a recurrent step-by step oxidation process. This means that for a quantitative polymerization, the concentration of initiators must be at least two times higher than that of monomers. Also, we demonstrated that the nature of the oxidizing species produced from water radiolysis determines the morphology as well as the physicochemical properties of the radiosynthesized PEDOT nanostructures.[17]

In order to demonstrate the versatility of radiolytic method, the original radiolytic methodology is extended here to the synthesis of another CP, the polypyrrole (PPy) in aqueous solution under N_2O atmosphere. Under these conditions, the hydroxyl radicals (HO•) produced by water radiolysis should act as an oxidizing species towards Py monomers leading to PPy polymers. For comparison purpose, PPy polymers are also synthesized by traditional chemical method using potassium persulfate ($K_2S_2O_8$) as oxidant and as polymerization initiator. The morphology and the properties of PPy synthesized by both methods are compared in details.

4.1 PPy synthesis methodologies and characterizations

4.1.1 Solution preparation

Pyrrole (Py) was used as the monomer and ultrapure water was used as the solvent. N_2O was used to degas the aqueous solutions of pyrrole before γ irradiation. Aqueous solutions containing different concentrations in pyrrole ranging between 1 and 20 mM were prepared. Note that these concentrations are both by far lower than Py solubility in water (0.9 M). Then, the samples were degassed with N_2O for 20 min and irradiated with a ^{60}Co γ source (Laboratoire de Chimie Physique, LCP, Paris-Sud University) at a dose rate of 6 $kGy \cdot h^{-1}$ in order to synthesize PPy polymers. For comparison purpose, chemical oxidant namely $K_2S_2O_8$ was used for chemical synthesis of PPy.

4.1.2 Radiolytical and chemical preparation of PPy

Radiolytic method. Upon irradiating N_2O-saturated diluted aqueous solutions at neutral pH, the radiolytic yield of formation of hydroxyl radicals (HO•) is 5.6×10^{-7} $mol \cdot J^{-1}$ (equation 2.15, chapter 2). The concentration of HO• produced by water radiolysis can then be expressed as a function of the irradiation dose, D expressed in Gray (Gy) according to:

$$[HO\bullet]\ (mol \cdot L^{-1}) = D\ (Gy) \times G\ (HO\bullet)\ (mol \cdot J^{-1}) \qquad (4.1)$$

As demonstrated in the previous part (section 3.2.2, chapter 3), for quantitative polymerization of CP, the concentration of oxidative species (HO•) should be twice that of Py monomers ($[Py]_0$).[16,17] As a consequence, the dose D_{max} needed for a quantitative polymerization of Py can be calculated as follows:

$$D_{max}\ (Gy) = \frac{2[Py]_0\ (mol\ L^{-1})}{G(HO\bullet)\ (mol\ J^{-1})} \qquad (4.2)$$

It thus amounts to 3.6 kGy for 1 mM in Py and to 72 kGy for 20 mM in Py. Py solutions were then irradiation at such doses.

Chemical method. For comparison purpose, PPy was also synthesized by a chemical method. Aqueous solution containing both pyrrole monomers (20 mM) and $K_2S_2O_8$ oxidant (40 mM) was prepared and stirred for another 24 h to ensure that Py monomers fully polymerize into polypyrrole.[18] As in the case of radiolytical method, the molar ratio of monomer to oxidant was 1:2 to ensure quantitative polymerization.

4.1.3 PPy characterization

In order to check whether the polymerization of pyrrole monomers occurred by both radiolytic method and chemical method, Ultraviolet-visible (UV-vis) spectra of pyrrole aqueous solutions or suspensions before and after polymerization were recorded in quartz cell with an optical path length of 0.2 cm. The reference was always ultrapure water. All the solutions of Py after polymerization were dried by to obtain dehydrated powders. After lyophilization, all the samples were further directly investigated by ATR-FTIR, SEM and TGA.

To further identify PPy and its chemical composition, the Fourier transform infrared (FTIR) spectra of lyophilized PPy were recorded. In order to observe the morphology of radiosynthesized PPy polymers in aqueous solutions, *in-situ* observation of the morphology of PPy was carried out on a transmission electron microscope in a cryogenic environment (Cryo-TEM). In order to check whether the radiosynthesized PPy maintained its original morphology during the drying process, after γ irradiation, a small drop of the solution was deposited onto the upper surface of ZnSe prism (transparent in the mid-IR) and dried naturally. The dried deposit

was observed by AFM-IR that combines the AFM with a pulsed infrared laser to perform spectromicroscopy.[19-21] In order to check the morphology of PPy polymers synthesized by radiolytic and chemical methods, PPy powders obtained after lyophilization were observed by scanning electron microscopy (SEM).

The thermal stability and composition analysis of PPy was performed on a thermogravimetric analysis instrument (TGA). To measure the conductivity of PPy, spin-coated films of PPy were obtained by spinning a small drop of PPy suspensions on an ITO substrate. Before measurements, the nanostructures of PPy solutions or suspensions were doped with $NOBF_4$ at a concentration of 10^{-2} M in acetonitrile. A four-point probe technique was used for measuring the resistance of PPy film and a surface profiler was used for the thickness measurement of the film. The conductivity, ρ ($S \cdot cm^{-1}$) of doped PPy film was determined according to equation 2.35, chapter 2.

4.2 HO•-induced oxidation of Py monomers

Aqueous solution containing 1 mM in Py was prepared under N_2O atmosphere. Its UV-vis absorption absorption spectrum displays the 205 nm characteristic peak of Py monomers which corresponds to a π-π^* transition (Figure 4.2, left).[22,23] The molar extinction coefficient of Py monomers amounts to: ε_{205} = 6730 $L \cdot mol^{-1} \cdot cm^{-1}$ (in hexane).[22] This solution was irradiated at increasing doses up to 3.6 kGy and UV-vis absorption spectra were recorded as a function of the dose (Figure 4.2, left). The absorption of Py monomers at 205 nm as a function of the dose is plotted (Figure 4.2, right). One can observe the decrease of the absorption as a function of the irradiation dose, which means that Py is progressively consumed (according to a pseudo-first order exponential decay).

The initial radiolytic yield of Py consumption, G_{-Py0}, corresponds to the value of the initial slope of the curve which can be deduced thanks to an exponential fit of the experiment curve:

$$G_{-Py\,0}\,(\text{mol J}^{-1}) = -\left(\frac{\text{d[Py] (mol L}^{-1})}{\text{dDose (Gy)}}\right)_0 = 6.0 \times 10^{-7}\ \text{mol J}^{-1} \qquad (4.3)$$

It is clear that: $G_{-Py0} \approx G(HO\bullet)$. This indicates that a concentration of 1 mM in Py is sufficient to scavenge all the HO• radicals produced by radiolysis and demonstrates that only HO• radicals

react with Py monomers. Indeed, HO• is a strong oxidizing species since its standard redox potential in neutral medium (pH=7) amounts to $E^{0'}(HO•/H_2O)$ = 2.3 V_{HSE} enabling oxidation of Py ($E^{0'}(Py^{+}/Py)$ = 0.76 V_{SHE}).[24,25] Therefore, it is clear that the radiation induced polymerization of pyrrole can be initiated by HO• as expected. Therefore, as previously explained, the dose needed for quantitative polymerization of Py could be easily calculated (equation 4.2). In particular, 72 kGy are needed for 20 mM in Py.

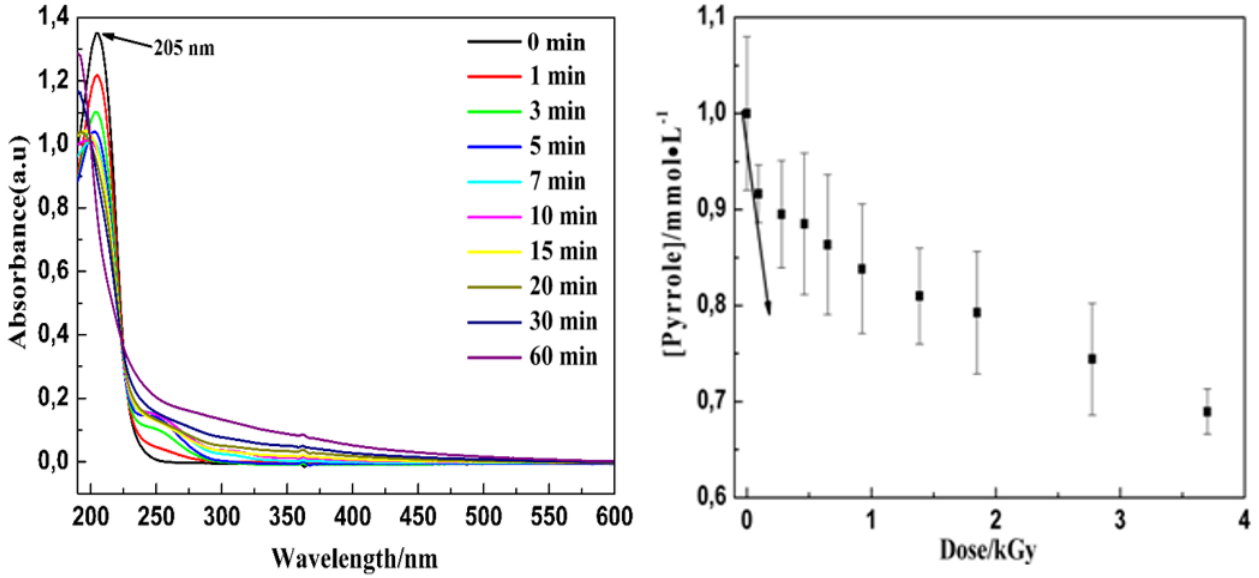

Figure 4.2 UV-vis absorption spectra of aqueous solution of pyrrole (1 mM) as a function of the dose (left). Evolution of pyrrole concentration as a function of the irradiation dose (right), l = 0.2 cm. Reference: water.[23]

4.3 Radiation induced synthesis of PPy, a comparison with chemical synthesis

While relatively low concentrations in Py monomers (1 mM, see previous section) were needed for succeeding in the follow-up of their oxidation mechanism, higher concentrations were necessary for the characterization of PPy polymers either in aqueous solution or after their deposition onto substrates as it will be presented in the case of 20 mM in Py.

Aqueous solutions containing 20 mM in Py were irradiated at 72 kGy (Figure 4.3).[23] It is noted that after irradiation (spectrum b), only a shoulder is observable at 205 nm indicating that polymerization is indeed almost quantitative at 72 kGy since only a small amount of Py monomers remains in solution.

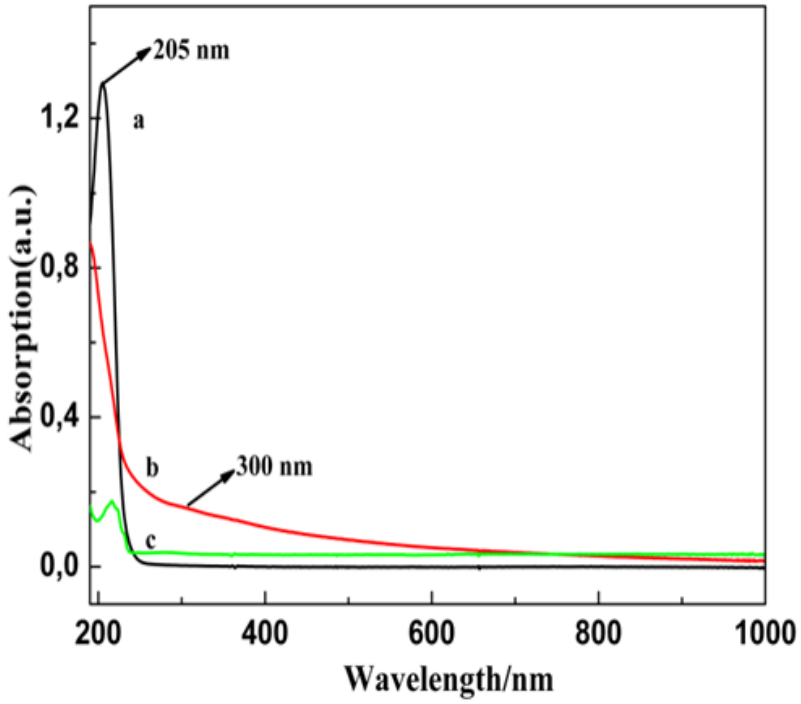

Figure 4.3 UV-vis absorption spectra of pyrrole before and after polymerization by radiolytic and chemical methods. (a) Aqueous solution of pyrrole (20 mM) before polymerization (diluted 20 times), (b) PPy synthesized by radiolytic method, γ-PPy (diluted 20 times), and (c) PPy synthesized by chemical method, χ-PPy (diluted 20 times), L= 0.2 cm, Reference: water.[23]

Py disappearance parallels the formation of species which absorb at 300 nm as observed in spectrum b. Vetter *et al.* reported that the shoulder at 300 nm should be attributed to terpyrrole.[26] Also, after a 72 kGy irradiation, continuous scattering (long absorption tail) in the range 400~1000 nm whose intensity increases with irradiation dose, is observed in the extinction spectrum b. This is characteristic of the π-π* transition of PPy with higher molecular weight.[26-28]

This scattering should result from the presence of a black suspension in the medium as observed (Figure 4.4, image b). This suspension becomes denser and the solution appears more turbid as the irradiation dose increases. As it will be demonstrated later, this suspension corresponds to PPy polymers formed at high doses thanks to the HO•-induced oxidation process. These polymers formed by radiolysis are called γ-PPy. Note that no sedimentation is observed in this case. This may be explained by a relatively low molecular weight of the polymers. Nevertheless, the absence of any deposition implies that γ-PPy polymers are not hydrophobic.

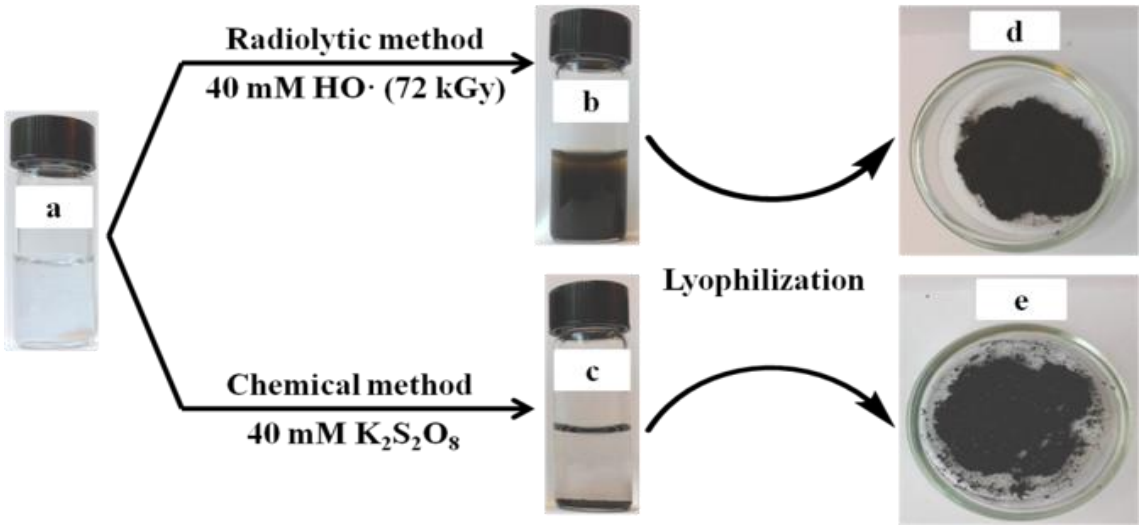

Figure 4.4 Photographs of Py samples before (a), after polymerization (b) and (c) and after lyophilization (d) and (e).[23]

In order to compare the radiolytic procedure with a more common chemical methodology, 40 mM of $K_2S_2O_8$ was added as oxidant to a solution containing 20 mM in Py (ratio Py/ $K_2S_2O_8$ = 1:2) under stirring. After 24 hours, the absorption spectrum of the solution was recorded (Figure 4.3, spectrum c). This spectrum is somewhat different from the spectrum b. Indeed, one can note the presence of residual Py monomers characterized by the absorption at 205 nm meaning that, in the present experimental conditions, chemical polymerization is less complete than radiation induced one. While no peak at 300 nm, characteristic of terpyrrole, is observed (Figure 4.3, spectrum c). Continuous absorption in the range 400~1000 nm is present such as in the case of radiolytical method. Nevertheless, the lower intensity of the extinction spectrum c in comparison with that of spectrum b could be explained by the sedimentation process observable in the case of chemical method. Indeed, contrarily to radiolytical method, a black powder deposits in this latter case at the bottom of the solution as observed (Figure 4.4, image c).

Thus, as in the case of radiolysis, PPy polymers are formed in aqueous solution thanks to chemical oxidation of Py. These polymers are called χ-PPy. Nevertheless, the chemically synthesized polymers (χ-PPy) should be more hydrophobic than radiosynthesized ones (γ-PPy) or could have higher molecular weight since they precipitate.

4.4 Highlighting γ-PPy radioinduced synthesis

In order to perform ATR-FTIR experiments for comparing the chemical nature of both γ-PPy and χ-PPy, the two samples (Figure 4.4, images b and c) were lyophilized. In both cases, black powders were obtained (Figure 4.4, images d and e). While the powder obtained after irradiation is only polymers, the powder obtained after chemical oxidation should also contain $K_2S_2O_8$ and its conjugated reducing species. According to the oxidation mechanism which involves persulfate ion ($S_2O_8^{2-}$), sulfate radical ($SO_4^{\bullet -}$) is formed (equation 2.1, chapter 2) then oxidizes Py monomers leading to Py radical cation ($Py^{\bullet +}$) and sulfate anion (SO_4^{2-}). We can assume that $Py^{\bullet +}$ dimerizes into Py_2 which undergoes a step-by-step polymerization process leading to the PPy polymers as demonstrated in the thesis of Cecilia Coletta.[11]

The ATR-FTIR spectrum of γ-PPy is presented (Figure 4.5, spectrum b) in the wavenumber region 600~4000 cm^{-1} together with those of χ-PPy (Figure 4.5, spectrum c) and pure non irradiated Py liquid sample (Figure 4.5, spectrum a).[23] Note that the deposition of Py liquid phase is translated by a better resolution when compared with the solid phase deposition of lyophilization polymer powders.

The three obtained spectra are in good agreement with those previously reported for Py and PPy in literature.[26,29,30] In addition, no considerable differences exist between spectra b and c. Only small shifts in the vibration modes can be observed. Starting from what is known in literature about Py, vibration at 3396 cm^{-1} observed in spectrum a can be attributed to the in plane stretching of N-H.[28,31] The bands at 1571 and 1467 cm^{-1} are due to C-C in-ring-stretch mode and stretching vibration of pyrrole rings respectively.[18,29] The band at 1047 cm^{-1} is mostly attributed to C-C out-of-plane deformation vibration.[29,31] The strong band at 726 cm^{-1} results from the C-H wag vibration at α, α′ positions.[30]

After polymerization, the C-H wag vibration and N-H in plane stretching in spectra b and c decrease obviously indicating that free pyrrole monomers are not observable here, suggesting that polymerization of pyrrole is relatively quantitative. In the case of chemically synthesized PPy (Figure 4.5, spectrum c), the broad band at 3120 cm^{-1} can't be due to the presence of water since samples were lyophilized. It corresponds to the stretch of N-H bond and the peak at 1700 cm^{-1} corresponds to the stretch of C=O.[32] It has been reported that the C=O structure at the β position of the pyrrole ring is typically due to the overoxidation of polypyrrole.[26] The bands at 1556, 1481

and 1043 cm^{-1} correspond to stretching mode of C=C, C-N and C-C out-of-plane vibration indicating the formation of PPy.[29] The bands at 1184 and 916 cm^{-1} are attributed to the S=O group and stretching vibration of PPy showing that chemically synthesized PPy is doped with the oxidant. [18,31]

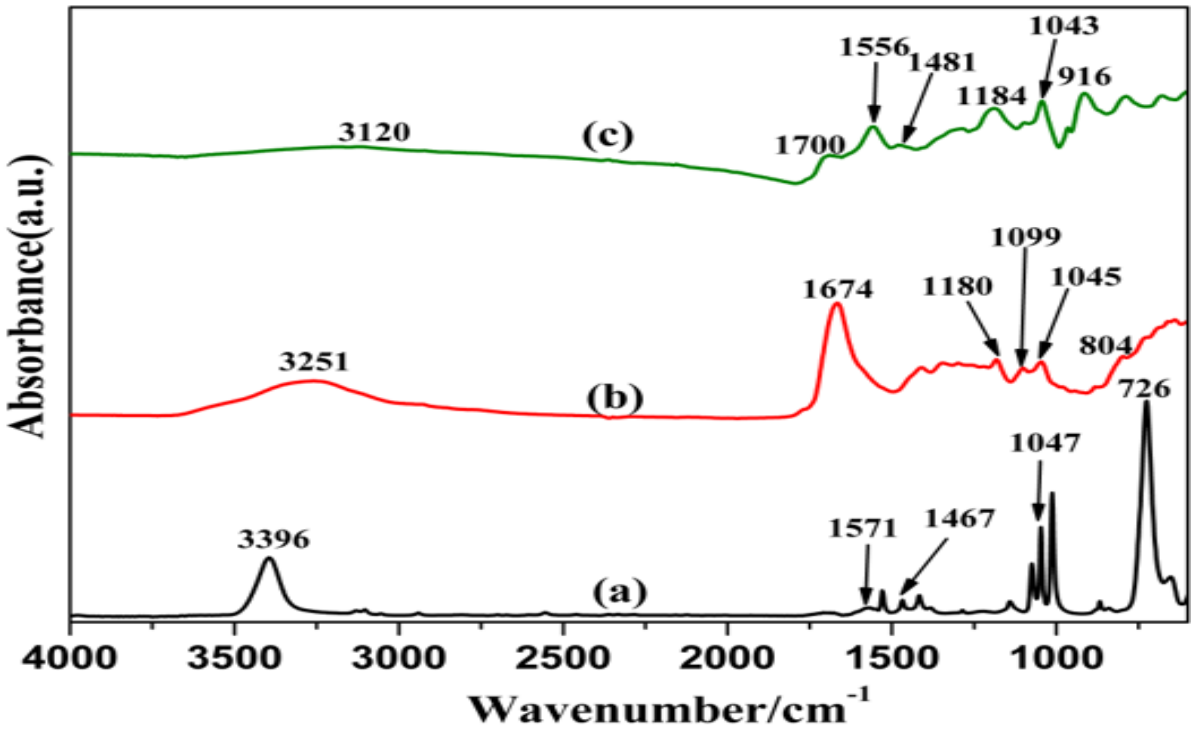

Figure 4.5 ATR-FTIR spectra of pure pyrrole before polymerization (a), radiosynthesized PPy after lyophilization (b), and chemically synthesized PPy after lyophilization (c).[23]

In the case of PPy synthesized by radiolytical method (Figure 4.5, spectrum b), some bands are more or less displaced. The bands at 1180, 1099 and 1045 correspond to C-H, =C-H in-plane and C-C out-of plane vibration proving the successful preparation of PPy.[26,29,31] Nevertheless, there is an obvious carbonyl C=O group peak at 1674 cm^{-1}, which is more intense than the C=O group peak at 1700 cm^{-1}in the case of χ-PPy. The presence of this peak obviously demonstrates that γ-PPy is overoxidized.[26,33] The spectrum of γ-PPy also exhibits a very large band around 3251 cm^{-1}. As in the case of χ-PPy (Figure 4.5, spectrum c), this band is attributed to the N-H bond. The observation of such a very large band should result from the N-H groups of the polymers. On the other hand, this very large and relatively intense band observed in the case of γ-PPy could also

come from the -OH functionalization of the polymers by HO• radicals. This has already been established in the case of radiation induced synthesis of PEDOT. This result is also in very good agreement with literature since HO• radicals are known to add to the double bonds of organic molecules and with pulse radiolysis study of Py polymerization which has been carried out in the thesis of Cecilia Coletta.[11,29,34,35]

Therefore, PPy was successfully synthesized by both radiolytical and chemical methods. Nevertheless, radiosynthesized PPy polymers could be functionalized by O-H and C=O groups which should then explain their higher hydrophilicity in comparison with that of χ-PPy.

4.5 Morphological observations of PPy

As the solubility in water of PPy synthesized by radiolytic method (γ-PPy) is relatively high, the *in-situ* observation of the morphology of γ-PPy is possible by Cryo-TEM. Aqueous solutions containing 20 mM in Py and irradiated at 72 kGy were observed by cryo-transmission electron microscopy just after irradiation. Representative images showed the presence of low density globular structures forming polydisperse spherical nanoparticles the diameter of which was comprised between 80 and 200 nm as observed (Figure 4.6, image a).[23]

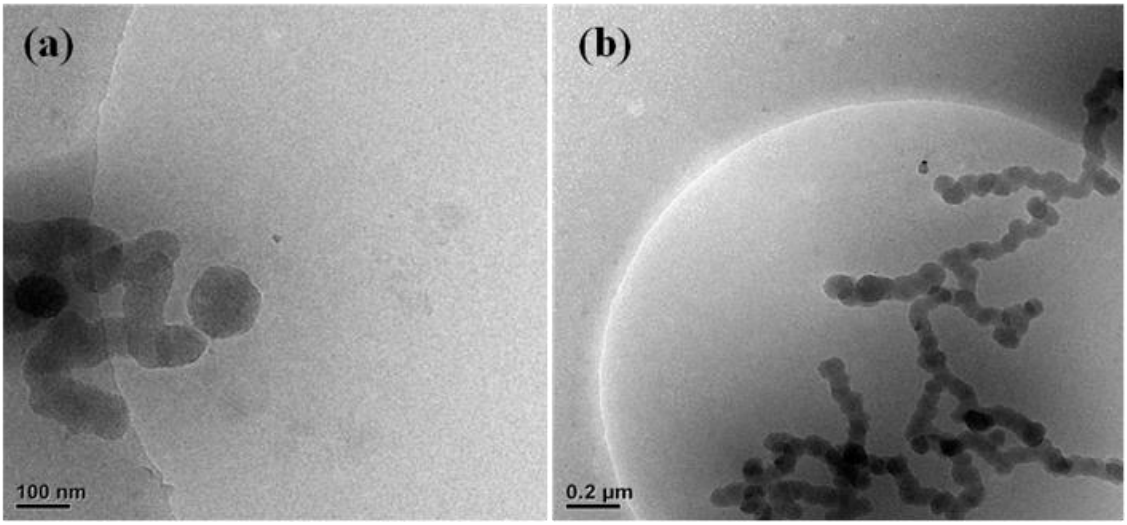

Figure 4.6 Cryo-TEM images of radiosynthesized PPy (γ-PPy) at 72 kGy.
(a) Nanostructures of γ-PPy, (b) full view of chaplets of γ-PPy.[23]

Also, these particles systematically appeared self-assembled into nanochaplets after lyophilization (Figure 4.6, image b). These results are in good agreement with previous observations reported in literature concerning such polymer systems.[36,37]

Since no other low density objects were observed during Cryo-TEM experiments, we deduce that these more or less spherical nanoparticles are made up of radiosynthesized PPy polymers. Each globular structure observed on Figure 4.6 should correspond to the self-assembly of independent amorphous PPy polymer chains which interact all together by hydrogen-bonds as already reported in literature.[35,38] Also, the packing and the structuration of the polymers into supramolecular nanochaplets should also result from such intermolecular interactions.

In order to definitely prove the PPy nature of these spherical nanoparticles and in order to characterize the morphology of the polymers after a deposition procedure and also to check whether a drying process is able to affect the morphology of PPy, a drop of the solution containing the PPy black suspension obtained after a 72 kGy-irradiation (polymers of Figure 4.6) was deposited onto a ZnSe prism, then dried, and finally imaged and characterized by AFM-IR (Figure 4.7).[23]

According to the AFM image of γ-PPy recorded in contact mode, the top dark areas having no thickness correspond to the substrate (Figure 4.7, image a).[23] The topography of γ-PPy displayed as the bright areas correspond to the thicker regions made up of isolated bigger spherical PPy nanoparticles and closely packed smaller ones (200~300 nm in average).[39] This AFM observation agrees well with the morphology of γ-PPy particles previously observed in aqueous solution by Cryo-TEM (Figure 4.6) without any significant change in the mean size and in the shape. Then, the packing of the particles and their flattening onto the substrate when deposited and dried do not seem to affect the nanostructuration of γ-PPy polymers.

In order to confirm that the nanoparticles already observed by Cryo-TEM and AFM contain only PPy polymers without any residual Py monomers, the sample was observed by AFM-IR in the range of 1600~1800 cm^{-1} (Figure 4.7, image b). The spectrum of image b in Figure 4.7 displays a peak at 1674 cm^{-1} which is characteristic of C=O bonds. Now, these bonds have been detected by ATR-FTIR spectroscopy in the γ-PPy polymers (Figure 4.5, spectrum b) and not in Py monomers (Figure 4.5, spectrum a). This demonstrates that the globular structures observed in both Figure 4.6 and Figure 4.7 (image a) do not contain close-packed Py monomers.

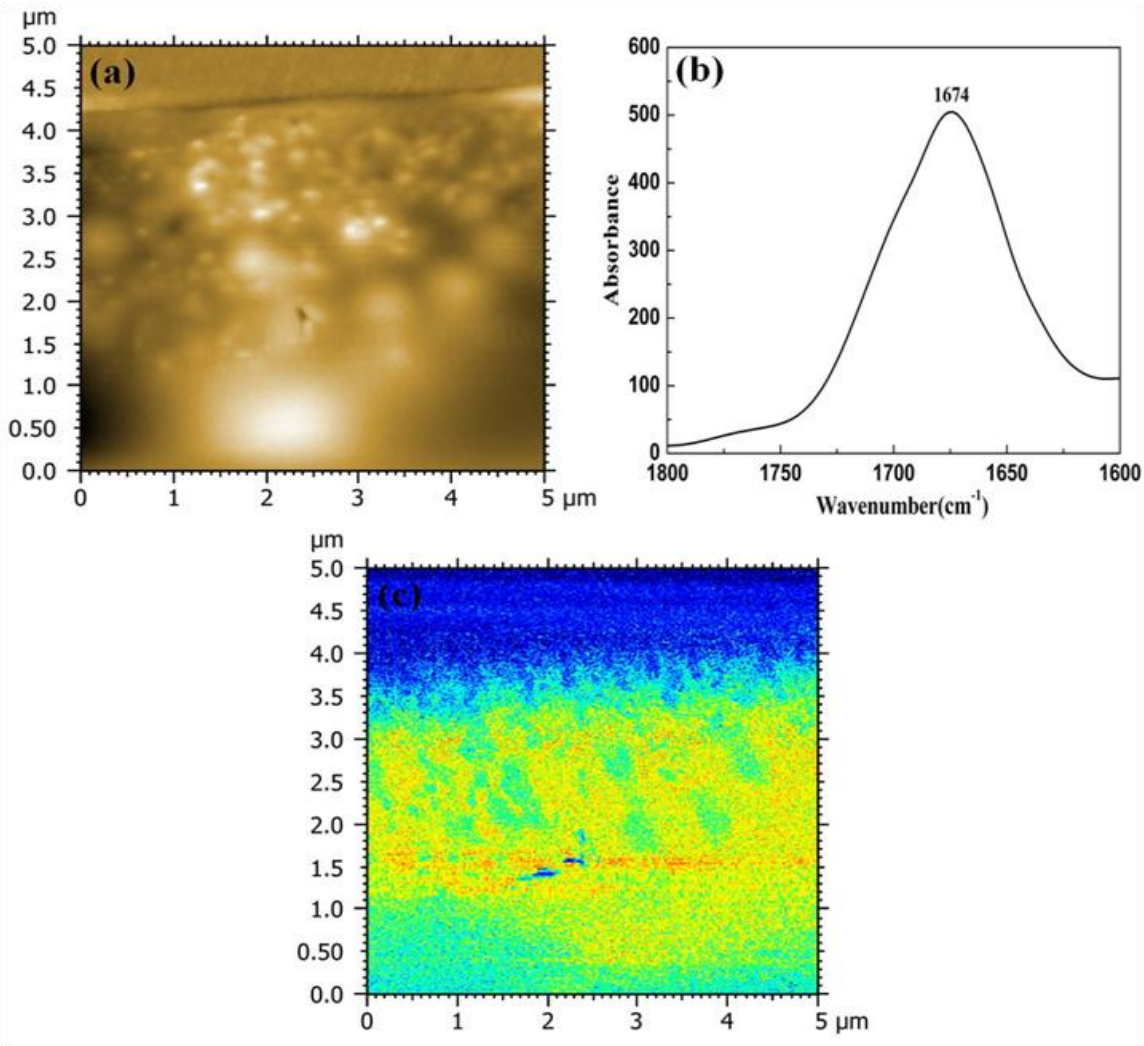

Figure 4.7 AFM topographic image of γ-PPy in contact mode, (b) AFM-IR spectrum of PPy, and (c) AFM-IR chemical mapping of PPy with the IR source tuned to the C=O band at 1674 cm^{-1}.[23]

Since the AFM-IR technique also enables the chemical mapping of the sample, this wavenumber 1674 cm^{-1} was chosen for AFM-IR chemical mapping of our sample (Figure 4.7, image c). In Figure 4.7 (image c), the red and yellow areas indicate a stronger absorption at the characteristic wavenumber which is caused by a thick layer of γ-PPy (~500 nm) linked onto the prism. Compared with the topography of the sample (Figure 4.7, image a), it is clear that these thick areas correspond to the bright regions of the γ-PPy. As the distribution of γ-PPy nanoparticles on the prism is inhomogeneous, the appearance of AFM-IR is not totally the same as its topography. Nevertheless, the signal of AFM-IR (Figure 4.7, image c) fits well with the

thickness of γ-PPy (Figure 4.7, image a). Thus, it is definitely assumed that the nanoparticles observed on Figure 4.7 (image a) are composed of γ-PPy polymers without any packed Py monomers.

This result does not only prove that radiosynthesized PPy are spherical nanoparticles but also further explains their hydrophilicity and their packing into nanochaplets. Indeed, the presence of C=O bonds at the surface of the PPy nanoparticles, as demonstrated by AFM-IR, should enhance the probable effect of O-H functionalities, leading to strong hydrogen-bonds interactions between the self-assembled nanoparticles as well as with the aqueous solvent.

In order to check whether the lyophilization procedure and whether the substrate nature affect the morphology of γ-PPy nanoparticles, the lyophilized PPy powder obtained after a 72 kGy-irradiation was observed by SEM microscopy. Typical image is displayed and γ-PPy polymers appear as more or less spherical nanoparticles with a mean size of 100 nm (Figure 4.8, image a).[23] This definitely proves that the presence of the solvent, that the lyophilization, that the nature of the substrate have no influence on the nanostructuration of the polymers. This would imply the existence of very strong hydrogen-bond interactions into each nanoparticle.

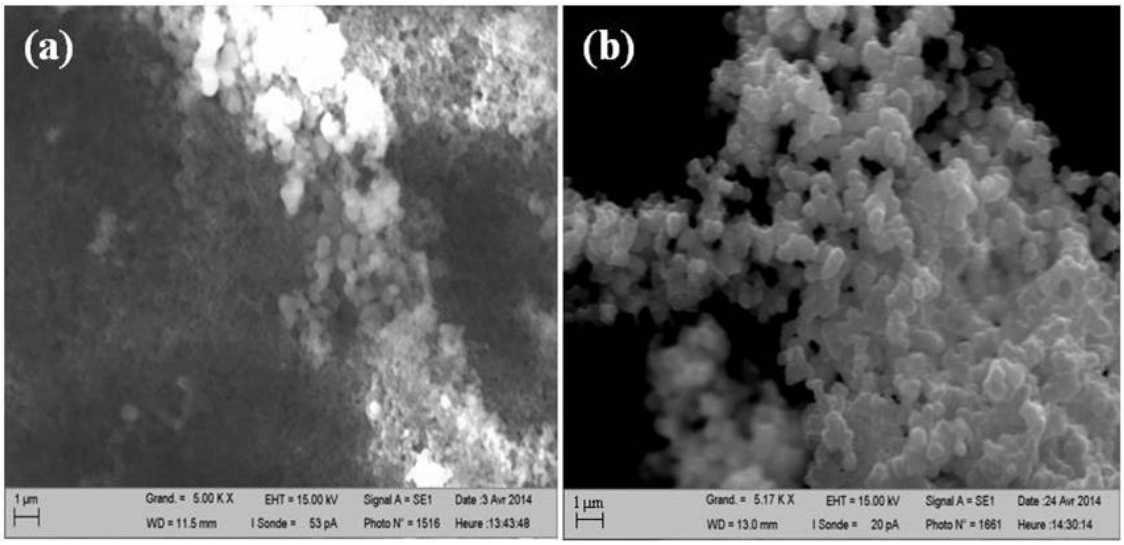

Figure 4.8 SEM images of PPy lyophilized after radiolytical (a) or chemical (b) synthesis.[23]

In order to compare the morphology of γ-PPy with that of χ-PPy, the lyophilized PPy powder obtained in the presence of 40 mM in $K_2S_2O_8$ was also observed by SEM (Figure 4.8, image b).

χ-PPy polymers also appear as more or less close-packed spherical nanoparticles.[40] However, the value of the mean-size (~200 nm) and that of the polydispersity are much higher than those corresponding to γ-PPy. This result proves that our radiolytic methodology does not only lead to more hydrophilic PPy polymers, but also to smaller and less polydisperse PPy nanoparticles. Due to the absence of O-H and C=O groups into χ-PPy, the bigger size of χ-PPy nanoparticles in comparison with that of γ-PPy structures, could explain their sedimentation observed after their chemical synthesis into water (Figure 4.4, image c).

4.6 Physico-chemical properties of γ-PPy, a comparison with χ-PPy

4.6.1 Thermal stability

We wanted to check and to compare the thermal stability of γ-PPy and χ-PPy previously synthesized and obtained as powders after lyophilization. The thermo gravimetric analysis (TGA) plots of both PPy polymers are shown (Figure 4.9).[23] The inset displays the temperature at which the weight loss of PPy occurs.

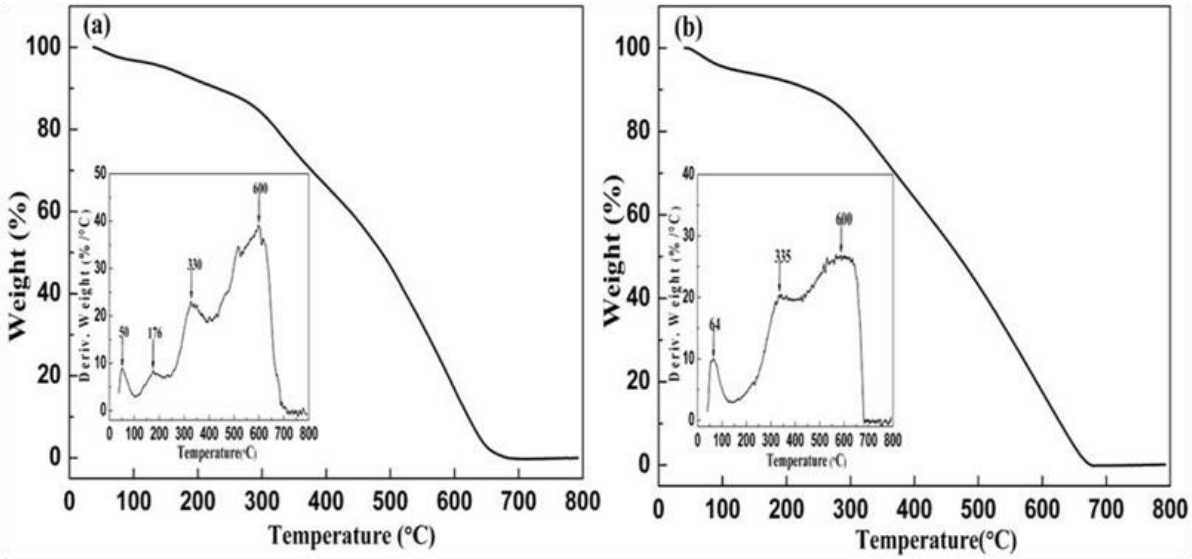

Figure 4.9 Thermo gravimetric analysis (TGA) plots of PPy synthesized by radiolytic method (a) or chemical method (b). Insert: the weight derivative curves of PPy as the temperature changes.[23]

In the case of γ-PPy (Figure 4.9, image a), the weight loss exhibits three stages of decomposition which is in agreement with literature.[41] From 40 to100 °C, the main loss of weight happens at 50 °C which may be caused by the loss of some unreacted pyrrole. Then, in the range 100-400 °C, the weight loss at 176 °C may be caused by the loss of terpyrrole which was observed by UV-visible absorption spectroscopy (Figure 4.3, spectrum b), while the main weight loss which occurs at about 330 °C may correspond to the decomposition of some γ-PPy oligomers characterized by low molecular weights.[26] Finally, the decomposition of the backbone of PPy occurs at around 600 °C. This TGA analysis is in very good agreement with TGA data already reported in literature concerning PPy polymers.[31,42] Note that the same thermal stability is found for χ-PPy (Figure 4.9, image b). This result indicates that the size of the PPy polymer nanoparticles as well as their functionalization by C=O or O-H groups seem to have no effect on their thermal behavior.

4.6.2 Electrical conductivity

In order to check and to compare the electrical conductivity of γ-PPy and χ-PPy by four point probe technique, both samples were doped with $NOBF_4$ (10 mM). It is found that the electrical conductivity of χ-PPy is 1.2 $\times 10^{-2}$ $S \cdot cm^{-1}$. This value is similar to those reported in literature.[43] Interestingly, the electrical conductivity of γ-PPy synthesized by the original radiolytical procedure was found to be higher: 5.7×10^{-2} $S \cdot cm^{-1}$. This result proves that, even if the thermal stability of γ-PPy is not better than that of χ-PPy, the value of the electrical conductivity of γ-PPy is nearly five times higher than that of χ-PPy. The higher conductivity of γ-PPy could be related to the smaller particles size and the bigger surface areas.[44,45] Indeed, as the diameter decreases, more ordered chains of connected structure of γ-PPy networks could counteract the influence of insulated cavities and bigger surface areas could enhance the delocalization of charge carriers over an extended region of the polymer chains. We think that both aspects contribute to a relatively higher electrical conductivity of γ-PPy.

4.7 Conclusions

In the previous chapter, we succeeded in the development of a new γ-radiolysis-based alternative way for synthesizing PEDOT polymers in aqueous solution. In the present chapter,

this radiolytic methodology was extended as an alternative green way for the synthesis of conducting PPy polymers in aqueous solution.

PPy polymers synthesized by radiolysis are characterized by a very good long-term stability at air in a humid environment. We showed that the as-prepared PPy polymers remain well-dispersed in water, can be easily dried and are quite simply redispersed in protic solvents. As revealed by ATR-FTIR spectroscopy, the probable presence along the polymeric chains of O-H and C=O functionalities, which should come from the addition of hydroxyl radicals during the polymer growth, could explain the hydrophilic properties of the radiosynthesized PPy polymers. This could also justify the existence in aqueous solution of the globular self-assembled structures made up of PPy polymeric chains and their packing into nanochaplets as observed by cryo-TEM.

After deposition onto substrate, the radiosynthesized PPy polymers appear as more or less spherical nanoparticles as revealed by AFM and SEM observations. Moreover, in an original way, high resolution atomic force microscopy, coupled with infrared nanospectroscopy was used to probe the local chemical composition of PPy nanostructures.

A detailed investigation enabled the comparison between the properties of radiosynthesized PPy and those of PPy synthesized by a conventional chemical polymerization. We found that radiosynthesized PPy nanoparticles are more hydrophilic, smaller and less polydisperse than chemically synthesized PPy. Besides, we demonstrated that radiosynthesized PPy nanostructures are characterized by a very good thermal stability and an electrical conductivity which is five times higher than that of chemically synthesized PPy.

In this chapter, the radiolytic procedure is extended to the successful synthesis of another representative CP (different from PEDOT), namely PPy. This definitely demonstrated the versatility of this original radiolytic methodology which should lead to the polymerization of other kinds of CPs in aqueous solution including: PANI, P3HT, PTAA, etc.

At this stage of the research project, PEDOT and PPy have been prepared by radiolysis, by using oxidizing radiolytical radicals in water in neutral medium. Now, the questions are: is it possible to synthesize such CPs in other experimental conditions? What is the influence of such conditions on the stability, the morphology and the properties of radiosynthesized CPs?

In the next chapter, further work is focusing on the study of the presence of surfactant and the influence of the pH on the radiation induced synthesis of PEDOT polymers.

References

[1] Groenendaal, L.; Jonas, F.; Freitag, D.; Pielartzik, H.; Reynolds, J. R., Poly(3,4-ethylenedioxythiophene) and Its Derivatives: Past, Present, and Future. *Adv. Mater.* **2000,** *12* (7), 481-494.

[2] De Jesus, M. C.; Fu, Y.; Weiss, R. A., Conductive polymer blends prepared by in situ polymerization of pyrrole: a review. *Polym Eng Sci* **1997,** *37*, 1936-1943.

[3] Uter, W.; Stropp, G.; Schnuch, A.; Lessmann, H., Aniline - a 'historical' contact allergen? current data from the ivdk and review of the literature. *Ann Occup Hyg* **2007,** *51*, 219-226.

[4] Harun, H. M.; Saion, E.; Kassim, A.; Yahya, N.; Mahmud, M., Conjugated conducting polymers: a brief overview. *J. Acoust. Soc. Am.* **2007,** *2*, 63-68.

[5] Khulbe, K. C.; Mann, R. S.; Khulbe, C. P., Polymerization of pyrrole by potassium persulfate. *J. Polym. Sci., Part A: Polym. Chem.* **1982,** *20*, 1089–1095.

[6] Li, X.; Wan, M. X.; Wei, Y.; Shen, J. Y.; Chen, Z. J., Electromagnetic functionalized and core-shell micro/nanostructured polypyrrole composites. *J. Phys. Chem. B.* **2006,** *110*, 14623-14626.

[7] Leonavicius, K.; Ramanaviciene, A.; Ramanavicius, A., Polymerization model for hydrogen peroxide initiated synthesis of polypyrrole nanoparticles. *Langmuir* **2011,** *27*, 10970-10976.

[8] Li, C.; Bai, H.; Shi, G. Q., Conducting polymer nanomaterials: electrosynthesis and applications. *Chemical Society reviews* **2009,** *38*, 2397-2409.

[9] Ramanaviciene, A.; Kausaite-Minkstimiene, A.; Oztekin, Y.; Carac, G.; Voronovic, J.; German, N.; Ramanavicius, A., Visualization of red-ox proteins on the gold surface using enzymatic polypyrrole formation. *Microchimica Acta* **2011,** *175* (1), 79.

[10] Camurlu, P., Polypyrrole derivatives for electrochromic applications. *RSC Advances* **2014,** *4* (99), 55832-55845.

[11] Coletta, C., Study of growth mechanism of conducting polymers by pulse radiolysis. *Ph.D thesis* **2016**, 148.

[12] Coletta, C.; Cui, Z. P.; Archirel, P.; Pernot, P.; Marignier, J. L.; Remita, S., Electron-Induced Growth Mechanism of Conducting Polymers: A Coupled Experimental and Computational Investigation. *The Journal of Physical Chemistry B* **2015,** *119* (16), 5282-5298.

[13] Zhang, X. T.; Zhang, J.; Song, W. H.; Liu, Z. F., Controllable synthesis of conducting polypyrrole nanostructures. *J. Phys. Chem. B* **2006,** *110*, 1158-1165.

[14] Wang, D.; Li, Y. X.; Shi, Z.; Qin, H. L.; Wang, L.; Pei, X. F.; Jin, J., Spontaneous growth of free-standing polypyrrole films at an air/ionic liquid interface. *Langmuir* **2010,** *15*, 8259–8264.

[15] Varmenot, N.; Remita, S.; Abedinzadeh, Z.; Wisniowski, P.; Strzelczak, G.; Bobrowski, K., Oxidation processes of N,S-diacetyl-l-cysteine ethyl ester: influence of S-acetylation. *J. Phys. Chem. A* **2001,** *105*, 6867-6875.

[16] Lattach, Y.; Besseau, A. D.; Guigner, J. A.; Remita, S., Radiation chemistry as an alternative way for the synthesis of PEDOT conducting polymers under ‘‘soft’’ conditions. *Radiation Physics and Chemistry* **2013,** *82*, 44–53.

[17] Lattach, Y.; Coletta, C.; Ghosh, S.; Remita, S., Radiation-induced synthesis of nanostructured conjugated polymers in aqueous solution fundamental effect of oxidizing species. *ChemPhysChem* **2014,** *15*, 208 – 218.

[18] Zhong, W. B.; Li, S. M.; Chen, X. H.; Wang, Y. X.; Yang, W. T., High-yield synthesis of superhydrophilic polypyrrole nanowire networks. *Macromolecules* **2006,** *39*, 3224-3230.

[19] Dazzi, A.; Prazeres, R.; Glotin, F.; Ortega, J. M., Local infrared microspectroscopy with subwavelength spatial resolution with an atomic force microscope tip used as a photothermal sensor. *Opt. Lett.* **2005,** *30*, 2388-2390.

[20] Policar, C.; Waern, J. B.; Plamont, M. A.; Clede, S.; Mayet, C.; Prazeres, R.; Ortega, J. M.; Vessieres, A.; Dazzi, A., Subcellular ir imaging of a metal–carbonyl moiety using photothermally induced resonance. *Angew. Chem., Int. Ed.* **2011,** *50*, 860–864.

[21] Dazzi, A.; Prater, C. B.; Hu, Q. C.; Bruce Chase, D.; Rabolt, J. F.; Marcott, C., AFM-IR: combining atomic force microscopy and infrared spectroscopy for nanoscale chemical characterization. *Appl. Spectrosc.* **2012,** *66*, 1365–1384.

[22] Silverstein, R. M.; Bassler, G. C., Spectrometric idenntification of organic compounds. *John Wiley & Sons, Inc.* **1998,** *7*, 311.

[23] Cui, Z.; Coletta, C.; Dazzi, A.; Lefrancois, P.; Gervais, M.; Neron, S.; Remita, S., Radiolytic method as a novel approach for the synthesis of nanostructured conducting polypyrrole. *Langmuir* **2014,** *30* (46), 14086-14094.

[24] Koppenol, W. H.; Stanbury, D. M.; Bounds, P. L., Electrode potentials of partially reduced oxygen species, from dioxygen to water. *Free radical biology & medicine* **2010,** *49*, 317-322.

[25] Mart ńez, M. W.; Thompson, T. T.; Smit, M. A., Characterization and electrocatalytic activity of carbon-supported polypyrrole-cobalt-platinum compounds. *Int. J. Electrochem. Sci.* **2010,** *5*, 931 - 943.

[26] Vetter, C. A.; Suryawanshi, A.; Lamb, J. R.; Law, B.; Gelling, V. J., Novel synthesis of stable polypyrrole nanospheres using ozone. In *Langmui*, 2011; Vol. 27, pp 13719-13728.

[27] Ye, S. J.; Fang, L.; Lu, Y., Contribution of charge-transfer effect to surface-enhanced IR for Ag@PPy nanoparticles. *Phys. Chem. Chem. Phys.* **2009,** *11*, 2480–2484.

[28] Li, X. G.; Hou, Z. Z.; Huang, M. R.; Moloney, M. G., Efficient synthesis of intrinsically conducting polypyrrole nanoparticles containing hydroxy sulfoaniline as key self-stabilized units. *J. Phys. Chem. C* **2009,** *113*, 21586–21595.

[29] Li, X. G.; Li, A.; Huang, M. R.; Liao, Y. Z.; Lu, Y. G., Efficient and scalable synthesis of pure polypyrrole nanoparticles applicable for advanced nanocomposites and carbon nanoparticles. *J. Phys. Chem. C* **2010,** *114*, 19244-19255.

[30] Scienza, L. C.; Thompson, G. E., Preparation and surface analysis of PPY/SDBS films on aluminum substrates. *Pol ́meros* **2001,** *11*, 142-148.

[31] Hazarika, J.; Kumar, A., Controllable synthesis and characterization of polypyrrole nanoparticles in sodium dodecylsulphate (SDS) micellar solutions. *Synthetic Metals* **2013,** *175*, 155-162.

[32] Hawkins, S. J.; Ratcliffe, N. M., A study of the effects of acid on the polymerisation of pyrrole, on the oxidative polymerisation of pyrrole and on polypyrrole. *J. Mater. Chem.* **2000,** *10*, 2057-2062.

[33] Wang, H. L.; Fernandez, J. E., Conducting polymer blends-polypyrrole and poly(vinyl methyl ketone). *Macromolecules* **1992,** *25*, 6179-6184.

[34] Choi, S.; Kim, K.; Nam, J.; Shim, S. E., Synthesis of silica-coated graphite by enolization of polyvinylpyrrolidone and its thermal and electrical conductivity in polymer composites. *Carbon* **2013,** *60*, 254-265.

[35] Talarico, A. M.; Szerb, E. I.; Mastropietro, T. F.; Aiello, I.; Crispini, A.; Ghedini, M., Tuning solid state luminescent properties in a hydrogen bonding-directed supramolecular assembly of bis-cyclometalated iridium(III) ethylenediamine complexes. *Dalton T* **2012,** *41* (16), 4919-4926.

[36] Chatterjee, S.; Shit, A.; Nandi, A. K., Nanochannel morphology of polypyrrole–ZnO nanocomposites towards dye sensitized solar cell application. *J. Mater. Chem. A* **2013,** *1*, 12302-12309.

[37] Jang, J.; Oh, J. H., Fabrication of a highly transpartent conductive thin film from polypyrrole/poly(methyl methacrylate) core/shell nanospheres. *Adv Funct Mater* **2005,** *15*, 494-502.

[38] Zang, J. F.; Bao, S. J.; Li, C. M.; Bian, H. J.; Cui, X. Q.; Bao, Q. L.; Sun, C. Q.; Guo, J.; Lian, K. R., Well-aligned cone-shaped nanostructure of polypyrrole/RuO2 and its electrochemical supercapacitor. *J Phys Chem C* **2008,** *112*, 14843-14847.

[39] Vasilyeva, S. V.; Vorotyntsev, M. A.; Bezverkhyy, I.; Lesniewska, E.; Heintz, O.; Chassagnon, R., Synthesis and characterization of palladium nanoparticle/polypyrrole composites. *J. Phys. Chem. C* **2008,** *112*, 19878–19885.

[40] Xu, P.; Han, X. J.; Wang, C.; Zhou, D. H.; Lv, Z. S.; Wen, A. H.; Wang, X. H.; Zhang, B., Synthesis of electromagnetic functionalized nickel/polypyrrole core/shell composites. *J Phys Chem B* **2008,** *112*, 10443-10448.

[41] Guo, J.; Gu, H. B.; Wei, H. G.; Zhang, Q. Y.; Haldolaarachchige, N.; Li, Y.; Young, D. P.; Wei, S. Y.; Guo, Z. H., Magnetite-polypyrrole metacomposites: dielectric properties and magnetoresistance behavior. *J Phys Chem C* **2013,** *117*, 10191-10202.

[42] Yang, C.; Liu, P., Polypyrrole/conductive mica composites: preparation, characterization, and application in supercapacitor. *Synthetic Metals* **2010,** *160*, 768-773.

[43] Shen, C.; Sun, Y.; Yao, W.; Lu, Y., Facile synthesis of polypyrrole nanospheres and their carbonized products for potential application in high-performance supercapacitors. *Polymer* **2014,** *55*, 2817-2824.

[44] Ghosh, S.; Remita, H.; Ramos, L.; Dazzi, A.; Deniset-Besseau, A.; Beaunier, P.; Goubard, F.; Aubert, P. H.; Brisset, F.; Remita, S., PEDOT nanostructures synthesized in hexagonal mesophases. *New J. Chem.* **2014,** *38*, 1106-1115.

[45] Peng, S. J.; Tian, L. L.; Liang, J.; Mhaisalkar, S. G.; Ramakrishna, S., Polypyrrole nanorod networks/carbon nanoparticles composite counter electrodes for high-efficiency dye-sensitized solar cells. *Acs Appl Mater Inter* **2012,** *4*, 397-404.

Chapter 5: Effect of synthetic conditions on radiation induced synthesis of PEDOT polymers

In chapter 4, the versatility of radiolytic method has been proved by the successful synthesis of polypyrrole (PPy). However, the morphology and properties of conducting polymers (CPs) can be affected and adjusted by the synthetic conditions (soft template and pH). Therefore, it is necessary to study the effect of the experimental conditions on the synthesis of CPs by using gamma (γ)-irradiation.

In the present chapter, synthesis of poly(3,4-ethylenedioxythiophene) (PEDOT) induced by γ-irradiation is selected as the research target and effects of synthetic conditions on the polymerization of 3,4-ethylenedioxythiophene (EDOT) monomers are discussed.

First, in order to control the morphology of PEDOT polymers, the effect of the presence of soft templates on the polymerization of EDOT monomers is studied. The radiation stability of soft templates formed by sodium dodecyl sulfate (SDS) is checked and the influence of SDS concentration on the polymerization of EDOT monomers is studied.

Second, in order to improve the properties of PEDOT polymers, the effect of pH on the synthesis of PEDOT polymers is studied. PEDOT polymers are prepared in acidic aqueous solution by using γ-irradiation. On the one hand, influence of concentration of acid on the polymerization of EDOT monomers is checked. On the other hand, effect of the nature of the acid on the polymerization is studied by choosing perchloric acid ($HClO_4$) and hydrochloric acid (HCl). In order to check the effect of ionic strength on the polymerization of EDOT monomers, sodium perchlorate ($NaClO_4$) is added instead of the inorganic acid.

5.1 PEDOT synthesis and characterization methodologies

5.1.1 Solution preparation and γ-irradiation

EDOT is selected as the monomer and deionized water is used as the solvent. SDS with a concentration which is below or above critical micelle concentration (CMC) is added to EDOT solutions to form soft template. $HClO_4$ or HCl are added to adjust the pH of EDOT solutions. $NaClO_4$ is used to adjust the ionic strength of the solutions. Nitrous oxide (N_2O) is applied for degassing. Nitrosyl tetrafluoroborate ($NOBF_4$) is dissolved in acetonitrile for *p*-

doping during the electrical conductivity test. Poly(4-styrenesulfonic acid) (PSSH) and dimethyl sulfoxide (DMSO) are applied to help PEDOT form PEDOT/PSS membranes.

Soft template. Aqueous solutions of SDS at concentrations of 1 (below CMC I), 10 (between CMC I and CMC II) and 200 (above CMC II) mM (chapter 2) are prepared at room temperature. EDOT monomers are solubilized in pure water at a concentration of 10 mM. To study the effect of soft template on the polymerization of EDOT monomers, EDOT aqueous solutions are added with SDS to prepare aqueous solutions containing concentration ratios of EDOT to SDS at 10:0, 10:1, 10:10 and 10:200.

Acidic medium. A series of acidic solutions containing EDOT and $HClO_4$ (or HCl) with molar ratios (in mM) of 10:0 (pH = 8), 10:1 (pH = 3), 10:10 (pH = 2), 10:100 (pH = 1) and 10:1000 (pH = 0) are prepared by adding $HClO_4$ (or HCl) into EDOT aqueous solutions (10 mM). In addition, for comparison purpose, EDOT solution (10 mM) is added with $NaClO_4$ with a concentration of 1000 mM.

γ-irradiation. Before γ-irradiation, aqueous solutions of SDS, EDOT solutions added with SDS, EDOT solutions added with $HClO_4$ (or HCl) and EDOT solutions added with $NaClO_4$ are all degassed with N_2O for 20 min. Then, all the solutions were irradiated for 72 kGy in the ^{60}Co source (Laboratoire de Chimie Physique, Paris-Sud University) at a dose rate of 4.1 $kGy \cdot h^{-1}$.

5.1.2 Radiolysis of acidic medium

It is well known that the radiolysis of water under nitrogen (N_2) atmosphere at neutral pH produces various species: HO•, H•, e_{aq}^-, H_3O^+, H_2O_2, H_2 (equation 2.2, chapter 2). Among these formed species, solvated electron (e^-_{aq}) and hydroxyl radical (HO•) are the most abundant species with high reactivity. As the pH of aqueous solution decreases, e_{aq}^- is transformed to hydrogen atom (H•) by reacting with hydrogen ions (H^+) in the acidic medium (equation 2.18, chapter 2) while the yield of HO• remains nearly the same. As a result, the radiolysis of water under N_2 atmosphere in acidic conditions (pH = 0) mainly produces HO• and H• and the radiolytic yields are 2.9×10^{-7} mol J^{-1} and 3.7×10^{-7} mol J^{-1} (Figure 2.5, chapter 2).

When irradiation of aqueous solution happens under N_2O atmosphere, e^-_{aq} is transformed into HO• (equation 2.14, chapter 2) which competes with the transformation of e^-_{aq} into H• (equation 2.18, chapter 2). Therefore, the main species produced by the radiolysis of water under N_2O atmosphere in acidic conditions are still HO• and H•. Nevertheless, under N_2O

atmosphere, radiolytic yield of production of HO• is higher than under N_2 atmosphere, while the yield of production of at least 2.9×10^{-7} mol J^{-1} while the maximum radiolytic yield of H• is necessarily lower.[1]

When $HClO_4$ is added to adjust the pH of aqueous solution, the main species produced by radiolysis of acidic aqueous solution under N_2O atmosphere containing $HClO_4$ are oxidizing HO• and reducing H• since ClO_4^- anions remain unreactive.

When HCl is used instead of $HClO_4$, HO• is converted to $Cl_2^{\cdot-}$ (reactions 2.19~2.21, chapter 2) which is very oxidative agent.[2] Therefore, the main species produced by γ-radiolysis of acidic aqueous solution containing HCl under N_2O atmosphere are $Cl_2^{\cdot-}$ as well as H•.

Therefore, γ-irradiation of acidic aqueous solutions of EDOT can induce polymerization of EDOT either by oxidation of EDOT either by HO• or $Cl_2^{\cdot-}$ depending on the nature of the used acid. Note in these conditions, the reactivity of H• should be taken into account due to the high concentration in hydrogen atoms.

5.1.3 Characterizations and measurements

To study the effect of γ-irradiation, Ultraviolet-visible (UV-vis) spectra of all the prepared solution before and after γ-irradiation were recorded without dilution or with 10 times dilution using a quartz cell with an optical path length of 0.2 cm. Acidic solutions of EDOT (10 mM) and $HClO_4$ (or HCl) (10:1000) after γ-irradiation were selected for further characterizations. To identify the formation of PEDOT and its chemical composition, attenuated total reflection fourier transform infrared (ATR-FTIR) absorption spectra were measured within the wavenumber range of 4000 to 600 cm^{-1} with a resolution of 4 cm^{-1}. The morphology of the as-prepared products in solution was observed by cryo-transmission electron microscopy (Cryo-TEM). The morphology samples dried by lyophilization were observed by scanning electron microscopy (SEM). In addition, energy dispersive X-Ray (EDX) analysis is carried out to identify the chemical composition of the materials during the SEM characterizations. Atomic force microscopy-based infrared spectroscopy (AFM-IR) was performed to further study the morphology and composition of the as-prepared samples.

The electrical conductivity measurements were done by spinning PEDOT suspension on a glass and doping with $NOBF_4$ (10 mM) solvated in acetonitrile. Similarly, the electrical conductivity of PEDOT was measured by using the same procedures applied for PPy (chapter 4).

5.2 Effect of SDS on the polymerization of EDOT monomers

SDS was used as surfactant building-block for the preparation of soft template in order to prepare architecture-controlled PEDOT polymers. Indeed, EDOT and PEDOT being mainly hydrophobic, EDOT monomers and PEDOT polymers should preferentially dissolve inside the micelles. The choice of concentration below CMC I, between CMC I and CMC II and above CMC II should enable the preparation of free PEDOT nanoparticles, PEDOT nanoparticles in the core of spherical micelles and PEDOT nanotubes in cylindrical micelles.

In order to study the influence of SDS on the polymerization of EDOT monomers in neutral aqueous solution, the stability of SDS upon irradiation under N_2O atmosphere in aqueous solution was checked first in the absence of EDOT monomers. The photographs of aqueous solutions of SDS (1, 10 and 200 mM) before and after γ-irradiation are shown (Figure 5.1).

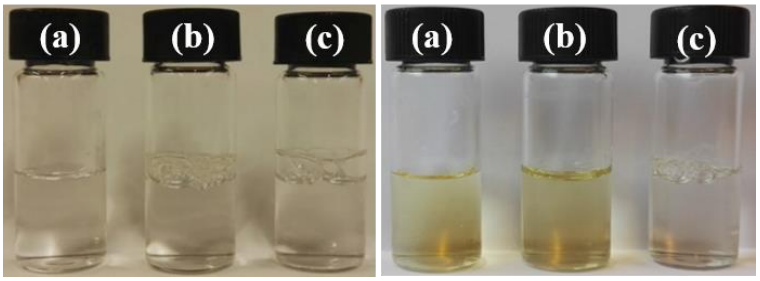

Figure 5.1 Photographs of aqueous solutions of SDS before (left) and after γ-irradiation at 72 kGy under N_2O atmosphere. The concentrations of SDS are 1 (a), 10 (b) and 200 (c) mM.

It is clear that all the SDS solutions are transparent before γ-irradiation indicating that SDS is completely solubilized in the concentration range of 1 to 200 mM. After γ-irradiation at 72 kGy, solutions (a) and (b) become light yellow while solution (c) remains almost the same as its appearance without γ-irradiation. Therefore, γ-irradiation of SDS solutions leads to slight color change at low concentration indicating the chemical instability of SDS surfactant upon irradiation.

In order to carry out spectroscopic comparison, Ultraviolet-visible (UV-vis) spectra of aqueous solutions of SDS before and after γ-irradiation are recorded (Figure 5.2). According to Figure 5.2, all aqueous solutions of SDS are overlapped and show no absorption above 250 nm without γ-irradiation (Figure 5.2, left). After γ-irradiation, all the solutions show clear absorption below 350 nm and UV-vis absorption spectra of solutions (a) and (b) (Figure 5.1)

show weak absorption within the wavelength number of 350~500 nm which may explain the light yellow color (Figure 5.2, right). The obvious changes of UV-vis absorption spectra of SDS indicate that γ-radiolysis of SDS solutions under N_2O atmosphere produces some species which absorb below 500 nm. This may result from the degradation of SDS by reacting with HO• forming SDS radicals.[3,4] Since no clear precipitates are observed and since SDS micelles have been widely used during the radiolysis, it is reasonable to suppose that SDS self assembles remain stable upon γ-radiolysis.[3,5-7] Even if SDS (dispersed or self-assembled into micelles) is relatively unstable upon high dose irradiation, it is worth checking whether PEDOT polymers could be synthesized in the presence of SDS surfactants. Indeed, since the rate constants of oxidation of SDS by HO• corresponding to 7.6×10^9 L mol^{-1} s^{-1} (below CMC I) and 0.5×10^9 L mol^{-1} s^{-1} (above CMC I) are comparable to the rate constant of EDOT oxidation by HO• with a rate constant of 5×10^9 L mol^{-1} s^{-1}, one can expect competitive reaction of HO• onto both EDOT (10 mM) and SDS (up to 200 mM) which should finally lead to the synthesis of PEDOT polymers.[4,8]

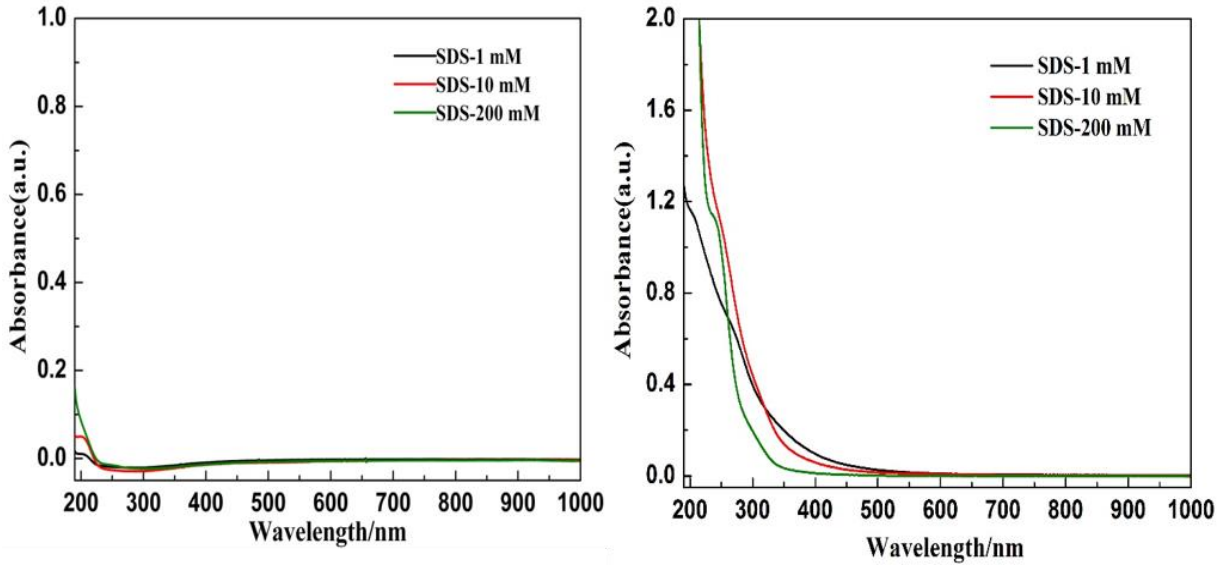

Figure 5.2 UV-vis absorption spectra of aqueous solutions of SDS before (left) and after (right) γ-irradiation for 72 kGy under N_2O atmosphere. All the spectra are recorded without dilution with l = 0.2 cm.

To study the effect of SDS on the polymerization of EDOT, EDOT solutions (10 mM) are added with SDS at different concentrations (1, 10 and 200 mM) and irradiated for 72 kGy (Figure 5.3). As the critical micelle concentrations (CMC) of SDS are 8.3 mM (CMC I, 25 ^{0}C) and 70 mM (CMC II, 25 ^{0}C) and the solubility of EDOT increases from 11 mM to 73 mM

(chapter 2), it is certain that EDOT is completely solubilized in solution or distributed in SDS micelles whatever the experimental conditions.

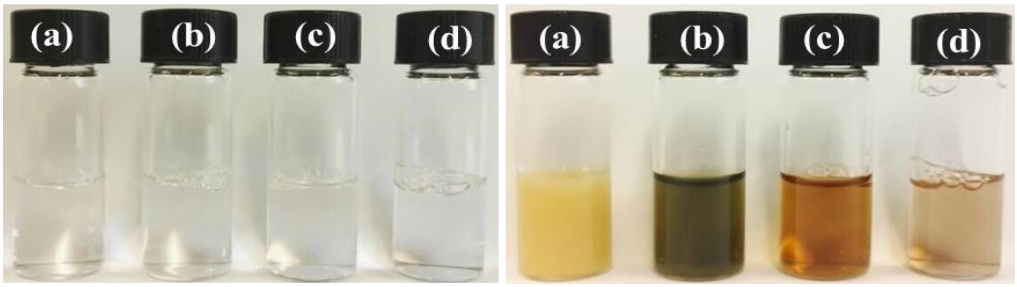

Figure 5.3 Photographs of EDOT solutions (10 mM) added with SDS before (left) and after (right) γ-irradiation for 72 kGy under N_2O atmosphere. The concentrations of SDS are 0 (a), 1 (b), 10 (c) and 200 (d) mM.

From Figure 5.3, it can be seen that all the EDOT solutions added with SDS appear to be transparent before irradiation as EDOT and SDS are completely solubilized. Therefore, EDOT has no effect on the solubilization of SDS. Also, when comparing the absorption spectra of EDOT in the absence or in the presence of SDS (1, 10 and 200 mM), one can observe that the absorption of EDOT at 235 and 255 nm decreases slightly with increasing SDS concentration (Figure 5.4, left).

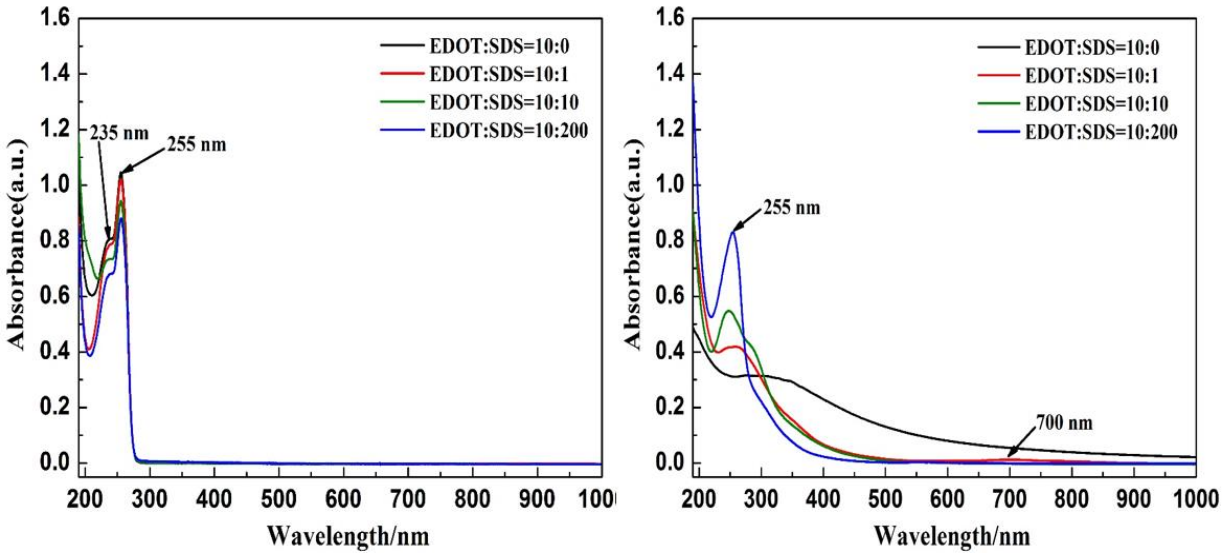

Figure 5.4 UV-vis absorption spectra of EDOT solutions (10 mM) added with SDS before (left) and after (right) γ-irradiation for 72 kGy under N_2O atmosphere. The concentrations of SDS are 0, 1, 10 and 200 mM. All the spectra are recorded after 10 times dilution with l = 0.2 cm.

This decrease can't be due to a lower solubility of EDOT in SDS micelles. This systematic error is due to the variation of the volume and then of EDOT concentration when SDS powder is added to the medium, to the dilution of the solution which is necessary before recording UV-vis absorption spectra and also to the bubbling of the solution which is more important when SDS concentration is higher.

After γ-irradiation, apparent color changes happen to all the solutions and all the EDOT solutions added with SDS have no precipitate (Figure 5.3). The appearance of EDOT solution is the same as reported results (Figure 3.7, chapter 3). In particular, in the absence of SDS, the yellow suspension is due to the formation of PEDOT polymers.

However, solution (b) added with 1 mM of SDS becomes yellow green while solution (c) with a concentration of SDS 10 mM becomes yellow brown. Compared with solutions (b) and (c), solution (d) added with SDS 200 mM becomes light brown. As the concentration of SDS increases, the color becomes lighter implying that less polymerization of EDOT happens. In general, the color of PEDOT is light blue (oxidized state) or dark blue (reduced state). Therefore, only the color of solution (b) is close to the color of PEDOT in reduced state indicating that low concentration of SDS favors the polymerization of EDOT.

The UV-vis absorption spectra of the irradiated solutions in the presence of SDS after 10 times dilution are displayed (Figure 5.4, right). While the absorption spectrum obtained in the absence of SDS is similar to that previously obtained (Figure 3.7, chapter 3) confirming the presence of PEDOT, the spectra obtained in the presence of SDS are quite different. No intense bands are observed at high wavelengths. On the contrary, after irradiation the characteristic band of EDOT at 255 nm remains. The intensity of this band increases with SDS concentration.

Solution (b) (Figure 5.3, right) added with 1 mM of SDS (ratio 10:1) shows decreasing absorption band at 255 nm suggesting the polymerization of EDOT happens. There is a new band around 700 nm which further proves that polymerization of EDOT happens and may explain the γ-irradiation induced yellow green color of solution (b) (Figure 5.3). However, at SDS concentration higher than 10 mM (ratios 10:10 and 10:200), the absorbancy at 255 nm remains confirming that EDOT polymerization is inhibited. In the absence of SDS, all EDOT monomers are consumed. On the contrary, in the presence of 200 mM in SDS, the intensity of the absorption band of EDOT monomers is nearly the same as before irradiation indicating the remaining of all EDOT monomers. It can be concluded that unfortunately the yield of EDOT oxidation decreases with SDS concentration. The competitive reaction of HO• radicals onto EDOT and SDS don't enable the efficient preparation of PEDOT polymers in the

presence of SDS surfactant when self-assembled into organic micelles. Therefore, the application of SDS-based soft template is not helpful for γ-irradiation induced synthesis of PEDOT while the addition of SDS with a concentration lower than CMC I contributes to the polymerization of EDOT. In this latter condition, PEDOT polymers display absorption band at around 700 nm which is in agreement with reported results.[9,10]

5.3 Effect of pH on the polymerization of EDOT monomers

In order to study the effect of pH on the polymerization of EDOT, EDOT solutions were added with either $HClO_4$ or HCl and irradiated under N_2O. Since γ-radiolysis of acidic aqueous medium produces different oxidizing species (HO• or $Cl_2^{\cdot -}$) (chapter 3), the effect of these different oxidizing species on the polymerization of EDOT are also discussed.

5.3.1 Effect of $HClO_4$

With the aim to check the influence of $HClO_4$ on the polymerization of EDOT, EDOT solutions were added with $HClO_4$ at different concentrations (0, 1, 10, 100 and 1000 mM) (Figure 5.5) and the pH values of all the solutions were measured with a pH-meter.

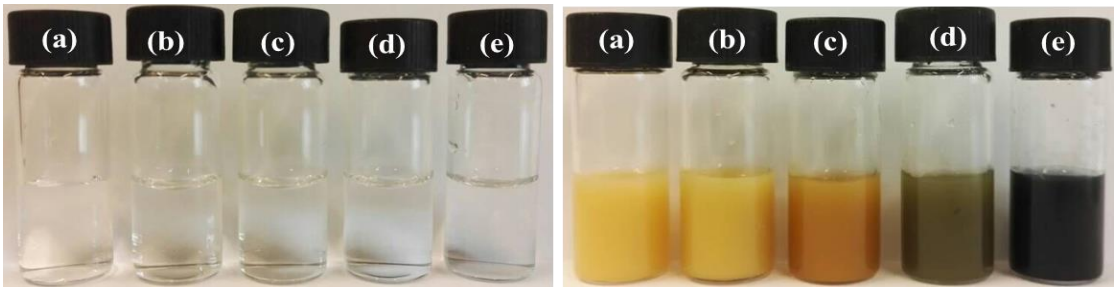

Figure 5.5 Photographs of EDOT solutions (10 mM) added with $HClO_4$ before (left) and after (right) γ-irradiation at 72 kGy under N_2O atmosphere. The concentrations of $HClO_4$ are 0 (a), 1 (b), 10 (c), 100 (d) and 1000 (e) mM and the pH values are 8, 3, 2, 1 and 0, respectively.

As is shown in Figure 5.5, before γ-irradiation, all the EDOT solutions added with $HClO_4$ are transparent and the pH values of all the solutions are 8, 3, 2, 1 and 0, respectively. After γ-irradiation, all the transparent solutions become colored suspensions and the color darkens as the concentration of $HClO_4$ increases. In particular, when the concentration of $HClO_4$ is 1000 mM (pH = 0), dark blue suspension is obtained which is the same as the color of PEDOT in

reduced state.[11,12] Therefore, pH has obvious effect on the polymerization of EDOT monomers and the polymerization of EDOT monomers at low pH is more favorable.

To further check the effect of pH, UV-vis absorption spectra of all EDOT solutions before and after γ-irradiation are recorded after 10 times dilution (Figure 5.6).

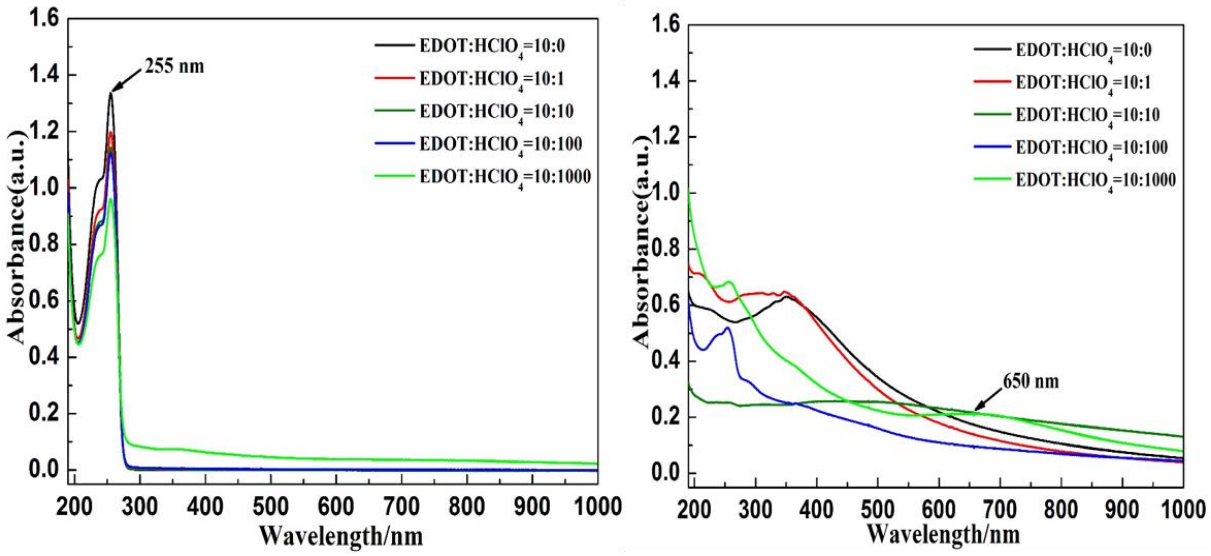

Figure 5.6 UV-vis absorption spectra of aqueous solutions of EDOT (10 mM) added with $HClO_4$ before irradiation (left) and after (right) irradiation for 72 kGy under N_2O atmosphere. The concentrations of $HClO_4$ are 0, 1, 10, 100 and 1000 mM and the pH values are 8, 3, 2, 1 and 0, respectively. All the spectra are recorded after 10 times dilution with l = 0.2 cm.

According to Figure 5.6, before γ-irradiation, UV-vis absorption spectra of all EDOT solutions (b), (c), (d) and (e) (Figure 5.5) added with $HClO_4$ are nearly the same as that of pure EDOT solution (a) (Figure 5.5). Only a slight decrease in the absorption is observed with increasing pH values. This should be due to the variation of the volume (and then of EDOT concentration) when $HClO_4$ is added and also to the dilution of solution which is needed for recording UV-vis absorption spectra. Therefore, the addition of $HClO_4$ has no effect of the absorption spectrum of EDOT which means that EDOT monomers remain stable in very acidic medium. After γ-irradiation, in the absence of $HClO_4$, the UV-vis absorption spectrum of EDOT solution is the same as before (Figure 5.4), while clear variations of UV-vis absorption spectra are observed as the pH decreases. In particular, a new band around 650 nm appears in the UV-vis absorption spectrum of solution (e) (Figure 5.5) which is added with $HClO_4$ at a concentration of 1000 mM (pH = 0). This new band may arise from PEDOT in reduced state. Taking into account its dark blue color, these results indicate that EDOT

polymerization occurs and PEDOT may be formed by reacting with radiolytic radicals obtained in acidic medium.

Let's consider the two competitive reactions (2.14 and 2.18, chapter 2) of e_{aq}^- onto N_2O (which leads to additional HO•) and H^+ (which leads to additional H•), respectively. Taking into consideration the concentration of $[N_2O]$ (0.0265 mol L^{-1}) and $[H^+]$ (10^{-pH}) as well as the rate constants k_{N_2O} (9×10^9 L mol^{-1} s^{-1}) and k_{H^+} (2.3×10^{10} L mol^{-1} s^{-1}) corresponding to reactions 2.14 and 2.18, the branching ratio (R) between the two reactions (2.14 and 2.18) can be estimated. It enables the quantification of the ratio between the additional amounts of HO• and H• produced by reactions 2.14 and 2.18. If the radiolytic yields of production of HO• and H• produced by reactions 2.14 and 2.18 are noted $G'_{HO\bullet}$ and $G'_{H\bullet}$, then R can be expressed as:

$$R = \frac{G'_{HO\bullet}}{G'_{H\bullet}} = \frac{k_{N_2O}\,[N_2O]}{k_{H^+}\,[H^+]} = \frac{9\times10^9\times0.0265}{2.3\times10^{10}\times[H^+]} = \frac{0.01}{[H^+]} \tag{5.1}$$

which evidently depends on the pH value. The lower the pH (the higher the $[H^+]$), the higher the amount of H• in comparison with that of HO•.

Taking into account the pseudo-first order decay of e_{aq}^- by its reaction with N_2O and H^+, one can consider its half-time to be:

$$t_{1/2} = \frac{\ln 2}{k_{N_2O}\,[N_2O] + k_{H^+}\,[H^+]} \tag{5.2}$$

which is around few ns.

For the calculation of $G'_{HO\bullet}$ and $G'_{H\bullet}$ which result from e_{aq}^- decay according to reactions 2.14 and 2.18, let's then consider the yield of production of e_{aq}^- at 3 ns for consideration which is:

$$G_{e_{aq}^-} = G'_{HO\bullet} + G'_{H\bullet} = 3.4\times10^{-7}\ \text{mol}\,J^{-1} \tag{5.3}$$

Knowing the dependence of $R = (G'_{HO\bullet}/G'_{H\bullet})$ as a function of H^+, it is then possible to evaluate the values of $G'_{HO\bullet}$ and $G'_{H\bullet}$ at pH 0, 1, 2 and 3 (Table 5.1). The total radiolytic yields of production of HO• and H• can then be calculated according to:

$$G(HO\bullet) = G_{HO\bullet} + G'_{HO\bullet} = 2.8 \times 10^{-7} \text{ mol J}^{-1} + G'_{HO\bullet} \quad (5.4)$$

$$G(H\bullet) = G_{H\bullet} + G'_{H\bullet} = 0.6 \times 10^{-7} \text{ mol J}^{-1} + G'_{H\bullet} \quad (5.5)$$

Table 5.1 Radiolytic yields of HO• and H• under N_2O atmosphere in acidic medium.

[EDOT]/ [$HClO_4$]	**pH**	**R**	**$G'_{HO\bullet}$** ($\times 10^{-7}$ mol J^{-1})	**$G'_{H\bullet}$** ($\times 10^{-7}$ mol J^{-1})	**G(HO•)** ($\times 10^{-7}$ mol J^{-1})	**G(H•)** ($\times 10^{-7}$ mol J^{-1})
10:1000	0	0.01	0	3.4	2.8	4
10:100	1	0.1	0.3	3.1	3.1	3.7
10:10	2	1	1.7	1.7	4.5	2.3
10:1	3	10	3.1	0.3	5.9	0.9

These calculations enable the evolution of the radiolytic yields of production of HO• and H• as a function of the pH under N_2O atmosphere. Evidently, at lower pH, the radiolytic yield of HO• is lower and that of H• is higher. Nevertheless, at this stage of the work, it is not possible to know if both HO• and H• react onto EDOT monomers. In order to find the answer, aqueous solutions containing 1 mM in EDOT in the presence of 1000 mM $HClO_4$ (pH = 0) are irradiated at increasing dose (Figure 5.7).

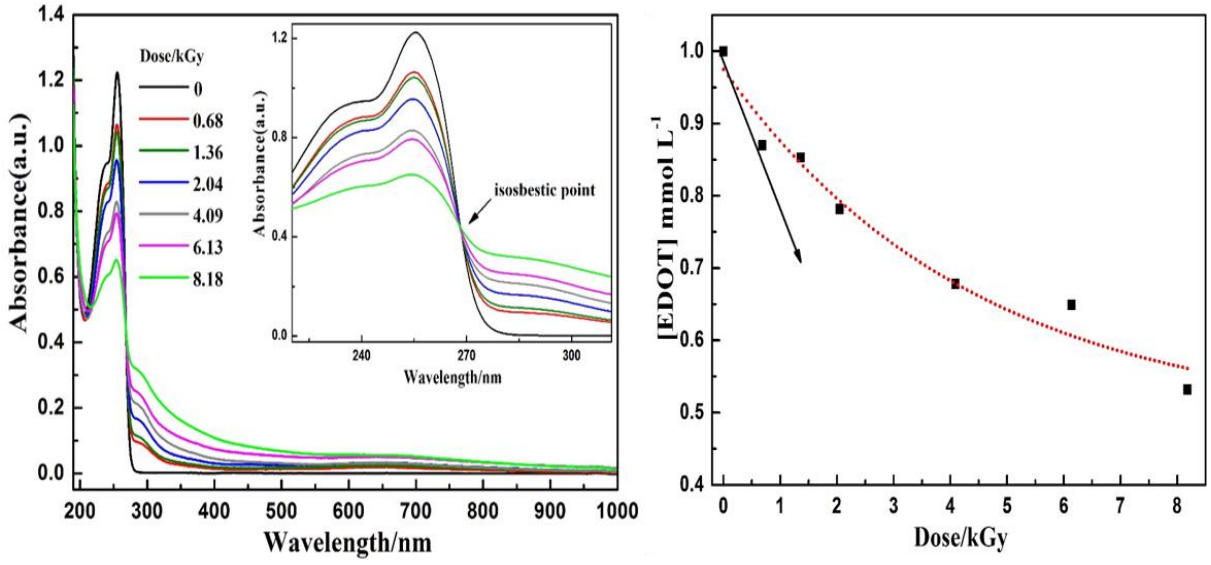

Figure 5.7 UV-vis absorption spectra of aqueous solutions of EDOT (1 mM) added with $HClO_4$ (1000 mM) (pH = 0) as a function of the dose under N_2O atmosphere (left) and evolution of EDOT concentration as a function of the irradiation dose (right). Insert: zoom which highlights the existence of an isosbestic point. All the spectra are recorded without dilution and l = 0.2 cm.

When the dose increases, one can observe the progressive decrease of the characteristic bands of EDOT at 235 and 255 nm (Figure 5.7, left). This decrease parallels an increase of the absorbancy at higher wavelength. Note that an isosbestic point is observed at around 270 nm (see insert). In order to calculate the radiolytic yield of EDOT consumption ($G_{-EDOT\ 0}$) at pH = 0, the evolution of EDOT concentration (deduced from the absorbancy at 255 nm) is displayed as a function of the dose (Figure 5.7, right). The initial slope of the curve enable to calculate $G_{-EDOT\ 0.}$ It amounts to：

$$G_{-EDOT\ 0} = 2.0 \pm 0.5 \text{ mol J}^{-1} \quad (5.6)$$

It is noted that this yield is close the value of G(HO•) at pH = 0 (Table 5.1) and much lower than that of G(HO•) + G(H•) at the same pH. This result shows that, as in the case of neutral medium, HO• reacts with EDOT leading to PEDOT polymers. H• atoms which are predominant in very acidic medium don't seem to be involved in the polymerization of EDOT monomers. Note that isopropanol or *tert*-butanol were added to scavenge HO• and H• during radiolysis. Nevertheless, the yield of EDOT disappearance was found to be the same. This should be due to the instability of alcohols in very acidic medium. Indeed, alcohols can undergo β-elimination or nucleophilic substitution which leads to ethylenic compounds and halogeno-compound.[13]

Considering the spectra of PEDOT polymers as function of the dose, the evolution couldn't be attributed to the nature of oxidizing radicals since only HO• seem to react with EDOT monomers. The difference which exists in the spectra could be due to the ionic strength which increases drastically with pH.

As the ionic strength is very high under extreme acidic conditions, it is necessary to check its effect on the polymerization of EDOT in neutral aqueous solutions. EDOT solution added with $NaClO_4$ (1000 mM) is then exposed to γ-irradiation up to 72 kGy under N_2O atmosphere and UV-vis absorption spectrum of the obtained solution is measured after 10 times dilutions (Figure 5.8).

Figure 5.8 shows that UV-vis absorption spectrum of EDOT solution added with $NaClO_4$ has weak absorption from 200 to 1000 nm and no characteristic bands are observed. Similarly, the solution after γ-irradiation appears to be yellow suspension. These results are different from that obtained with $HClO_4$ implying that ionic strength has no effect on the polymerization of EDOT. Therefore, the effect of ionic strength on the polymerization of EDOT can be excluded while pH has critical effect. The differences which exist in the spectra

of PEDOT obtained at different pH values are certainly due to the concentration of H^+ which could affect the morphology of the polymers as well as the doping level.

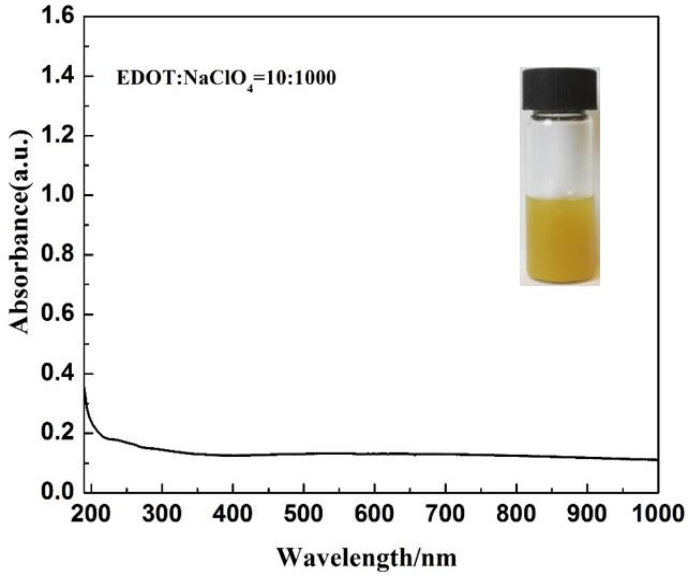

Figure 5.8 UV-vis absorption spectrum of aqueous solution of EDOT (10 mM) added with $NaClO_4$ (1000 mM) irradiated for 72 kGy under N_2O atmosphere. The spectrum is recorded after 10 times dilution with l = 0.2 cm. Insert: photograph of the solution after γ-irradiation.

5.3.2 Effect of HCl

In order to check whether the original results obtained in the presence of $HClO_4$ could be obtained in the presence of another inorganic acid, HCl is considered. As in the case of $HClO_4$, HCl is added into EDOT solutions at different concentrations (0, 1, 10, 100 and 1000 mM) to study the effect of pH on the polymerization of EDOT (pH = 8, 3, 2, 1, 0) (Figure 5.9).

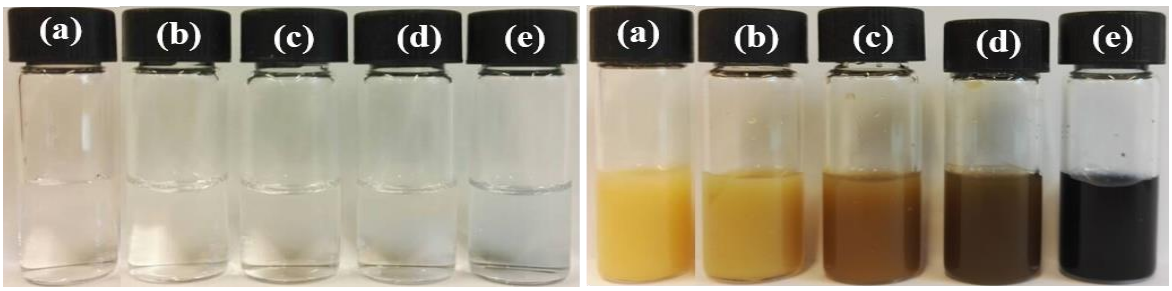

Figure 5.9 Photographs of EDOT solutions (10 mM) added with HCl before (left) and after (right) γ-irradiation for 72 kGy under N_2O atmosphere. The concentrations of HCl are 0 (a), 1 (b), 10 (c), 100 (d) and 1000 (e) mM and the pH values are 8, 3, 2, 1 and 0, respectively.

In Figure 5.9, all EDOT solutions added with different concentrations of HCl are transparent and the pH values of all the solutions are 8, 3, 2, 1 and 0, respectively. After γ-irradiation, all transparent solutions become colored suspensions and solution (e) appears to be dark blue. These results are the same as those obtained in the case of EDOT added with $HClO_4$. Dark blue suspension is only formed under extremely acidic medium (pH = 0) indicating that the polymerization of EDOT under acidic is more favorable.

In order to verify the effect of pH, UV-vis absorption spectra of all EDOT solutions before and after γ-irradiation are recorded after 10 times dilution (Figure 5.10). From Figure 5.10, it is clear that all EDOT solutions show characteristic bands of EDOT at 233 and 255 nm before γ-irradiation confirming that HCl has no absorption within this wavelength range. Also, EDOT monomers remain stable in the presence of HCl. The slight variation in the absorption of EDOT should be once again due to the dilution. After γ-irradiation, quite different absorption spectra are recorded and all the characteristic bands of EDOT disappear indicating that the polymerization of EDOT quantitatively occurs. UV-vis absorption spectrum of solution (e) (Figure 5.9, right) after γ-irradiation has a new absorption band around 685 nm which may correspond to PEDOT polymers in reduced state formed in the present experimental conditions.

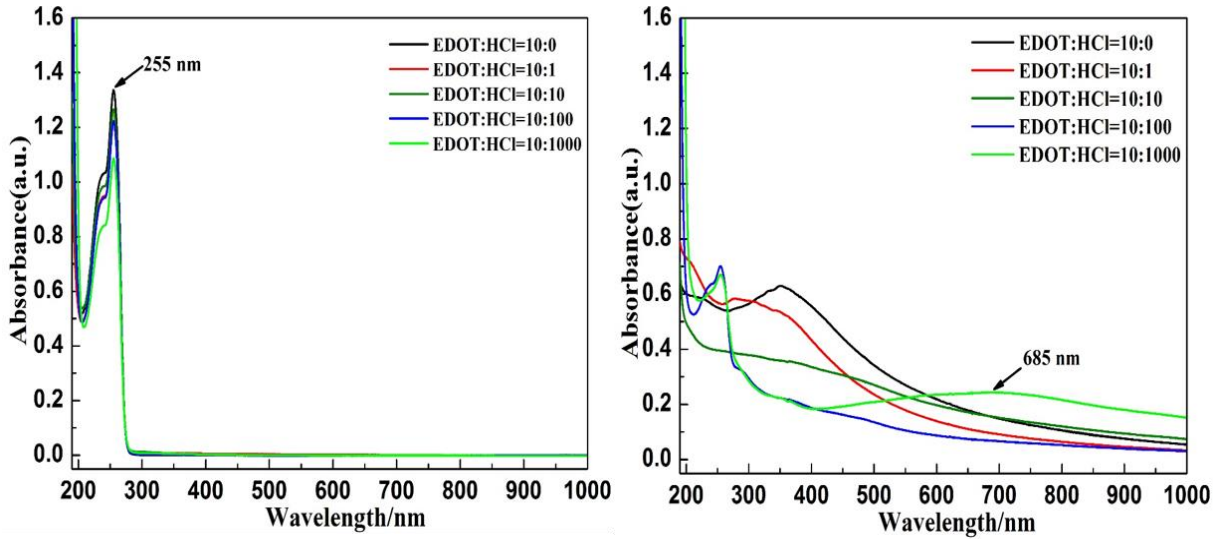

Figure 5.10 UV-vis absorption spectra of aqueous solutions of EDOT (10 mM) added with HCl before irradiation (left) and after (right) irradiation for 72 kGy under N_2O atmosphere. The concentrations of HCl are 0, 1, 10, 100 and 1000 mM and the pH values are 8, 3, 2, 1 and 0, respectively. All the spectra are recorded after 10 times dilution with l = 0.2 cm.

As demonstrated above with $HClO_4$ (equation 5.1), the radiolytic yields of HO• and H• depend on the pH of the medium. If HO• is quantitatively converted into $Cl_2^{\cdot -}$ (with HCl), one

can evaluate once again the radiolytic yields of production of $Cl_2^{\cdot -}$ and H• as a function of the pH. Evidently, at lower pH, the radiolytic yield of $Cl_2^{\cdot -}$ is lower and that of H• is higher. If considering that H• atoms don't react with EDOT monomers, the formation of PEDOT polymers is certainly exclusively due to $Cl_2^{\cdot -}$ which should quantitatively oxidize EDOT monomers thanks to its high redox potential. Since similar results are obtained with both $HClO_4$ and HCl, we can conclude that the reactivity of $Cl_2^{\cdot -}$ onto EDOT monomers is comparable with that of HO•, leading to PEDOT polymers with similar absorption properties (compare Figure 5.6 and 5.10). As the UV-vis absorption spectra obtained with $HClO_4$ and HCl are similar at a given pH, this means that the concentration of H^+ is the crucial parameter which determines the morphology and the doping level of the PEDOT polymers.

Based on the above results, it is easy to see that both $HClO_4$ and HCl have nearly the same effect on the polymerization. Although the oxidizing species produced by γ-radiolysis of acidic medium, containing either $HClO_4$ or HCl are different (HO• or $Cl_2^{\cdot -}$), the color and absorption spectra of final products are quite similar suggesting that both HO• and $Cl_2^{\cdot -}$ can initiate the polymerization of EDOT monomers and lead to the same polymeric compound.

5.4 Spectroscopic characterization of PEDOT polymers synthesized at pH = 0

In order to characterize PEDOT polymers formed at pH = 0 in the presence of $HClO_4$ (Figure 5.5, solution (e)) and HCl (Figure 5.9, solution (e)) and to identify the chemical composition and functional groups of the as-prepared products, EDOT solutions added with $HClO_4$ or HCl after γ-irradiation are dried by lyophilization and attenuated total reflection fourier transform infrared (ATR-FTIR) spectra are recorded (Figure. 5.11). The obtained products after lyophilization are noted PEDOT-$HClO_4$ and PEDOT-HCl. For comparison, the ATR-FTIR spectrum of pure EDOT is also displayed.

According to Figure 5.11, it is clear that the ATR-FTIR spectrum of EDOT monomers shows the characteristic band at 755 cm^{-1} which corresponds to the C-H out-of-plane bending vibration at α,α' positions.[14] After γ-irradiation, this characteristic band disappears in FTIR spectra of PEDOT-$HClO_4$ and PEDOT-HCl indicating that polymerization of EDOT monomers occurs totally via α, α' coupling reactions.[15]

Furthermore, all the characteristic bands of PEDOT polymers can be clearly identified which confirms the polymerization of EDOT monomers into PEDOT polymers. In the FTIR spectrum of PEDOT-HCl, the absorption bands at 835, 902 and 981 cm^{-1} correspond to the vibrations of C-S bond.[16] The band at 1054 is attributed to the ethylenedioxy group (C-O-R-

O-C).[16] The stretching vibrations of C=C in thiophen ring are seen at 1390 and 1471 cm^{-1}.[16,17] The bands at 1226 and 1349 cm^{-1} originate from of C-C bond.[17,18] Note that observation of Cl^- is not possible by FTIR since no characteristic band of chloride based functional group is recorded. The FTIR spectrum of PEDOT-$HClO_4$ is quite similar to that of PEDOT-HCl proving that PEDOT polymers are formed. Nevertheless, in the case of PEDOT-$HClO_4$, there are two weak peaks at 620 and 1016 cm^{-1} which arise from the ClO_4^- anions which remain in the sample after lyophilization. FTIR spectra clearly identify the characteristic peaks of PEDOT polymers confirming successful synthesis of PEDOT polymers with $HClO_4$ and HCl at pH = 0. Therefore, the synthesis of PEDOT in acidic medium is successful and offers another synthetic approach for the preparation of CPs.

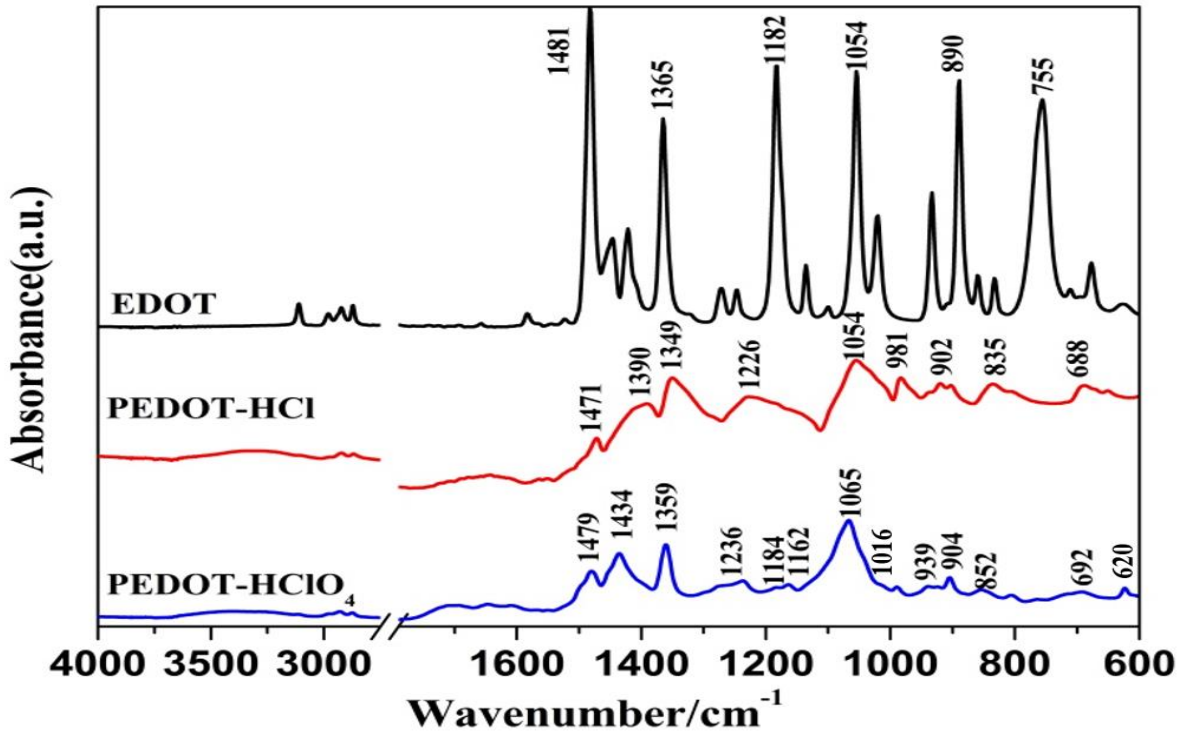

Figure 5.11 ATR-FTIR spectra of pure EDOT, PEDOT-$HClO_4$ and PEDOT-HCl after a 72 kGy γ-irradiation at pH = 0 under N_2O atmosphere.

5.5 Morphological observations of PEDOT polymers synthesized at pH = 0

In order to observe the morphology of PEDOT polymers, EDOT solutions added with $HClO_4$ or HCl after γ-irradiation (solutions (e), Figure 5.5 and Figure 5.9) are characterized by cryo-transmission electron microscopy (Cryo-TEM). Typical Cryo-TEM images of PEDOT-$HClO_4$ are exhibited (Figure 5.12).

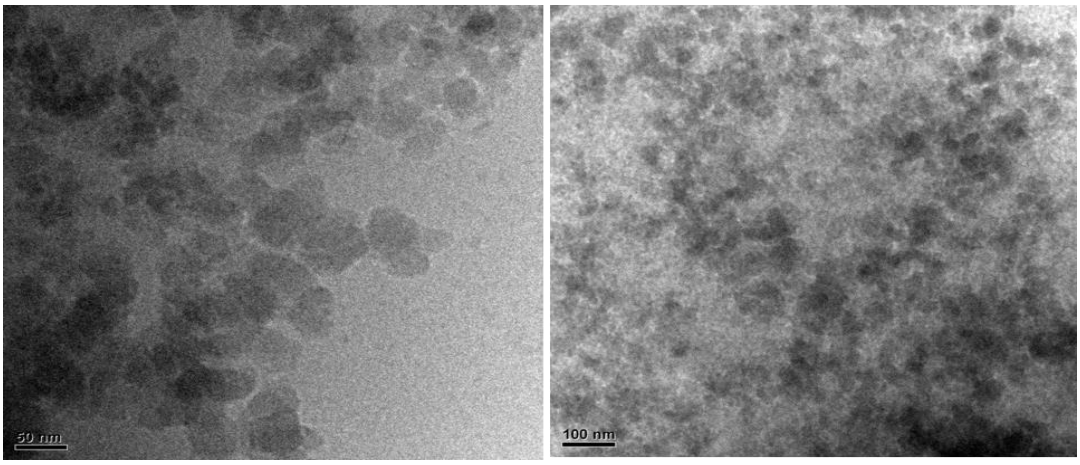

Figure 5.12 Cryo-TEM images of PEDOT-$HClO_4$ synthesized by a 72 kGy irradiation of EDOT aqueous solution at pH = 0 under N_2O atmosphere.

Figure 5.12 shows Cryo-TEM images of PEDOT in acidic solution added with $HClO_4$. It can be found that PEDOT-$HClO_4$ appears to be amorphous in acidic medium. Although some granular-like (~50 nm) and aggregated structures are observed, PEDOT-$HClO_4$ shows no specific features which is different from that of PEDOT obtained in neutral aqueous solution (Figure 3.10, chapter 3).[18,19] The morphological difference may result from the random aggregation of small size of PEDOT formed in acidic medium.[20,21] Maybe, this amorphous aspect and the high level of aggregation observed are responsible of the characteristic UV-vis absorption spectra obtained in the presence of $HClO_4$ at very low pH (Figure 5.6).

Similarly, in order to observe the morphology of PEDOT-HCl in solution, Cryo-TEM images of PEDOT-HCl are recorded (Figure 5.13).

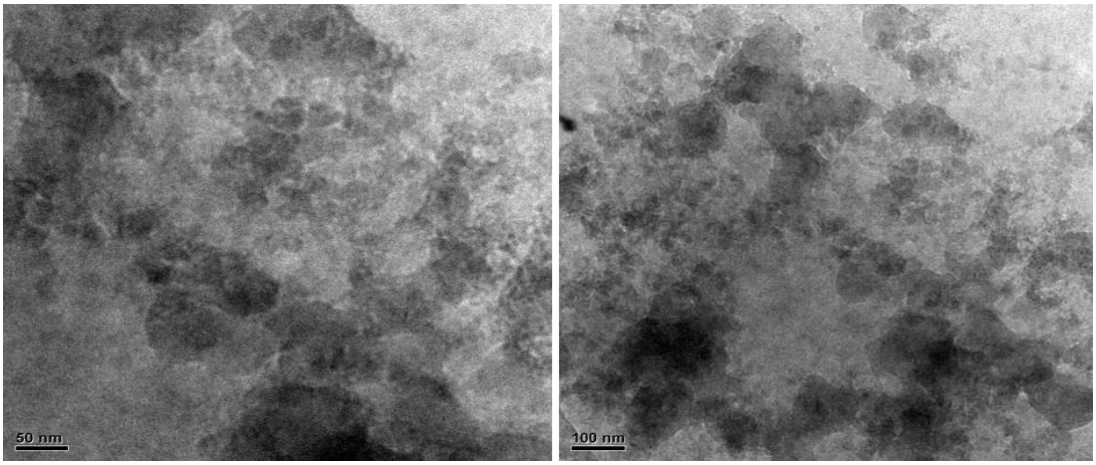

Figure 5.13 Cryo-TEM images of PEDOT-HCl synthesized by a 72 kGy irradiation of EDOT aqueous solution at pH = 0 under N_2O atmosphere.

As is shown in this figure, the morphology of PEDOT-HCl appears to be amorphous in acidic medium as in the case of $HClO_4$ and aggregated structures are observed. This result is the same as that of PEDOT-$HClO_4$ further proving that the polymerization of EDOT is favorable whatever the kind of acid.

In order to observe the morphology of PEDOT polymers after deposition, the solutions previously observed by Cryo-TEM are dried by lyophilization and characterized by scanning electron microscopy (SEM). In order to get highly contrasted SEM images, the obtained powders are coated with gold before SEM characterization. The typical SEM images of PEDOT-$HClO_4$ and PEDOT-HCl are presented (Figure 5.14).

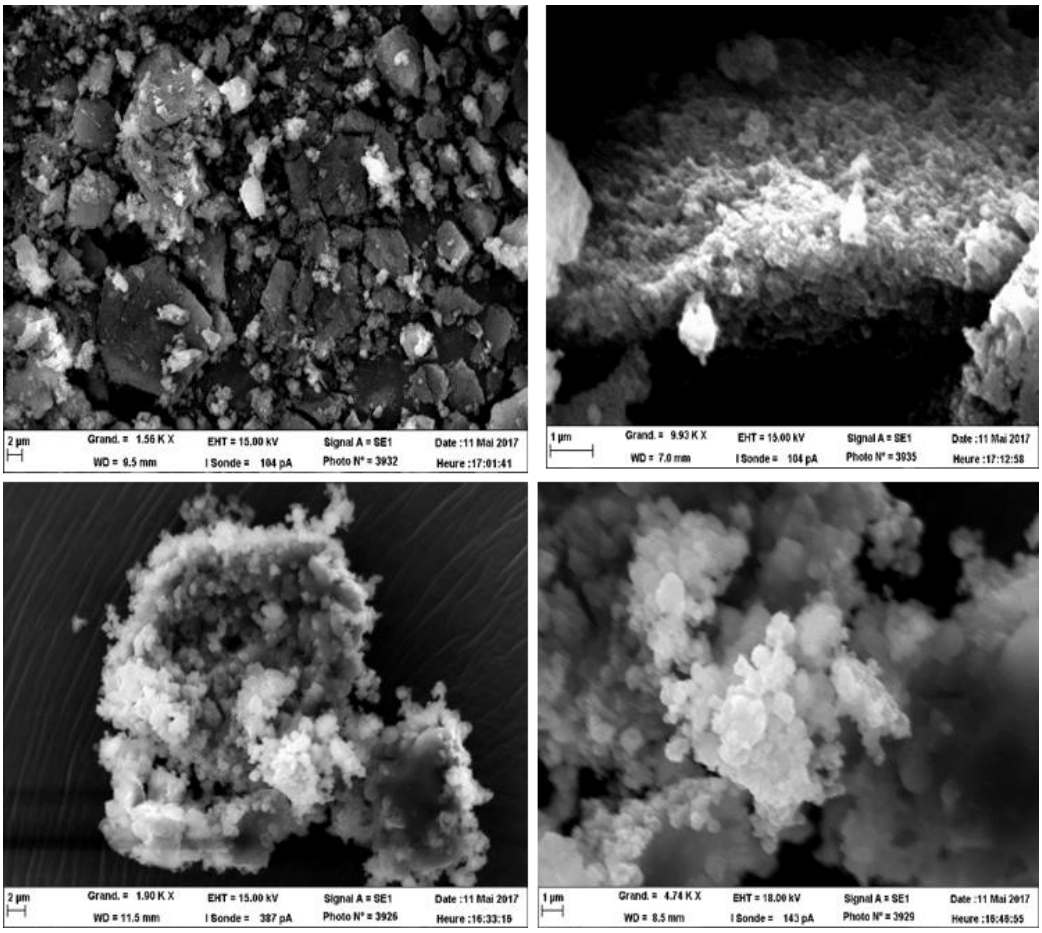

Figure 5.14 SEM images of PEDOT-$HClO_4$ (up) and PEDOT-HCl (down) synthesized by a 72 kGy irradiation of EDOT aqueous solution at pH = 0 under N_2O atmosphere.

In Figure 5.14, different morphologies of PEDOT-$HClO_4$ (up) and PEDOT-HCl (down) can be found. To PEDOT-$HClO_4$, big blocks and compact aggregation of granular particles can be seen. This result may result from the perchlorate anions (ClO_4^-) which absorb humid

making PEDOT-$HClO_4$ wettish. However, the SEM images of PEDOT-HCl highlight the existence of compact aggregates of granular particles. These aggregations are formed by amorphous and granular structures observed by Cryo-TEM (Figure 5.13). Therefore, the morphological difference of PEDOT polymers may result from the presence of ClO_4^- in one case and of Cl^- which is less hygroscopic in the other case.

In order to study the chemical composition of the obtained powders, energy dispersive X-Ray (EDX) analysis is carried out during the SEM characterization within a selected area. The EDX spectra of the PEDOT-$HClO_4$ and PEDOT-HCl are recorded (Figure 5.15).

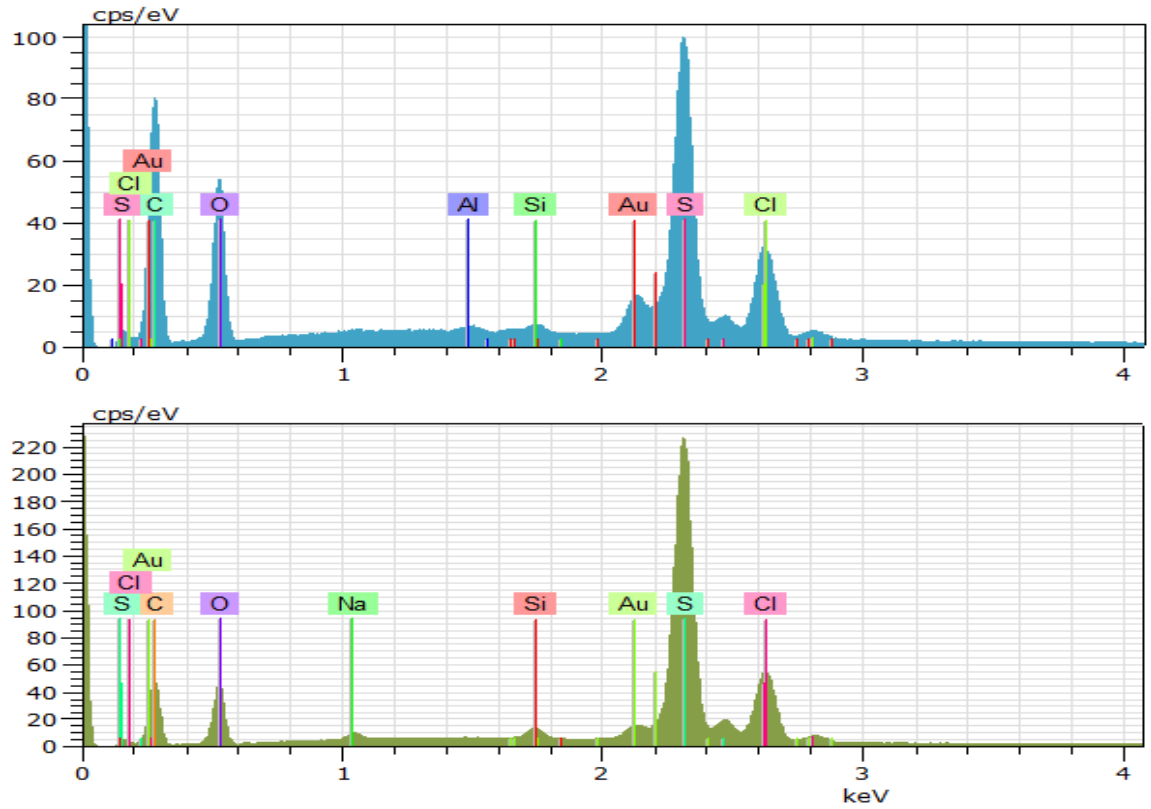

Figure 5.15 EDX spectra of PEDOT-$HClO_4$ (up) and PEDOT-HCl (down) synthesized by a 72 kGy irradiation of EDOT solution at pH = 0 under N_2O atmosphere..

From the EDX spectra of both PEDOT polymers, the peaks of C, O, S and Cl can be clearly seen indicating that the PEDOT powders contain Cl. Since the ATR-FTIR spectra of the PEDOT polymers show no characteristic vibration bands of functional groups containing Cl, Cl atoms are not bounded to polymer chains. But, the Cl element may exist in the form of counter ions of ClO_4^- or Cl^- which can't be removed by lyophilization. This may explain the wettish character of PEDOT-$HClO_4$ during the SEM characterization.

In order to further observe the morphology of PEDOT polymers and check their chemical compositions, a few drops of acidic solutions of PEDOT-$HClO_4$ and PEDOT-HCl are deposited onto the ZnSe prism, dried naturally and characterized by atomic force microscopy-based infrared spectroscopy (AFM-IR). The results of AFM-IR characterizations of PEDOT-$HClO_4$ are shown (Figure 5.16).

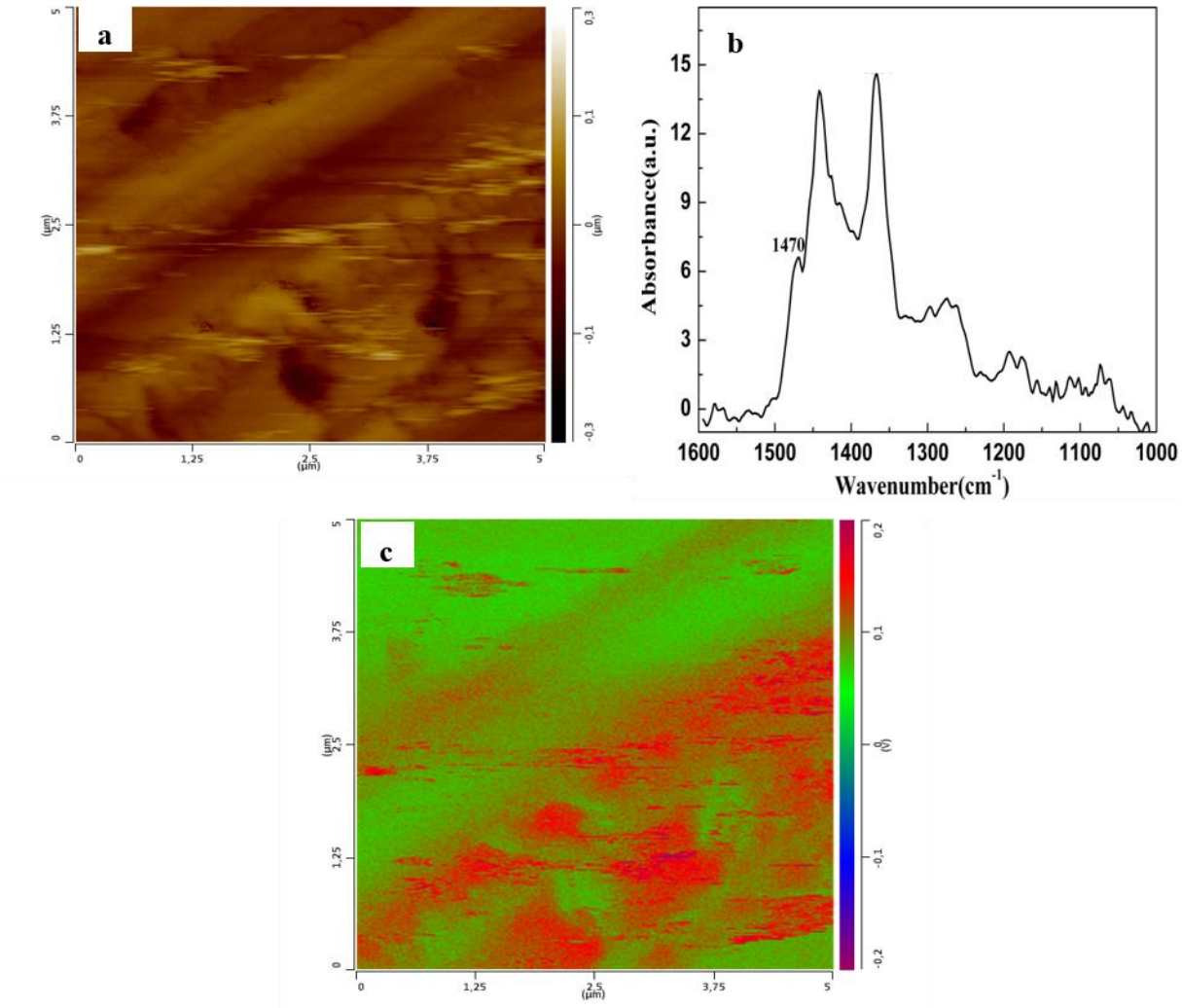

Figure 5.16 AFM-IR characterization of PEDOT-$HClO_4$ synthesized by a 72 kGy irradiation of EDOT solution at pH = 0 under N_2O atmosphere. (a) AFM topographic image of PEDOT-$HClO_4$ polymers in contact mode, (b) AFM-IR spectrum of PEDOT-$HClO_4$ and (c) Chemical map of PEDOT-$HClO_4$ polymers with the IR source tuned to the C=C bond at 1480 cm^{-1}.

As is shown in Figure 5.16, topography of PEDOT-$HClO_4$ (Figure 5.16, image a) appears to be very loose granular structures when dried naturally. It is clear that PEDOT-$HClO_4$ is not dry enough due to the presence of ClO_4^- which absorbs humid. During the AFM-IR test, PEDOT-$HClO_4$ is scratched by the tip and moves making the topography unclear. The wettish

property and loose granular structure are in agreement with the results obtained by SEM characterization (Figure 5.14, up). The IR spectrum (Figure 5.16, image b) of PEDOT-$HClO_4$ shows the vibration band of C=C at 1471 cm^{-1} indicating the presence of PEDOT polymers. The chemical map (Figure 5.16, image c) of PEDOT-$HClO_4$ is recorded with the IR sourced tuned to the absorption of C=C band at 1480 cm^{-1}. The red color indicates regions absorbing stronger at the selected IR wavenumber 1480 cm^{-1} while the green color shows the contrary. The fact that chemical mapping (Figure 5.16, image c) fits well with topography (Figure 5.15, image c) indicates that the loose structures are made of PEDOT polymers. This result further confirms that PEDOT polymers are successfully synthesized in acidic medium.

Similarly, AFM-IR test is applied to PEDOT-HCl and results are presented (Figure 5.17).

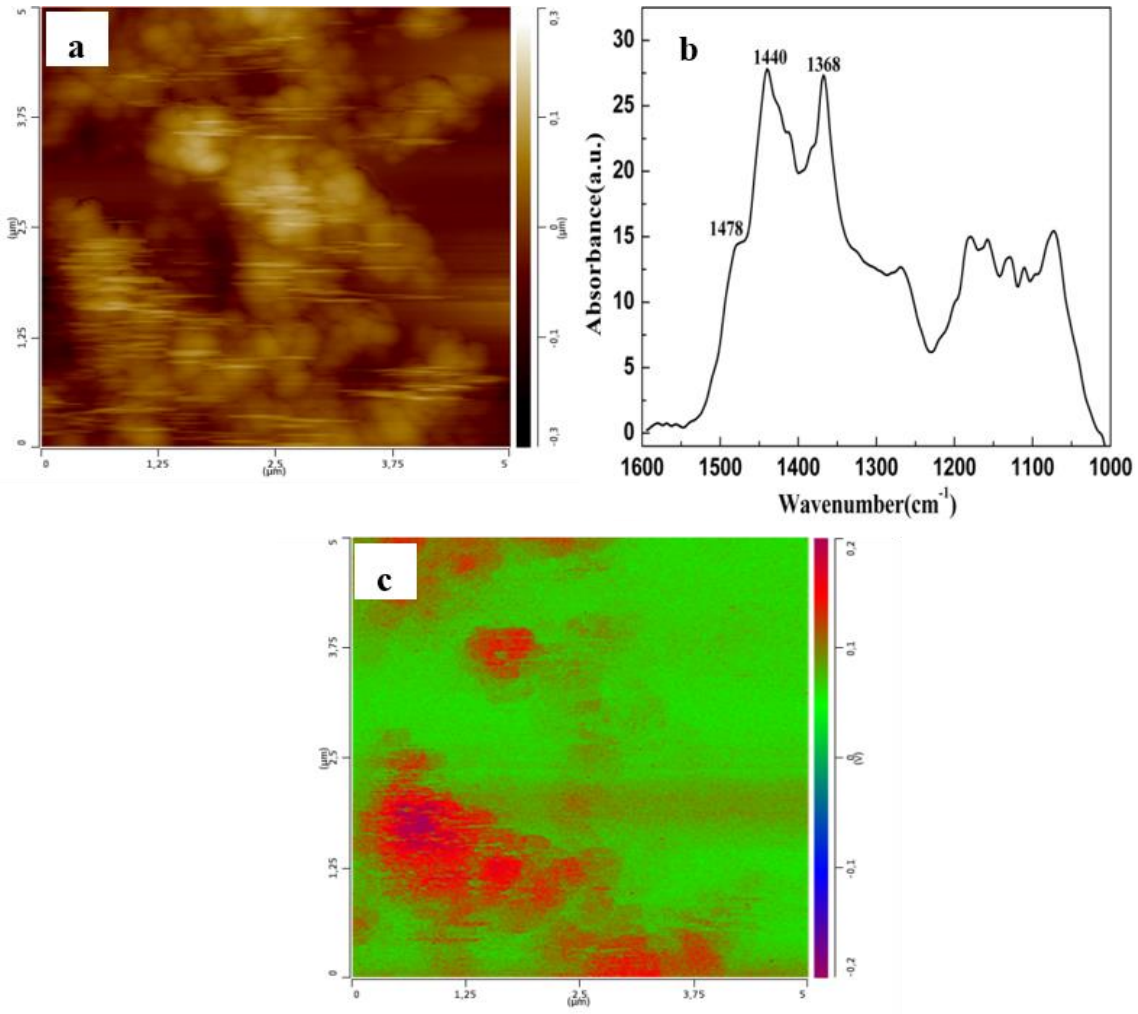

Figure 5.17 AFM-IR characterization of PEDOT-HCl synthesized by a 72 kGy irradiation of EDOT solution at pH = 0 under N_2O atmosphere. (a) AFM topographic image of PEDOT-HCl polymers in contact mode, (b) AFM-IR spectrum of PEDOT-HCl and (c) Chemical map of PEDOT-HCl polymers with the IR source tuned to the C=C bond at 1480 cm^{-1}.

From the topography of PEDOT-HCl (Figure 5.17 a), it is clear that PEDOT polymers appear as aggregated granular particles after drying. This result is in agreement with the morphology of PEDOT-HCl observed by SEM (Figure 5.14, down). Therefore, dried from the acidic solution, PEDOT-HCl appears to be granular particles.

The collected AFM-IR spectrum (Figure 5.17, image b) of the granular deposit displaying the absorption band of C=C stretching band at 1478 cm^{-1} which is also observed in the ATR-FTIR spectrum of PEDOT-HCl polymers (1471 cm^{-1}). The chemical map (Figure 5.17, image c) is scanned with the laser tuned to 1480 cm^{-1} which is the characteristic absorption band of PEDOT polymers and the absorption strength is recorded. Compared with the topography (Figure 5.17, image a), the chemical map shows stronger absorption areas corresponding to the regions where more nanoparticles compactly aggregate. The features of both topography and chemical map are quite similar indicating that the granular particles are mainly composed by PEDOT polymers. Therefore, it can be concluded that amorphous PEDOT polymers synthesized by γ-irradiation induced polymerization in aqueous solution sin acidic medium form granular particles after deposition.

5.6 Electrical conductivity of PEDOT polymers synthesized at pH = 0

The electrical conductivity of PEDOT polymers prepared in acidic medium (pH = 0) by γ-irradiation is measured by using the same procedures as those already described in the case of PPy and PEDOT polymers (chapter 4). After p-doping, the electrical conductivity of PEDOT-$HClO_4$ and PEDOT-HCl are determined to be 7.7×10^{-4} and 3.3×10^{-3} $S\cdot cm^{-1}$. These values are comparable with the electrical conductivity of PEDOT prepared by electron beam, which is 9×10^{-4} S cm^{-1} (chapter 3) and the low electrical conductivity of PEDOT prepared in acidic medium suggests that acidic condition is not so good for the enhancement of electrical conductivity of PEDOT even when doped with counter anions (ClO_4^- or Cl^-).

5.7 Preparation of PEDOT/PSS membranes

As the membranes composed by PEDOT and poly(4-styrenesulfonic acid) (PSSH) have various applications, the prepared PEDOT polymers in very acidic solutions (pH = 0) are mixed with PSSH to form PEDOT/PSS membranes (Figure 5.18). The ratio of PEDOT to PSS is fixed at 1:2.5 (wt%) and DMSO is added (5%) to help the distribution of PEDOT.

As is shown in Figure 5.18, the PEDOT/PSS membranes appear to be dark blue and clear cracks are seen after drying in the oven. As the membranes are very fragile, it is necessary to check the effect of ratio on the mechanical stability of PEDOT/PSS.

Figure 5.18 PEDOT/PSS membranes prepared by mixing PEDOT-$HClO_4$ (left) or PEDOT-HCl with PSS and DMSO. PEDOT-$HClO_4$ and PEDOT-HCl are synthesized by a 72 kGy irradiation of EDOT solution at pH = 0 under N_2O atmosphere.

5.8 Conclusions

In this chapter, the effect of synthetic conditions (soft template, pH and ionic strength) on the polymerization of EDOT is studied. First, the presence of SDS micelles didn't allow the synthesis of PEDOT polymers due to the competitive reaction of HO• onto SDS molecules. On the contrary, a very acidic medium ($HClO_4$ or HCl) enabled the synthesis of PEDOT polymers thanks to the oxidation of EDOT monomers by HO• or $Cl_2^{\cdot -}$. A dark blue precipitate is obtained after γ-irradiation at pH=0. Spectroscopic studies prove that PEDOT polymers in reduced state are synthesized. Next, it is proved that the kind of acid and ionic strength have no effect on the polymerization of EDOT. Microscopic observations (Cryo-TEM and SEM) showed that the produced PEDOT appears to be amorphous in solution while compact aggregates of granular particles are observed after deposition. These granular particles are mainly composed of PEDOT polymers as confirmed by AFM-IR. PEDOT polymers prepared in acidic medium possess electrical conductivity in the order of 10^{-3} $S \cdot cm^{-1}$ which comparable to that of PEDOT prepared in neutral medium. In conclusion, synthesizing conducting PEDOT polymers using gamma irradiation in acidic medium is feasible and may offer a new approach for the synthesis of CPs. Finally, even if the fabrication of PEDOT/PSS membrane

is successful, the preparation conditions needs to be optimized in order to improve the mechanical stability of the layer.

References

[1] Spinks, J. W. T.; Woods, R. J., An introduction to radiation chemistry. *John Wiley & Sons, Inc.* **1990**, *3*, 276.

[2] Schwarz, H. A.; Dodson, R. W., Equilibrium between Hydroxyl Radicals and Thallium(I I) and the Oxidation Potential of OH (aq). *The Journal of Physical Chemistry* **1984**, *88* (16), 3643-3647.

[3] Evers, E. L.; Jayson, G. G.; Swallow, A. J., Pulse radiolysis study of protoferrihaem IX intercalated in sodium dodecyl sulphate micelles. *Journal of the Chemical Society, Faraday Transactions 1: Physical Chemistry in Condensed Phases* **1978**, *74* (0), 418-426.

[4] Rodgers, M. A. J.; Lindig, B. A., Radiolytic Studies of Micelles and Other Aggregated Systems. *The Study of Fast Processes and Transient Species by Electron Pulse Radiolysis* **1982**, 551-571.

[5] Evers, E. L.; Jayson, G. G.; Robb, I. D.; Swallow, A. J., Determination by pulse radiolysis of the distribution of solubilizates between micellar and nonmicellar phases. Naphthalene and its reduced free radical in aqueous sodium dodecyl sulphate solutions. *Journal of the Chemical Society, Faraday Transactions 1: Physical Chemistry in Condensed Phases* **1980**, *76* (0), 528-536.

[6] Guha, S. N.; Mittal, J. P., Pulse radiolysis study of redox reactions of safranine T in sodium dodecylsulphate (SDS) micellar medium. *Proceedings of the Indian Academy of Sciences - Chemical Sciences* **1992**, *104* (4), 497-507.

[7] Meisel, D.; Matheson, M. S.; Rabani, J., Photolytic and radiolytic studies of tris(2,2'-bipyridine)ruthenium(2+) in micellar solutions. *Journal of the American Chemical Society* **1978**, *100* (1), 117-122.

[8] Coletta, C., Study of growth mechanism of conducting polymers by pulse radiolysis. *Ph.D thesis* **2016**, *1*, 37.

[9] Sakmeche, N.; Aeiyach, S.; Aaron, J. J.; Jouini, M.; Lacroix, J. C.; Lacaze, P. C., Improvement of the Electrosynthesis and Physicochemical Properties of Poly(3,4-ethylenedioxythiophene) Using a Sodium Dodecyl Sulfate Micellar Aqueous Medium. *Langmuir* **1999**, *15* (7), 2566-2574.

[10] Han, M. G.; Foulger, S. H., Facile synthesis of poly(3,4-ethylenedioxythiophene) nanofibers from an aqueous surfactant solution. *Small* **2006**, *2* (10), 1164-1169.

[11] Kirchmeyer, S.; Reuter, K., Scientific importance, properties and growing applications of poly(3,4-ethylenedioxythiophene). *Journal of Materials Chemistry* **2005**, *15* (21), 2077.

[12] Heuer, H. W.; Wehrmann, R.; Kirchmeyer, S., Electrochromic window based on conducting poly(3,4-ethylenedioxythiophene)-poly(styrene sulfonate). *Adv. Funct. Mater.* **2002**, *12* (2), 89-94.

[13] Simic, M.; Neta, P.; Hayon, E., Pulse radiolysis study of alcohols in aqueous solution. *The Journal of Physical Chemistry* **1969**, *73* (11), 3794-3800.

[14] Hagiwara, T.; Yamaura, M.; Sato, K.; Hirasaka, M.; Iwata, K., Synthesis and properties of poly(3,4-dimethoxythiophene). *Synth. Met.* **1989**, *32*, 367-369.

[15] Akimoto, M.; Furukawa, Y.; Takeuchi, H.; Harada, I., Correlation between vibrational spectra and electrical conductivity of polythiophene. *Synth. Met.* **1986**, *15*, 353-360.

[16] Kvarnström, C.; Neugebauer, H.; Blomquist, S.; H.J. Ahonenc; J. Kankarec; Ivaska, A., In situ spectroelectrochemical characterization of poly(3,4-ethylenedioxythiophene). *Electrochim. Acta* **1999**, *44*, 273-2750.

[17] Ghosh, S.; Remita, H.; Ramos, L.; Dazzi, A.; Deniset-Besseau, A.; Beaunier, P.; Goubard, F.; Aubert, P. H.; Brisset, F.; Remita, S., PEDOT nanostructures synthesized in hexagonal mesophases. *NewJ.Chem.* **2014**, *38* (3), 1106-1115.

[18] Lattach, Y.; Coletta, C.; Ghosh, S.; Remita, S., Radiation-induced synthesis of nanostructured conjugated polymers in aqueous solution: fundamental effect of oxidizing species. *Chemphyschem* **2014**, *15* (1), 208-218.

[19] Cui, Z.; Coletta, C.; Rebois, R.; Baiz, S.; Gervais, M.; Goubard, F.; Aubert, P. H.; Dazzi, A.; Remita, S., Radiation-induced reduction-polymerization route for the Synthesis of PEDOT conducting polymers. *Radiat. Phys. Chem.* **2016**, *119*, 157-166.

[20] Zhou, J.; Anjum, D. H.; Lubineau, G.; Li, E. Q.; Thoroddsen, S. T., Unraveling the Order and Disorder in Poly(3,4-ethylenedioxythiophene)/Poly(styrenesulfonate) Nanofilms. *Macromolecules* **2015**, *48* (16), 5688-5696.

[21] Kim, N.; Kee, S.; Lee, S. H.; Lee, B. H.; Kahng, Y. H.; Jo, Y. R.; Kim, B. J.; Lee, K., Highly conductive PEDOT:PSS nanofibrils induced by solution-processed crystallization. *Advanced materials* **2014**, *26* (14), 2268-72, 2109.

Chapter 6: Development of a radiation-induced reduction–polymerization route for the synthesis of PEDOT polymers

Conducting polymers (CPs) have been widely investigated due to their potential applications in many areas.[1] A large variety of CPs have been developed among which poly(3,4-ethylenedioxythiophene) (PEDOT) polymers have attracted great interests for their easy synthesis, good environmental stability and high electrical conductivity[2-4]. PEDOT polymers have many potential applications as conducting coating, organic transistor, sensor, electrochromic display and photovoltaic device.[4-7]

As an important kind of CPs, PEDOT polymers are normally prepared by the traditional chemical or electrochemical polymerization of 3,4-ethylenedioxythiophene (EDOT) monomers.[8-11] PEDOT is usually synthesized by oxidation–polymerization routes thanks to the initial oxidation EDOT monomers and to the further coupling reactions in α,α′ positions (Figure 2.2, chapter 2).

To initiate the polymerization of EDOT monomers, both the chemical and electrochemical methods involve the oxidation of EDOT monomers to the EDOT cations. Both chemical oxidants and applied electrochemical oxidation potential can oxidize the EDOT monomers into EDOT cations which form EDOT dimers by α-α' coupling reactions. Two H atoms are subtracted from α and α' positions of EDOT monomers forming a new C-C bond. Then, the formed EDOT dimers undergo similar chemical or electrochemical oxidation and coupling reactions produce EDOT oligomers. Finally, elongation of the EDOT oligomers with the similar procedures produces PEDOT polymers (Figure 6.1).

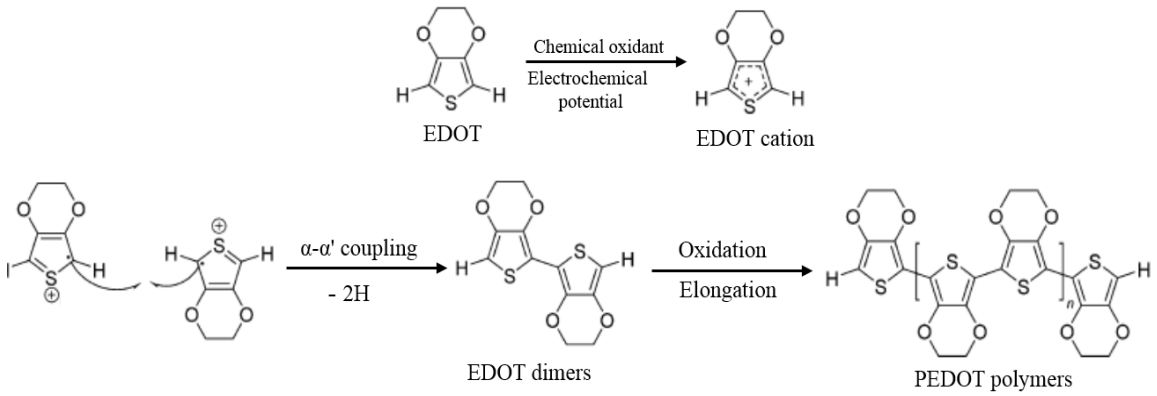

Figure 6.1 Schematic of chemical and electrochemical polymerization of EDOT monomers into PEDOT polymers.

While the more traditional oxidation–polymerization ways consist in chemical or electrochemical methods, some alternative approaches such as plasma deposition and enzyme-catalyzed polymerization to synthesize PEDOT polymers have been reported.[12-14] It has also been reported that the combination of chemical oxidation and gamma (γ)-irradiation was applied for the synthesis of CPs.[15-17] Contrary to the traditional oxidation-polymerization approach, the reduction polymerization route has been rarely applied and only the chemical reduction polymerization of halothiophene is reported.[18] To the best of my knowledge, the synthesis of PEDOT polymers by reduction polymerization has not been reported.

In chapter 3, an easy and "green" methodology has been developed by using exclusively γ-rays to induce oxidation-polymerization of EDOT monomers in aqueous solution.[19] Also, by adjusting polymerization conditions, different oxidizing species, namely hydroxyl and azide radicals, were produced under N_2O atmosphere by γ-radiolysis of water and leaded to the self-assembled PEDOT polymers with different morphologies.[20] In chapter 4, this radiolytic methodology has also been extended to the synthesis of polypyrrole (PPy) polymers. Therefore, radiolytic methodology, especially γ-irradiation, has definitely proved to be a useful alternative approach for the oxidation–polymerization of nanostructured CPs. Nevertheless, to the best of our knowledge, radiation chemistry has never been used, in reducing conditions, as a route for conducting polymers reduction–polymerization procedure.

In this chapter, simple γ-rays-based reduction–polymerization route for synthesizing conducting polymers under N_2 atmosphere is described at room temperature. The originality of the work comes from the use, during the initiation step of polymerization, of reducing species produced from water radiolysis, namely hydrated electrons (e_{aq}^-), instead of oxidizing radicals, such as hydroxyl radicals (HO•) or azide radicals (N_3•). Morphology and physicochemical properties of PEDOT synthesized by reduction–polymerization (action of e_{aq}^- under N_2 atmosphere), noted $PEDOT_{red}$, are checked and compared with those of PEDOT already synthesized by γ-irradiation under oxidative conditions, noted $PEDOT_{ox}$ (action of HO• under N_2O atmosphere).

6.1 PEDOT synthesis stragety and characterization

6.1.1 Solution preparation

Aqueous solutions containing different concentrations in EDOT (1 and 10 mM) were prepared at room temperature and in the dark to prevent any photochemical reaction. The

chosen EDOT concentrations, which are lower than EDOT solubility in water, were always checked by UV–vis absorption spectroscopy since the spectrum of EDOT had earlier been determined.[19] EDOT concentrations higher than 10 mM were not used in order to avoid the direct ionization of EDOT molecules which could occur during radiolysis. The pH of the solutions was, in all the cases, found to be close to 7. Note that no drastic change in the pH was observed after irradiation.

For $PEDOT_{red}$ synthesis, EDOT aqueous solutions were added with isopropanol (0.2 M), degassed with N_2 for 20 min and then irradiated with increasing doses up to 72 kGy in order to achieve complete polymer synthesis. For comparison purpose and in order to quantitatively synthesize $PEDOT_{ox}$, EDOT aqueous solutions were degassed by bubbling with nitrous oxide, N_2O, for 20 min, in the absence of isopropanol and then irradiated at 72 kGy. All irradiations were carried out at a dose rate of 5 kGy h^{-1}.

6.1.2 Water radiolysis and radiation-induced polymerization

γ-radiolysis of aqueous solutions under N_2 atmosphere at neutral produces two main species, namely hydroxyl radicals (HO•) and hydrated electrons (e_{aq}^-) with the same radiolytic yields of 2.8×10^{-7} mol J^{-1} (equations 2.4 and 2.5, chapter 2). Note that HO• is a strong oxidant (2.2 V_{SHE} at pH = 7) and e_{aq}^- is a very reducing species (-2.8 V_{SHE}). Due to these two extremal redox potential values, one can consider the possible oxidation of EDOT (1.4 $V_{Ag/AgCl}$) by HO• as well as its possible reduction by e_{aq}^-.[21]

In order to reduce EDOT monomers and then to synthesize $PEDOT_{red}$ polymers, HO• must be scavenged. This is possible, under N_2 atmosphere, in the presence of isopropanol, $(CH_3)_2CHOH$. Indeed, when isopropanol is present (at a relatively high concentration, 0.2 M for instance), HO• is quantitatively converted into isopropanol radical, $(CH_3)_2C•OH$ (reaction 2.23, chapter 2). In addition, γ-radiolysis of water produces hydrogen atoms (H•) which also quantitatively reacts with $(CH_3)_2CHOH$ producing $(CH_3)_2C•OH$ (reaction 2.24, chapter 2).

As a consequence, when irradiating N_2-saturated aqueous solutions in the presence of isopropanol, as in the case of EDOT solutions, in addition to e_{aq}^- ($G_{e_{aq}^-} = 2.8\times10^{-7}$ mol•J^{-1}), only an additional short-lived transient species is quantitatively formed, namely $(CH_3)_2C•OH$, the radiolytic yield of which being 3.4×10^{-7} mol J^{-1} (equation 2.26, chapter 2). Note that

$(CH_3)_2C•OH$ cannot oxidize EDOT. In fact, it is almost a reducing species, the redox potential of which amounts to −1.8 V_{SHE} at pH = 7.[22]

On the contrary, in order to oxidize EDOT and then to synthesize $PEDOT_{ox}$, hydrated electrons must be scavenged. As described before (chapter 3), this is possible under N_2O atmosphere. As a consequence, when irradiating N_2O-saturated aqueous solutions at neutral pH, as in the case of EDOT solutions, only one short-lived transient species is quantitatively formed, namely HO• radicals, the radiolytic yield of which becoming 5.6×10^{-7} mol J^{-1} (equation 2.15, chapter 2).

The concentration, C, of a radiolytic species produced by water radiolysis can be expressed as a function of the irradiation dose, D, expressed in Grays according to:

$$[e_{aq}^-] = D\ (Gy) \times G_{e_{aq}^-}\ (mol\ J^{-1}) \qquad (6.1)$$

$$[HO•] = D\ (Gy) \times G(HO•)\ (mol\ J^{-1}) \qquad (6.2)$$

Then, under N_2 atmosphere in the presence of isopropanol, a dose of 3.6 kGy produces 1 mM in hydrated electrons (and 1 mM in isopropanol radicals), while under N_2O atmosphere, a dose of 1.8 kGy is needed for the production of 1 mM in hydroxyl radicals.

As demonstrated in chapter 3, the yield of EDOT monomers oxidation by hydroxyl radicals is strictly equal to the yield of HO• formation.[19,20] It is also demonstrated that the quantitative synthesis of $PEDOT_{ox}$ polymers throughout oxidation–polymerization mechanism implies the use of two HO ·radicals per EDOT molecule. This is consistent with the fact that, in a polymer, all the monomers apart from the terminal ones, are bound to two neighbors in α and α′ positions. Thus, the theoretical irradiation dose (D_{max}) which should lead to the quantitative formation of $PEDOT_{ox}$ under N_2O atmosphere is twice the dose necessary for the total oxidation of EDOT monomers. In a N_2O-saturated aqueous solution containing 10 mM in EDOT, according to (equation 2.4, chapter 2 and equation 6.2), the dose which is necessary for the total oxidation of EDOT (10 mM) by hydroxyl radicals, amounts to 18 kGy, while the dose D_{max} which is necessary for the complete synthesis of $PEDOT_{ox}$ amounts to 36 kGy.

One can suppose that the quantitative synthesis of $PEDOT_{red}$ polymers throughout reduction–polymerization mechanism implies also the use of two reducing radicals per EDOT molecule. The theoretical irradiation dose (D_{max}) which should lead to the quantitative formation of $PEDOT_{red}$, under N_2 atmosphere in the presence of isopropanol, is then twice the dose necessary for the total reduction of EDOT monomers. Since, isopropanol radicals do not

reduce EDOT as it will be further demonstrated and since only hydrated electrons react onto EDOT molecules, due to equation 2.5 (chapter 2) and equation 6.1, the doses which are necessary for the total reduction of 1 mM and 10 mM in EDOT, amount to 3.6 and 36 kGy respectively, while the doses D_{max} which are necessary for the complete synthesis of $PEDOT_{red}$, amount to 7.2 and 72 kGy respectively.

6.1.3 $PEDOT_{red}$ and $PEDOT_{ox}$ characterization

UV-visible absorption spectra of EDOT (before irradiation) and of radiosynthesized $PEDOT_{ox}$ or $PEDOT_{red}$ (after irradiation) solutions were recorded by putting the obtained aqueous solutions in a quartz cell with an optical path length of 0.2 cm. Due to the relatively high extinction coefficient of EDOT, aqueous solutions containing 10 mM EDOT monomers were diluted 10 times before measurement. The morphology of PEDOT polymers in solution was directly observed by Cryo-TEM before any deposition.

To further identify radiosynthesized polymers and their chemical composition, the Fourier transform infrared (FTIR) spectra of lyophilized $PEDOT_{ox}$ and $PEDOT_{red}$ were recorded. In order to check the morphology of radiosynthesized polymers after deposition, $PEDOT_{red}$ powder obtained after lyophilization was sprinkled onto carbon tape adhered to aluminum mounts and SEM images were obtained.

AFM-IR measurement were carried out by depositing a small drop of $PEDOT_{red}$ solution onto the upper surface of ZnSe prism (transparent in the mid-IR) and dried naturally in air. The thermal stability and composition analysis of lyophilized $PEDOT_{ox}$ and $PEDOT_{red}$ was performed under a nitrogen flow of 50 mL/min. The temperature ranged from 40 to 900 ℃ at a heating rate of 20 ℃/min.

To measure the conductivity of $PEDOT_{ox}$ and $PEDOT_{red}$, spin-coated films of PEDOT were obtained by spinning a small drop of PEDOT suspensions on a glass substrate. Before measurements, the nanostructures of PEDOT solutions or suspensions were doped with $NOBF_4$ at a concentration of 10 mM in acetonitrile. A four-point probe technique was used for measuring the resistance of $PEDOT_{ox}$ and $PEDOT_{red}$ films and surface profiler was used for the thickness measurement of the films. The conductivity, ρ (S cm^{-1}) was determined thanks to equation2.35 (chapter 2).

6.2 Hydrated electrons-induced EDOT reduction

In chapter 3, it has already been demonstrated that, at air and under N_2O atmosphere, hydroxyl radicals quantitatively oxidize EDOT molecules, the yield of EDOT monomers oxidation being strictly equal to the yield of formation of HO• radicals.[19,20] In order to check whether EDOT molecules can be alternatively reduced by radical species produced by water radiolysis, we irradiated aqueous solutions containing 1 mM in EDOT at increasing doses up to 7.2 kGy under N_2 in the presence of 0.2 M isopropanol.

The UV–vis absorption spectrum of aqueous solution containing 1 mM in EDOT displays as already highlighted two absorption maxima at 235 and 255 nm as shown (Figure 6.2).[23]

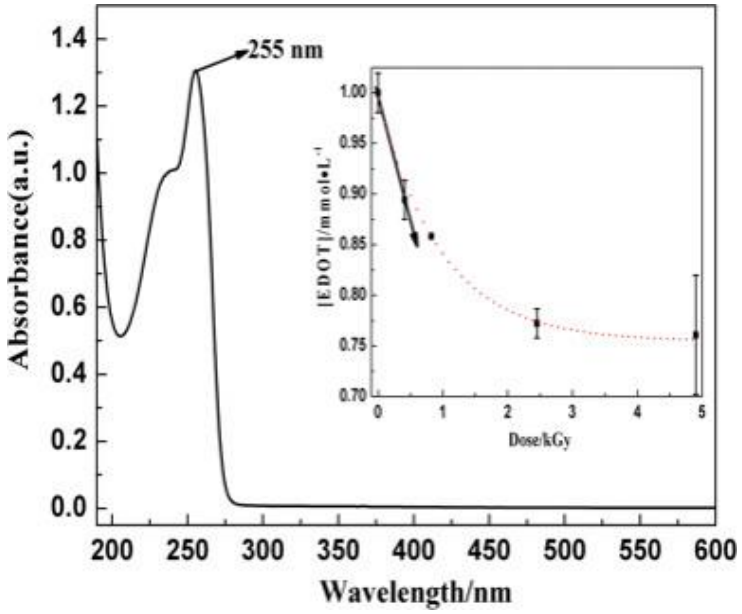

Figure 6.2 UV-vis absorption spectrum of EDOT monomer (1 mM) aqueous solution (l=0.2 cm, reference: water). Insert: evolution of EDOT concentration of as a function of the dose. The initial radiolytic yield of EDOT consumption corresponds to the initial slope of the curve.[23]

The characteristic peak of EDOT monomers at 255 nm arises from π→π* electronic transitions in the thiophene ring and its extinction coefficient value was estimated to be 7048 L mol^{-1} cm^{-1} which is in agreement with the results obtained (section 3.2.2, chapter 3).[19] The evolution of the UV–visible absorption spectrum of this solution as a function of the irradiation dose displays a continuous decrease in the absorption at 235 and 255 nm (results not shown) indicating the progressive consumption of EDOT (according to a pseudo-first-

order exponential decay). From the value of the extinction coefficients at 255 nm, we deduced the variation in EDOT concentration with the irradiation dose (Inset of Figure 6.2). The initial radiolytic yield of EDOT consumption, $G_{-EDOT\ 0}$, is given by the value of the initial slope of the curve which can be deduced thanks to an exponential fit of the experimental curve:

$$G_{-EDOT\ 0}\,(\text{mol J}^{-1}) = -\left(\frac{\text{d[EDOT] (mol L}^{-1})}{\text{dDose (Gy)}}\right)_0 = 2.6 \times 10^{-7}\ \text{mol J}^{-1} \tag{6.3}$$

The same yield is obtained when irradiations are performed in the presence of *tert*-butanol (instead of isopropanol) which is also a scavenger of HO• radicals. Nevertheless, contrarily to isopropanol radicals, *tert*-butanol radicals are known to be unreactive. These results demonstrate that, under N_2 in the presence of isopropanol, only hydrated electrons react with EDOT monomers. In addition, we clearly find that:

$$G_{-EDOT\ 0} \sim G_{e_{aq}^-} \tag{6.4}$$

This indicates that a concentration of 1 mM in EDOT is sufficient to scavenge all the hydrated electrons produced by radiolysis of water and that e_{aq}^- quantitatively reduces EDOT monomers. Also, the reactivity of e_{aq}^- onto EDOT was checked by pulse radiolysis and the rate constant of reduction of EDOT has been determined as it will be presented in the next part (chapter 7).

6.3 Radiation-induced reduction–polymerization of PEDOT

In chapter 3, it has been demonstrated that, at air and under N_2O atmosphere, HO•-induced oxidation of EDOT implies the formation of a transient species, namely $EDOT^{\bullet+}$ cation radical, which dimerizes and deprotonates leading to a stable product, namely $EDOT_2$ dimer.[24] This result proves that $PEDOT_{ox}$ growth is not a chain reaction. On the contrary, it proceeds through a step-by-step mechanism made up of the following recurrent steps: (i) oxidation/activation, (ii) growth/chain length increase, (iii) deprotonation. As a consequence, $PEDOT_{ox}$ radioinduced synthesis proceeds through a recurrent oxidation process: HO ·reacts with EDOT monomers, then with dimers, then with oligomer. This means that the quantitative synthesis of $PEDOT_{ox}$ polymers throughout oxidation–polymerization mechanism implies the use of two HO• radicals per EDOT molecule. This has also been

demonstrated since doses higher than 36 kGy enabled the quantitative radiation-induced oxidation polymerization of 10 mM in EDOT under N_2O atmosphere.[12,19]

While hydroxyl radicals oxidize EDOT monomers leading to $PEDOT_{ox}$ polymers, hydrated electrons are able to reduce EDOT and, by comparison, should lead to $PEDOT_{red}$ polymers. The fact that the yield of EDOT consumption is equal to that of e_{aq}^- production (equation 6.4) means that the process initiated by hydrated electrons and which will be further attributed to $PEDOT_{red}$ radioinduced synthesis does not proceed through a chain reaction. Then, one can suppose that the quantitative synthesis of $PEDOT_{red}$ polymers throughout a reduction-polymerization process implies also a step-by-step mechanism and then needs the use of two hydrated electrons per EDOT molecule.

In order to check whether reduction of EDOT monomers by e_{aq}^- is accompanied by a radiation-induced polymerization process, under N_2 atmosphere in the presence of 0.2 M isopropanol, aqueous solutions containing 10 mM in EDOT were irradiated at increasing doses up to 72 kGy (Figure 6.3 spectrum b).[23]

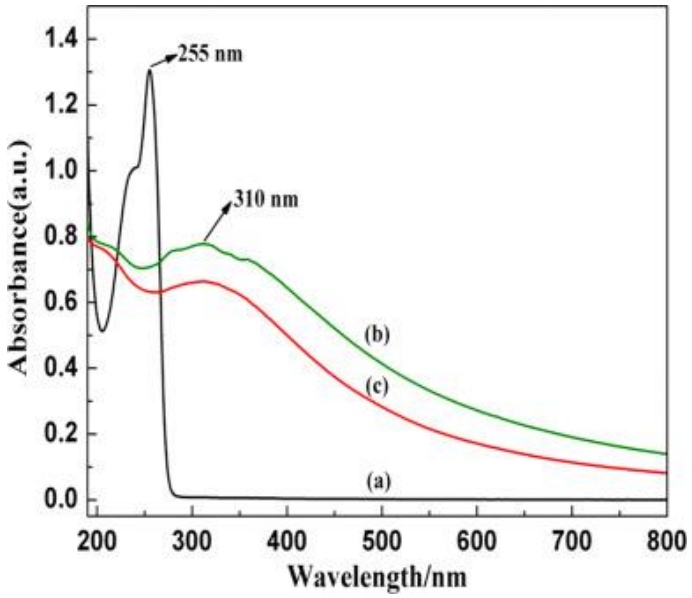

Figure 6.3 UV-vis absorption spectra of an aqueous solution containing 10 mM in EDOT (a) before irradiation, (b) irradiated at 72 kGy under N_2 in the presence of isopropanol ($PEDOT_{red}$), (c) irradiated at 72 kGy under N_2O ($PEDOT_{ox}$). The optical path length was 0.2 cm. The reference was water.[23]

This used dose is that needed for the total reduction of EDOT in case of a step-by-step reduction–polymerization mechanism. Note that while low concentrations in EDOT monomers (1 mM) were needed for succeeding in the follow-up of their reduction mechanism,

higher concentrations in EDOT were necessary for the characterization of $PEDOT_{red}$ polymers, either in aqueous solution or after their deposition onto substrate as it will be further presented in the case of 10 mM in EDOT.

In Figure 6.3, the UV–visible absorption spectrum of the solution irradiated (at 72 kGy) under N_2 in the presence of isopropanol (spectrum b) is similar to the spectrum obtained for $PEDOT_{ox}$ (at the same dose) under N_2O (spectrum c).[20] Only a small difference between the intensities of the spectra is observed. In both cases, the two absorption bands of EDOT monomers at 235 and 255 nm (spectrum a) have completely disappeared, which should indicate that oxidation–polymerization as well as reduction–polymerization are quantitative at 72 kGy (D_{max}) as expected. Both spectra display an absorption maximum around 310 nm, which has been attributed to EDOT dimers and oligomers (section 3.2.2, chapter 3).[25,26] Such a band was also observed in the case of oxidation–polymerization (section 3.3.2, chapter 3).[20] Also, spectra are characterized by a continuous scattering in the range of 400–800 nm which should correspond to longer oligomers and polymers of PEDOT.[27-29] The observed light scattering traduces the presence in the irradiated solutions of a dense yellow suspension such as that observed in the case of EDOT solution irradiated under N_2 (Figure 6.4, image b).[23] As it will be later demonstrated thanks to ATR-FTIR spectroscopic measurements, these suspensions correspond to $PEDOT_{red}$ and $PEDOT_{ox}$ polymers formed at high doses thanks respectively to the reduction–polymerization and the oxidation–polymerization processes.

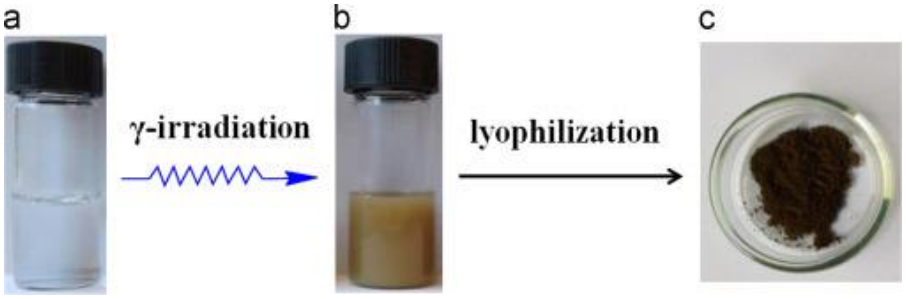

Figure 6.4 Photographs of EDOT samples (a) at a concentration of 10 mM before irradiation, (b) after a 72 kGy-irradiation under N_2 in the presence of isopropanol ($PEDOT_{red}$), (c) after lyophilization.[23]

6.4 Highlighting $PEDOT_{red}$ radioinduced synthesis

After a 72 kGy-irradiation under N_2, the original transparent aqueous solution of EDOT monomers in the presence of isopropanol (Figure 6.4, image a) becomes turbid (Figure 6.4,

image b). The yellow suspension was then dried by lyophilization in order to eliminate any residual water molecules which could be trapped in the polymer-containing dark solid phase obtained (Figure 6.4, image c). For comparison, EDOT aqueous solution irradiated at 72 kGy under N_2O was also lyophilized. The lyophilized samples were then characterized by ATR-FTIR spectroscopy in order to investigate the chemical nature of the solid phases and to confirm the presence of PEDOT polymers in both of them.

The ATR-FTIR spectra of both powders, radiosynthesized at 72 kGy under reducing (spectrum b) and oxidizing conditions (spectrum c), are presented in the wave number region 4000–600 cm^{-1} together with the spectrum of pure non irradiated EDOT (spectrum a) (Figure 6.5).[23]

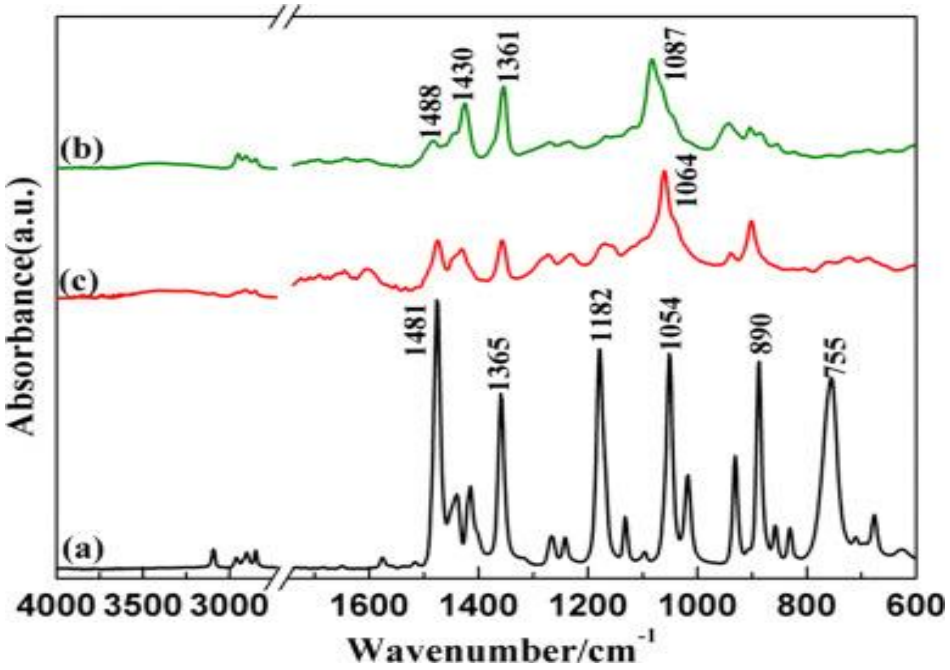

Figure 6.5 ATR-FTIR spectra of (a) pure EDOT monomers, (b) $PEDOT_{red}$ powder obtained by reduction–polymerization at 72 kGy, (c) $PEDOT_{ox}$ powder obtained by oxidation–polymerization at 72 kGy.[23]

Between 1600 and 600 cm^{-1}, the three obtained spectra are in good agreement with those previously reported for PEDOT and EDOT in literature. The absorption bands at 890, 1054 and 1182 cm^{-1} correspond to the stretching vibrations of ethylenedioxy group (C–O–R–O–C). The stretching vibrations of C–C and C=C in thiophene ring are also observed at 1365 and 1481 cm^{-1}.[11] The absorption bands at 1361, 1430 and 1488 cm^{-1} originating from C–C and C=C can be seen in the ATR-FTIR spectra of both powders.[26] All the characteristic bands of

PEDOT are then present in spectra b and c of Figure 6.5 even if they appear relatively slightly displaced. For instance, the absorption band assigned to ethylenedioxy group is observed at 1087 cm^{-1} in the case of the powder obtained by reduction–polymerization, while it appears at 1064 cm^{-1} in the case of the powder obtained by oxidation. Nevertheless, this demonstrates, without any ambiguity, that PEDOT polymers are obtained by radiolysis either by reduction–polymerization or by oxidation–polymerization.

Note that the characteristic peak at 755 cm^{-1}, attributed to the C–H out-of-plane bending vibration at α, α′ positions of EDOT (spectrum a), totally disappears after irradiation (spectra b and c). This result proves the successful synthesis of $PEDOT_{red}$ and $PEDOT_{ox}$ via α, α′ coupling reactions and definitely demonstrates that EDOT polymerization is complete at 72 kGy, in agreement with a step-by-step PEDOT growth mechanism in both oxidizing and reducing conditions.[20]

6.5 Morphological observation of $PEDOT_{red}$

Aqueous solutions containing 10 mM in EDOT and irradiated at 72 kGy under N_2 in the presence of isopropanol were observed by cryo-transmission electron microscopy just after irradiation and before any sedimentation. Representative images showed the presence of low density globular structures forming polydisperse spherical nanoparticles with a diameter comprised between 100 and 500 nm as observed (Figure 6.6, images a and b at two different magnifications).[23]

Since no other low density objects were observed during our cryo-TEM experiments, we deduce that these spherical nanoparticles are made up of $PEDOT_{red}$ polymers. The mean size, the shape and the polydispersity of $PEDOT_{red}$ polymer nanostructures obtained in the present work, through reduction–polymerization, are the same as those of $PEDOT_{ox}$ polymers already synthesized through oxidation–polymerization routes induced either by γ-rays or by accelerated electrons (chapter 3).[19,20,24]

Such as in the case of PEDOT obtained by radiation induced oxidation polymerization, each observed nanoparticle should be composed of interdigitated polymer chains. Since no parasite α-β′ linkages could occur during polymerization, radiosynthesized $PEDOT_{red}$ nanostructures must be composed of linear chain polymers which are not branched nor networked. Thus, each globular structure observed on Figure 6.6 should correspond to a self-assembly of independent amorphous PEDOT chains.

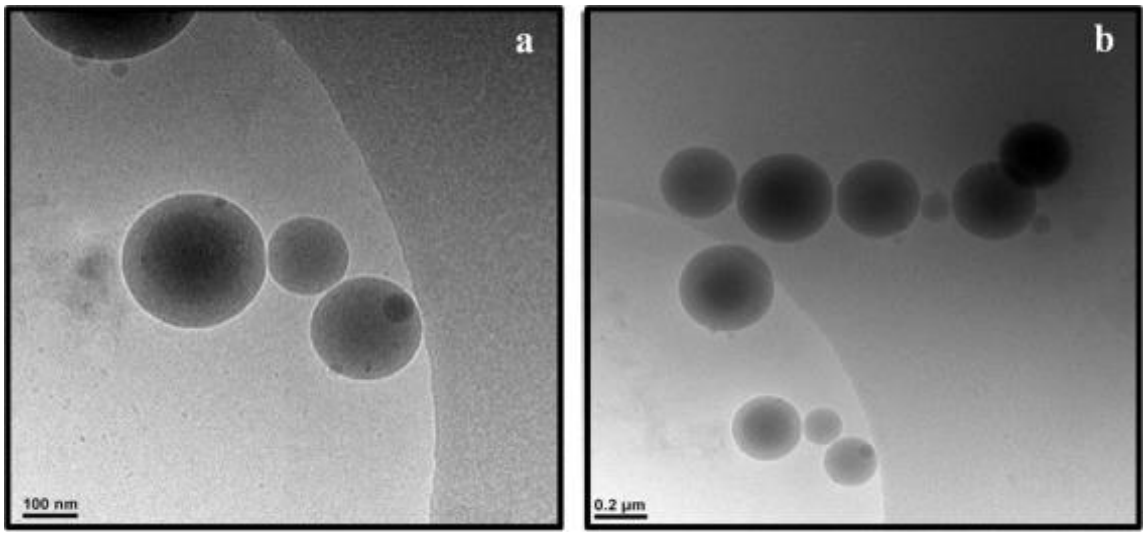

Figure 6.6 Cryo-TEM images of aqueous samples containing 10 mM in EDOT irradiated at 72 kGy under N_2 in the presence of isopropanol. They exhibit spherical nanoobjects with diameters comprised between 100 and 500 nm attributed to self-assembled $PEDOT_{red}$ polymers.[23]

In order to characterize the morphology of the polymers after drying and deposition procedures, $PEDOT_{red}$-containing lyophilized powder obtained after a 72 kGy-irradiation was deposited onto carbon tape adhered to aluminum mounts and dried. The surface was then imaged by SEM (Figure 6.7).[23]

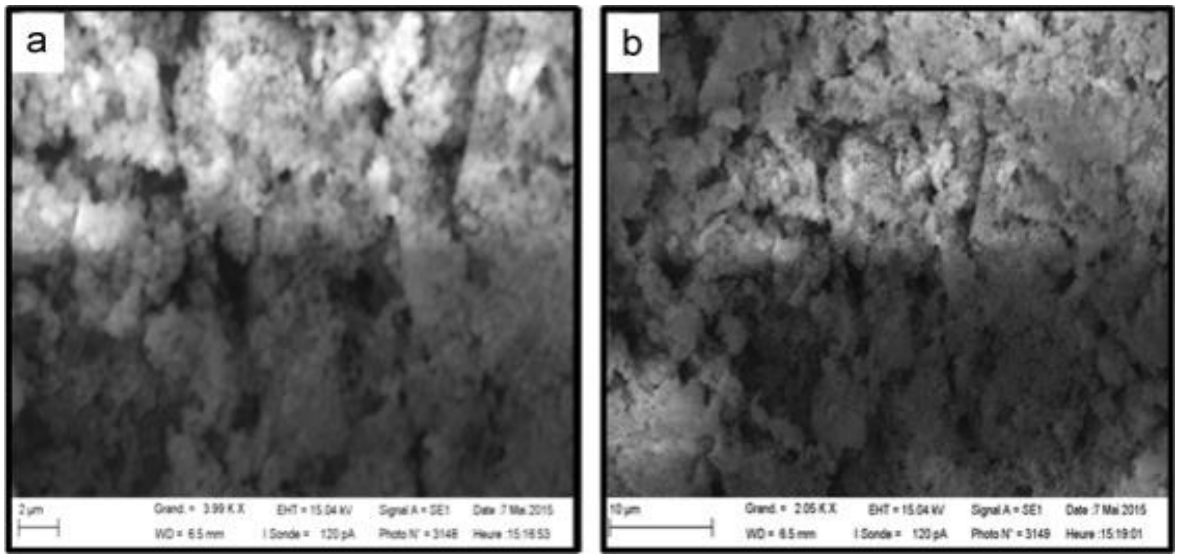

Figure 6.7 SEM images of $PEDOT_{red}$ polymers after lyophilization and deposition onto carbon tape adhered to aluminum mounts. Polymers were obtained after a 72 kGy-irradiation of an aqueous solution containing 10 mM in EDOT under N_2 in the presence of isopropanol.[23]

The images of Figure 6.7 displayed at two different magnifications (images a and b), indicate the presence of very close-packed spheroid polymeric particles. These structures should come from the globular nanostructures already observed in aqueous solution by Cryo-TEM (Figure 6.6). All these observations are consistent with the reported characterizations of $PEDOT_{ox}$ polymers synthesized by oxidation–polymerization (chapter 3).[20] The particles observed by SEM after deposition are polydisperse in size with a diameter comprised between 100 and 500 nm. These SEM observations agree well with the morphology of $PEDOT_{red}$ particles previously observed in aqueous solution by Cryo-TEM (Figure 6.6) without any significant change in the mean size and in the shape. Then, the packing of the particles and their flattening onto the substrate when deposited and dried do not seem to affect the nanostructuration of $PEDOT_{red}$ polymers.

In order to further prove that the spherical nanoparticles already observed by Cryo-TEM and SEM are made up of PEDOT polymer chains, a drop of the yellow suspension (Figure 6.4, image b, obtained after the irradiation at 72 kGy of an aqueous solution containing 10 mM in EDOT under N_2 in the presence of isopropanol) was deposited on the upper surface of a ZnSe prism, dried naturally and finally imaged and characterized by AFM-IR (Figure 6.8).[23]

According to the AFM image of $PEDOT_{red}$ recorded in contact mode (Figure 6.8, image a), the bottom dark areas having no thickness correspond to the substrate. The topography of $PEDOT_{red}$ displayed as the bright areas correspond to the thicker regions made up of close-packed spherical nanoparticles (100-300 nm in diameter). This AFM observation agrees well with the morphology of $PEDOT_{red}$ globular particles previously observed in aqueous solution by Cryo-TEM (Figure 6.6) without any significant change in the mean size and in the shape. Then, the packing of the particles and their flattening onto ZnSe substrate when deposited and dried do not seem to affect the nanostructuration of polymer nanostructures.

In order to confirm that these nanoparticles are made up of PEDOT polymers, the sample was observed by AFM-IR in the range of 1000–1500 cm^{-1} (Figure 6.8, image b). The spectrum of Figure 6.8b displays a peak at 1370 cm^{-1} which corresponds to the C–C stretching band of PEDOT as observed in ATR-FTIR spectra at 1361 cm^{-1} (Figure 6.5, spectrum b). This definitely demonstrates that the nanoparticles observed (Figure 6.8, image a, Figure 6.6 and Figure 6.7) contain close-packed $PEDOT_{red}$ polymer chains.

Since the AFM-IR technique also enables the chemical mapping of the sample, this wavenumber 1370 cm^{-1} was chosen for AFM-IR chemical mapping of our sample. The chemical map was scanned and the absorption strength was recorded. (Figure 6.8, image c).

In image c, the red areas indicate a stronger absorption at the characteristic wavenumber which is caused by a thick layer of $PEDOT_{red}$ (~300 nm) linked onto the prism.

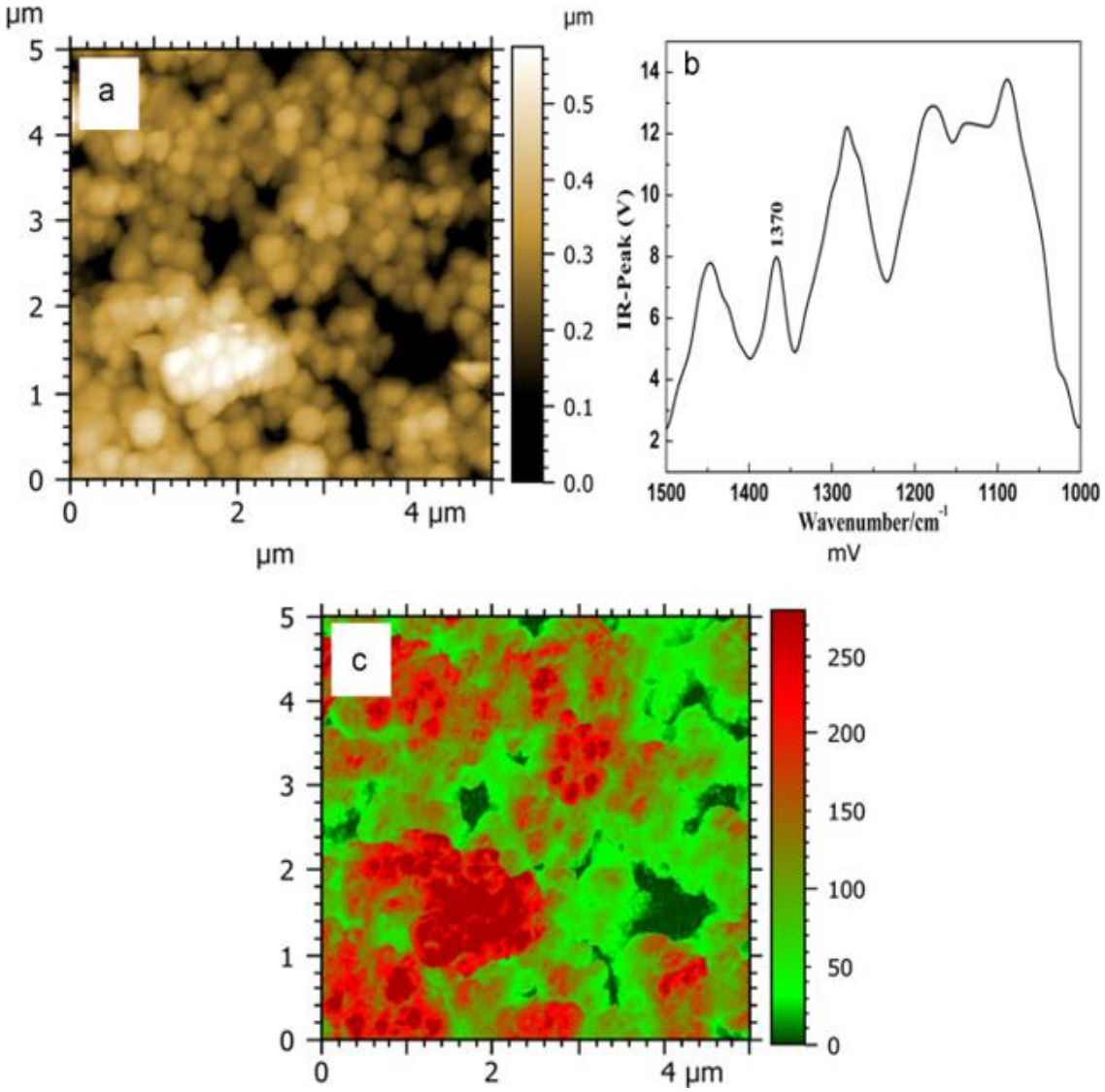

Figure 6.8 AFM-IR characterization of PEDOT polymers synthesized according to reduction–polymerization (a) AFM topographic image of $PEDOT_{red}$ polymers in contact mode, (b) AFM-IR spectrum of $PEDOT_{red}$ polymers and (c) AFM-IR chemical mapping of $PEDOT_{red}$ polymers with the IR source tuned to the C–C band at 1370 cm^{-1}. Samples containing 10 mM in EDOT were irradiated at 72 kGy under N_2 in the presence of isopropanol, then deposited onto ZnSe prism after lyophilization.[23]

When comparing the topography (Figure 6.8, image a) and the chemical mapping (Figure 6.8, image c), one can observe that the stronger absorbing areas fit very well with the thicker regions, which implies that the spherical nanoparticles are mainly composed by PEDOT polymer chains.[30] Therefore, we conclude, without any ambiguity that radiation chemistry in

reducing conditions (in the presence of hydrated electrons) leads to the reduction of EDOT monomers and to the growth of PEDOT polymers which self-assemble into spherical nanoparticles (of few hundred nanometers in diameter), those we observed in this work by Cryo-TEM, SEM and AFM (Figure 6.6, Figure 6.7 and Figure 6.8 respectively).

6.6 Physicochemical properties of $PEDOT_{red}$, a comparison with those of $PEDOT_{ox}$

In order to check and to compare the thermal stability of $PEDOT_{red}$ and $PEDOT_{ox}$ previously synthesized (under reducing conditions and oxidative conditions, respectively) and obtained as powders after lyophilization, the thermogravimetric analysis (TGA) plots of both polymers are recorded and displayed (Figure 6.9).[23] The degradation curves (green lines), which indicate the remaining weight of PEDOT powders as a function of temperature, are represented together with the weight derivative curves (red lines).

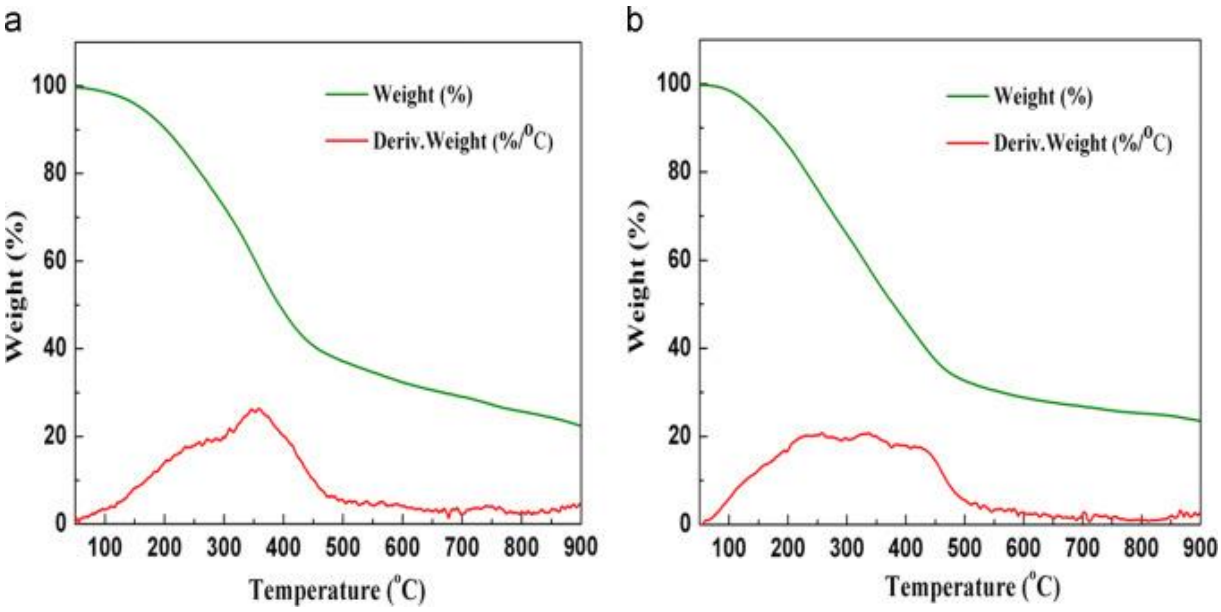

Figure 6.9 Thermogravimetric analysis (TGA) plots and weight derivative curves of (a) $PEDOT_{red}$ polymers synthesized under N_2 in the presence of isopropanol with a 72 kGy-irradiation, (b) $PEDOT_{ox}$ polymers synthesized under N_2O with a 72 kGy-irradiation.[23]

In the case of $PEDOT_{red}$ (Figure 6.9a), it can be found that a slow weight loss takes place before 150 ℃ due to the evaporation of water and the degradation of PEDOT oligomers.[31] Then, a continuous decomposition occurs between 250 and 450 ℃ due to PEDOT fragmentation and carbon oxidation. This decomposition results in about a 70% weight lost.

The quick degradation observed with temperature may be caused by the relatively small PEDOT particles size. Indeed, smaller particles are characterized by higher surface area for heat transfer.[32] After 450 °C, weight loss of residuals is negligible. For comparison purpose, the TGA curve of $PEDOT_{ox}$ was also recorded (Figure 6.9b) and the degradation processes are quite similar for both PEDOT synthesized by reduction–polymerization and oxidation–polymerization. The present results, which are in good agreement with earlier reports on PEDOT polymers, indicate that $PEDOT_{red}$ is characterized by a good thermal stability, at least comparable to that of PEDOT polymers usually synthesized by oxidative routes.[33]

At the end, in order to check and to compare the electrical conductivity of $PEDOT_{red}$ and $PEDOT_{ox}$ (synthesized under reducing conditions and oxidative conditions, respectively), they were characterized by four point probe technique. In this aim, both samples were doped with $NOBF_4$ (10 mM). The average electrical conductivity of $PEDOT_{red}$ was found to be 3.4×10^{-3} S cm^{-1}. This value is close to PEDOT conductivity values already reported in literature.[31,34] Thus, the synthesis of conducting materials thanks to this original radiation-induced reduction–polymerization route is successful. Nevertheless, it is found that $PEDOT_{red}$ conductivity, which has not been optimized yet, remains somewhat lower than that of $PEDOT_{ox}$ polymers, which amounts to 9.8×10^{-3} S cm^{-1}.

6.7 Conclusions

Current research aims to develop new synthesis strategies and new conducting polymers with tuned morphologies and properties. For the first time in literature, the development of a new radiolysis-based alternative methodology for synthesizing conducting polymers in aqueous solution was attempted. High energy γ-rays as well as high energy electrons irradiator were successfully used to generate oxidizing species, namely hydroxyl radicals, through water radiolysis, inducing first oxidation of monomers and then polymers growth.[19,20,24] This radiation-induced oxidation-polymerization route, which has been shown to proceed through a step-by-step oxidation process, enabled the preparation of nanostructured PEDOT (chapter 3 and chapter 5) conducting polymers as well as polypyrrole (PPy) (chapter 4).[23]

In this chapter, radiolysis was used, in a different way, to generate reducing species (instead of oxidizing radicals), namely hydrated electrons, in order to reduce monomers and to induce polymers growth. Starting from EDOT monomers dissolved in water, for the first time this

simple γ-rays-based reduction–polymerization route was described for synthesizing PEDOT conducting polymers in aqueous solution ($PEDOT_{red}$).

$PEDOT_{red}$ polymers synthesized by radiation-induced reduction polymerization are characterized by a very good long-term stability at air in a humid environment. We showed that the as-prepared $PEDOT_{red}$ polymers remain well dispersed in water, can be easily dried and are quite simply redispersed in protic solvents. The chemical nature of $PEDOT_{red}$ polymers was confirmed by ATR-FTIR spectroscopy while their morphology was checked in solution by Cryo-TEM microscopy and after lyophilization and deposition by SEM microscopy and AFM-IR nanospectroscopy. $PEDOT_{red}$ polymers were found to form polydisperse spherical nanoparticles whose morphology was kept after deposition onto solid substrates. Finally, the electrical conductivity of $PEDOT_{red}$ was evaluated at 3.4×10^{-3} S cm^{-1}.

This conductivity is comparable to conductivities already reported in literature concerning PEDOT polymers synthesized by conventional oxidative methodologies, but remains somewhat lower than that of $PEDOT_{ox}$ polymers we previously synthesized by oxidation–polymerization.

In this part, the radiolytic procedure is extended to the synthesis of CPs by the way of a reduction route instead of an oxidation procedure. This novel route, not really used in literature, should lead to the preparation of different kinds of CPs in water. In the next chapter, this original reduction route will be used for the synthesis of CP nanocomposites composed by PEDOT and silver (Ag) nanoparticles.

References

[1] Heeger, A. J., Semiconducting and metallic polymers: the fourth generation of polymeric materials (nobel lecture). *Angew. Chem. Int. Ed.* **2001**, *40*, 2591-2611.

[2] Roncali, J.; Blanchard, P.; Frère, P., 3,4-Ethylenedioxythiophene (EDOT) as a versatile building block for advanced functional π-conjugated systems. *J. Mater. Chem.* **2005**, *15* (16), 1589-1610.

[3] Wang, Y., Research progress on a novel conductive polymer–poly(3,4-ethylenedioxythiophene) (PEDOT). *JPCS* **2009**, *152*, 012023.

[4] Kirchmeyer, S.; Reuter, K., Scientific importance, properties and growing applications of poly(3,4-ethylenedioxythiophene). *J. Mater. Chem.* **2005**, *15* (21), 2077-2088.

[5] Cho, B.; Park, K. S.; Baek, J.; Oh, H. S.; Koo Lee, Y. E.; Sung, M. M., Single-crystal poly(3,4-ethylenedioxythiophene) nanowires with ultrahigh conductivity. *Nano Lett.* **2014**, *14* (6), 3321-3327.

[6] Jang, J.; Chang, M.; Yoon, H., Chemical sensors based on highlyconductive poly(3,4-ethylene-dioxythiophene) nanorods. *Adv. Mater.* **2005**, *17*, 1616-1620.

[7] Heuer, H. W.; Wehrmann, R.; Kirchmeyer, S., Electrochromic window based on conducting poly(3,4-ethylenedioxythiophene)-poly(styrene sulfonate). *Adv. Funct. Mater.* **2002**, *12* (2), 89-94.

[8] Jiang, C. Q.; Chen, G. M.; Wang, X., High-conversion synthesis of poly(3,4-ethylenedioxythiophene) by chemical oxidative polymerization. *Synt. Met.* **2012**, *162* (21-22), 1968-1971.

[9] Atanasov, S. E.; Losego, M. D.; Gong, B.; Sachet, E.; Maria, J. P.; Williams, P. S.; Parsons, G. N., Highly conductive and conformal poly(3,4-ethylenedioxythiophene) (PEDOT) thin films via oxidative molecular layer deposition. *Chem. Mater.* **2014**, *26* (11), 3471-3478.

[10] Li, C.; Bai, H.; Shi, G., Conducting polymer nanomaterials: electrosynthesis and applications. *Chem. Soc. Rev.* **2009**, *38* (8), 2397-2409.

[11] Kvarnström, C.; Neugebauer, H.; Blomquist, S.; H.J. Ahonenc; J. Kankarec; Ivaska, A., In situ spectroelectrochemical characterization of poly(3,4-ethylenedioxythiophene). *Electrochim. Acta* **1999**, *44*, 273-2750.

[12] Lawal, A. T.; Wallace, G. G., Vapour phase polymerisation of conducting and non-conducting polymers: a review. *Talanta* **2014**, *119*, 133-143.

[13] Dams, R.; Vangeneugden, D.; Vanderzande, D., Plasma Deposition of Thiophene Derivatives Under Atmospheric Pressure. *Chem Vapor Depos* **2006**, *12* (12), 719-727.

[14] Rumbau, V.; Pomposo, J. A.; Eleta, A.; Rodriguez, J.; Grande, H.; Mecerreyes, D.; Ochoteco, E., First enzymatic synthesis of water-soluble conducting poly(3,4-ethylenedioxythiophene). *Biomacromolecules* **2007**, *2*, 315-317.

[15] Karim, M. R.; Lee, C. J.; Kim, H. J.; Bhuiyan, M. T. I.; Lee, M. S., Preparation of Buckyball-Shaped Conducting Polythiophene by the Gamma Radiation-Induced Polymerization Method. *Macromol Symp* **2007**, *249-250* (1), 234-240.

[16] Karim, M. R.; Lee, C. J.; Lee, M. S., Synthesis of conducting polypyrrole by radiolysis polymerization method. *Polym Advan Technol* **2007**, *18* (11), 916-920.

[17] Pillalamarri, S. K.; Blum, F. D.; Tokuhiro, A. T.; Story, J. G.; Bertino, M. F., Radiolytic Synthesis of Polyaniline Nanofibers: A New Templateless Pathway. *Chemistry of Materials* **2005**, *17* (2), 227-229.

[18] Kitada, K.; Ozaki, S., Reductive Polymerization of Halothiophene. *Polym Journal* **1995**, *27* (12), 1161-1166.

[19] Lattach, Y.; Deniset-Besseau, A.; Guigner, J. M.; Remita, S., Radiation chemistry as an alternative way for the synthesis of PEDOT conducting Polymers under "soft" Conditions. *Radiat. Phys. Chem.* **2013**, *82*, 44-53.

[20] Lattach, Y.; Coletta, C.; Ghosh, S.; Remita, S., Radiation-induced synthesis of nanostructured conjugated polymers in aqueous solution: fundamental effect of oxidizing species. *Chemphyschem : a European journal of chemical physics and physical chemistry* **2014**, *15* (1), 208-218.

[21] Hart, E. J., Research potentials of the hydrated electron. *Acc. Chem. Res.* **1969**, *2*, 161-167.

[22] Belloni, J.; Mostafavi, M.; Remita, H.; Marignier, J. L.; Delcourt, M. O., Radiation-induced synthesis of mono- and multi-metallic clusters and nanocolloids. *New J. Chem.*, **1998**, 1239-1255.

[23] Cui, Z. P.; Coletta, C.; Rebois, R.; Baiz, S.; Gervais, M.; Goubard, F.; Aubert, P. H.; Dazzi, A.; Remita, S., Radiation-induced reduction–polymerization route for the synthesis of PEDOT conducting polymers. *Radiat. Phys. Chem.* **2016**, *119*, 157-166.

[24] Coletta, C.; Cui, Z.; Archirel, P.; Pernot, P.; Marignier, J. L.; Remita, S., Electron-induced growth mechanism of conducting polymers: a coupled experimental and computational investigation. *J. Phys. Chem. B* **2015**, *119* (16), 5282-5298.

[25] Hulvat, J. F.; Stupp, S. I., Anisotropic properties of conducting polymers prepared by liquid crystal templating. *Adv. Mater.* **2004**, *16* (7), 589-592.

[26] Tran-Van, F.; Garreau, S.; Louarn, G.; Froyer, G.; Chevrot, C., Fully undoped and soluble oligo(3,4-ethylenedioxythiophene)s: spectroscopic study and electrochemical characterization. *J. Mater. Chem.* **2001**, *11* (5), 1378-1382.

[27] Zhao, Q.; Jamal, R.; Zhang, L.; Wang, M. C.; Abdiryim, T., The structure and properties of PEDOT synthesized by template-free solution method. *Nanoscale Res. Lett.* **2014**, *9:557*.

[28] Hohnholz, D.; MacDiarmid, A. G.; Sarno, D. M.; Jones, J. W. E., Uniform thin films of poly-3,4-ethylenedioxythiophene (PEDOT) prepared by in-situ deposition. *Chem. Commun.* **2001**, 2444-2445.

[29] Han, M. G.; Foulger, S. H., Facile synthesis of poly(3,4-ethylenedioxythiophene) nanofibers from an aqueous surfactant solution. *Small* **2006**, *2* (10), 1164-1169.

[30] Ghosh, S.; Remita, H.; Ramos, L.; Dazzi, A.; Deniset-Besseau, A.; Beaunier, P.; Goubard, F.; Aubert, P. H.; Brisset, F.; Remita, S., PEDOT nanostructures synthesized in hexagonal mesophases. *NewJ.Chem.* **2014**, *38* (3), 1106-1115.

[31] Nagarajan, R.; Kumar, J.; Bruno, F. F.; Samuelson, L. A.; Nagarajan, R., Biocatalytically synthesized poly(3,4-ethylenedioxythiophene). *Macromolecules* **2008**, *41*, 3049-3052.

[32] Paradee, N.; Sirivat, A., Synthesis of poly(3,4-ethylenedioxythiophene) nanoparticles via chemical oxidation polymerization. *Polym. Int.* **2014**, *63* (1), 106-113.

[33] Feng, Z. Q.; Wu, J.; Cho, W.; Leach, M. K.; Franz, E. W.; Naim, Y. I.; Gu, Z. Z.; Corey, J. M.; Martin, D. C., Highly aligned poly(3,4-ethylene dioxythiophene) (pedot) nano- and microscale fibers and tubes. *Polymer* **2013**, *54* (2), 702-708.

[34] Jones, B. H.; Cheng, K. Y.; Holmes, R. J.; Lodge, T. P., Nanoporous poly(3,4-ethylenedioxythiophene) derived from polymeric bicontinuous microemulsion templates. *Macromolecules* **2012**, *45* (1), 599-601.

Chapter 7: Extension of the radiolytic procedure to the synthesis of PEDOT/Ag nanocomposites

The combination of conducting polymers (CPs) with inorganic nanoparticles produces composites of CPs which can not only maintain the properties of CPs and inorganic nanoparticles but also endow the CPs composites new properties.[1-3] Among various CPs composites, nanocomposites composed by CPs and noble metal nanoparticles have been of great research interest.[4,5] CPs such as poly(3,4-ethylenedioxythiophene) (PEDOT), polypyrrole (PPy) and polyaniline (PANI), are organic polymers which exhibit inherent electrical conductivity due to the unique π-conjugated system in their structures, while noble metal (Au, Ag) nanoparticles constitute inorganic components which have already been widely studied and applied in a variety of fields.[3,5-7]

Generally, synthesis of CPs nanocomposites can be achieved by traditional chemical and electrochemical routes.[2,5,8] According to the synthetic methodologies, two-step method or one-pot method are usually applied to synthesize CPs nanocomposites.[9,10] These latter usually show core-shell structure, the composition of which fundamentally depends on the preparation procedure.[11-13] In literature, PEDOT/Ag nanocomposites have already been successfully synthesized by the means of either chemical or electrochemical methods and have also been shown to possess various potential applications.[11,14-18]

In previous works, radiation-induced synthesis of shape controlled silver nanoparticles in aqueous solution has been successfully conducted in our lab, on the one hand, and the radiolytic preparation of nanostructured conducting PEDOT polymers has been realized as previously highlighted in this manuscript on the other hand.[19-23] This evidently represents good omens for the successful synthesis of PEDOT/Ag composites by radiolysis. Starting from an aqueous solution containing metal ions and organic monomers, this work intends to originally use radiation chemistry for the *in situ* production of hydrated electrons and hydroxyl radicals as reducing and oxidizing species respectively, in order to synthesize CPs/metal nanocomposites.

In this work, starting from EDOT monomers and Ag^+ silver ions dissolved in water, simple γ-rays-based radiolytic methodology which enables the synthesis of CPs/metal nanocomposites is described in details. In fact, PEDOT/Ag nanocomposites are prepared by both two-step and one-

pot methods. According to the two-step method, PEDOT polymers are first synthesized by either oxidation or reduction of EDOT monomers and then, PEDOT/Ag nanocomposites are prepared by the further reduction of silver ions into metal nanoparticles. Differently, according to the one-pot method, polymerization and metal ions reduction are achieved in parallel, in one step. Pulsed radiolysis experiments are additionally performed in order to find the rate constants and also to understand the mechanism involved in such a one-pot procedure.

7.1 Nanocomposites synthesis strategy and characterization

7.1.1 Solution preparation

3,4-ethylenedioxythiophene (EDOT) is used as organic monomer for PEDOT production. Silver perchlorate salt ($AgClO_4$) is used as Ag^+ source for silver nanoparticles synthesis. Note that, ClO_4^- anion is unreactive under radiolysis. Isopropanol and *tert*-butanol are added to the solutions as hydroxyl radicals scavengers. N_2O and N_2 are used to degas the aqueous solutions before γ-irradiation.

Aqueous solutions containing EDOT (10 mM) and different concentrations in Ag^+ ions (ranging from 0 to 20 mM) are prepared at room temperature, in the dark, to prevent any photochemical reaction. In all cases, the pH of the solutions is found to be close to 7. EDOT concentration is always checked by UV-vis absorption spectroscopy.[21] Also, concentrations used in this work remain lower than EDOT and $AgClO_4$ solubilities in water.[24,25] Note that such relatively low concentrations avoid direct ionization of EDOT molecules and Ag^+ ions by γ rays.

After degassing, all solutions are irradiated with a ^{60}Co γ at a dose rate of 5 kGy h^{-1}, up to doses enabling the total consumption of EDOT molecules and Ag^+ ions.

Starting from 10 mM in EDOT and 10 mM in silver ions, if considering that, at high doses, EDOT polymerization into PEDOT, on one hand, and Ag^+ reduction into metal nanoparticles, on the other hand, are quantitative, then the weight ratio W_{PEDOT}/W_{Ag} should amount, after radiolysis, to 1.3/1 whatever the preparation procedures.

7.1.2 Synthetic methodologies of PEDOT/Ag composites

γ-radiolysis of aqueous solution at neutral pH under N_2 atmosphere produces two main species, hydroxyl radicals (HO•) and hydrated electrons (e_{aq}^-), which are respectively strong oxidant and reducing species.[26-29]

In the presence of an alcohol, such as isopropanol, $(CH_3)_2CHOH$, (at a relatively high concentration, 0.2 M), HO• and H• radicals are quantitatively scavenged, producing a reducing $(CH_3)_2C•OH$ secondary radical (reactions 2.23 and 2.24, chapter 2).[30-32] As a consequence, when irradiating N_2-saturated aqueous solutions in the presence of isopropanol, two short-lived reactive transient species are formed, namely e_{aq}^- and $(CH_3)_2C•OH$ radicals, the radiolytic yields (G-values) of which amount to 2.8×10^{-7} mol J^{-1} and 3.4×10^{-7} mol J^{-1} (equations 2.25 and 2.26, chapter 2).[33] Note that isopropanol radical is a reducing species with a redox potential of - 1.8 V_{SHE} at pH = 7 (section 2.3.4, chapter 2).

When diluted aqueous solutions, containing Ag^+ ions, are irradiated by γ-rays, both $(CH_3)_2C•OH$ and e_{aq}^- quantitatively act as reducing species towards silver ions, leading to silver atoms which aggregate into silver nanoparticles.[34] As a consequence, under N_2 atmosphere, in the presence of isopropanol, the radiolytic yield, G-value, of reduction of silver ions is:[35]

$$G_{red}(Ag^+) = 6.2\times10^{-7} \text{ mol } J^{-1} \quad (7.1)$$

Differently, when diluted EDOT aqueous solutions are irradiated by γ-rays, $(CH_3)_2C•OH$ radicals don't reduce EDOT monomers as demonstrated (section 6.2, chapter 6).[23] Only e_{aq}^-, as reducing species, react onto EDOT molecules, leading to PEDOT polymers. As a consequence, under N_2 atmosphere, in the presence of isopropanol, the G-value of EDOT reduction is:[23]

$$G_{red}(EDOT) = 2.8\times10^{-7} \text{ mol } J^{-1} \quad (7.2)$$

While silver nanoparticles can only be obtained by reduction of silver ions, PEDOT polymers can be synthesized either by reduction or by oxidation of EDOT molecules as demonstrated in chapter 6.[22,23] In order to specifically oxidize EDOT, hydrated electrons must be scavenged. This is possible under nitrous oxide (N_2O) atmosphere as described (section 2.3.3, chapter 2),

evidently in the absence of isopropanol. In these conditions, only one transient species is quantitatively formed, namely HO• radicals, with a radiolytic yield of 5.6×10^{-7} mol J^{-1} (equation 2.15, chapter 2).[26]

When diluted aqueous solutions, containing EDOT monomers, are irradiated by γ-rays under N_2O, HO• radicals quantitatively act as oxidizing species, leading to PEDOT polymers. As a consequence, under N_2O atmosphere, in the absence of isopropanol, the G-value of EDOT oxidation is:[22]

$$G_{ox}(EDOT) = 5.6\times10^{-7} \text{ mol } J^{-1} \quad (7.3)$$

Then, under nitrogen in the presence of isopropanol, knowing the yield of reduction of silver ions ($G_{red}(Ag^+)$), 10 mM of Ag^+ are totally reduced and silver nanoparticles are quantitatively synthesized at doses higher than 16 kGy. Also, in the same experimental conditions, knowing the yield of EDOT reduction ($G_{red}(EDOT)$), 10 mM of EDOT are totally reduced above 36 kGy. Now, when irradiating N_2O-saturated aqueous solutions, due to the yield of EDOT oxidation ($G_{ox}(EDOT)$), 10 mM of EDOT are totally oxidized at about 18 kGy.

Two-step method

In this method, the first step corresponds to the synthesis of PEDOT, while the second step is related to the reduction of silver ions into inorganic nanoparticles. Two different procedures (procedures ① and ②) are used (Figure 7.1):[36]

- Procedure ① (Figure 7.1). In the first step, aqueous solution of EDOT monomers (10 mM) is prepared and degassed with N_2O for 20 min (sample a), then irradiated by γ-rays at 36 kGy in order to quantitatively oxidize EDOT monomers and to synthesize PEDOT polymers (sample b). In the second step, the solution is added with $AgClO_4$ (10 mM) and isopropanol (0.2 M), degassed with N_2 for 20 min and then irradiated at 36 kGy in order to quantitatively reduce silver ions (sample c).
- Procedure ② (Figure 7.1). In the first step, aqueous solution of EDOT monomers (10 mM) added with isopropanol (0.2 M) is first degassed with N_2 for 20 min (sample a) and irradiated at

36 kGy in order to quantitatively reduce EDOT monomers and synthesize PEDOT polymers (sample e).

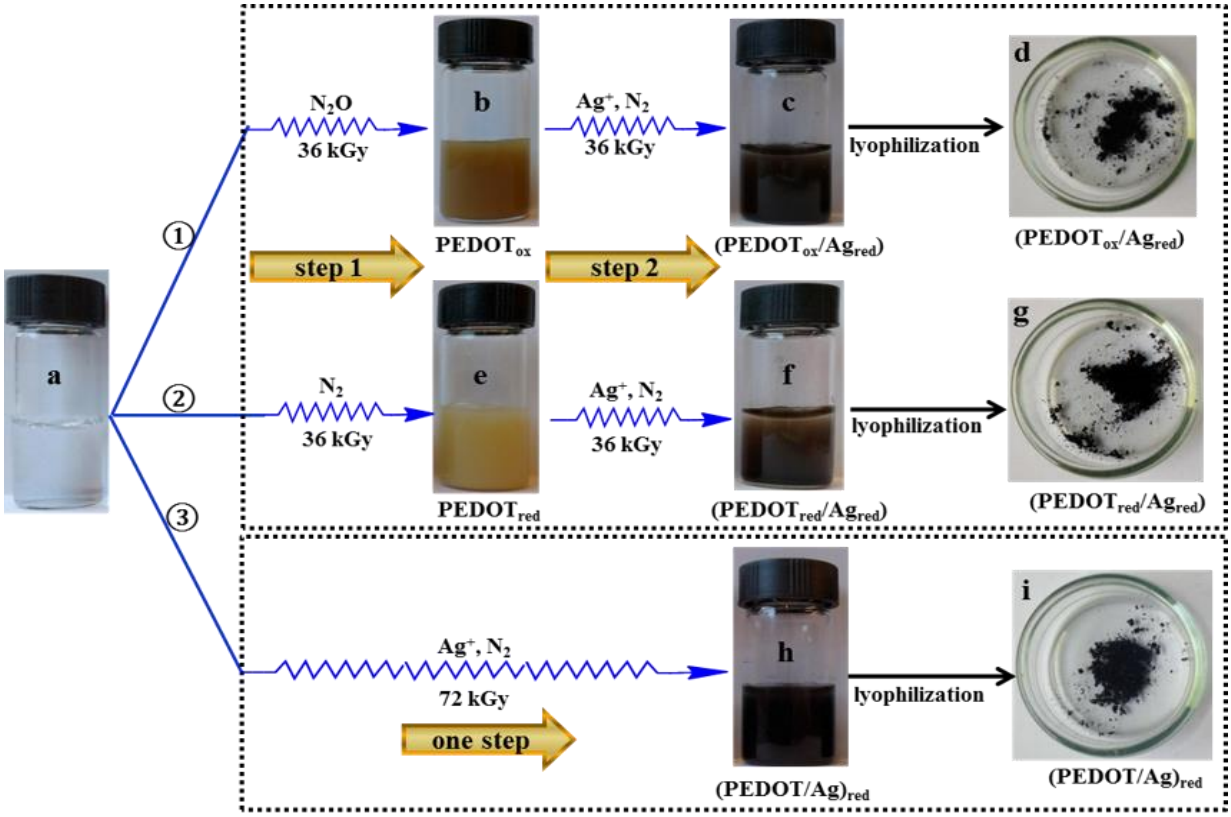

Figure 7.1 Radiation-induced synthesis of PEDOT/Ag nanocomposites, starting from an aqueous solution of EDOT (10 mM), sample a. Different ways were used. In procedure ①, which is a two-step method, EDOT solution is first irradiated at 36 kGy, under N_2O (sample b), in order to quantitatively oxidize EDOT monomers into PEDOT ($PEDOT_{ox}$). In the second step, the solution was added with Ag^+ (10 mM) and isopropanol (0.2 M), then irradiated at 36 kGy under N_2 (sample c), in order to quantitatively reduce silver ions. Lyophilization leads to the nanocomposites called ($PEDOT_{ox}/Ag_{red}$) (sample d). In procedure ②, which is also a two-step method, EDOT solution is first irradiated at 36 kGy, under N_2 (sample e), in order to quantitatively reduce EDOT monomers into PEDOT ($PEDOT_{red}$). In the second step, the solution was added with Ag^+ (10 mM) and isopropanol (0.2 M), then irradiated at 36 kGy under N_2 (sample f), in order to quantitatively reduce silver ions. Lyophilization leads to the nanocomposites called ($PEDOT_{red}/Ag_{red}$) (sample g). In procedure ③, which is a one-pot method, EDOT solution is added with Ag^+ (10 mM) and isopropanol (0.2 M), then irradiated at 72 kGy under N_2 (sample h), in order to quantitatively reduce, at the same time, EDOT monomers and Ag^+ ions. Lyophilization leads to the nanocomposites called $(PEDOT/Ag)_{red}$ (sample i).[36]

In the second step, the solution is added with $AgClO_4$ (10 mM) and isopropanol (0.2 M), degassed again with N_2 for 20 min and finally irradiated at 36 kGy in order to quantitatively reduce silver ions (sample f).

One-pot method

In this method, reduction of EDOT (production of PEDOT) and reduction of silver ions (production of silver nanoparticles) are considered concurrently, at the same time (procedure ③, Figure 7.1): aqueous solutions containing 10 mM in EDOT, 10 mM in $AgClO_4$ (EDOT/Ag ratio = 10:10) and 0.2 M in isopropanol are prepared, degassed with N_2 for 20 min and irradiated at 72 kGy (sample h). This dose is enough to ensure the total reduction of both EDOT molecules and Ag^+ ions.

According to this one-pot method, for the ratio 10:10, the irradiation dose is varied from 0 to 72 kGy. Also, the EDOT/Ag ratio is changed, from 10:1 to 10:20, by varying the amount of $AgClO_4$. Whatever the ratio of EDOT to Ag, the aqueous solutions are always added with isopropanol (0.2 M), degassed with N_2 for 20 min and irradiated at 72 kGy, which enables in all cases the total reduction of both EDOT and Ag^+.

7.1.3 Characterizations of PEDOT/Ag nanocomposites

Radiosynthesized PEDOT/Ag nanocomposites were characterized by different experimental techniques: UV-Vis absorption spectrophotometry, EDX spectroscopy and Cryo-TEM microscopy in solution, ATR-FTIR spectroscopy and SEM microscopy after deposition. The thermal stability and composition analysis of lyophilized PEDOT polymers (prepared in the absence of silver) and of PEDOT/Ag nanocomposites were performed by thermogravimetric analysis (TGA). The electrical conductivity of PEDOT/Ag nanocomposites were measured by four-point probe technique**.**

7.2 Synthesis of PEDOT/Ag nanocomposites by two-step method

In this method, the first step corresponds to the synthesis, in aqueous solution, of PEDOT polymers by either oxidation (procedure ①) or reduction (procedure ②) of EDOT monomers. An

aqueous solution containing 10 mM in EDOT is first prepared. This aqueous solution is found transparent (Figure 7.1, sample a). In this solution, EDOT monomers display two absorption maxima at 235 and 255 nm (Figure 7.2, spectrum a) in agreement with results obtained before (section 6.2.1, chapter 6).[21,22,36]

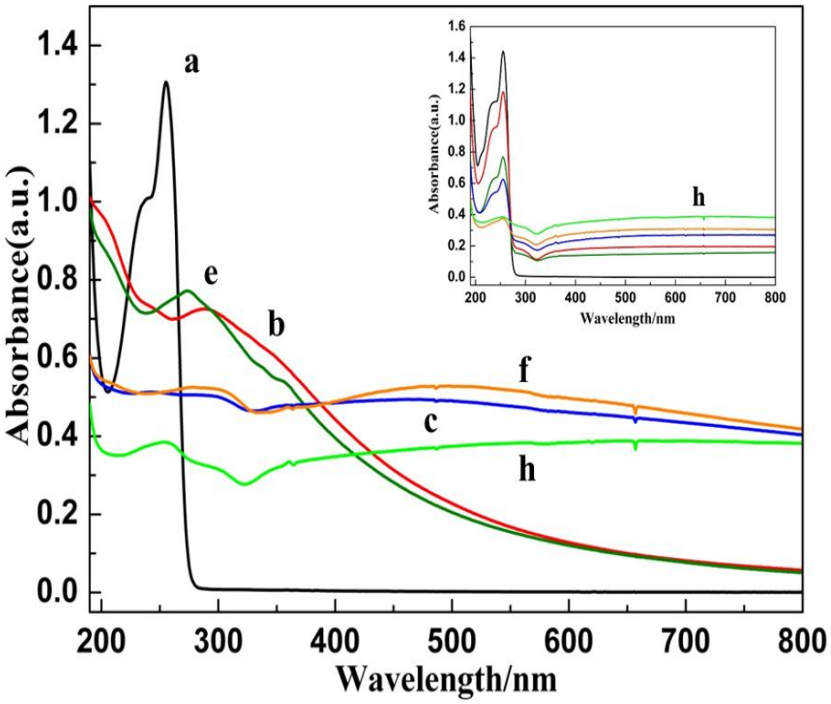

Figure 7.2 UV-visible absorption spectra of sample a (containing 10 mM in EDOT before irradiation), sample b and sample c (containing respectively $PEDOT_{ox}$ and ($PEDOT_{ox}/Ag_{red}$), both synthesized according to procedure ①), sample e and sample f (containing respectively $PEDOT_{red}$ and ($PEDOT_{red}/Ag_{red}$), both synthesized according to procedure ②) and sample h (containing $(PEDOT/Ag)_{red}$ prepared according to procedure ③. Inset: evolution of the UV-vis absorption spectrum of sample h with the irradiation dose according to the one-pot method (the dose was 0, 10, 20, 30, 50 and 70 kGy). All solutions were diluted 10 times. Optical path was 0.2 cm and water was used as reference.[36]

According to procedure ① (Figure 7.1), in the first step, the transparent aqueous solution of EDOT monomers (10 mM) is degassed with N_2O, then irradiated at 36 kGy. In these conditions, hydroxyl radicals generated by radiolysis should quantitatively oxidize EDOT monomers. After irradiation, a yellow-brown suspension is observed (Figure 7.1, sample b). Its absorption spectrum (Figure 7.2, spectrum b) displays an absorption band at 290, a shoulder at 350 nm and a

long absorption tail in the range of 400-800 nm, which are attributed to PEDOT oligomers and polymers.[21-23] One can note, in this spectrum, the absence of absorption bands at 235 and 255 nm. This definitely proves that, after a 36 kGy-irradiation, EDOT monomers have completely disappeared, as expected. Indeed, they are quantitatively converted by oxidation into PEDOT polymers, called $PEDOT_{ox}$.

In the second step of procedure ① (Figure 7.1), the irradiated solution is added with $AgClO_4$ (10 mM) and isopropanol (0.2 M), degassed with N_2, then irradiated again at 36 kGy. In these conditions, e_{aq}^- and $(CH_3)_2C•OH$ radicals generated by radiolysis should quantitatively reduce Ag^+ ions. After the second irradiation, a black suspension, which slowly precipitates, is clearly observed (Figure 7.1, sample c). Its absorption spectrum (Figure 7.2, spectrum c) displays the well-known plasmon absorption band of silver nanoparticles at around 450 nm.[33] The asymmetric shape of the surface plasmon resonance (SPR) band could be due to the aggregation of silver nanoparticles or to their interaction (adsorption) with organic molecules.[19,37-39] Note that the two shoulders at 290 and 350 nm, attributable to PEDOT, are still present in the absorption spectrum. This demonstrates that, according to procedure ①, both PEDOT (obtained by oxidation) and silver nanoparticles (obtained by reduction) are present in the aqueous medium. The corresponding composites will be called ($PEDOT_{ox}/Ag_{red}$).

In a different way, according to procedure ② (Figure 7.1), the aqueous solution containing 10 mM in EDOT is degassed with N_2, then irradiated at 36 kGy. In these conditions, hydrated electrons generated by radiolysis should quantitatively reduce EDOT monomers. After irradiation, as in the case of procedure ①, a yellow suspension is observed (Figure 7.1, sample e). Its UV-Visible absorption spectrum (Figure 7.2, spectrum e) does not display bands at 235 and 255 nm, but highlights absorption bands in the UV and a long absorption tail in the range of 400-800 nm, which are attributed in a previous work to PEDOT oligomers and polymers.[23] Once again, it can be concluded that, after a 36 kGy-irradiation, but this time under N_2, EDOT monomers are quantitatively converted by reduction into PEDOT oligomers and polymers, called $PEDOT_{red}$.

In the second step of procedure ② (Figure 7.1), which is similar to the second step of procedure ①, the irradiated solution is added with $AgClO_4$ and isopropanol, then irradiated again at 36 kGy under N_2 atmosphere. At the end of the procedure, a black suspension, which sediments, is clearly observed (Figure 7.1, sample f). Its absorption spectrum (Figure 7.2, spectrum f), which, once again, displays the plasmon absorption band of silver nanoparticles at around 500 nm, is

very similar to that obtained at the end of procedure ① (Figure 7.2, spectrum c). This demonstrates that, according to procedure ②, both PEDOT (obtained by reduction) and silver nanoparticles (also obtained by reduction) are present in the aqueous medium. The corresponding composites will be called ($PEDOT_{red}/Ag_{red}$).

Irradiated solutions, corresponding to the black suspensions of sample c and sample f, are dried by lyophilization in order to quantitatively eliminate water and isopropanol from the two dark powders obtained (Figure 7.1, sample d and sample g respectively). Naturally, due to the previous spectrophotometric results, these powders are expected to contain an organic component, PEDOT, in addition to an inorganic phase, Ag. In addition, perchlorate anions, ClO_4^-, should also remain present in the sample after lyophilization. PEDOT/Ag composite, contained in sample d, which is obtained at the end of procedure ① and which implies first the oxidation-polymerization of EDOT and second the reduction of silver ions, is called ($PEDOT_{ox}/Ag_{red}$). The second composite, contained in sample g, which is obtained at the end of procedure ② and which implies first the reduction-polymerization of EDOT and second the reduction of silver ions, is differently called ($PEDOT_{red}/Ag_{red}$).

Both lyophilized samples (sample d and sample g) are characterized by ATR-FTIR spectroscopy in order to investigate the chemical nature of the solid phases and to confirm the presence of PEDOT polymers in the powders. The ATR-FTIR spectra of both powders, ($PEDOT_{ox}/Ag_{red}$) and ($PEDOT_{red}/Ag_{red}$) are presented in the wave number region 4000-600 cm^{-1}, together with the spectra of pure non irradiated EDOT and of pure $AgClO_4$ salt (Figure 7.3).[36]
In ATR-FTIR spectrum of EDOT, the characteristic peak at 755 cm^{-1} corresponds to the C-H out-of-plane bending vibration in the thiophen ring.[21] The stretching vibrations of C-C and C=C in thiophene ring are also seen at 1365 and 1481 cm^{-1}.[40] ATR-FTIR spectra of ($PEDOT_{ox}/Ag_{red}$) (Figure 7.3, spectrum d) and ($PEDOT_{red}/Ag_{red}$) (Figure 7.3, spectrum g) are in good agreement with PEDOT spectra found in literature.[41] Indeed, all the characteristic bands of PEDOT are present, even if they appear slightly displaced. The bands at 1062 cm^{-1} (spectrum d) and 1087 cm^{-1} (spectrum g) are attributed to the ethylenedioxy group.[21,23] The peaks at 1430 and 1361 cm^{-1} originating from C-C and C=C stretching vibrations are also observed in both cases.[41] Nevertheless, one can note the absence, in spectrum d and spectrum g, of the C-H vibration peak at 755 cm^{-1}, which definitely proves that quantitative polymerization of EDOT, through α, α'-

coupling reaction, took place in both cases (procedures ① and ②), leading to organic/inorganic composites made of PEDOT.

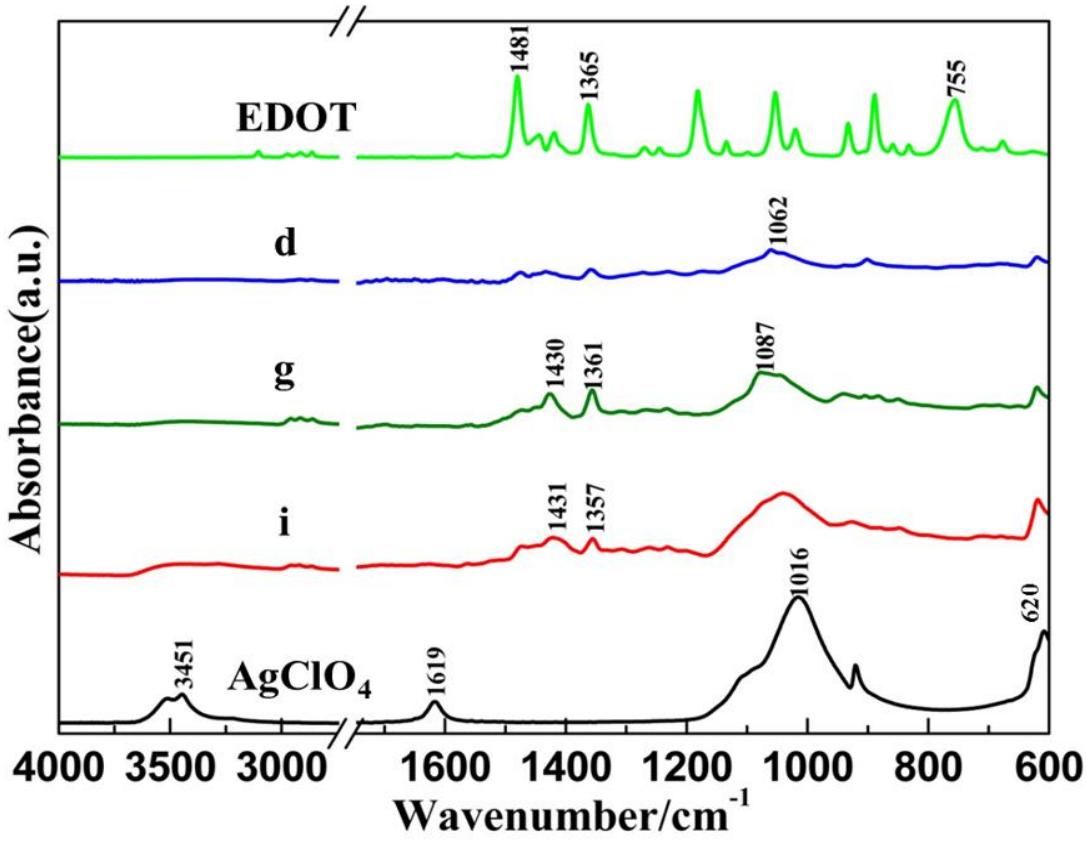

Figure 7.3 ATR-FTIR spectra of pure EDOT and pure $AgClO_4$ salt together with spectra of sample d containing ($PEDOT_{ox}/Ag_{red}$) composites prepared according to procedure ①, sample g containing ($PEDOT_{red}/Ag_{red}$) composites prepared according to procedure ② and sample i containing $(PEDOT/Ag)_{red}$ composites prepared according to procedure ③. Samples d, g and i were obtained after lyophilization of samples c, f and h respectively.[36]

In ATR-FTIR spectrum of $AgClO_4$ salt, the stretching vibrations of coordinated and free ClO_4^- anions are observed at 1016 and 620 cm^{-1}, while the peaks at 1619 and 3451 cm^{-1} are due to the bending and stretching vibrations of O-H groups, which is explained by the hygroscopic nature of $AgClO_4$ salt.[42-44] In ATR-FTIR spectra of ($PEDOT_{ox}/Ag_{red}$) (spectum d) and ($PEDOT_{red}/Ag_{red}$) (spectrum g), one can observe the presence of large intense bands around 1016 and 620 cm^{-1}, which let guess the presence of ClO_4^-, as doping anions, into ($PEDOT_{ox}/Ag_{red}$) and

($PEDOT_{red}/Ag_{red}$) dried composites. In fact, these anions come from silver perchlorate salt and are well-known to remain unreactive in the present radiolytic conditions.[33]

In order to investigate, in liquid phase before any deposition, the structure and morphology of ($PEDOT_{ox}/Ag_{red}$) and ($PEDOT_{red}/Ag_{red}$) composites, the black suspensions obtained at the end of procedures ① and ② (sample c and sample f respectively), are observed by cryo-transmission electron microscopy just after irradiation and before any sedimentation (Figure 7.4, image c and image f respectively).[36] The observations made on ($PEDOT_{ox}/Ag_{red}$) and ($PEDOT_{red}/Ag_{red}$) aqueous samples are totally similar, as can be seen when comparing images c and f. In both cases, representative images show the presence of low density globular structures forming polydisperse spherical nanoparticles with a diameter comprised between 100 and 500 nm. This result is in very good agreement with the observations already made in the case of PEDOT synthesized, alone (in the absence of silver) by radiolysis, either by EDOT oxidation or by EDOT reduction.[21-23] Thus, these low density globular objects are made of PEDOT polymers. Each globular structure should correspond to the self-assembly of independent amorphous PEDOT chains.

As can be seen in images c and f, smaller nanoparticles (from few nm to 50 nm), which appear very more contrasted (darker), are systematically found adsorbed onto the bigger globular PEDOT nanoparticles. The relatively high contrast of these small particles suggests their metal nature.[45] Since no other objects are observed during our Cryo-TEM experiments, we suppose that these small spherical nanoparticles are made up of silver.

During Cryo-TEM observations, *in situ* Energy-Dispersive X-ray (EDX) spectroscopy is used to check the chemical composition of our radiosynthesized materials in order to prove the presence of sulfur atoms (which are only present in PEDOT polymers, one sulfur atom per EDOT molecule) and of silver atoms (which would be the signature of silver nanoparticles). The aim is also to check the molar ratio between both atoms in radiosynthesized PEDOT/Ag composites. EDX spectra (Figure 7.4, spectrum c and spectrum f) which correspond respectively to the elemental analysis of the surrounded areas of image c and image f of Figure 7.4, highlight the presence, in both samples, of the following chemical elements: O (Kα 0.525 keV), C (Kα 0.277 keV), S (Kα 2.31 keV) and Ag (Lα 2.98 keV and L_β 3.15 keV). The presence of oxygen and carbon atoms in both samples may be related to the presence of PEDOT polymers. Nevertheless, their preponderance in EDX spectra is certainly due to the ice which surrounds all the observed nanomaterials and to the carbon-coated grid itself (which is used for Cryo-TEM observations).

Contrarily to oxygen and carbon atoms, the detection of sulfur and silver elements definitely demonstrates, as expected, the concomitant presence, in the analyzed areas of images c and f of Figure 7.4, of both PEDOT polymers and silver nanoparticles. A quantitative analysis enabled us to estimate S and Ag atomic percentages in the surrounded areas of Figure 7.4. It is found 39 % S and 61 % Ag in spectrum c and 67 % S and 33 % Ag in spectrum f. Even if these percentages are not far from those expected (50 % S and 50 % Ag) starting from 10 mM in EDOT and 10 mM in $AgClO_4$, they are found to be dependent on the analyzed area. In fact, sulfur and silver are systematically detected in all the nanoparticles observed by Cryo-TEM. But their atomic percentage is found to vary from 20 % to 80 %. Note that sulfur and silver atoms are only observed into the nanomaterials and are never found in the surrounding aqueous medium.

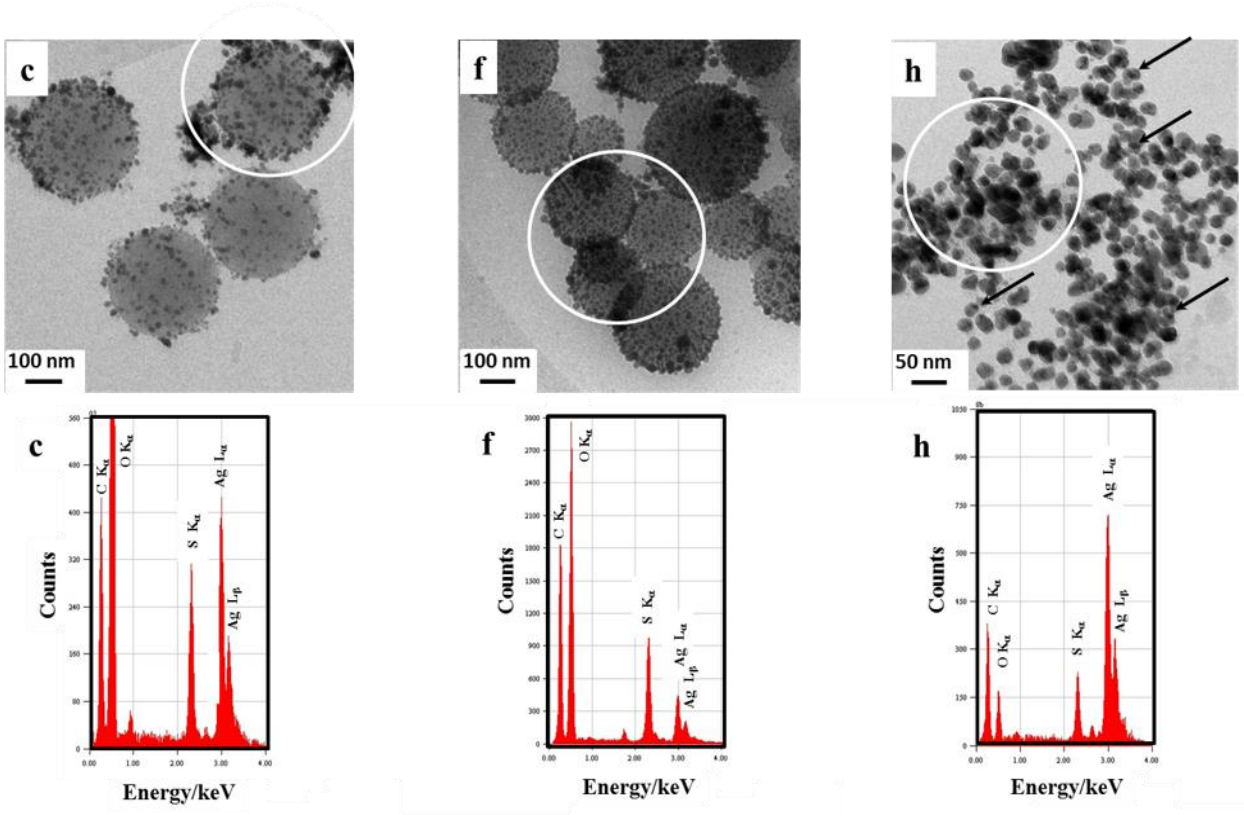

Figure 7.4 Cryo-TEM images of sample c containing ($PEDOT_{ox}/Ag_{red}$) synthesized according to procedure ①, sample f containing ($PEDOT_{red}/Ag_{red}$) synthesized according to procedure ② and sample h containing $(PEDOT/Ag)_{red}$ prepared according to one-pot procedure ③. Energy-Dispersive X-ray (EDX) spectra corresponding to the elemental analysis of the surrounded areas in Cryo-TEM images.[36]

As demonstrated by Cryo-TEM microscopy and EDX spectroscopy, composites prepared by two-step method are made of large spherical PEDOT nanoparticles at the surface of which smaller silver nanoparticles adsorb. The deposition and the aggregation of these silver nanoparticles onto PEDOT organic compounds should explain their characteristic asymmetric plasmon absorption bands which are found by UV-Vis absorption spectroscopy (Figure 7.2, spectra c and f).

Due to the two-step method used in procedures ① and ②, PEDOT polymers are first synthesized, in the absence of inorganic ions, and self-assemble thanks to Van der Waals interactions into globular organic nanoparticles. Silver nanoparticles are formed only during the second step. This explains their presence outside PEDOT nanoparticles. Nevertheless, in spite of all our Cryo-TEM investigations, metal nanoparticles are never found isolated in the aqueous phase. They are always found adsorbed onto PEDOT spherical nanostructures. Maybe, during the second step, silver nanoparticles are radiolytically synthesized in the bulk of the aqueous solution and then diffuse and adsorb at the surface of PEDOT thanks to weak Van der Waals interactions. But, more probably, prior to irradiation, silver ions first strongly interact with PEDOT particles and bind, as soft Lewis acids, with the sulfur atoms (soft Lewis bases) present all along the polymer chains. These coordinated silver ions are further reduced by hydrated electrons in the vicinity of PEDOT nanoparticles.

In order to check the morphology of ($PEDOT_{ox}/Ag_{red}$) and ($PEDOT_{red}/Ag_{red}$) composites, after deposition procedure and drying step, PEDOT-containing lyophilized powders (sample d and sample g) are deposited onto carbon tape adhered to aluminum mounts. The surface is then imaged by Scanning Electron Microscopy (Figure 7.5, image d and image g respectively).[36]

The images d and g of Figure 7.5 indicate the presence of very close-packed spheroid particles. Some of these particles are surrounded for clarity. These structures should come from the globular nanostructures already observed in aqueous solution by cryo-TEM (Figure 7.4, image c and image f respectively). All these observations are consistent with the reported characterizations of PEDOT polymers synthesized by oxidation-polymerization or reduction polymerization routes.[21,23] The composite nanoparticles observed by SEM after deposition are polydisperse in size with a diameter comprised between 100 and 500 nm. These SEM observations agree well with the size and the shape of ($PEDOT_{ox}/Ag_{red}$) and ($PEDOT_{red}/Ag_{red}$)

particles previously observed in aqueous solution by Cryo-TEM (Figure 7.4). Then, deposition and drying do not seem to affect the nanostructuration of PEDOT/Ag nanocomposites.

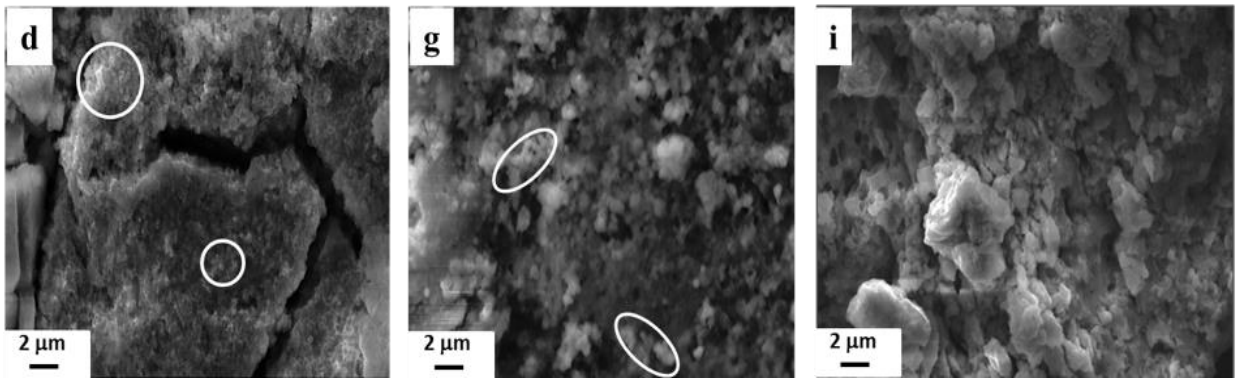

Figure 7.5 SEM images of sample d containing ($PEDOT_{ox}/Ag_{red}$) composites prepared according to procedure ①, sample g containing ($PEDOT_{red}/Ag_{red}$) composites prepared according to procedure ② and sample i containing $(PEDOT/Ag)_{red}$ composites prepared according to procedure ③. Samples d, g and i were obtained after lyophilization of samples c, f and h respectively.[36]

7.3 Synthesis of PEDOT/Ag nanocomposites by one-pot method

After the successful synthesis of PEDOT/Ag nanocomposites according to two-step method (procedures ① and ②, Figure 7.1), we tried to simplify the synthesis methodology by using a reduction-based one-pot method (procedure ③, Figure 7.1). The aim is also to compare the morphology and the properties of the composites prepared by procedure ③ with those of nanocomposites differently prepared according to procedures ① and ②. For the success of the one-pot method, production of PEDOT and of silver nanoparticles should be concomitant. This is conceivable only if reduction of silver ions and oxidation of EDOT monomers take place simultaneously.

While, both $(CH_3)_2C•OH$ and e_{aq}^- act as reducing species towards silver ions, only hydrated electrons can reduce EDOT monomers, leading probably to EDOT anion radicals, $EDOT•^-$.[23] As a consequence, the success of procedure ③ depends on the rate constant values of the two following reactions:

$$Ag^+ + e_{aq}^- \rightarrow Ag^0 \qquad (7.4)$$

$$EDOT + e_{aq}^{-} \rightarrow EDOT\bullet^{-} \qquad (7.5)$$

While the rate constant of reaction (7.4) amounts to $k_{7.4} = 3 \times 10^{10}$ L mol^{-1} s^{-1}, the rate constant of reaction (7.5), $k_{7.5}$, remains unknown.[46]

In order to understand the mechanism involved in the one-pot method and, more particularly, to determine the rate constant of reduction of EDOT molecules by hydrated electrons, pulse radiolysis experiments are carried out on the picosecond laser-triggered electron accelerator (ELYSE at Paris-Sud University) coupled with a time-resolved absorption spectroscopic detection system.[47,48]

In pulse radiolysis, an aqueous solution irradiated by a short pulse of high-energy electrons produces a significant concentration of radical species, according to reaction 2.2 (chapter 2). In order to study the specific action of hydrated electrons, e_{aq}^{-}, onto EDOT molecules and in order to determine its rate constant, an aqueous solution containing 1 mM in EDOT and 0.2 M in tert-butanol, $(CH_3)_3COH$, is prepared, degassed with N_2 and then studied by pulse radiolysis. Such as isopropanol, tert-butanol is an efficient scavenger of HO• radicals (with a rate constant of 6.8×10^8 M^{-1} s^{-1}), according to the following reaction:[32,49]

$$(CH_3)_3COH + HO\bullet \rightarrow \bullet CH_2(CH_3)_2COH + H_2O \qquad (7.6)$$

Tert-butanol radicals, $\bullet CH_2(CH_3)_2COH$, are known to be totally unreactive, which enables us to be sure that, in the present experimental conditions, only hydrated electrons can act, as reducing species towards EDOT molecules.

The transient absorption spectra of the irradiated solution are then recorded at different timescales from 200 ns to 1 s after the electron pulse (Figure 7.6).[36] One can observe at 200 ns a large and intense absorption band at around 600 nm, which is the well-known signature of hydrated electrons generated in the medium by water radiolysis. At longer times, this absorption band progressively decreases, demonstrating the decay of e_{aq}^{-}, while a weaker peak grows up at around 290 nm. Since no other bands are observed in the spectrum over the first 800 ns, one can conclude that the species absorbing at 290 nm comes from the reaction (7.5) of hydrated electrons onto EDOT monomers and should correspond to $EDOT\bullet^{-}$ anion radical.

The evolution with time, over 800 ns, of the absorbancies at 290 and 600 nm are displayed in inset of Figure 7.6 (absorbancies are normalized here for clarity). One can find that the time evolution of the absorbance of hydrated electrons at 600 nm fits well with a first-order decay. On the other hand, the growth of EDOT•$^{-}$ at 290 nm, which is very well correlated with e_{aq}^{-} decay, fits well with a pseudo-first order reaction, in good agreement with reaction (7.5) since EDOT is present in excess in the irradiated medium (1 mM). The kinetic study of the decay at 600 nm and of the growth at 290 nm enabled us to find, two times, the same value for the effective rate constant of reaction (7.5): $k_{7.5} = 3 \times 10^9$ L mol^{-1} s^{-1}.

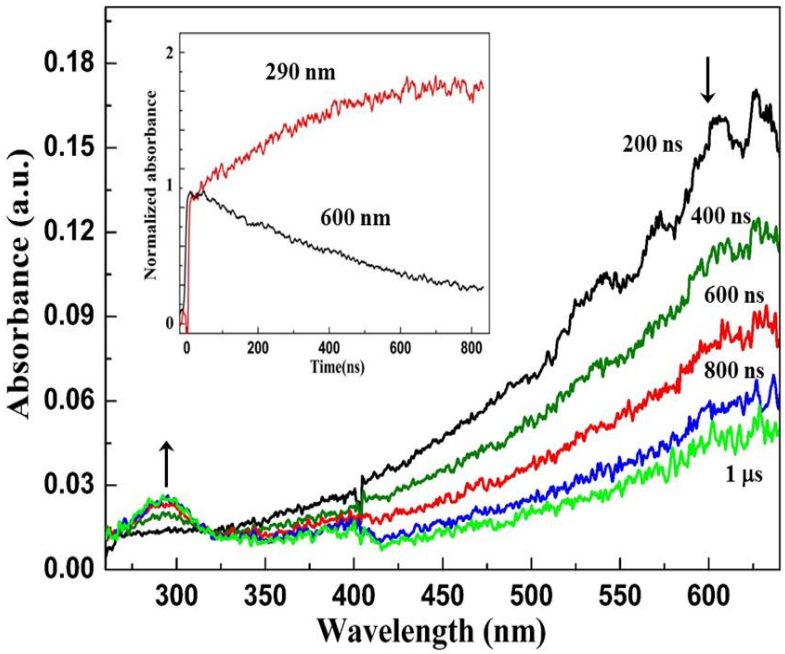

Figure 7.6 Optical absorption spectra recorded in the first 1 ms after the electron pulse and obtained by pulse radiolysis of an aqueous solution containing 1 mM in EDOT and 0.2 M in tert-butanol under N_2 in a cell of 10 mm. **Inset:** Kinetic profiles over 800 ns of the absorbancies at 290 nm and 600 nm, which were normalized for clarity.[36]

One can note that even if the value of $k_{7.5}$ is relatively high, it remains ten times smaller than that of $k_{7.4}$. This result means that starting from an aqueous solution containing equimolar amounts of EDOT monomers and Ag^+ ions (10 mM in both for instance), the reduction of EDOT should be ten times slower than that of silver ions. Therefore, according to procedure ③, PEDOT polymers and silver nanoparticles can be produced simultaneously. Nevertheless, the production of Ag nanoparticles should be faster than that of polymers.

According to procedure ③ (Figure 7.1), aqueous solutions containing 10 mM in EDOT, 10 mM in $AgClO_4$ (EDOT/Ag ratio = 10:10) and 0.2 M in isopropanol are prepared, degassed with N_2 for 20 min and irradiated at 72 kGy. Let's remember that, whatever the rate constants of reduction, this irradiation dose is enough to ensure the total reduction of both EDOT molecules and Ag^+ ions.

After irradiation of the transparent aqueous solution containing both EDOT and silver ions, a brown-black suspension, which slowly precipitates, is observed (Figure 7.1, sample h). Its absorption spectrum (Figure 7.2, spectrum h) displays an asymetric plasmon absorption band, between 400 and 800 nm, which is once again characteristic of silver nanoparticles.[68] Nevertheless, the shape of the spectrum is quite different from that of spectra c and f. This could be due to the synthesis by the way of procedure ③ of silver nanoparticles with new morphology and which could interact differently with PEDOT polymers. One can also note in spectrum h, the absence of the absorption bands of EDOT at 235 and 255 nm. This proves that, after a 72 kGy-irradiation, at the end of procedure ③, EDOT monomers have completely disappeared, as expected.

The simultaneous production of PEDOT polymers and of silver nanoparticles according to this one-pot method is checked by following the evolution of the UV-visible absorption spectrum of the aqueous solution (inset of Figure 7.2) as a function of the irradiation dose (0, 10, 20, 30, 50 and 70 kGy). One can note that even if silver ions reduction is faster as demonstrated by pulse radiolysis, EDOT reduction is noticeable from the lower doses. Indeed, at 10 kGy, which is a dose lower than the dose which is necessary for the total reduction of 10 mM in Ag^+ (16 kGy), the decay of EDOT at 235 and 255 nm is evident. Also, with increasing the irradiation dose, the growth of the plasmon band of silver nanoparticles between 400 and 800 nm and the decay of the absorption bands of EDOT at 235 and 255 nm are concomitant. This definitely demonstrates that, according to procedure ③, PEDOT polymers and silver nanoparticles are formed simultaneously and are thus finally present in the aqueous medium of sample h. The corresponding composites will be called $(PEDOT/Ag)_{red}$.

Irradiated solution, corresponding to the black suspension of sample h, is dried by lyophilization into a black powder (Figure 7.1, sample i). Lyophilized sample i, which is expected to contain $(PEDOT/Ag)_{red}$ nanocomposites, is then characterized by ATR-FTIR spectroscopy. As observed in Figure 7.3, its infrared spectrum (spectrum i) is found very similar

to spectrum d and spectrum g. This definitely proves that, such as sample d and sample g, sample i, obtained at the end of procedure ③, contains PEDOT polymers, silver nanoparticles as well as perchlorate anions.

According to this one-pot method, we changed the EDOT/Ag ratio, from 10:1 to 10:20, by varying the concentration of $AgClO_4$ from 1 mM to 20 mM. Whatever the ratio of EDOT to Ag, the aqueous solutions are all added with isopropanol (0.2 M), degassed with N_2 for 20 min then irradiated at 72 kGy. This dose enables, in all cases, the total reduction of both EDOT and Ag^+. In all cases, black suspensions are obtained after irradiation and black powders are got after lyophilization. The absorption spectra obtained after irradiation are all very close to spectrum h of Figure 7.2 (obtained for the ratio 10:10) (results not shown). Also, the ATR-FTIR spectra are all similar to spectrum i of Figure 7.3 (Figure 7.7).

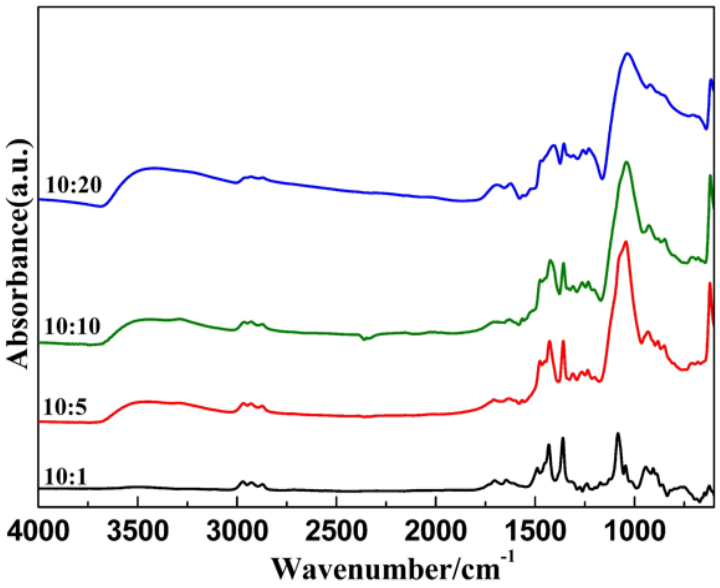

Figure 7.7 ATR-FTIR spectra of $(PEDOT/Ag)_{red}$ composites prepared according to procedure ③ with EDOT/Ag ratios ranging from 10:1 to 10:20.

This indicates, that, even if silver ions reduction is faster than that of EDOT monomers, $(PEDOT/Ag)_{red}$ composites can be formed according to the one-pot method whatever the EDOT/Ag ratio from 10:1 to 10:20.

In order to investigate, in liquid phase before any deposition, the structure and morphology of $(PEDOT/Ag)_{red}$ composites, the black aqueous suspension obtained at the end of procedure ③

(sample h), is observed by Cryo-transmission electron microscopy just after irradiation and before any sedimentation (Figure 7.4, image h). $(PEDOT/Ag)_{red}$ nanocomposites appear as granular mixtures.[16,50] Representative images of $(PEDOT/Ag)_{red}$ aqueous sample are very different from those obtained in the case of ($PEDOT_{ox}/Ag_{red}$) and ($PEDOT_{red}/Ag_{red}$) (Figure 7.4, images c and f respectively). Indeed, image h of Figure 7.4, shows the presence of low density globular structures forming polydisperse spheroidal nanoparticles with a diameter comprised between 10 and 50 nm. These organic particles, made of PEDOT polymers and obtained by one-pot method, are ten times smaller than PEDOT nanoparticles obtained by two-step method. On another hand, as can also be observed in image h of Figure 7.4, smaller nanoparticles which appear very more contrasted (darker), are found embedded into the core of the bigger globular PEDOT nanoparticles. Some of these dark nanoparticles are indicated on the figure by arrows. The relatively high contrast of these smaller particles suggests once again that they are made of silver.[33,45] The presence of organic molds around these silver nanoparticles should explain their characteristic asymmetric plasmon absorption band which is found by UV-Vis absorption spectroscopy (Figure 7.2, spectrum h).

EDX spectrum (Figure 7.4, spectrum h) which corresponds to the elemental analysis of the surrounded area of image h, highlights, the presence, in sample h, of all the chemical elements already detected in spectrum c and spectrum f of Figure 7.4, namely O, C, Ag and S. This definitely demonstrates, as expected, the presence, in the analyzed area of image h, of both PEDOT polymers and silver nanoparticles. In this area, S and Ag atomic percentages are found to be 21 % and 79 % respectively. Nevertheless, these percentages are found very dependent on the analyzed area.

In procedures ① and ②, PEDOT nanoparticles are first synthesized, then in a second step, silver ions are reduced at the surface of these polymer nanoparticles. Differently, in procedure ③, silver ions reduction takes place in parallel with EDOT reduction. Then, since silver reduction is faster than that of EDOT, metal nanoparticles can form prior to the existence of PEDOT nanoparticles. In one-pot method, according to procedure ③, all silver nanoparticles are found surrounded by an organic shell (Figure 7.4, image h). This could mean that EDOT reduction and polymerization happen in the vicinity of silver nanoparticles. Such a growth mechanism could be explained by the strong interaction which exists between silver ions (or even atoms) and the sulfur atoms of EDOT monomers. Or maybe, PEDOT polymers are formed far from silver

nanoparticles, in the bulk of the aqueous solution, and then diffuse and adsorb at their surface, thanks to weak Van der Waals interactions, enabling the thermodynamic stabilization of silver particles and avoiding their aggregation and sedimentation. This effect of polymers onto silver nanoparticles has already been reported in literature.[51]

In order to characterize the morphology of $(PEDOT/Ag)_{red}$ composites, after drying and deposition procedures, PEDOT-containing lyophilized powder (sample i) is observed by SEM (Figure 7.5, image i). Contrarily to the observations made on images d and g of Figure 7.5 concerning ($PEDOT_{ox}/Ag_{red}$) and ($PEDOT_{red}/Ag_{red}$) respectively, no spherical nanoparticles are observed in image i. Maybe their relatively small size avoids their observation by SEM microscopy. In fact, SEM characterization shows that $(PEDOT/Ag)_{red}$ composites become compact hybrid after deposition.

According to this one-pot method, we changed the EDOT/Ag ratio, from 10:1 to 10:20, by varying the concentration of $AgClO_4$ from 1 mM to 20 mM. Whatever the ratio of EDOT to Ag, $(PEDOT/Ag)_{red}$ nanocomposites appear as granular mixtures with silver nanoparticles embedded into organic molds. This indicates that, whatever the EDOT/Ag ratio from 10:1 to 10:20, $(PEDOT/Ag)_{red}$ composites have the same morphology in aqueous solution. Nevertheless, when the amount of silver is higher, the size of the nanocomposites increases and a more important aggregation takes place (Figure 7.8).[38]

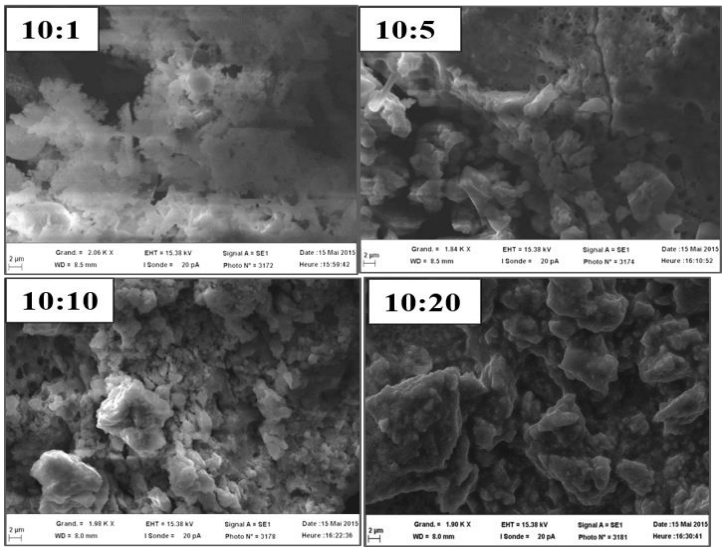

Figure 7.8 SEM images of $(PEDOT/Ag)_{red}$ composites prepared according to procedure ③ with EDOT/Ag ratio ranging from 10:1 to 10:20.

7.4 Physico-chemical properities of PEDOT/Ag nanocomposites

As demonstrated previously, PEDOT/Ag nanocomposites can be prepared by both two-step method (($PEDOT_{ox}/Ag_{red}$) and ($PEDOT_{red}/Ag_{red}$) composites) and one-pot method ($(PEDOT/Ag)_{red}$ composites) thanks to γ-radiolysis. The obtained PEDOT/Ag nanocomposites display very close UV-vis absorption spectra and similar ATR-FTIR spectra. All composites which are found to be made of PEDOT polymers and silver nanoparticles are shown to be doped with perchlorate anions.

Contrarily to their chemical composition which is the same, the morphology of PEDOT/Ag nanocomposites in aqueous solution and after deposition is almost different. In aqueous solution, while ($PEDOT_{ox}/Ag_{red}$) and ($PEDOT_{red}/Ag_{red}$) composites are made of large spherical PEDOT nanoparticles at the surface of which smaller silver nanoparticles adsorb, $(PEDOT/Ag)_{red}$ composites are made of silver nanoparticles embedded in the core of small irregular spheroidal PEDOT nanoparticles. After deposition, while ($PEDOT_{ox}/Ag_{red}$) and ($PEDOT_{red}/Ag_{red}$) composites are made of very close-packed polydisperse spheroidal particles, $(PEDOT/Ag)_{red}$ composites appear denser and form more compact blocks.

In order to check the influence of the morphology of PEDOT/Ag nanocomposites onto their physico-chemical properties, thermal stability and composition analysis of lyophilized ($PEDOT_{ox}/Ag_{red}$), ($PEDOT_{red}/Ag_{red}$) and $(PEDOT/Ag)_{red}$ composites are performed by thermogravimetric analysis (TGA). Also, in order to check the influence of the presence of silver component onto the stability of radiosynthesized polymers, lyophilized PEDOT polymers prepared in the absence of silver ions according to procedures ① and ②, $PEDOT_{ox}$ and $PEDOT_{red}$ respectively (Figure 7.1), are also analyzed by TGA from 50 to 900 ^{0}C.

The degradation curves of PEDOT polymers and PEDOT/Ag composites, which indicate the remaining weight of the powders as a function of temperature, are all displayed (Figure 7.9).[36]
TGA curves of PEDOT/Ag nanocomposites show quite similar tendency in the whole temperature range. Before 150 ℃, a small weight loss is caused by the evaporation of water and degradation of PEDOT oligomers. Then, progressive weight loss happens from 150 to 450 ℃ resulting from PEDOT fragmentation and carbon oxidation.[52] After 450 ℃, the degradation curves tend to be constant up to 900 ℃. At this temperature, the remaining weights of PEDOT/Ag nanocomposites are about 45 %. The residues should contain silver nanoparticles, perchlorate and

undecomposed PEDOT.[17] The similarity in the degradation curves of ($PEDOT_{ox}/Ag_{red}$), ($PEDOT_{red}/Ag_{red}$) and $(PEDOT/Ag)_{red}$ composites means that the morphology of the composites has no clear influence on their thermal stability. This similarity in the curves is certainly due to the fact that the three materials have, as already demonstrated, the same chemical composition (even if the synthesis methodologies are different).

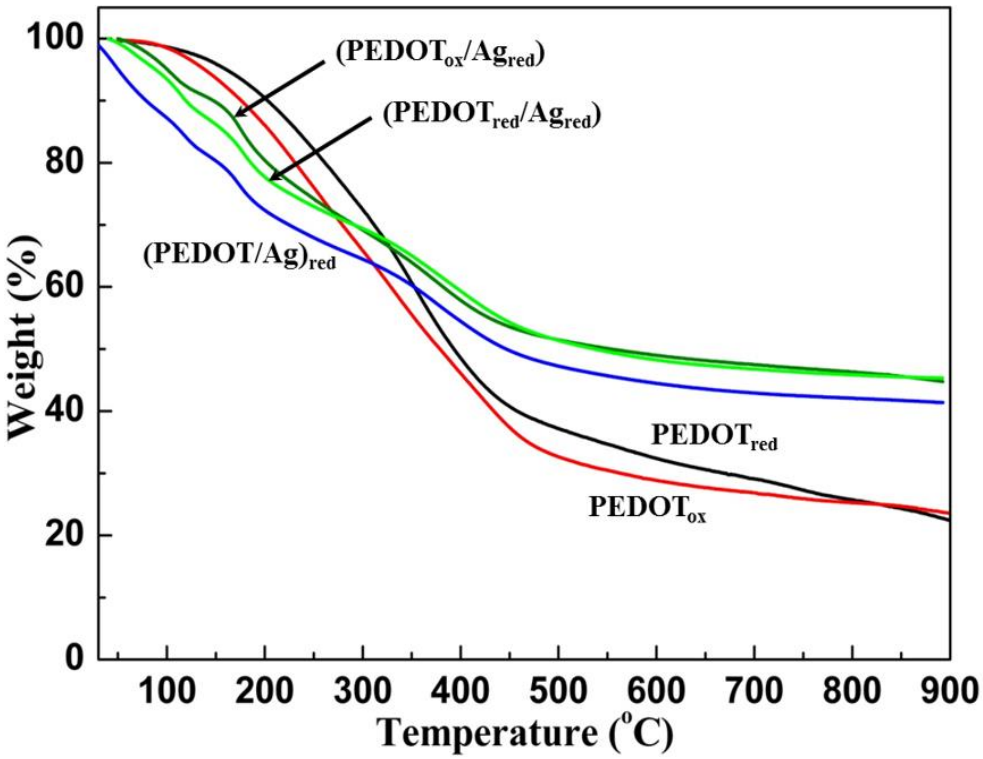

Figure 7.9 Thermogravimetric analysis (TGA) plots of $PEDOT_{ox}$ and ($PEDOT_{ox}/Ag_{red}$), both synthesized according to procedure ① (two-step method), $PEDOT_{red}$ and ($PEDOT_{red}/Ag_{red}$), both synthesized according to procedure ② (two-step method) and $(PEDOT/Ag)_{red}$ prepared according to procedure ③ (one-pot method).[36]

TGA curves of pure PEDOT polymers, $PEDOT_{ox}$ and $PEDOT_{red}$, prepared in the absence of silver perchlorate, show quite similar tendency in the whole temperature range (Figure 7.9). Before 150 ℃, contrarily to what is observed in the case of composites, no weight loss is observed in the case of pure PEDOT. This could be explained by the existence of a smaller amount of PEDOT oligomers resulting from a higher level of polymerization. Above 150 ℃ and up to 450 ℃, a progressive weight loss happens resulting from PEDOT fragmentation and carbon oxidation. Note that, in this range of temperature, degradation rate of pure PEDOT is faster than

that of PEDOT/Ag nanocomposites. This result indicates a superior thermal stability of PEDOT/Ag composites compared with that of pure PEDOT. Thus the presence of silver nanoparticles into the composites increases the thermal stability of PEDOT polymers.[11] Above 450 ℃, the degradation curves of pure PEDOT tend to be constant up to 900 ℃, only a small weight loss is observed. Besides, one can note that the final weight loss is more important in the case of pure PEDOT than in the case of composites. This result is logical. Indeed, in the case of pure PEDOT, the residue should contain only undecomposed PEDOT, while in the case of composites, it should also contain silver nanoparticles together with perchlorate. In conclusion, thanks to the presence of silver, PEDOT/Ag composites display a thermal stability which is globally higher than that of pure PEDOT over a wide range of temperatures.

Besides, when varying EDOT/Ag ratio, from 10:1 to 10:20 in the case of $(PEDOT/Ag)_{red}$ composites, as the proportion of silver perchlorate increases, one can note an increase in the remaining weight of the composites at 900 ℃ (Figure 7.10). In particular, the remaining weight reaches 60 % for the ratio 10:20.

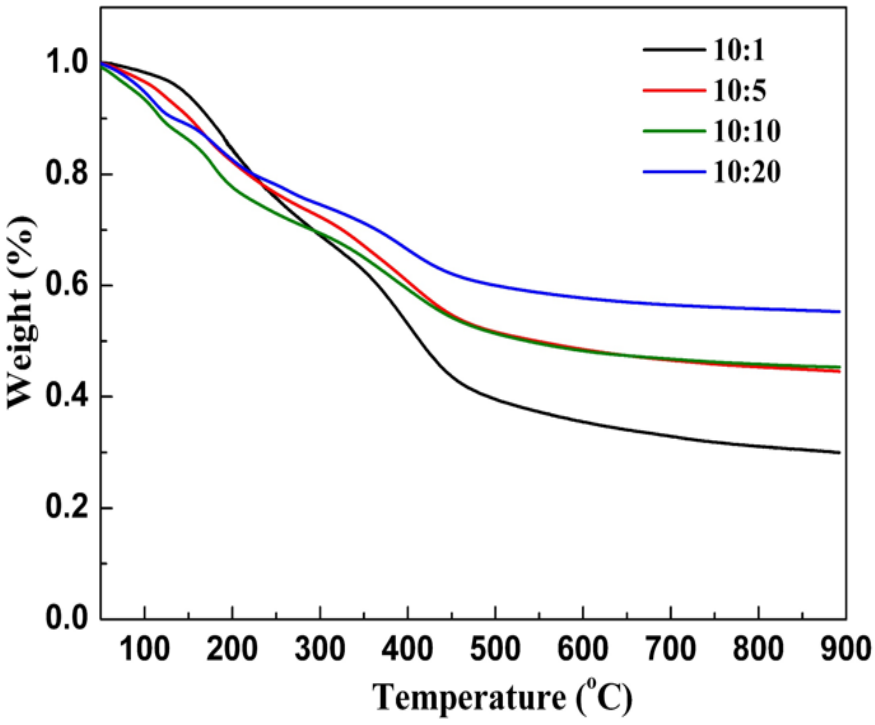

Figure 7.10 TGA curves of $(PEDOT/Ag)_{red}$ composites prepared according to procedure ③ with EDOT/Ag ratio ranging from 10:1 to 10:20.

Finally, in order to measure and to compare the electrical conductivities of the differently prepared PEDOT/Ag nanocomposites and in order to check the influence of the morphology and of the presence of silver, spin-coated films of ($PEDOT_{ox}/Ag_{red}$), ($PEDOT_{red}/Ag_{red}$), $(PEDOT/Ag)_{red}$, $PEDOT_{ox}$ and $PEDOT_{red}$ are prepared and a four-point probe technique is used for measuring the resistance of all PEDOT and PEDOT/Ag films. Note that before measurements, all PEDOT and PEDOT/Ag solutions are doped with $NOBF_4$ at a concentration of 10 mM in acetonitrile.

The electrical conductivities measured by four-point probe technique are all reported (Table 7.1).[36] The values found in the case of PEDOT/Ag composites are in the same order of magnitude, even if that of ($PEDOT_{red}/Ag_{red}$) appears slightly higher. These values are comparable to those already reported in literature for PEDOT nanocomposites prepared according to other methods.[9] Also, when varying EDOT/Ag ratio, from 10:1 to 10:20 in the case of $(PEDOT/Ag)_{red}$ composites, as the proportion of silver perchlorate increases, one can note a slight increase in the electrical conductivity from 3.2×10^{-3} to 3.9×10^{-3} S cm^{-1} (results not reported in Table 7.1).

Table 7.1 Electrical conductivities of $PEDOT_{ox}$ and ($PEDOT_{ox}/Ag_{red}$), both synthesized according to procedure ① (two-step method), $PEDOT_{red}$ and ($PEDOT_{red}/Ag_{red}$), both synthesized according to procedure ② (two-step method) and $(PEDOT/Ag)_{red}$ prepared according to procedure ③ (one-pot method).[36]

Sample	Conductivity / S cm^{-1}
$PEDOT_{ox}$	9.8×10^{-3}
$PEDOT_{red}$	3.4×10^{-3}
($PEDOT_{ox}/Ag_{red}$)	3.2×10^{-3}
($PEDOT_{red}/Ag_{red}$)	5.6×10^{-3}
$(PEDOT/Ag)_{red}$	3.6×10^{-3}

The measured electrical conductivities of $PEDOT_{ox}$ and $PEDOT_{red}$ are also reported in Table 7.1. The value found in the case of $PEDOT_{red}$ (3.4×10^{-3} S cm^{-1}) is somewhat lower than that of $PEDOT_{ox}$ (9.8×10^{-3} S cm^{-1}). Nevertheless, both values are close to those already reported in literature for PEDOT polymers.[53,54] Moreover, conductivities of pure PEDOT polymers and those of PEDOT/Ag composites are found in the same order of magnitude. Definitely, this proves that

neither the morphology of the composites, nor their chemical composition (amount of silver and perchlorate) have a clear influence on the electrical conductivity. The main factor which seems to determine the final conductivity is the amount of PEDOT conducting polymers, which is the same in all samples. Note that the oxidation or reduction methodologies used for the production of PEDOT polymers seem to have no influence.

7.5 Conclusions

Hybrid nanocomposites, made of organic conducting polymers and inorganic metal nanoparticles attracted intensive research interests due to their remarkable properties. These nanocomposites are generally synthesized by traditional chemical and electrochemical routes. Nevertheless, in our knowledge, radiolysis has never been used for the preparation of such conducting polymers-based nanocomposites. Herein, an original methodology based on radiation chemistry is used for the first time for the synthesis of hybrid organic-inorganic composites in aqueous solution.

Starting from an aqueous solution containing both metal ions and organic monomers, we originally used gamma-radiolysis for the *in situ* production of hydrated electrons and hydroxyl radicals as reducing and oxidizing species respectively, in order to synthesize hybrid CPs/metal nanocomposites.

Starting from EDOT monomers and silver perchlorate salt, preparation of PEDOT/Ag composites, made of PEDOT conducting polymers and silver nanoparticles, is achieved by using different radiolytical procedures. According to the two-step method, PEDOT polymers are first synthesized by either oxidation or reduction of EDOT monomers and then, silver nanoparticles are produced in the presence of PEDOT by reduction of silver ions. Differently, according to the one-pot method, polymerization and metal ions reduction are achieved in parallel, in one step, thanks to the concomitant reduction of EDOT monomers and of silver ions, as demonstrated by pulse radiolysis experiments.

As highlighted by UV-Vis absorption spectrophotometry, ATR-FTIR spectroscopy and EDX spectroscopy, all prepared nanocomposites are made of PEDOT polymers and silver nanoparticles. Also, they are found to be doped with perchlorate anions. On the contrary, the morphologies of PEDOT/Ag nanocomposites are almost different and depend on the preparation

procedure, as demonstrated respectively by Cryo-TEM observations in aqueous solution and SEM microscopy after deposition. While composites prepared by two-step method are made of large spherical PEDOT nanoparticles at the surface of which smaller silver nanoparticles adsorb, composites produced according to one-pot method are made of silver nanoparticles embedded in the core of small irregular spheroidal PEDOT nanoparticles.

Four-point probe measurements demonstrated that electrical conductivities of all radiosynthesized PEDOT/Ag composites, which are close to those reported in literature for PEDOT nanocomposites prepared according to other methodologies, are in the same order of magnitude. Moreover, these conductivities are close to those measured in the case of pure PEDOT polymers synthesized by radiolysis in the absence of silver. This proves that neither the morphology, nor the presence of silver have a clear influence on the electrical conductivity of the composites. The main factor which seems to determine the final conductivity is the amount of PEDOT conducting polymers, which is the same in all our nanocomposites. More interestingly, TGA analysis revealed that, whatever their morphology, all PEDOT/Ag composites are characterized by the same thermal stability, which remains higher, over a wide range of temperatures, than that of pure PEDOT synthesized by radiolysis. Also, this thermal stability can be enhanced by increasing the amount of silver into the composites.

As demonstrated in previous chapters (chapter 3, 4, 5 and 6), that PEDOT and PPy conducting polymers can be produced in aqueous solution by radiolysis.[19,21,55] According to oxidation or reduction route. In this chapter, the radiolytic procedure was extended to the synthesis of CPs nanocomposites. In particular, thanks to radiation chemistry, the preparation of hybrid nanocomposites made of PEDOT conducting polymers and of silver nanoparticles was realized. This novel methodology, never used in literature, should enable us to prepare in aqueous solution different kinds of CPs/metal nanocomposites containing, for instance, PPy as CPs and gold as inorganic component.

References

[1] Kao, J.; Thorkelsson, K.; Bai, P.; Rancatore, B. J.; Xu, T., Toward functional nanocomposites: taking the best of nanoparticles, polymers, and small molecules. *Chemical Society reviews* **2013,** *42* (7), 2654-2678.

[2] Gangopadhyay, R.; De, A., Conducting Polymer Nanocomposites: A Brief Overview. *Chem Mater* **2000,** *12* (3), 608-622.

[3] Zhan, C.; Yu, G.; Lu, Y.; Wang, L.; Wujcik, E.; Wei, S., Conductive polymer nanocomposites: a critical review of modern advanced devices. *Journal of Materials Chemistry C* **2017,** *5* (7), 1569-1585.

[4] Folarin, O. M.; Sadiku, E. R.; Maity, A., Polymer-noble metal nanocomposites: Review. *International Journal of the Physical Sciences* **2011,** *6* (21), 4869-4882.

[5] Xu, P.; Han, X.; Zhang, B.; Du, Y.; Wang, H., Multifunctional polymer-metal nanocomposites via direct chemical reduction by conjugated polymers. *Chemical Society reviews* **2014,** *43* (5), 1349-1360.

[6] Zhu, C.; Du, D.; Eychmuller, A.; Lin, Y., Engineering Ordered and Nonordered Porous Noble Metal Nanostructures: Synthesis, Assembly, and Their Applications in Electrochemistry. *Chemical reviews* **2015,** *115* (16), 8896-8943.

[7] Zou, X. X.; Zhang, Y., Noble metal-free hydrogen evolution catalysts for water splitting. *Chemical Society reviews* **2015,** *44*, 5148-5180.

[8] Armel, V.; Winther-Jensen, B.; Kerr, R.; MacFarlaneb, D. R.; Winther-Jensena, B., Designed electrodeposition of nanoparticles inside conducting polymers. *J. Mater. Chem.* **2012,** *22* (37), 19767–19773.

[9] Pillalamarri, S. K.; Blum, F. D.; Tokuhiro, A. T.; Bertino, M. F., One-Pot Synthesis of Polyaniline-Metal Nanocomposites. *Chem. Mater.* **2005,** *17*, 5941-5944.

[10] Mo, Z. L.; Zuo, D. D.; Chen, H.; Sun, Y. X.; Zhang, P., Synthesis of graphite nanosheets/AgCl/polypyrrole composites via two-step inverse microemulsion method. *Eur. Polym. J.* **2007,** *43* (2), 300-306.

[11] Fujii, S.; Aichi, A.; Akamatsu, K.; Nawafune, H.; Nakamura, Y., One-step synthesis of polypyrrole-coated silver nanocomposite particles and their application as a coloured particulate emulsifier. *J.Mater.Chem.* **2007,** *17* (36), 3777-3779.

[12] Feng, X. M.; Huang, H. P.; Ye, Q. Q.; Zhu, J. J.; Hou, W. H., Ag/Polypyrrole Core-Shell Nanostructures: Interface Polymerization, Characterization, and Modification by Gold Nanoparticles. *J. Phys. Chem. C* **2007,** *111*, 8463-8468.

[13] Muñoz-Rojas, D.; Oró-Solé, J.; Ayyad, O.; Gómez-Romero, P., Shaping hybrid nanostructures with polymer matrices: the formation mechanism of silver–polypyrrole core/shell nanostructures. *J. Mater. Chem.* **2011,** *21* (7), 2078-2086.

[14] Roncali, J.; Blanchard, P.; Frère, P., 3,4-Ethylenedioxythiophene (EDOT) as a versatile building block for advanced functional π-conjugated systems. *J. Mater. Chem.* **2005,** *15* (16), 1589-1610.

[15] Groenendaal, L. B.; Jonas, F.; Freitag, D.; Pielartzik, H.; Reynolds, J. R., Poly(3,4-ethylenedioxythiophene) and Its Derivatives: Past, Present, and Future. *Adv. Mater.* **2000,** *12*, 481-494.

[16] Jung, H. R.; Lee, W. J., Ag/poly(3,4-ethylenedioxythiophene) nanocomposites as anode materials for lithium ion battery. *Solid State Ionics* **2011,** *187* (1), 50-57.

[17] Mumtaz, M.; Cloutet, E.; Labrugère, C.; Hadziioannou, G.; Cramail, H., Synthesis of hybrid semiconducting polymer–metal latexes. *Polym. Chem.* **2013,** *4* (3), 615-622.

[18] Radhakrishnan, S.; Sumathi, C.; Umar, A.; Jae Kim, S.; Wilson, J.; Dharuman, V., Polypyrrole-poly(3,4-ethylenedioxythiophene)-Ag (PPy-PEDOT-Ag) nanocomposite films for label-free electrochemical DNA sensing. *Biosensors & bioelectronics* **2013,** *47*, 133-140.

[19] Remita, S.; Mostafavi, M.; Delcourt, M. O., Stabilization, growth and reactivity of silver aggregates produced by radiolysis in the presence of EDTA. *New J.Chem.* **1994,** *18*, 581-588.

[20] Mostafavi, M.; Remita, S.; Delcourt, M. O.; Belloni, J., Ligand effects on solvated metal cluster properties. *J. Chim. Phys.* **1996,** *93*, 1828-1842.

[21] Lattach, Y.; Deniset-Besseau, A.; Guigner, J. M.; Remita, S., Radiation chemistry as an alternative way for the synthesis of PEDOT conducting Polymers under "soft" Conditions. *Radiat. Phys. Chem.* **2013,** *82*, 44-53.

[22] Lattach, Y.; Coletta, C.; Ghosh, S.; Remita, S., Radiation-induced synthesis of nanostructured conjugated polymers in aqueous solution: fundamental effect of oxidizing species. *C hemphyschem* **2014,** *15* (1), 208-218.

[23] Cui, Z. P.; Coletta, C.; Rebois, R.; Baiz, S.; Gervais, M.; Goubard, F.; Aubert, P. H.; Dazzi, A.; Remita, S., Radiation-induced reduction–polymerization route for the synthesis of PEDOT conducting polymers. *Radiat. Phys. Chem.* **2016,** *119*, 157-166.

[24] Hanynes, W. M., *Handbook of Chemistry and Physics* **2012,** *84* (CRC Press, New York, United States), 112.

[25] Sakmeche, N.; Aeiyach, S.; Aaron, J.-J.; Jouini, M.; Lacroix, J. C.; Lacaze, P.-C., Improvement of the Electrosynthesis and Physicochemical Properties of Poly(3,4-ethylenedioxythiophene) Using a Sodium Dodecyl Sulfate Micellar Aqueous Medium. *Langmuir* **1999,** *15*, 2566-2574.

[26] Spinks, J. W. T.; Woods, R. J., An introduction to radiation chemistry. *John Wiley & Sons, Inc. New York, United States* **1990**, pp. 251-256.

[27] Ferradini, C.; Jay-Gerin, J.-P., La radiolyse de l'eau et des solutions aqueuses: historique et actualité. *Can. J. Chem.* **1999,** *77*, 1542-1575.

[28] Ferradini, C.; Jay-Gerin, J. P., The effect of pH on water radiolysis: A still open question - A minireview. *Res. Chem. Intermed.* **2000,** *26* (6), 549-565.

[29] Hart, E. J., Research Potentials olf the Hydrated Electron. *Acc. Chem. Res.* **1969,** *2*, 161-167.

[30] Song, L. Y.; Wang, M. Z.; Cong, Y. H.; Liu, W. J.; Ge, X. W.; Zhang, Z. C., The mechanism of 60Co γ-ray radiation induced interfacial redox reaction in inverse emulsion and its application in the synthesis of polymer microcapsules. *Polymer* **2007,** *48* (1), 150-157.

[31] Belloni, J.; Mostafavi, M.; Remita, H.; Marignier, J.-L.; Delcourt, M.-O., Radiation-induced synthesis of mono- and multi-metallic clusters and nanocolloids. *New J. Chem.* **1998**, 1239-1255.

[32] Buxton, G. V.; Greenstock; Helman, W. P.; Ross, A. B., Critical riview of rate constants for reactions of hydrated electrons, hodrogen atoms and hodroxyl radicals(·OH/·O-) in aqueous solution. *J. Phys. Chem. Ref. Data* **1988,** *17* (2), 513-886.

[33] Remita, S., Effect of ligands on thermadynamics, kinetics and spectral properties of metalic aggregates synthesized by radiloysis. *Doctoral thesis* **1995**.

[34] Mostafavi, M.; Dey, G. R.; Francöois, L.; Belloni, J., Transient and Stable Silver Clusters Induced by Radiolysis in Methanol. *J. Phys. Chem. A* **2002,** *106*, 10184-10194.

[35] Remita, S.; Fontaine, P.; Rochas, C.; Muller, F.; Goldmann, M., Radiation induced synthesis of silver nanoshells formed onto organic micelles. *EPJD* **2005,** *34*, 231-233.

[36] Cui, Z. P.; Coletta, C.; Bahry, T.; Marignier, J.-L.; Guigner, J.-M.; Gervais, M.; Baiz, S.; Goubard, F.; Remita, S., A novel radiation chemistry-based methodology for the synthesis of PEDOT/Ag nanocomposites. *Materials Chemistry Frontiers* **2017,** *1* (5), 879-892.

[37] Paramelle, D.; Sadovoy, A.; Gorelik, S.; Free, P.; Hobley, J.; Fernig, D. G., A rapid method to estimate the concentration of citrate capped silver nanoparticles from UV-visible light spectra. *Analyst* **2014,** *139*, 4855–4861.

[38] Henglein, A.; Giersig, M., Formation of Colloidal Silver Nanoparticles: Capping Action of Citrate. *J. Phys. Chem. B* **1999,** *103*, 9533-9539.

[39] Rajesh, D.; Sunandana, C. S., XRD, optical and AFM studies on pristine and partially iodized Ag thin film. *Results in Physics* **2012,** *2*, 22-25.

[40] Kvarnström, C.; Neugebauer, H.; Blomquist, S.; Ahonenc, H. J.; Kankarec, J.; Ivaska, A., In situ spectroelectrochemical characterization of poly(3,4-ethylenedioxythiophene). *Electrochim. Acta* **1999,** *44*, 2739-2750.

[41] Ghosh, S.; Remita, H.; Ramos, L.; Dazzi, A.; Deniset-Besseau, A.; Beaunier, P.; Goubard, F.; Aubert, P. H.; Brisset, F.; Remita, S., PEDOT nanostructures synthesized in hexagonal mesophases. *New J.Chem.* **2014,** *38* (3), 1106-1115.

[42] Chen, Y.; Zhang, Y. H.; Zhao, L. J., ATR-FTIR spectroscopic studies on aqueous $LiClO_4$, $NaClO_4$, and $Mg(ClO_4)_2$ solutions. *Phys. Chem. Chem. Phys.* **2004,** *6* (3), 537-542.

[43] Yang, J. S.; Hsiue, G. H., Novel dry poly[(1-trimethylsilyl)-1-propyne]-AgClO4 complex membranes for olefin/paraffin separations. *J. Membrane Sci.* **1996,** *120*, 69-76.

[44] He, S. Q.; Wu, J. G.; Zhang, Q. L., Mid-infrared spectra of the crown ether complexes of lithium perchlorate. *Acta Chim. Sinica* **1984,** *42*, 1183-1187.

[45] Attia, J.; Remita, S.; Jonic, S.; Lacaze, E.; Faure, M.-C.; Larquet, E.; Goldmann, M., Radiation-Induced Synthesis and Cryo-TEM Characterization of Silver Nanoshells on Linoleate Spherical Micelles. *Langmuir* **2007,** *23* (19), 9523-9526.

[46] Beaumont, P. C.; Powers, E. L., Radiation sensitivity of DNA-metal complexes: A pulse, radiolysis study. *Int. J. Radiat. Biol. Relat. Stud. Phys. Chem. Med.* **1983**, 485-494.

[47] Belloni, J.; Monard, H.; Gobert, F.; Larbre, J. P.; Demarque, A.; De Waele, V.; Lampre, I.; Marignier, J. L.; Mostafavi, M.; Bourdon, J. C.; Bernard, M.; Borie, H.; Garvey, T.; Jacquemard, B.; Leblond, B.; Lepercq, P.; Omeich, M.; Roch, M.; Rodier, J.; Roux, R., ELYSE—A picosecond electron accelerator for pulse radiolysis research. *Nucl. Instr. Meth. Phys. Res. A* **2005,** *539* (3), 527-539.

[48] Marignier, J. L.; de Waele, V.; Monard, H.; Gobert, F.; Larbre, J. P.; Demarque, A.; Mostafavi, M.; Belloni, J., Time-resolved spectroscopy at the picosecond laser-triggered electron accelerator ELYSE. *Radiat. Phys. Chem.* **2006,** *75* (9), 1024-1033.

[49] Piechowski, M. V.; Thelen, M.-A.; Hoigne, J.; Biihler, R. E., tert-Butanol as an OH-Scavenger in the Pulse Radiolysis of Oxygenated Aqueous Systems. *Ber. Bunsenges. Phys. Chem.* **1992,** *96*, 1448-1453.

[50] Mahendia, S.; Tomar, A. K.; Kumar, S., Electrical conductivity and dielectric spectroscopic studies of PVA–Ag nanocomposite films. *J. Alloys Compd.* **2010,** *508* (2), 406-411.

[51] Remita, S.; Orts, J. M.; Feliu, J. M., STM identification of silver oligomer clusters prepared by radiolysis in aqueous solution. *Chem. Phys. Lett.* **1994,** *218*, 115-121.

[52] Wu, J.; Cho, W.; Martin, D. C.; Feng, Z. Q.; Leach, M. K.; Franz, E. W.; Naim, Y. I.; Gu, Z. Z.; Corey, J. M., Highly Aligned Poly(3,4-ethylene dioxythiophene) (PEDOT) Nano- and Microscale Fibers and Tubes. *Polymer* **2013,** *54* (2), 702-708.

[53] Jones, B. H.; Cheng, K.-Y.; Holmes, R. J.; Lodge, T. P., Nanoporous Poly(3,4-ethylenedioxythiophene) Derived from Polymeric Bicontinuous Microemulsion Templates. *Macromolecules* **2012,** *45* (1), 599-601.

[54] Nagarajan, R.; Kumar, J.; Bruno, F. F.; Samuelson, L. A.; Nagarajan, R., Biocatalytically synthesized poly(3,4-ethylenedioxythiophene). *Macromolecules* **2008,** *41*, 3049-3052.

[55] Coletta, C.; Cui, Z. P.; Dazzi, A.; Guigner, J.-M.; Néron, S.; Marignier, J.-L.; Remita, S., A pulsed electron beam synthesis of PEDOT conducting polymers by using sulfate radicals as oxidizing species. *Radiat. Phys. Chem.* **2016,** *126*, 21-31.

Conclusions and perspectives

In this thesis, synthesis of conducting polymers (CPs) and CPs nanocomposites with radiolytic method has been studied. The radiolytic method was developed by Samy Remita's team (Laboratoire de Chimie Physique, LCP) and this new method opens a novel approach for the synthesis of CPs. Based on the radiolytic method, synthesis of different kinds of CPs has been carried out and the effect of synthetic conditions on the polymerization has been investigated. In addition, new synthetic routes based on oxidation or reduction of monomers have been tried for the synthesis of CPs and CPs nanocomposites. During the study, some general conclusions are drawn and some unsolved questions are proposed for perspectives.

In chapter 3, the original radiolytic methodology was developed for the synthesis of poly(3,4-ethylenedioxythiophene) (PEDOT) polymers from aqueous solutions of 3,4-ethylenedioxythiophene (EDOT) monomers. Different oxidizing species produced by gamma (γ)-radiolysis were applied to oxidize EDOT monomers leading to PEDOT polymers with different morphologies. With pulse radiolysis study, a step-by-step mechanism has been established for the polymerization of EDOT monomers and accelerated electron beam also enables the synthesis of PEDOT polymers.

In chapter 4, the versatility of γ-radiolysis-based alternative way for synthesizing CPs is proved by the successful synthesis of polypyrrole (PPy) polymers by using hydroxyl radicals (HO•) produced from γ-radiolysis of water as the oxidizing species. Radiosynthesized PPy polymers show good stability and can be well dispersed in polar solvents. PPy polymers show globular self-assembled structures and pack into nanochaplets in aqueous solution. Compared with the PPy polymers prepared by traditional chemical method by using potassium persulfate ($K_2S_2O_8$), radiosynthesized PPy nanoparticles are more hydrophilic, smaller and less polydisperse than chemically synthesized PPy. In addition, the radiosynthesized PPy nanostructures are characterized by a very good thermal stability and an electrical conductivity which is five times higher than that of chemically synthesized PPy. The successful synthesis of PPy polymers extends the application of radiolytic method for the synthesis of CPs.

In chapter 5, the effect of synthetic conditions including soft template, pH and ionic strength on the polymerization of EDOT monomers are studied in detail. It is found that the addition of SDS surfactant does not affect the polymerization of EDOT at a concentration lower than its

CMC I. Nevertheless, the use of self-assembled surfactants in micelles inhibits the polymerization of SDS due to the competitive reaction of radiolytic radicals onto highly concentrated SDS molecules. The effect of pH on the polymerization of EDOT is obvious. Dark blue precipitate is obtained after γ-irradiation at pH = 0. Spectroscopic studies prove that poly(3,4-ethylenedioxythiophene) (PEDOT) polymers in reduced state are obtained in very acidic medium. Microscopic observations show that PEDOT prepared in these conditions appears to be amorphous. It forms granular particles in solution and compact aggregates after deposition. It is noted that the kind of acid and the nature of oxidizing species hydroxyl radicals (HO•) or dichloride anion radicals ($Cl_2^{\cdot -}$) have no effect on the polymerization of EDOT. In addition, it is proved that the ionic strength has no effect on the polymerization of EDOT. PEDOT polymers prepared in very acidic medium possess electrical conductivity in the order of 10^{-3} S·cm^{-1}. Also, the as-prepared PEDOT has successfully been mixed with poly(4-styrenesulfonic acid) (PSSH) to form PEDOT/PSS membranes.

In chapter 6, the polymerization of EDOT is initiated by hydrated electrons (e_{aq}^-) produced from γ-radiolysis of water. For the first time, such a simple γ-rays-based reduction polymerization route solution is described for synthesizing PEDOT conducting polymers in aqueous. PEDOT polymers synthesized by radiation-induced reduction polymerization are characterized by a very good long-term stability at air in a humid environment. PEDOT polymers are found to form polydisperse spherical nanoparticles after deposition with an electrical conductivity of 3.4×10^{-3} S cm^{-1}.

In chapter 7, based on the results of chapter 6, starting from EDOT monomers and silver perchlorate salt, preparation of PEDOT/Ag composites, made of PEDOT conducting polymers and silver nanoparticles, is achieved by using different radiolytical procedures. According to a two-step method, PEDOT polymers are first synthesized by either oxidation or reduction of EDOT monomers and then, silver nanoparticles are produced in the presence of PEDOT by reduction of silver ions. As a result, composites prepared by two-step method are made of large spherical PEDOT nanoparticles at the surface of which smaller silver nanoparticles adsorb. Differently, according to an one-pot method, polymerization and metal ions reduction are achieved in parallel, in one step, thanks to the concomitant reduction of EDOT monomers and of silver ions, as demonstrated by pulse radiolysis experiments. Therefore, composites produced according to one-pot method are made of silver nanoparticles embedded in the core of small

irregular spheroidal PEDOT nanoparticles. All PEDOT/Ag composites are characterized by the same thermal stability, which remains higher, over a wide range of temperatures, than that of pure PEDOT synthesized by radiolysis. Also, their electrical conductivity are in the same order of magnitude.

All in all, the synthesis of CPs and CPs nanocomposites has been tried in this thesis for primary study. The versatility of radiolytic methodology has been proved to be a potential alternative method. However, there are also few questions that worth further investigation for better understanding and application of the radiolytic method.

For the synthesis of PPy using radiolytic method, the oxidation polymerization of pyrrole introduces the new carbonyl band into the PPy polymers. It is necessary to check the reaction for the formation of this new group and check whether PPy polymers are overoxidized. In addition, the extension of radiolytic method for the synthesis of different kinds of CPs including polyaniline (PANI), polythiophene (PTs) and poly(3-thiophene acetic acid) (P3TAA) is worth studying. Moreover, the synthesis of CPs directly onto conducting or nonconducting substrates by γ-irradiation or accelerated electron beams may offer synthetic routes.

In the study of the effect of synthetic conditions on the polymerization of EDOT, the effect of soft template formed by SDS needs to be checked in detail below CMC I. To control the morphology of CPs, use of hexagonal mesophases or microemulsions is worth trying. It is worth studying the mechanism of polymerization of EDOT in acidic medium and determining the role of H• during the polymerization of EDOT. To the preparation of PEDOT/PSS membranes, it is necessary to optimize the ratios and add other supporting reagents. In order to enhance the electrical conductivity of radiosynthesized CPs, we will work on increasing the doping level by adding chemical oxidant and increasing the polymer chain length thanks to the decrease of the dose rate during irradiation.

To the polymerization of EDOT by reduction polymerization with e_{aq}^-, the mechanism for the reduction induced polymerization has not been reported which is worth studying. During the synthesis of PEDOT/Ag nanocomposites, the interaction between PEDOT and Ag nanoparticles needs further study. In addition, the application of PEDOT/Ag nanocomposites for catalytic applications is of great mean. The synthesis of poly(3-hexylthiophene) (P3HT) or poly(diphenylbutadiyne) (PDPB) or mixture of PEDOT/P3HT, PEDOT/PSS for photovoltaic, electrochromic, solar cell applications is meaningful.

Therefore, the improvement of synthetic conditions as well as potential applications of CPs and CPs nanocomposites needs further research.

université PARIS-SACLAY
ÉCOLE DOCTORALE
Sciences chimiques : molécules, matériaux, instrumentation et biosystèmes

Titre : Synthèse radio-induite de polymères conducteurs et de leurs nanocomposites métalliques

Mots clés : Irradiation gamma, Polymères conducteurs, Nanocomposites

Résumé : L'objectif du présent travail est de démontrer la versatilité de méthodologie radiolytique et de l'étendre à la synthèse de différents PCs dans l'eau. Le poly(3,4-ethylènedioxythiophène), PEDOT, et le polypyrrole, PPy, ont ainsi été préparés avec succès et caractérisés en solution aqueuse, ou après dépôt sur substrat, par des techniques spectroscopiques et microscopiques. La stabilité thermique et la conductivité électrique de ces matériaux radiosynthétisés ont été étudiées et comparées aux propriétés des PCs produits par les méthodologies traditionnelles. Nous avons étudié l'influence de la nature des espèces radiolytiques oxydantes, de la force ionique du milieu, du pH de la solution et de la présence de surfactants, sur le mécanisme de croissance des PCs, sur le rendement de polymérisation, sur la morphologie des matériaux radiosynthétisés ainsi que sur les propriétés optiques et électriques de ces derniers.

Nous avons utilisé la radiolyse pour la synthèse de nanocomposites hybrides à base de PCs et de métaux de transition. Plusieurs voies de synthèse ont été développées : synthèse en une ou deux étapes, par oxydation ou réduction des monomères.

La nouvelle stratégie de synthèse par radiolyse, qui est décrite dans ce manuscrit, ouvre la voie à la préparation de très nombreuses familles de PCs et de leurs composites, que ce soit en solution aqueuse ou dans des environnements alternatifs (en milieu organique, sur support, en milieu hétérogène), ce qui laisse augurer de nombreuses applications fort prometteuses.

Title : Radiation induced synthesis of conducting polymers and their metal nanocomposites

Keywords : Gamma irradiation, Conducting polymers, Nanocomposites

Abstract : The aim of the present work is to demonstrate the versatility of the gamma (γ)-rays based radiolytic method and to extend our methodology to the synthesis of various conducting polymers (CPs) in water in different experimental conditions. Poly(3,4-ethylenedioxythiophene) (PEDOT) and polypyrrole (PPy) conjugated polymers were successfully prepared and characterized in solution and after deposition by complementary spectroscopic and microscopic techniques. Also their thermal stability and their electrical conductivity were studied and compared with those of CPs prepared by conventional methods. The influence of the nature of radiation-induced oxidizing radicals, of the ionic strength, of the medium, of the pH, of the presence of surfactant-based soft templates on the growth mechanism, on the efficiency of polymerization, on the morphology of the obtained CPs as well as on their absorption and conducting properties was checked.

Also, the radiolytic method was extend to the synthesis of CPs/noble metal nanocomposites. Different preparation methodologies were developed based on two-step method and one-pot method, by using oxidation route or reduction route.

Our new radiolytic strategy described and extended in this manuscript opens the way for the preparation of different kinds of CPs and CPs nanocomposites not only in aqueous solutions but also in various environments foreshadowing many promising applications.

Université Paris-Saclay
Espace Technologique / Immeuble Discovery
Route de l'Orme aux Merisiers RD 128 / 91190 Saint-Aubin, France